AD _____

CONTRACT NO: DAMD17-93-C-3042

TITLE: PRODUCTION AND ENZYME ENGINEERING OF HUMAN ACETYLCHOLINESTERASE AND ITS MUTANT DERIVATIVES

PRINCIPAL INVESTIGATOR: Avigdor Shafferman Ph.D.

CONTRACTING ORGANIZATION: Israel Institute for Biological Research

70450 Ness-Ziona
ISRAEL

REPORT DATE: May 1996

TYPE OF REPORT: Final

PREPARED FOR: Commander
U.S. Army Medical Research, and Materiel Command
Fort Detrick, Frederick, Maryland, 21702-5012.

DISTRIBUTION STATEMENT: Approved for public release;
distribution unlimited

The views, opinions and/or findings contained in this report are those of the author(s) and should not be construed as an official Department of the Army position, policy or decision unless so designated by other documentation.

19961218 063

DTIC QUALITY INSPECTED 1

REPORT DOCUMENTATION PAGE

Form Approved
OMB No. 0704-0188

Public reporting burden for this collection of information is estimated to average 1 hour per response, including the time for reviewing instructions, searching existing data sources, gathering and maintaining the data needed, and completing and reviewing the collection of information. Send comments regarding this burden estimate or any other aspect of this collection of information, including suggestions for reducing this burden, to Washington Headquarters Services, Directorate for Information Operations and Reports, 1215 Jefferson Davis Highway, Suite 1204, Arlington, VA 22202-4302, and to the Office of Management and Budget, Paperwork Reduction Project (0704-0188), Washington, DC 20503.

1. AGENCY USE ONLY *(Leave blank)*	2. REPORT DATE	3. REPORT TYPE AND DATES COVERED
	May 1996	Final (15 Jan 93 - 31 Mar 96)

4. TITLE AND SUBTITLE
Production and Enzyme Engineering of Human Acetylcholinesterase and Its Mutant Derivatives

5. FUNDING NUMBERS
DAMD17-93-C-3042

6. AUTHOR(S)
Avigdor Shafferman, Ph.D.

7. PERFORMING ORGANIZATION NAME(S) AND ADDRESS(ES)
Israel Institute for Biological Research
70450 Ness-Ziona, Israel

8. PERFORMING ORGANIZATION REPORT NUMBER

9. SPONSORING/MONITORING AGENCY NAME(S) AND ADDRESS(ES)
U.S. Army Medical Research and Materiel Command
Fort Detrick
Frederick, Maryland 21702-5012

10. SPONSORING/MONITORING AGENCY REPORT NUMBER

11. SUPPLEMENTARY NOTES

12a. DISTRIBUTION / AVAILABILITY STATEMENT
Approved for public release; distribution unlimited

12b. DISTRIBUTION CODE

13. ABSTRACT *(Maximum 200)*

Studies toward the design of pharmacologically useful bio-scavengers against organophosphate poisoning, were pursued in two main directions: a. structure-reactivity characteristics of human acetylcholinesterase (HuAChE) derivatives and of the corresponding phosphyl conjugates; b. molecular surface properties of HuAChE derivatives affecting biosynthesis, stability and clearance. Combination of recombinant DNA technology, kinetic studies and molecular modeling was employed to identify some of the residues involved in direct interactions with organophosphates and phosphonates and in the subsequent aging processes. Our findings allow to define the structural determinants in the active center facilitating the bio-scavenging and conferring resistance to aging. In addition, we identified residues at the peripheral anionic site (PAS), participating in modulation of HuAChE reactivity, and defined a possible structural link for transmission of the allosteric signal to the active center. Such mechanism probably involves the conformational mobility of the surface loop (Cys69-Cys96) containing specific elements of the PAS and the active center. Alterations of the molecular surface properties of HuAChE including replacements of up to seven acidic residues, failed to alter significantly the catalytic properties of the mutants relative to the wild type HuAChE. Manipulation of the level of glycosylation sites by mutagenesis affected biosynthesis, secretion, thermal stability and the rates of clearance. It was demonstrated that a control over the number of vacant sialic acid attachment sites may improve the enzyme residence time in the bloodstream.

14. SUBJECT TERMS
Human Acetylcholinesterase, Production, Mutagenesis
Molecular Modeling, Enzyme Engineering, Organophosphorus
Inhibitors, Bioscavengers

15. NUMBER OF PAGES
276

16. PRICE CODE

17. SECURITY CLASSIFICATION OF REPORT	18. SECURITY CLASSIFICATION OF THIS PAGE	19. SECURITY CLASSIFICATION OF ABSTRACT	20. LIMITATION OF ABSTRACT
Unclassified	Unclassified	Unclassified	Unlimited

FOREWORD

Opinions, interpretations, conclusions and recommendations are those of the author and are not necessarily endorsed by the US Army.

_____ Where copyrighted material is quoted, permission has been obtained to use such material.

_____ Where material from documents designated for limited distribution is quoted, permission has been obtained to use the material.

_____ Citations of commercial organizations and trade names in this report do not constitute an official Department of Army endorsement or approval of the products or services of these organizations.

___X___ In conducting research using animals, the investigator(s) adhered to the "Guide for the Care and Use of Laboratory Animals," prepared by the Committee on Care and Use of Laboratory Animals of the Israel Institute for Biological Research.

_____ For the protection of human subjects, the investigator(s) adhered to policies of applicable Federal Law 45 CFR 46.

___X___ In conducting research utilizing recombinant DNA technology, the investigator(s) adhered to current guidelines promulgated by the National Institutes of Health.

___X___ In the conduct of research utilizing recombinant DNA, the investigator(s) adhered to the NIH Guidelines for Research Involving Recombinant DNA Molecules.

_____ In the conduct of research involving hazardous organisms, the investigator(s) adhered to the CDC-NIH Guide for Biosafety Microbiological and Biomedical Laboratories.

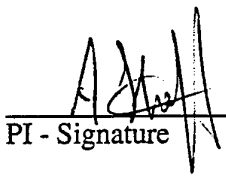

20.6.96

PI - Signature Date

PRODUCTION AND ENZYME ENGINEERING OF HUMAN ACETYLCHOLINESTERASE AND ITS MUTANT DERIVATIVES

FINAL REPORT

BARUCH VELAN*
ARIE ORDENTLICH*
NAOMI ARIEL*
SHAUL REUVENI‡
YOFFI SEGALL#
DANA STEIN*
ARIE LAZAR‡
SARA COHEN*
ABRHAM BROMBERG+
DOV BARAK#
CHANOCH KRONMAN*
DINO MARCUS‡
TAMAR SERRY*
NEHAMA ZELIGER*
LEA SILBERSTEIN‡
TAMAR BINO*
LEVANA MOTULA*
THEODOR CHITLARU*

AVIGDOR SHAFFERMAN*‡

We greatly appreciate the contribution of Mrs ESTHER HABERMAN≠ to the administrative management of the contract

*Department Of Biochemistry
#Department of Organic Chemistry
‡Department of Biotechnology
+Department of Physical Chemistry
≠Division of Biology

CONTENTS

CONTENTS (Cont'd) Page

CONTENTS (Cont'd) Page

CONTENTS (Cont'd) Page

CONTENTS (Cont'd) Page

LIST OF FIGURES

LIST OF FIGURES (Cont'd) Page

LIST OF TABLES

LIST OF TABLES (Cont'd)

I. General Introduction

The primary role of acetylcholinesterase (acetylcholine acetylhydrolase, 3.1.1.7 AChE), is the termination of impulse transmission in cholinergic synapses by rapid hydrolysis of the neurotransmitter acetylcholine (ACh). A second ACh hydrolysing enzyme butyrylcholinesterase (alcholine acyl hydrolase 3.1.1.8, BChE), often appears together with AChE in various tissues. BChE differs from AChE in its substrate specificity and in susceptibility to inhibitors. Several cholinesterase inhibitors remain of value as medicinal agents and pesticides while others possess the potential for use as chemical warfare agents. Some AChE inhibitors (e.g. phospholineiodide and physostigmine) are useful therapeutic agents in the treatment of glaucoma. In addition, the quaternary carbamates neostigmine and pyridostigmine are currently used for the treatment of myasthenia gravis (Taylor, 1990). Modifications in the levels of human brain AChE have been reported in several neurological and genetic disorders, such as Alzheimer disease (Coyle *et al.,* 1983) and Down's Syndrome (Yates *et al.,* 1980). Indeed the first drug approved recently by the FDA to treat Alzheimer disease is an AChE inhibitor - tacrine. Some organophosphorus (OP) inhibitors of ChEs such as malathion and diazinon, act as efficient insecticides and have been widely used in combating medfly and other agricultural pests. Other OP compounds, such as the nerve agents sarin and soman, inhibit AChE irreversibly by rapid phosphorylation of the serine residue in the enzyme active site. The acute toxicity of these nerve agents is elicited in motor and respiratory failure following inhibition of AChE in the peripheral and central nervous system. The current treatment regimes against nerve agent exposure are designed to protect life but are not able to prevent severe incapacitation. The use of exogenous scavengers such as AChE and BChE has been successfully demonstrated in animals (Wolf *et al.,* 1987; Raveh *et al.,* 1989; Broomfield *et al.,* 1991; Doctor *et al.,* 1992) for sequestration of highly toxic OPs before they reach their physiological target.

Elucidation of the primary structure of various cholinesterases (Schumacher *et al.,* 1986; Hall and Spierer 1986; Lockridge *et al.,* 1987; Prody *et al.,* 1987; Sikarov *et al.,* 1987; Chatonnet and Lockridge 1989; Olson *et al.,* 1990; De la Escalera *et al.,* 1990; Rachinsky *et al.,* 1990; Doctor *et al.,* 1990) and the recent solution of the crystal structure of a AChE (Sussman *et al.,* 1991) added new perspectives to cholinesterase research. Recently we developed (under U.S. contract no. DAMD17-89-C-9117) efficient mammalian expression systems for recombinant

human AChE (Velan *et al.* 1991a; Kronman *et al.* 1992). We also developed experimental systems for generating AChE mutants and methods for evaluation of their activity and conformation (Shafferman *et al.*, 1992a,b). All these developments provide the basis for the current research which should allow the design of enzymes with specifically altered activity (e.g. an AChE capable of undergoing reversible inhibition by irreversible inhibitors of the native enzyme) or an enzyme with extended stability. We believe that information derived from the studies described below, as well as the information accumulated by others, already provides a better understanding of the catalysis of AChE and will allow us in the near future to design and prepare novel AChE muteins tailored to need.

This report covers the various aspects of the proposed R&D. In the following section (Section II) we describe the identification of some of the critical elements of the active center such as the amino acids that constitute the "anionic" or the choline binding subsite, the acyl pocket and residues that determine specificity for the hydrophobic moiety of ligands and substrates. In the next section (Section III) we describe the analysis that led to the identification of the peripheral anionic subsite. In sections IV and V we analyze the relationship between aromatic moieties in the active center , specifically those involved the choline binding subsite, and the peripheral anionic subsite in modulation catalysis and allosteric effects in AChE. Other aspects related to catalysis such as the potential role of surface charge and the hypothesis of the "back door" are described in Sections VI and VII. In the following sections (VIII and IX) we describe how specific residues in the active center of human AChE (HuAChE) determine the specificity towards different OP-inhibitors and demonstrate the ability to generate novel enzymes that are either more efficient in OP scavenging or highly resistant to the aging process. Section X provides an update on the large scale production of the recombinant HuAChE enzyme for various research purposes including pharmacological studies and x-ray crystallography. The role and contribution of the three N-glycosylation sites to the catalytic activity, production efficiency and thermal stability is provided in Section XI. The manipulation of secretion pathways of recombinant HuAChE molecules from mammalian cells is described in Section XII. The role of oligosaccharide side chains and oligomerization in clearance of cholinesterases from the circulation is analysed in Section XIII. Each of the major sections includes a brief background introduction, methods and a result and discussion subsection. A summary of the main findings of the research, Section XIV, concludes this report.

II. Human Acetylcholinesterase Active Center - Identification of Residues Constituting the Anionic, and Hydrophobic Subsites and the Acyl Pocket.

INTRODUCTION

Acetylcholinesterase (AChE[1], EC 3.1.1.7) is a serine hydrolase selectively reacting with its natural substrate acetylcholine (ACh) at close to diffusion control rate (Bazelyansky *et al.*, 1986; Quinn, 1987). Kinetic studies with different substrates, as well as reversible and irreversible inhibitors, imply that the AChE active center consists of several major domains: a) an esteratic site containing the active serine; b) an anionic site that accommodates the positive pole of ACh; and c) hydrophobic sites which bind aryl substrates, other uncharged ligands and the alkyl portion of the acyl moiety (Quinn, 1987; Hucho *et al.*, 1991).

The location and spatial organization of the active site serine (MacPhee-Quigley *et al.*, 1985) and histidine (Krupka, 1966) constituting the esteratic site of AChE were determined by site-directed mutagenesis (Gibney *et al.*, 1990; Shafferman *et al.*, 1992a) and X-ray crystal structure studies (Sussman *et al.*, 1991). Mutagenesis studies identified and provided biochemical evidence for the involvement of a glutamic residue in the catalytic triad (Shafferman *et al.*, 1992a,c), as also predicted by the X-ray crystal structure of *Torpedo californica* AChE (TcAChE; Sussman *et al.*, 1991).

The high catalytic efficiency of AChE is attributed to the esteratic triad, as well as to structural elements of recognition such as the anionic and hydrophobic subsites, which confer specificity for particular alcoholic (X) and alkyl (R) groups (see Scheme 1).

Scheme 1

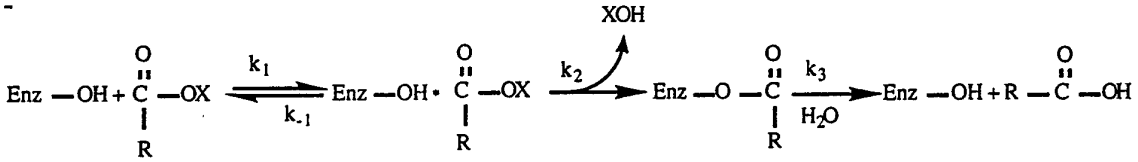

Earlier studies have postulated that the anionic site contains multiple charges (Nolte *et al.*, 1980). On the other hand, the pronounced catalytic activity of AChE towards neutral substrates (Cohen *et al.*, 1985) led to the proposal of a hydrophobic trimethyl binding site for accommodation of the quaternary functionality (Hassan *et al.*, 1980). Distinct binding

subsites for charged and neutral alcohol moieties (X in Scheme 1 and in Fig. 1) of the substrates also have been proposed (Berman and Decker, 1986). Recently several specific amino acids were implicated in stabilization of the charged X moiety of ACh. In HuAChE replacement of W86(W*84*) (Amino acids and numbers in parenthesis refer to the position of analogous residues in TcAChE, according to the recommended nomenclature, Massoulie *et al.*, 1992) resulted in at least a 100-fold reduction in the catalytic potential of the enzyme (Shafferman *et al.*, 1992c). The same tryptophan residue in TcAChE was labeled by phenyl aziridinium and the reaction was blocked by edrophonium, an active center inhibitor (Kreienkamp *et al.*, 1991; Weise *et al.*, 1990). According to the X-ray structure data, the W84 residue of TcAChE is located within a suitable distance from the esteratic site for accommodation of ACh (Sussman *et al.*, 1991). In addition to W86(W*84*), residues Y337(F*330*) and F338(F*331*) appear to interact with the substrate as well, since mutations Y337A and F338A in HuAChE resulted in a significant decrease in k_{cat} of acetylthiocholine (Shafferman *et al.*, 1992b,c). Involvement of residues F330 and F331 in the active center of TcAChE was also indicated by labeling studies (Kieffer *et al.*, 1986, Schalk *et al.*, 1992).

Another aspect of AChE specificity is exemplified by the different rates of hydrolysis for ACh and butyrylcholine (BCh) (Augustinsson and Nachmansohn, 1949). Structure-activity relationship studies with acylcholine substrates were rationalized by postulating a hydrophobic pocket (Jarv, 1984) of a limited size that accommodates a methyl group better than bulkier R groups (Scheme 1) . Size restrictions of this pocket were also implicated in the stereo-selectivity of AChE toward chiral phosphonates (Benshop and De Jong, 1988). Modeling of the butyrylcholinesterase (BChE)-BCh adduct (Harel *et al.*, 1992a) and of the HuAChE adducts with chiral phosphonates (Barak *et al.*, 1992) identified the size restricting elements of the acyl-pocket as residues F295(F*288*) and F297(F*290*). A careful analysis of the role of these residues in the formation of the initial enzyme-substrate complex or during the acylation-deacylation stages is yet to be performed.

In an attempt to further explore the structure-function relationships underlying the complex AChE substrate specificity, we employ site directed mutagenesis and molecular modelling techniques, together with examination of the kinetic behavior of the resulting muteins towards substrates and inhibitors. We identify some of the major structural elements of the hydrophobic subsite, provide evidence that this site is distinct from the anionic subsite, which is determined by HuAChE W86, and demonstrate a role for F295 and F297 in the acyl pocket.

METHODS

Mutagenesis of Recombinant HuAChE and Construction of Expression Vectors- Mutagenesis of AChE was performed by DNA cassette replacement into a series of HuAChE sequence variants which conserve the wild type (Soreq *et al.*, 1990) coding specificity, but carry new unique restriction sites (Velan *et al.*,1991a; Kronman *et al.*, 1992; Shafferman *et al.*, 1992a). Generation of mutants W86A(W*84*), W286A(W*279*), Y337A(F*330*) Y337F, and F338A(F*331*) was described previously (Shafferman *et al.*, 1992b). Substitution of residues F295(F*288*) and F297(F*290*) was carried out by replacement of the *Mlu*I- *Nar*I DNA fragment of the AChE-w7 variant (Shafferman *et al.*, 1992a) with synthetic DNA duplexes carrying the mutated codons. The TTC codon of F295 was changed to CTG(Leu) or GCC(Ala) and that of F297 to GTG(Val) or GCC(Ala). The codon of Gly121 was changed to Ala(GCC) on a synthetic DNA fragment cloned between the NruI-NarI sites of ACHE-w4 plasmid. All the synthetic DNA oligodeoxynucleotides were prepared using the automatic Applied Biosystems DNA synthesizer. The sequences of all new clones were verified by the dideoxy sequencing method (USB sequenase kit). The rHuAChE cDNA mutants were expressed in tripartite vectors which allows expression of the *cat* reporter gene and the *neo* selection marker (Kronman *et al.*, 1992, Shafferman *et al.*, 1992a).

Transient Transfection and Quantitation of AChE- Human embryonal 293 cells were transfected by purified plasmid preparations using the calcium phosphate method. Transient transfection was carried on as described previously (Shafferman *et al.*, 1992 a,b) and stably transfected colony-pools (Velan *et al.*, 1991b) were generated by G418 selection. AChE secreted by transiently, or stably transfected cells was collected by incubating cells in 2 ml AChE-depleted medium (Shafferman *et al.*, 1992a) per 100mm plate for 48 hours. AChE activity in cell supernatant was tested as described below and AChE-protein mass was determined by a specific enzyme linked immunosorbent assay (ELISA) (Shafferman *et al.*, 1992a). Efficiency of transfection was monitored (Kronman *et al.*, 1992) by levels of the coexpressed CAT (chloramphenicol acetyl transferase) activity (Gorman *et al.*, 1982).

Substrates and Inhibitors- Purified human serum butyrylcholinesterase (HuBChE),

acetylthiocholine iodide (ATC), butyrylthiocholine iodide (BTC), propionylthiocholine iodide (PTC), 5:5'-dithiobis (2-nitrobenzoic acid) (DTNB), *p*-nitrophenyl acetate (PNPA), 3,8 diamino-5-3'-(trimethylammonium)propyl-6-phenyl phenanthridinium iodide (propidium), ethyl(m-hydroxyphenyl)-dimethylammonium chloride (edrophonium), di(*p*-allyl-N-methylaminophenyl)-pentane-3-one (BW284C51) and tetraisopropylpyrophosphoramide (iso-OMPA) were all purchased from Sigma. S - n - propyl thioacetate ($CH_3C(O)SC_3H_7$ - TPA) was synthesized from n - propylmercaptane and acetyl chloride with triethylamine. Distillation afforded 95% yield of the product, b.p 53°C/20mmHg. Structural assignment was confirmed by NMR spectroscopy. S - 3,3 - dimethylbutyl thioacetate ($CH_3C(O)SC_2H_4C(CH_3)_3$ - TB) was synthesized using the following steps: a) 3,3 - dimethylbutanol was obtained by $LiAlH_4$ reduction of 3,3 - dimethylbutyric acid. Distillation resulted in 55% yield of the alcohol b.p. 68°C/25mmHg. b) 3,3 - dimethylbutyl bromide was obtained from the alcohol and aqueous HBr 48%. Distillation gave 91% yield of the bromide b.p. 40°C/20mmHg. c) The final product was obtained by reacting the dimethylbutyl bromide with thioacetic acid and KOH in ethanol. Distillation gave 90% yield of the thioacetate b.p. 79°C/20mmHg. Structural assignment was confirmed by NMR spectroscopy.

Determination of AChE Activity and Analysis of Kinetic Data- AChE activity with thioesters was assayed according to Ellman *et al.* (1961). Standard assays were performed in the presence of 0.1 mg/ml BSA, 0.3mM DTNB 50mM sodium-phosphate buffer pH-8.0 and varying substrate (ATC, BTC, PTC, TB, or TPA) concentrations. Hydrolysis of PNPA was performed in the buffer solution described above but without DTNB, and the reaction product was monitored by the absorbance of the *p*-nitrophenylate anion at 405 nm. The assays were carried out at 27°C and monitored by a Thermomax microplate reader (Molecular Devices). Michaelis-Menten constant (Km) values were obtained from the double reciprocal Lineweaver Burk plots and k_{cat} calculations were based on ELISA quantitations (Shafferman *et al.*, 1992a). Interactions with inhibitors were monitored by determining residual activity following preincubation of rHuAChE or its mutants for 20 minutes with increasing concentrations of edrophonium , propidium, iso-OMPA or BW284C51. Ki values for the reversible competitive inhibitor edrophonium were calculated from the equation $K_i=IC_{50}/[1+([S]/Km)]$ as described by Hobbiger and Peck (1969), where IC_{50} is the concentration resulting in 50% inhibition and [S] the substrate concentration.

Kinetic data for inhibition by propidium were analyzed according to the kinetic treatment developed by Barnet and Rosenberry (1977) and Berman and Leonard (1990) for the reaction described in the following scheme.

Scheme 2:

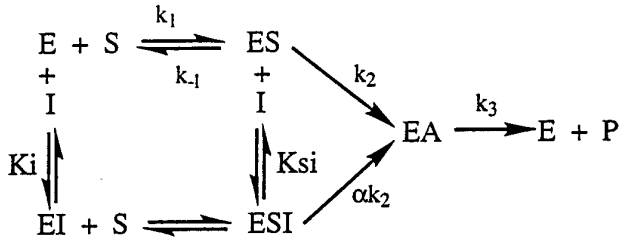

In this scheme Ki is the competitive inhibition constant and Ksi the noncompetitive inhibition constant. A kinetic solution for the dependence of the reciprocal rate on the inverse concentration of substrate is provided in equation 1. The expressions of relative slopes (Rs) and relative intercepts (Ri), in presence and absence of inhibitor, are provided by equations 2 and 3, respectively. Values of Rs and Ri can be computed from the double reciprocal plots of rate versus substrate concentration.

(1)

$$\frac{1}{V}=\frac{1}{Vm}\left[\frac{k_{cat}}{k_2}\left(1+\frac{[I]}{K_{si}}\right)+K_{app}\left(1+\frac{[I]}{K_i}\right)\cdot\frac{1}{[S]}\right]\cdot\left[\left(1+\frac{\alpha[I]}{K_{si}}\right)\right]^{-1}$$

(2)

$$Rs=\left[\left(1+\frac{[I]}{K_i}\right)\right]\cdot\left[\left(1+\frac{\alpha[I]}{K_{si}}\right)\right]^{-1}$$

(3)

$$Ri=\left[\left(1+\frac{[I]}{K_{si}}\right)\right]\cdot\left[\left(1+\frac{\alpha[I]}{K_{si}}\right)\right]^{-1}$$

If replots of Rs versus inhibitor concentration ([I]) are linear, $\alpha/Ksi = 0$; and Ki is given by the reciprocal of the slope of Rs versus [I]. In such cases Ksi is derived from the reciprocal of

the slope of Ri versus [I]. When replots of Rs are not linear, the enzyme can not be completely inhibited, Ki can then be derived from the double reciprocal plots of (Rs - 1) versus [I] (Barnett and Rosenberry 1977). In such cases an independent Ksi value can not be derived.

Structure Analysis and Molecular Graphics- Building and analysis of the three dimensional molecular models was performed on Silicon Graphics work station IRIS70/GT, using the SYBYL modelling software (Trypos Inc.). Construction of models for HuAChE mutants and the corresponding adducts with substrates and inhibitors were based on a model structure of the enzyme obtained by comparative modelling (Barak *et al.*, 1992) from coordinates of TcAChE (Sussman *et. al.* 1991). Structural refinement by molecular mechanics was done using the MAXMIN force field and zone refinement procedure Anneal, both included in SYBYL. The zone of refinement included 33 amino acids within the active site gorge and in its close vicinity.

RESULTS

Reactivity of HuAChE and Selected Mutants Towards Substrates Containing Charged and Uncharged Alcohol Moieties : To study enzyme specificity towards the alcoholic domain (X in Scheme 1 and Fig. 1) several substrates with a common acyl moiety (acetyl), were analyzed. Besides the charged choline moiety of ATC, three uncharged X-residues (Fig. 1) with different properties were selected for study: a reactive alkyl acetate (TB), a relatively unreactive alkyl acetate (TPA), and an aryl ester (PNPA). TB contains a t - butyl moiety which is isosteric with the trimethyl ammonium group of ATC and should therefore allow examination of the net effect of charge on reactivity. The aromatic amino acids in the active center that were previously implicated (see introduction) in interactions with the choline moiety of ACh, namely W86, F338 and Y337, were selected for study. In addition to wild type HuAChE and to the active center mutants, W86A, Y337A and F338A, we also included an alanine mutant of W286, an amino acid located at the rim (Barak *et al.*, 1992) of the HuAChE active center 'gorge'. We have previously shown that W286 may be involved in substrate inhibition by triggering a conformational change of Y337 in the active center (Shafferman *et al.*, 1992b). According to Scheme 1, the Michaelis-Menten constant (Km)

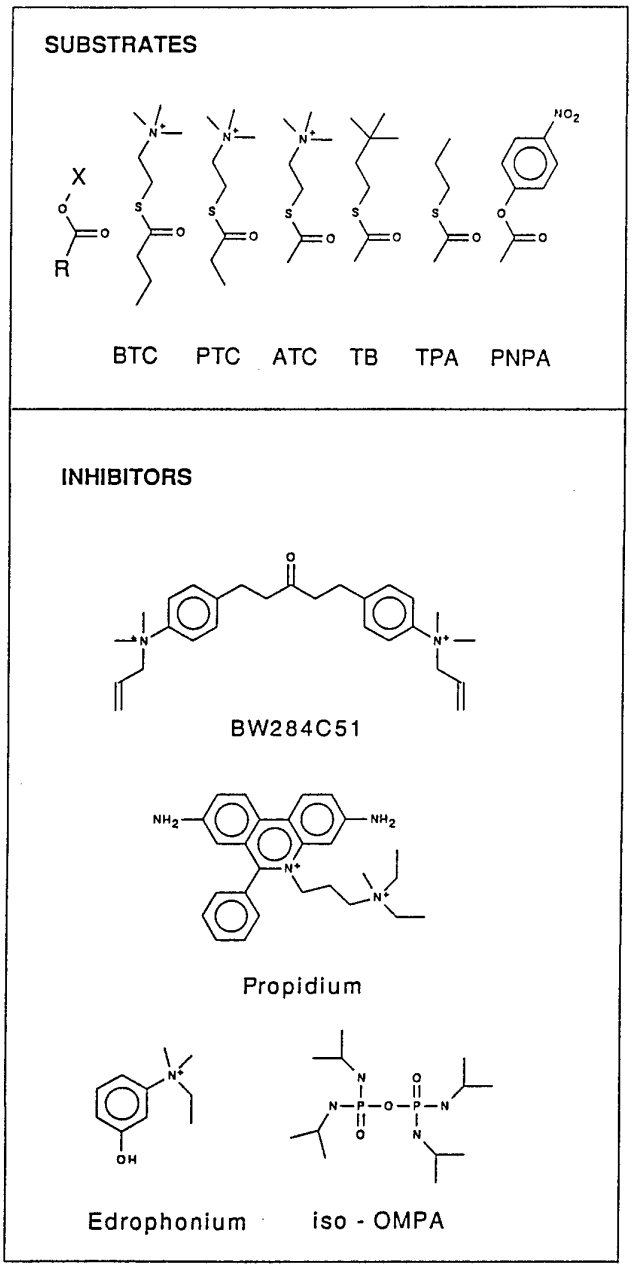

Fig. 1 Chemical formula of substrates and inhibitors used.

corresponds to $(k_{-1}/k_1+k_2/k_1)[(k_3/(k_2+k_3)]$. The apparent catalytic first order rate constant (k_{cat}) corresponds to the ratio of first order rate constants for acylation (k_2) and deacylation (k_3) and is equal to $(k_2k_3)/(k_2+k_3)$. Using the Lineweaver-Burk analysis, Km, k_{cat} and the apparent bimolecular rate constants (k_{cat}/Km) were calculated for the hydrolysis of the various substrates by HuAChE and its mutants (Table 1). The Km value of the wild type enzyme for ATC was about two orders of magnitude higher than that for TPA and PNPA and about 3-folds higher than that for TB (Table 1). Considering the differences in enzyme source and assay conditions, these values are in good agreement with those published (see Table 1) for AChE from *Electrophorus electricus* (Rosenberry, 1975; Hassan *et al.*, 1980; Salih, 1992) and from *Naja naja oxiama* (Jarv *et al.*, 1976). Mutations at positions 286, 337 and 338 had no major effect on the Km for the various substrates. The most striking effect was the increase of over 660 fold in the Km value for ATC in the W86A mutant. The Km value of the isosteric substrate TB, which is devoid of the cationic charge (Fig. 1), is hardly affected by the replacement of W86 with alanine. These results demonstrate that the tryptophan-86 residue is involved in stabilization of the charge in the enzyme-substrate complex and constitutes the classical 'anionic' subsite of the active center.

The k_{cat} and the apparent bimolecular rate constants values of the wild type recombinant HuAChE for the various substrates are again in good agreement with those determined previously (Rosenberry 1975; Jarv *et al.*, 1976; Hassan *et al.*, 1980; Salih, 1992; Table 1). Mutation of residues F338 and W86 resulted in a decrease in catalytic efficiency towards ATC, TB and TPA , yet only mutation of F338 resulted in a decrease in k_{cat} for PNPA (Table 1). Mutation of W86 had the most deleterious effect on the apparent first order rate constant of hydrolysis of ATC, TB and TPA, suggesting a major role of this residue not only in stabilization of the Michaelis- Menten complex but also in hydrolysis. The combined effects on Km and k_{cat} resulted in over 3000 fold reduction in the apparent bimolecular rate constant of W86A for ATC as compared to the wild type. Replacement of Y337 and W286 by alanine had no major effect on the apparent bimolecular rate constant with any of the uncharged substrates tested, and for ATC the change did not exceed a factor of four.

Replacement of Gly121 by alanine generated enzymes devoid of a detectable catalytic activity toward any of the substrates tested. This observation is consistent with its proposed role (Sussman *et al.*, 1991) as an element of the HuAChE 'oxyanion hole'.

Table 1: Kinetic constants for the hydrolysis of ATC, TB, TPA and PNPA by HuAChE and selected HuAChE mutants

Substrate / HuAChE	Km (mM)				k_{cat} ($x10^{-3}$ x min^{-1})				k_{cat}/Km ($x10^{-6}$) (M^{-1}xmin^{-1})			
	ATC	TB	TPA	PNPA	ATC	TB	TPA	PNPA	ATC	TB	TPA	PNPA
WT	0.14	0.45	11.0	5.6	370	52	11.0	110	2640	116	1.00	20.0
D74N	1.10	0.35	10.0	4.2	270	50	14.5	200	460	143	1.45	47.6
D74K	5.80	0.50	12.0	4.1	350	58	8.5	70	80	116	0.70	17.0
E202D	0.25	0.50	16.5	3.6	15	8.6	6.0	166	80	17	0.50	46.1
E202Q	0.35	0.48	8.5	2.9	56	65	1.25	40	160	12	0.15	13.8
W286A	0.40	0.40	8.2	4.6	400	46	9.6	130	1000	114	1.20	28.0
Y337A	0.14	0.50	10.0	5.4	100	83	15.0	96	710	166	1.50	18.0
F338A	0.30	0.30	11.7	8.6	170	13	4.8	20	570	43	0.40	2.3
W86A	93.3	0.55	11.5	3.0	80	28	1.4	190	0.86	51	0.12	63.0
W86E	57.9	0.63	19.5	8.3	20	30	2.2	270	0.34	48	0.11	32.5
Other AChE [a-d]	0.10 [a] 0.13 [c]	1.4 [d] 2.6 [d]	55 [b] 33 [d]	5.0 [a] 4.9 [c]	960 [a] 900 [c]	194 [b] 180 [d]	22.0 [b] 15.6 [d]	76.8 [a] 78 [c]	9600 [a] 6900 [c]	138 [b] 28 [d]	0.40 [b] 0.48 [d]	15.0 [a] 15.6 [c]

[a] Rosenberry, (1975); [b] Jarv *et al.*, (1976); [c] Salih, (1992); [d] Hassan *et al.*, (1980). [a,c,d] *Electrophorus electricus* AChE; [b] *Naja naja oxiama* AChE.
[a-d] Values for hydrolysis of either oxy or thiocholine acetates.

Inhibition by Edrophonium : Inhibition of the hydrolysis of various substrates by edrophonium, a reversible active center inhibitor, for HuAChE and the four mutants is summarized in Table 2. We have previously shown that an aromatic amino acid at position 337 is required for better interaction of edrophonium with the active center of AChE (Shafferman *et al.*, 1992b,c). Indeed, irrespective of the substrate used, the Y337A mutant exhibits about 10-40 increase in edrophonium inhibition constants compared with the values for the wild type enzyme. The effects of W86A were even more pronounced. Edrophonium at 150μM, a concentration 100-fold higher than the that required to achieve 50% inhibition (IC_{50}) of wild type enzyme, was insufficient to inhibit the catalysis of any of the substrates tested by the W86A mutant. These results suggest that W86 is a part of the edrophonium binding site, which is in agreement with X-ray crystal data (Sussman *et al.*, 1992), and with our assignment of the anionic subsite to this residue.

Inhibition by Propidium : The inhibitory effect of propidium , a peripheral anionic site ligand (Taylor and Lappi , 1975), on hydrolysis of ATC, TB and PNPA by HuAChE mutants and by the wild type enzyme are summarized in Figures 2,3 and Table 3. The results demonstrate complex inhibition patterns depending on both the nature of the substrate as well as the structure of the enzyme. For the wild type enzyme we observe that propidium exhibits mixed linear inhibition of catalysis for both ATC and TB and that the values derived for the competitive and the noncompetitive components are similar ranging between 1-2μM. For PNPA, on the other hand, a mixed nonlinear inhibition is observed. Similar phenomena of linear inhibition of ATC hydrolysis and nonlinear inhibition of uncharged substrate hydrolysis in the presence of propidium was reported previously (Berman and Leonard, 1990). In the W286A mutant the competitive inhibition constants are increased approximately 10 folds and, as expected, this increase does not depend on the nature of the tested substrate. On the other hand the inhibition constants and kinetic behavior of the ternary complexes (ESI, scheme 2) are substrate dependent (Table 3 and Fig. 3). Since ATC, TB and PNPA should generate a common acyl intermediate the differential effect of propidium should be related to interaction of inhibitor with the different enzyme substrate complexes.

Table 2: Edrophonium inhibition of hydrolysis of various substrates by HuAChE and selected mutants [a]

Substrate / HuAChE	K_i (μM) Edrophonium			
	ATC	TB	TPA	PNPA
WT [b]	0.3	0.7	0.24	0.4
W286A	0.7	0.6	0.30	0.6
Y337A	11.2	17.1	3.00	4.2
F338A	1.1	1.8	0.40	1.0
W86A	[>150] [c]	[>150] [c]	[>150] [c]	[>150] [c]

[a] Enzyme inhibition by edrophonium was determined as described in 'Methods'. Values represent mean of triplicate determinations, with standard deviations not exceeding 20%.

[b] Wild type recombinant HuAChE.

[c] Values in parenthesis refer to the highest concentration of edrophonium(150 μM) used, yet this concentration was still insufficient to cause inhibition of activity.

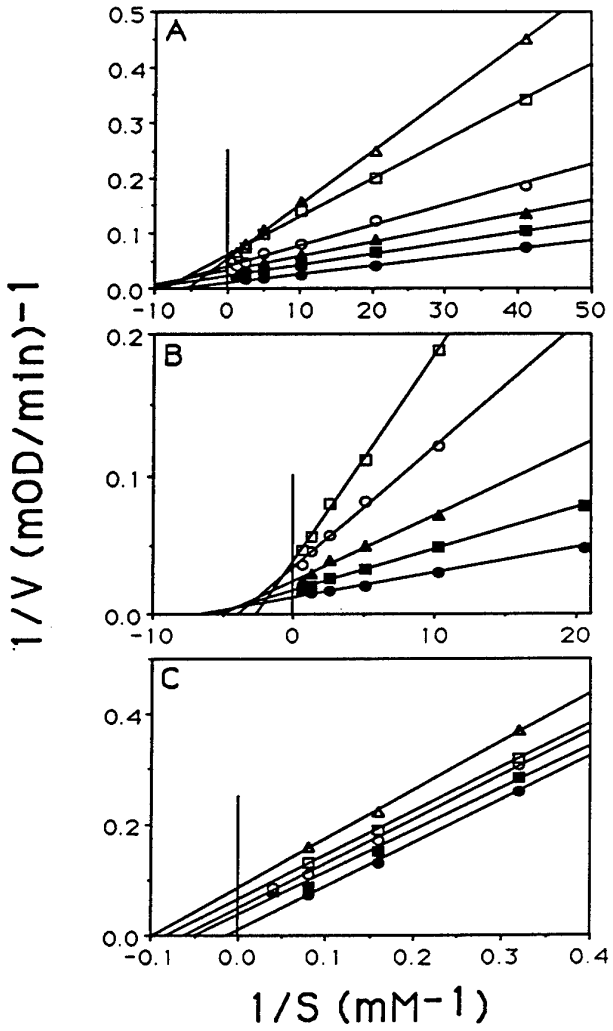

Fig 2. Double reciprocal plots of reaction velocity versus acetylthiocholine concentration in presence and absence of propidium. Panel A - Wild type enzyme (●) no inhibitor, (■) 0.75 μM, (▲) 1.5 μM, (O) 3.0 μM, (□) 6.0 μM and (Δ) 7.5 μM propidium. Panel B - W286A mutant (●) no inhibitor, (■) 7.5 μM, (▲) 20 μM, (O) 50 μM and (□) 100 μM propidium. Panel C - W86A mutant (●) no inhibitor, (■) 20 μM, (O) 30 μM, (□) 75 μM and (Δ) 100 μM propidium.

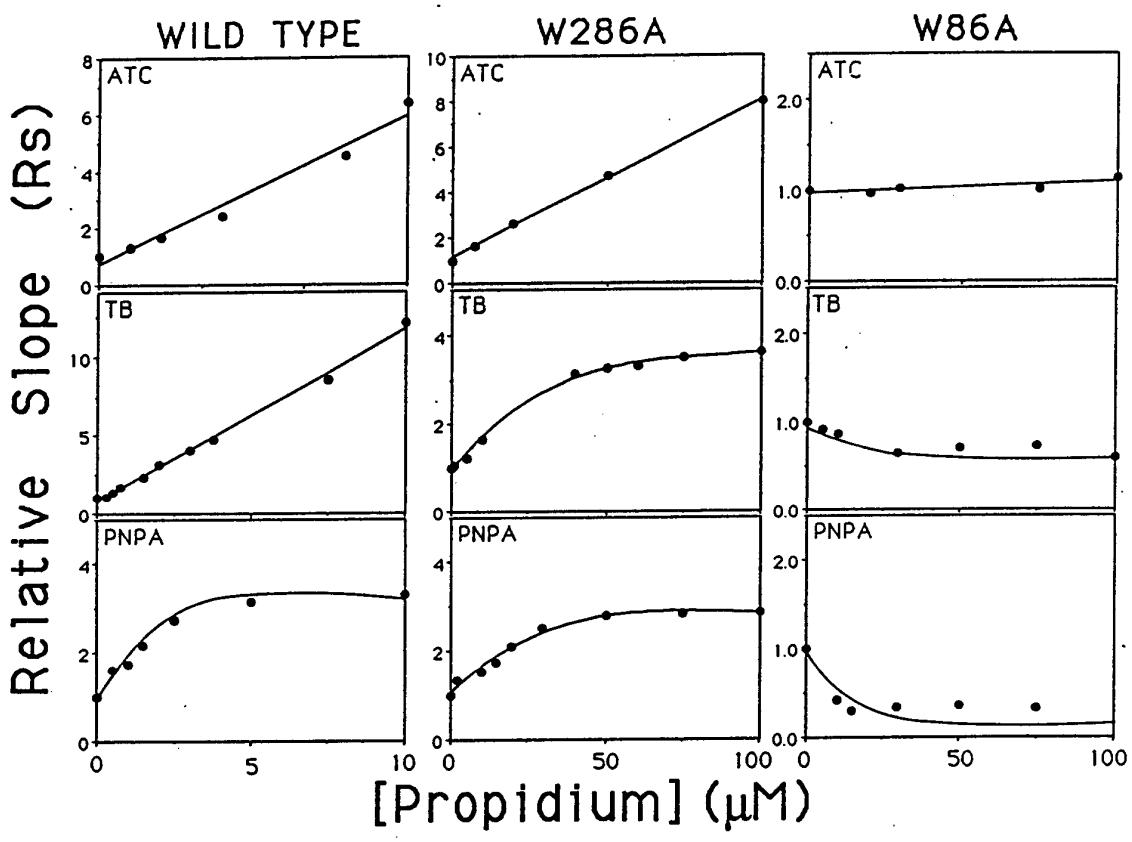

Fig 3. Compilation of replots of relative slopes (Rs values) versus concentration of propidium, for hydrolysis of ATC, TB and PNPA by the various mutants. Concentration of substrates used were 0.02-25 mM for ATC (see Fig. 2) and 0.1 - 1.0 mM for TB and PNPA. Computation of Rs values were as described in Methods

Table 3: Inhibition constants of propidium for hydrolysis of various substrates by HuAChE and selected mutants[a]

Substrate / HuAChE	ATC		TB		PNPA	
	Ki(μM)	Ksi(μM)	Ki(μM)	Ksi(μM)	Ki(μM)	Ksi(μM)
WT [b]	1.4	1.8	0.9	1.0	0.9	*[c]
W286A	14.3	28.3	12.3[c]	*[c]	12.4	*[c]
W86A	870.0	13.5	*[d]	*[d]	*[d]	*[d]

[a] Enzyme inhibition by propidium was determined as described in 'Methods'. Values represent mean of triplicate determinations, with standard deviations not exceeding 20%.
[b] Wild type recombinant HuAChE.
[c] Nonlinear inhibition pattern was observed (see Figure 3). The values of the competitive inhibition constant (Ki) were calculated from the slopes and intercepts of the double reciprocal plots of (Rs-1) versus inhibitor concentration, while Ksi values could not be extracted in these cases (see methods and text).
[d] For the substrates TB and PNPA kinetic behavior did not follow mixed linear or nonlinear inhibition pattern and at high inhibitor concentrations indication of acceleration was observed (see Fig. 3 and text).

The most striking observation is the inefficiency of propidium to inhibit catalysis in the W86A mutant for all the tested substrates. In the case of ATC hydrolysis, in the W86A mutant only 35% inhibition could be achieved at very high propidium concentrations (0.15mM) and plots of double reciprocals of rate versus substrate concentration (Fig 2C) manifest an almost pure uncompetitive inhibition pattern . Accordingly, a 700 fold increase in Ki and only 10 fold increase in Ksi value relative to the wild type is observed (Table 3). The above observations clearly demonstrate that mutation in position W86 reduces the ability of propidium to inhibit the mutant enzyme and that the residual inhibition proceeds through the ternary complex ESI (see scheme 2; Ki >>Ksi). In the cases of TB and PNPA hydrolysis by the W86A mutant, propidium is not only inefficient as inhibitor but actually accelerates the catalysis (Fig 3). Altogether, the propidium inhibition patterns obtained with the active center mutant W86A strongly suggest coupling between the peripheral anionic site at the exterior, and the W86 residue which is buried deeply within the protein.

Reactivity of HuAChE and Selected Mutants Towards Substrates Containing Different Acyl Moieties: Molecular modelling of HuAChE adducts with chiral methyl phosphonates (Barak *et al.*, 1992) and modelling of the BChE -BCh complex (Harel *et al.*, 1992a) showed that the two phenylalanine residues at position 295 and 297, which are replaced by leucine and valine respectively in butyrylcholinesterase (BChE), may prevent accommodation of large acyl moieties. Based on our modelling studies with HuAChE (see below), the F338 and Y337 residues may also take part in accommodation of the acyl moiety. Accordingly we studied the following AChE mutants: F295L, F295A, F297V, F297A, F295L/F297V, Y337F, Y337A and F338A. The substrates ATC, BTC, and PTC, which have a common X (choline) residue but differ in their R substituent (see Scheme 1 and Fig. 1), were selected for probing the effect of different acyl moieties on substrate specificity. Results from kinetic studies, summarized in Table 4, demonstrate that any of the substitutions of F295 by leucine or alanine and of F297 by valine or alanine resulted in a significant increase in k_{cat} for BTC relative to wild type (Fig. 4). The same substitutions hardly affected the k_{cat} for PTC but reduced to some extent the k_{cat} for ATC. These results clearly demonstrate the importance of both F295 and F297 in determining substrate specificity. In contrast to the effect of these

mutations on k_{cat}, their effect on Km differentiate between F295 and F297 mutations. HuAChE F295L and F295A mutants had lower Km for BTC than the wild type HuAChE or the F297 mutants (Table 4 and Fig. 4). Moreover Km values for ATC and PTC were somewhat higher for F297 mutant (relative to wild type). The double mutant F295L/F297V and the F295L mutant, had similar Km values for BTC, suggesting that residue 295 is the major contributor to the improved interaction of BTC with the mutein enzyme. We note that BChE has the L295/V297 configuration and the Km for butyrylthiocholine is similar to that of the HuAChE double mutant (F295L/F297V) (Table 4). Moreover, comparison of the Km values between the HuAChE F295A mutant and BChE, suggests that an engineered AChE mutant could be more specific for BTC than BChE. Recently the analogous double mutant in TcAChE (F*288*L/*290*V) was reported to have increased hydrolytic activity towards BTC (Harel *et al.*, 1992b).

Replacement of Y337 or F338 by alanine reduced the k_{cat} for ATC, PTC and BTC (Table 4). When the tyrosine at position 337 was replaced by another aromatic amino acid as in the Y337F mutant values similar to those of wild type were obtained. The results suggest that, the aromatic side chains, Y337 and F338, play some role in the stabilization of the acyl moiety during acylation or deacylation. The F338 mutant, unlike the Y337 mutant, appears to have an effect on the Km values with the substrates tested. Thus the F338 residue could be involved in stabilizing the acyl moiety of the substrate in the noncovalent enzyme-substrate complex. We note that F338 had similar effects on the X moiety of the substrate (see above and Table 1).

Interaction with Reversible and Irreversible Inhibitors : The inhibition of the 295 and 297 mutants by selective BChE and AChE inhibitors further supports the kinetic data suggesting the involvement of these residues in determining substrate specificity. Although iso-OMPA, a selective BChE inhibitor, is a slow irreversible inhibitor, we used the IC_{50} values as a crude indicator for relative inhibition. Accordingly, iso-OMPA IC_{50} values for the F295L, F295A, F297V, F297A mutants and for the double F295L/297V mutant are all lower by 5-60 folds than that for wild type AChE (Table 5). Interestingly, the specificity of the AChE F295A and F297A mutants towards the selective HuAChE reversible inhibitor BW284C51 is maintained and IC_{50} values do not vary by more than a factor of 2 relative to wild type AChE while being still three orders of magnitude higher than that for BChE . The

Table 4: Kinetic constants for hydrolysis of ATC, PTC and BTC by HuAChE, selected HuAChE mutants and HuBChE [a]

Substrate / HuAChE	Km (mM)			k_{cat} ($x10^{-5}$x min^{-1})			k_{cat}/Km ($x10^{-8}$)(M^{-1}xmin^{-1})		
	ATC	PTC	BTC	ATC	PTC	BTC	ATC	PTC	BTC
WT [b]	0.14	0.25	0.30	3.7	1.6	0.075	26.4	6.4	0.25
F295L	0.20	0.25	0.03	1.2	0.9	0.30	6.0	3.6	10.0
F295A	0.13	0.06	0.009	3.8	1.0	0.30	29.2	16.7	33.3
F297V	1.20	0.70	0.38	2.2	1.0	0.60	1.8	1.4	1.6
F297A	0.55	0.78	0.36	1.2	1.0	0.50	2.2	1.3	1.4
F295L/F297V	0.40	0.43	0.03	0.9	0.9	0.42	2.2	2.1	14.0
Y337F	0.20	0.15	0.11	3.7	1.4	0.10	18.5	9.3	0.9
Y337A	0.13	0.17	0.27	1.0	0.1	0.03	7.7	0.6	0.1
F338A	0.30	0.34	0.80	1.7	0.5	0.035	5.7	1.5	0.04
HuBChE [c]	0.035	0.055	0.05	0.5	1.0	1.10	14.3	18.2	22.0

[a] Values represent mean of triplicate determinations with standard deviations not exceeding 20%.
[b] Wild type recombinant HuAChE.
[c] Values for HuBChE were determined using purified human serum butyrylcholinesterase.

Table 5: Inhibition of HuAChE, selected HuAChE mutants and HuBChE by iso-OMPA, BW284C51, propidium and edrophonium [a]

Inhibitor / HuAChE	IC_{50} (μM)		K_i (μM)	
	iso-OMPA	BW284C51	Propidium	Edrophonium
WT [b]	150	0.008	1.6	0.30
F295L	5	0.036	1.2	0.43
F295A	30	0.0015	0.8	0.21
F297V	30	0.0047	3.7	1.00
F297A	12	0.0013	1.9	2.00
F295L/F297V	2.3	0.02	3.6	2.00
Y337F	15	0.008	1.3	0.43
Y337A	15	0.104	2.5	11.20
F338A	2250	0.024	1.4	1.10
HuBChE	35	62.0	3.2	53.6

[a] Inhibition by the various ligands was determined as described in 'Methods'.Values represent mean of triplicate determinations with standard deviation not exceeding 20%.
[b] Recombinant HuAChE wild type.

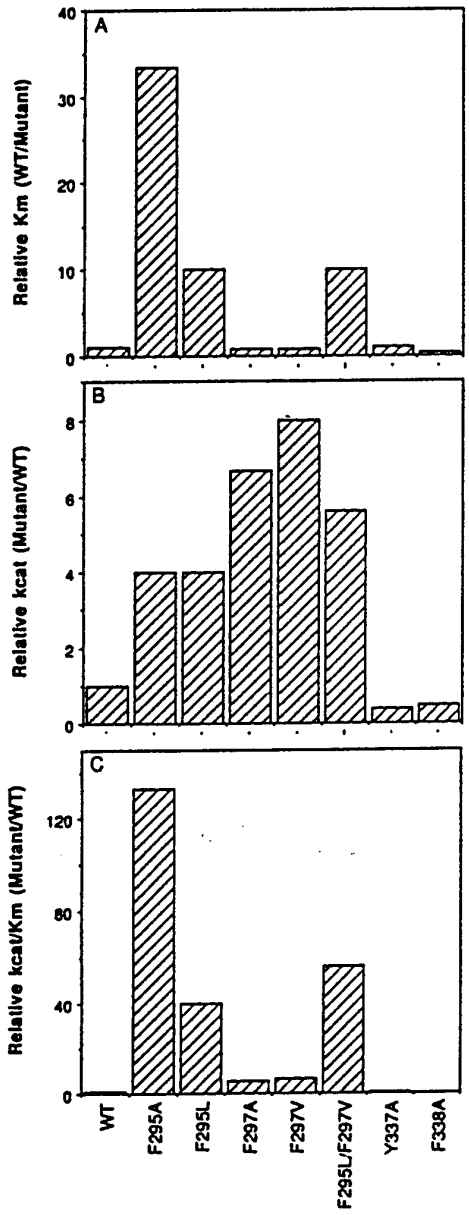

Fig. 4 The ratio of kinetic constants for butyrylthiocholine hydrolysis by HuAChE mutants and the wild type enzyme. Relative kinetic constants were calculated from values presented in Table 4.

most notable effect of mutation on susceptibility to BW284C51 results from replacement of Y337 by alanine but not by phenylalanine (Table 5; Shafferman *et al.*, 1992c). This could indicate stacking interaction between the aromatic residue at 337 with the aryl moiety of BW284C51.

Substitution of the HuAChE aromatic residues Y337, and F295/F297 by the corresponding residues of HuBChE (Y337A and F295L/F297V) increased the Ki values for inhibition of the mutated enzymes by edrophonium by a factor of 30 and 7 respectively, as compared to wild type HuAChE . This observation is in accordance with the overall 178-folds higher Ki for edrophonium in BChE than in AChE. Mutations at position 295 and 297 appear to have a small effect on susceptibility to propidium (Table 5).

Molecular Modelling of HuAChE, its Mutants and their Substrate Adducts :

Models of the HuAChE mutants and enzyme-substrate adducts were constructed by replacing the appropriate amino acid and ligand followed by zone refinement (see methods). Since, in all cases considered here, the mutants retained some of the original catalytic activity we assumed that the structure of the molecule and in particular the spatial architecture of the active site gorge was only locally perturbed (Bone and Agard, 1991). The initial model for docking ACh within the active site of HuAChE (Barak *et al.*, 1992), which is analogous to that reported for TcAChE - ACh adduct (Sussman *et al.*, 1991), included positioning of a tetrahedral carbon within bonding distance of Oγ - S203. The model places the quaternary ammonium group within an interaction distance from W86 and E202. The main stabilizing interaction is that of the acyl oxygen nested within the 'oxyanion hole' (hydrogen bonds to the amide nitrogens of G121; G122 and A204). Additional stabilization is conferred by the choline oxygen bound to Nε - H447 and the methyl group of the acyl moiety forming close contacts (hydrophobic interactions) with the aromatic rings of F295 and F297 (Fig. 5a). This basic model served as a template for modelling experiments of HuAChE - substrate adducts since the interactions involving the three oxygen substituents of the tetrahedral carbon are assumed to provide most of the stabilization energy. Such models reflect better the tetrahedral intermediate of the acylation reaction than the product of noncovalent association (e.g Michaelis complex) and therefore are more relevant to the molecular events influencing k_{cat} rather than those influencing Km.

Models of HuAChE-ATC adducts : The constructed model (Fig. 5a) closely resembles our basic HuAChE-ACh structure. The only noticeable difference is in the shorter distance (4.45Å vs. 4.05Å) of the quaternary ammonium nitrogen from the centroid of the indole ring of W86 due to the longer S-C bond compared to the O-C bond.

Model of HuAChE-PNPA adducts: For initial modelling the atomic positions of the tetrahedral carbon attached to Oγ - S203 and its substituents were retained as in the HuAChE - ACh model and then the dihedral angles around bonds C-O and O-$C_{aromatic}$, determining the orientation of the aryl moiety relative to the fixed tetrahedral carbon, were changed systematically. The most energetically probable orientation was achieved when the *p*-nitrophenyl ring was stacked against the phenyl moiety of F338 while in the latter the dihedral angle χ_2 (χ_1 and χ_2 denote dihedral angles for bonds C_α–C_β and C_β-C_γ, of amino acid side chains, respectively) changed from -77° to -101° (Fig. 5d). Further zone refinement of the model did not result in significant changes of the structure. The two interesting features of this model are first, the identification of F338 as an important structural element interacting with aryl acetates in the active site and second, the demonstration that the aryloxy moiety cannot assume the spatial orientation with respect to W86, that was postulated for choline esters (compare Fig. 5a and 5d). Indeed, our kinetic data show that while replacement of F338 by alanine reduces k_{cat} for PNPA, the replacement of W86 by alanine actually resulted in a small increase in k_{cat} for this substrate (Table 1). The edgewise interaction (Burley and Petsko, 1988) of the *p*-nitrophenyl ring with the π electrons of F337 in the final model was marginal, again in accordance with the minimal effect of the Y337A mutation on the PNPA kinetic parameters (Table 1).

Models of HuAChE-TB and HuAChE-TPA adducts: Adducts were constructed following a procedure similar to that described for HuAChE-ATC, but without the constrain of positioning the quaternary ammonium group. In both cases the conformational search, results in the trans-conformation for the alkylthio moiety. This conformation is different from the one found for the choline part of ATC adduct and suggests a different spatial orientation of the possible interaction of W86 with the alcohol portion of substrates like TB and TPA (Fig. 5b,c). Stabilization energies for these alkylthio residues originate mainly from hydrophobic interactions which are a consequence of the complementarity of surface areas between the ligand and the active site gorge. The observed kinetic differences (k_{cat}) between TB and TPA support this conclusion and the proposed models are in agreement with related correlations of

volume - activity for the alkyloxy moieties (Cohen *et al.*, 1985).

Optimization of the surface complementarity for the TB and TPA adducts included examination of the side chain flexibility of W86 since the indole ring could provide part of the active site 'gorge' surface in contact with the ligand. Surprisingly, the results indicated a relatively unrestrained movement of the indole moiety within a certain range of dihedral angles χ_1 and χ_2 for the adducts of uncharged substrates. Furthermore, and not less important, such motion could be observed also for the unoccupied enzyme. The torsional strain resulting from W86 side chain reorientation is counterbalanced by van der Waals interactions with elements of the active site gorge and with the ligands when present. The feasibility of such movement is evident particularly in the case of TPA adduct. In the latter the thiopropyl group is too short to interact with the indole moiety in its unmodified conformation unless W86 is allowed to rotate as described above (see Fig. 5c). Comparison of the extent of W86 side chain movement, for the adducts examined , indicates that in the TPA adduct, as in the unoccupied enzyme, such motion can occur over the χ_2 range 183° - 150° while $\chi_1 = 84°$ within 2.5 kcal/mole (the unmodified conformation is $\chi_2 = 183°$; $\chi_1 = 120°$). For TB and PNPA adducts this motion is restricted by the size of the ligand (χ_2 range 183° - 165°) while for ATC no such motion is possible. Indeed, the experimental data (k_{cat}) clearly demonstrate the involvement of W86 in stabilization of the transition state for acylation in the cases of TB and TPA (Table 1).

Modelling of adducts of PTC and BTC with HuAChE and mutants : The modelling of these adducts (Fig. 6) corroborates our previous observations regarding the steric interference for bulky substituents equivalent to the alkyl part of the acyl moiety (Barak *et al.*, 1992). Residues F338, F295, F297 and the main chain of G122 form a hydrophobic pocket the size of which allows for accommodation of a methyl group (Fig. 6a). To accommodate the ethyl group of the propionyl moiety a nearly eclipsed conformation of PTC has to be assumed. For the BTC adduct, the lowest energy conformation for the alkyl group within hydrophobic pocket indicates a less stable adduct than that for ATC and PTC (Fig. 6a). Most of the destabilization in this conformation comes from interactions with F297. Other orientations of the alkyl group, in the BTC adduct, are blocked by either F295 and F338 or by W236. Models of HuAChE(F297A) - BTC (Fig. 6b) and of HuAChE(F297V) - BTC (not shown) indicate that removal of the phenyl 297 group from the immediate vicinity of the propyl group removes

most of the interference. Indeed, replacement of F297 by either alanine or valine improves k_{cat} for BTC hydrolysis (Table 4, Fig. 4). One of the different alternative conformations examined for the HuAChE - BTC adduct was energetically unfavorable mainly due to strong interference from the phenyl portion of F295 (Fig. 6a). Modelling of BTC adducts with HuAChE mutated at the 295 position by alanine or leucine predicted that the alkyl group will assume an energetically probable conformation (Fig. 6c), as is indeed demonstrated by the increase in k_{cat} values for the two mutants F295A and F295L (Table 4). Although rigorous comparison of conformational energies for the different BTC adducts (of the F297A vs. the F295A mutant) could not be carried out by the methods employed, the relative stabilizations of the alkyl group in adducts with 295 and with 297 mutants appeared to be similar. Again, this conclusion from the models is supported by the observed similar k_{cat} values for the 295 and 297 mutants as well as for the double mutant F295L/F297V (Fig. 4, Table 4). Thus, modelling of BTC adducts with wild type HuAChE and mutants at positions 295 or 297 could predict the higher turnover numbers for the mutants. However one of the more intriguing results from our kinetic studies is the differential effect of mutation in position 295 and in position 297 on Km values. Yet we note that our model is based on a covalent adducts and therefore is not expected to predict the stabilities of Michaelis -Menten complexes.

DISCUSSION

The structure - function relationship underlying AChE substrate specificity was investigated by employing site directed mutagenesis, kinetic studies of the mutants towards substrates and inhibitors and molecular modelling. Each of these approaches can provide useful insights into the nature of enzymatic activity and each has been used to probe the catalytic activity of AChE. It is however the combination of these methods that is recently emerging as a most powerful tool for investigation of structure - property relationships in biological systems. We have recently applied this approach to the study of substrate inhibition in AChE (Shafferman *et al.*, 1992b). Here we describe the identification and the mode of action of some structural elements within the architecture of the AChE active center which determine specificity towards: a. the positive charge of the quaternary ammonium, b. the structure of the alcoholic part (X, see Scheme 1) and c. the structure of the acyl moiety.

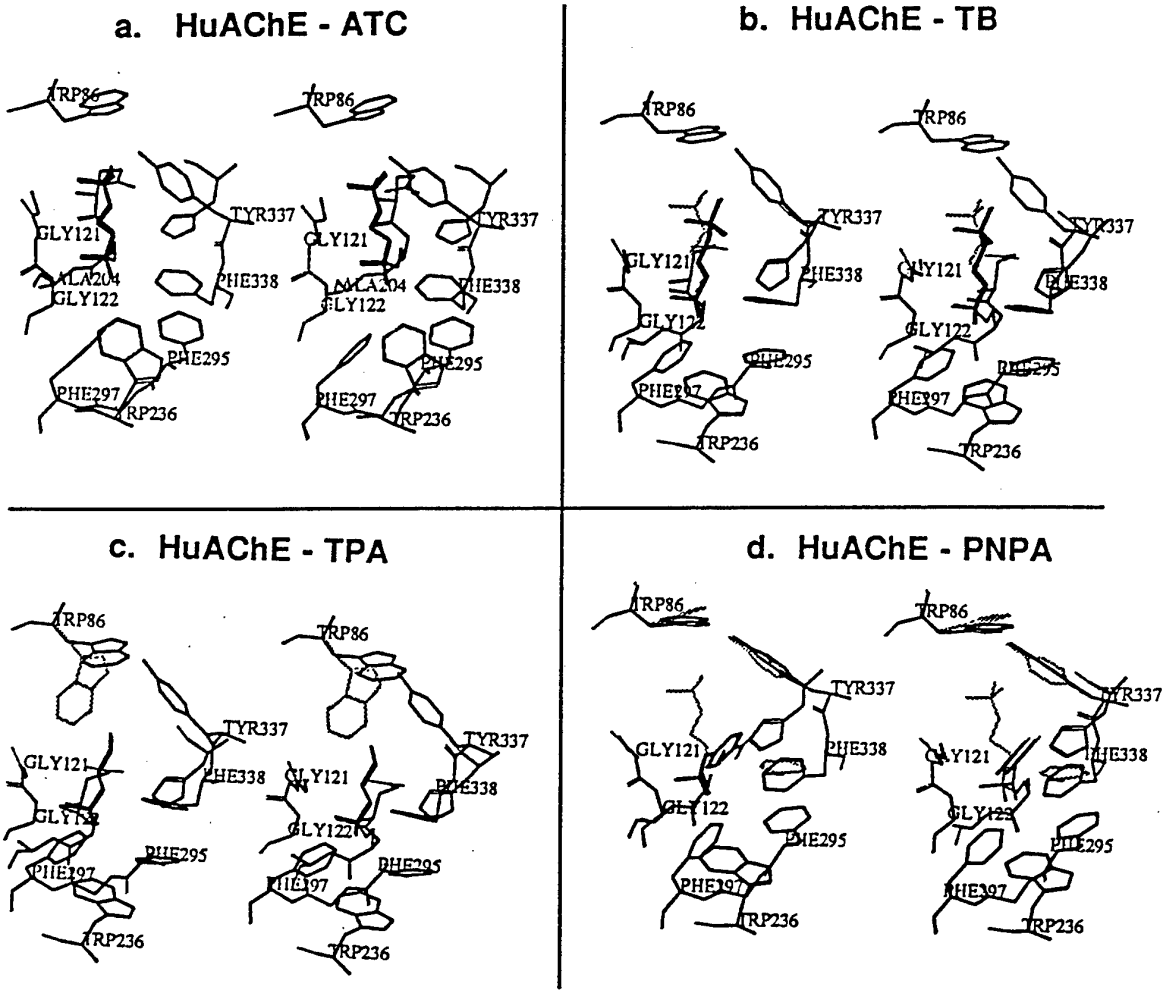
a. HuAChE - ATC
TRP86
TRP86
TYR337
GLY121
ALA204
GLY122
PHE338
PHE295
PHE297
TRP236
TYR337
GLY121
ALA204
GLY122
PHE338
PHE295
PHE297
TRP236
b. HuAChE - TB
TRP86
TRP86
TYR337
GLY121
PHE338
GLY122
PHE295
PHE297
TRP236
TYR337
GLY121
PHE338
GLY122
PHE295
PHE297
TRP236
c. HuAChE - TPA
TRP86
TRP86
TYR337
GLY121
PHE338
GLY122
PHE295
PHE297
TRP236
TYR337
GLY121
PHE338
GLY122
PHE295
PHE297
TRP236
d. HuAChE - PNPA
TRP86
TRP86
TYR337
GLY121
PHE338
GLY122
PHE295
PHE297
TRP236
TYR337
GLY121
PHE338
GLY122
PHE295
PHE297
TRP236

Fig. 5 Stereo view of adducts of HuAChE with charged and uncharged acetate-esters (Opposite page). Only the amino acids in the immediate vicinity of the ligand are displayed and hydrogen atoms are omitted for clarity. The ligand is marked by heavy line:

a. HuAChE-ATC adduct - Distances of the negatively charged oxygen from amide nitrogens of G121, G122 and A204 are 2.64Å, 2.60Å and 2.82Å respectively; distances of the terminal methyl from aromatic C_4 of F297 and from aromatic C_3 of F295 are 4.07Å and 3.65Å respectively. The above distances are similar for all adducts b. to d. Distances of the quaternary ammonium N-methyl carbons from the centroids of corresponding pyrol and phenyl parts of the indole moiety are 3.41Å and 3.37Å respectively;

b. HuAChE-TB adduct - Relative position of choline moiety is added for comparison (light line). Rotation around C-S bond places the three methyl carbon group in a hydrophobic environment created by aryl rings of Y337 and F338, the participation of W86 in this stabilization was also considered (see text).

c. HuAChE-TPA adduct - Conformation of the S-alkyl chain is similar to that observed for TB adduct; An alternative conformation of W86 side chain ($\chi_1 = 84^\circ$;$\chi_2 = 150^\circ$) is shown in light line.

d. HuAChE-PNPA adduct - Side chain positions of residues F337, F338 and W86 are shifted compared to ATC adduct (light lines). Relative position of choline moiety is added for comparison (light line). Position of W86 changed slightly during energy optimization.

a. HuAChE - BTC

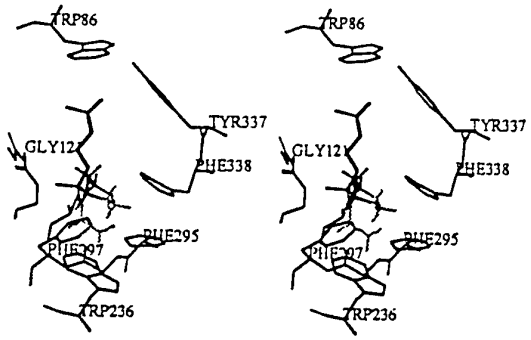

b. HuAChE(F297A) - BTC

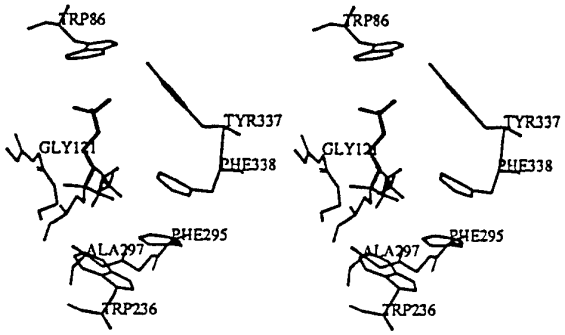

c. HuAChE(F295A) - BTC

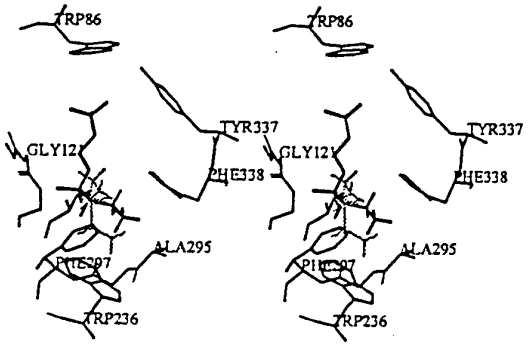

Fig. 6 Stereo views of BTC adducts with wild type, F295A and F297A mutants of HuAChE. Amino acids in the immediate vicinity of the ligand are displayed and hydrogen atoms are omitted; BTC is emphasized by heavy line. The preferred position of the propyl moiety of BTC is shown in heavy line. Few of the additional conformations considered are shown for comparison (light line). Similar conformation of the propyl chain are suggested for wild type and F297A mutant adducts while a different conformation is proposed for the F295A mutant adduct.

G121 Appears to Participate in the 'Oxyanion Hole': Residue Gly121 in HuAChE is analogous to Gly118 in TcAChE which has been suggested as a part of the binding subsite accommodating the carbonyl oxygen of the substrate (oxyanion hole, Sussman *et al.*, 1991). The replacement of Gly121 by alanine was therefore expected to severily impair the proper alignment of substrate in the active center, due to steric interference of the additional methyl group. Indeed, the resulting protein was devoid of any detectable catalytic activity, although its proper folding and secretion levels were not affected. This is evident from the efficient interaction of the Gly121Ala mutant with polyclonal antibodies (raised against native HuAChE) in the antigen capture ELISA (Shafferman *et al.*, 1992b). Such phenotype was also found for mutants of the HuAChE catalytic triad (Ser203; His447; Glu334), where replacements by alanine yielded nonfunctional HuAChE-like proteins.

W86 Constitutes the Classical 'Anionic ' Subsite : Based on the interaction of AChE with various types of positively charged compounds, the active center of AChE was suggested to contain a negatively charged anionic subsite (Nolte *et al.*, 1980). This hypothesis was criticized on the basis of correlations between AChE reactivity and the partial molal volume of substituent X (Scheme 1) for a series of charged and uncharged substrates (Hassan *et al.*, 1980). Accordingly, an alternative hypothesis was advanced which postulated a hydrophobic trimethyl binding site that accommodates the quaternary functionality of ACh as well as the X groups of uncharged substrates and inhibitors. Yet, by comparing the kinetic properties of the covalent adducts of AChE with isosteric charged and uncharged methyl phosphonates (Berman and Decker, 1986) it was concluded that the anionic and the hydrophobic subsites are not equivalent but constitute two partially overlapping regions.

The three dimensional models (Sussman *et al.*, 1991, Barak *et al.*, 1992) indicate that the only potential negative charge in the vicinity of the esteratic site is that of E202(E*199*) but this residue has been shown to affect the acylation - deacylation steps and not the noncovalent complex formation (Shafferman *et al.*, 1992b,c; Radic *et al.*, 1992). On the other hand results from labeling studies (Weise *et al.*, 1990), X - ray crystallography (Sussman *et al.*, 1991) and site directed mutagenesis studies (Shafferman *et al.*, 1992b) implicate W86 as the locus of interaction with the positively charged 'head group' of the substrate. The charge distribution in the indole ring is characterized by a partial negative charge in the π system (Schneider, 1991).

Such 'diffuse' negative pole might be better suited to interact with a tetraalkyl ammonium cation as suggested previously (Satow *et al.,* 1986; Dougherty and Stauffer, 1990).

The function of W86 in orienting and accommodating the charged part of the substrate is clearly demonstrated in the kinetic behavior of the W86A mutant. The dramatic 660 fold decrease in the value of Km for ATC in the W86A mutant as compared to the value of the wild type enzyme (Table 1), attests to the loss of stabilization of the enzyme - substrate complex. On the other hand k_{cat} for this mutant is less than five fold lower than that for the wild type indicating that other functions of the active center are relatively unaffected. The fact that for the W86A mutant the Km values of all the uncharged substrates, including TB the isosteric substrate of ATC, are comparable to those of the wild type demonstrate that W86 does not participate in accommodation of uncharged X groups in the *noncovalent* complexes. It also shows that the integrity of the hydrophobic binding sites, occupied by the uncharged substrates in the noncovalent complexes, is not affected by the replacement of W86. In the above discussion it is assumed that Km for the W86A mutant reflects the affinity of the enzyme towards the substrate which in turn implies that $k_{-1}>k_2$ (see scheme 1). Alternatively, if $k_{-1}<k_2$ then the effect in W86A on Km should be related to a decrease in k_1 (or the apparent bimolecular rate constant k_{cat}/Km). However, the latter is not compatible with the apparent bimolecular rate constant for reaction of the uncharged substrate TB with W86A mutant and the fact that the same constant for the isosteric ATC in this mutant is over 50 fold lower. Comparison of Km values for ATC and TB, in the wild type and the W86A mutant (Table 1), underscores the fact that although the site accommodating TB remains unchanged it does not bind ATC. Thus, at the stage of noncovalent complex formation the charged and the uncharged substrates bind to two different molecular environments.

The role of W86 as the main interaction locus for orienting the positive charge in the active center is further demonstrated by inhibition experiments with edrophonium. The low affinity of the W86A mutant for edrophonium correlates well with the low affinity towards ATC. A recently published X - ray structure of TcAChE - edrophonium complex shows that the trialkyl- ammonium moiety is positioned within interaction distance from the indole plane of the TcAChE W84 (Sussman *et al.,* 1992). The pronounced effects on Km for ATC and on K_i for edrophonium, of the W86A mutation (Tables 1,2) may indicate that the region for the noncovalent interaction for the two molecules is similar, and operates through cation-π interaction (McCury *et al*. 1992).

Amino Acids W86, Y337 and F338 are Elements of the Hydrophobic Subsite for the Covalent Adduct in the Active Center: Mutation of W86 resulted in a decrease of k_{cat} for hydrolysis of ATC, TB and TPA but not of PNPA (Table 1). This effect of W86 replacement on the acylation rates should depend upon the nature of X group (Fig. 1) since all four substrates are acetates. For ATC, TB and TPA the effect of the mutation on k_{cat} is comparable (4-8 fold), indicating a participation of W86 in stabilization of the corresponding transition intermediates for the acylation reactions. The manner in which W86 can interact with uncharged substrates was suggested by the modelling experiments. The feasibility of W86 side chain rotation, in the adducts of uncharged substrates, provides a mechanism for the adjustment of its distance from the group X as is best demonstrated by the movement of the W86 side chain in the TPA adduct (Fig. 5c). The fact that replacement of W86 by alanine did not affect k_{cat} for PNPA may be explained by the different orientation of residue X (*p*-nitrophenyl) through stacking interaction with the aromatic residue F338 (Fig. 5d). This conclusion is supported by the marked effect of F338A mutation on the value of k_{cat} for PNPA. The significance of the conformational flexibility of W86 aromatic side chain will be discussed further in the context of the crosstalk between the peripheral anionic site and the active center.

Molecular modelling indicates that, besides W86, residues Y337 and F338 can also interact with group X in the covalent adduct. However, the change of the k_{cat} values upon substitution of Y337 by alanine, is much less significant than that resulting from a similar substitution of F338. This discrepancy between the kinetic data and the prediction of the model, could suggest that the positioning of the aryl moiety of Y337 in the model needs further refinement. In this context it is relevant to mention that conformational flexibility of Y337 has been proposed and demonstrated before (Sussman *et al.*, 1992, Shafferman *et al.*, 1992b). Kinetic data for the F338A mutant are in good agreement with the prediction of the model as mentioned above regarding the PNPA adduct (Fig. 5d). Replacement of F338 by alanine affects the stability of the TB adduct to a greater extent than that of the isosteric ATC, which also is in good agreement with the different conformations of the two X moieties in the model (compare Fig. 5a to Fig. 5b). All these observations support the notion that the hydrophobic subsite is distinct from the anionic subsite. This conclusion helps to clarify the ambiguity in the literature regarding the structure and function of these two subsites and supports previous

interpretation of kinetic data suggesting the nonequivalence of the two subsites (Berman and Decker, 1986).

In summary, the hydrophobic interactions in the *covalent* adducts appear to be different from those in the *noncovalent* complexes. This conclusion is supported by the fact that mutations in HuAChE at positions 338 and 86 have marginal effects on Km but a substantial effect on k_{cat} with all the three uncharged substrates TB, TPA and PNPA . Furthermore the results indicate that for uncharged substrates the noncovalent adducts are formed in a different hydrophobic environment from the one referred to as the hydrophobic subsite of covalent adduct (tetrahedral intermediate) in the active center.

Residues F295 and F297 Confer Specificity for the Acyl Moiety : Molecular modelling of the adducts of ATC, PTC and BTC with HuAChE and the relevant mutants (Fig. 6) predict that replacement of the aromatic moieties in either the 295 or the 297 position removes most of the steric strain imposed upon the propyl group in the HuAChE-BTC adduct. The increase in values of k_{cat} for BTC in the F295 and F297 mutants as well as in the F295/F297 mutant (Table 4, Fig. 4) supports this conclusion. The prediction based on the model was also tested by examination of the relative stabilization of PTC adducts. In this case, mutations in positions 295,297 were not expected to affect the stability of the enzyme - PTC adduct, as was indeed found from the corresponding values of k_{cat} (Table 4). The model predicts further that due to hydrophobic interactions the stabilization of the methyl group of ATC is optimal in the wild type. Indeed, replacement of either one of the residues F295 or F297 results in a decrease of the k_{cat} value for ATC. The value for ATC in the double mutant F295L/F297V is close to that in BChE indicating that the difference in the ATC k_{cat} values for AChE and BChE is due to the loss of stabilization of the methyl group. The prediction concerning the size of the methyl binding pocket can be extended also to suggest that replacement of F297 by a bulkier residue would lower the reactivity towards ACh. Indeed this appears to be valid, since replacement of F368 in *Drosophila melanogaster* AChE (a position analogous to 297 in HuAChE) by tyrosine lowers the reactivity towards ACh and increases the resistance to organophosphorous inhibitors (Fournier *et al.,* 1992). A study, analyzing amino acid residues controlling mouse AChE and BChE specificity was published (Vellom *et al.*, 1993) which are in good agreement with the results presented above regarding the role of F295 and F297 in determining acyl pocket selectivity. The influence of residues F295 and F297 on

ligand selectivity was also demonstrated for the BChE - specific organophosphorous inhibitor iso-OMPA in the corresponding mutants. In the case of BW284C51, a selective inhibitor for AChE, replacement of either F295 or F297 indicates that the pronounced selectivity of BW284C51 towards AChE does not depend on these residues.

A surprising observation was the differential effect of mutation in positions 295 and 297 on the values of Km for the various substrates (Table 4). This effect becomes more pronounced as the size of the acyl moiety increases from ATC to BTC. The fact that no such difference was observed in the k_{cat} values could be interpreted as a difference in the stabilization of the acyl moiety in the *noncovalent* complex as compared to that in the *covalent* adduct. This may be due to the difference of the planar versus the tetrahedral carbon configurations in the two states. The enhanced affinity for BTC in the F295A and F295L mutants provides the major contribution to the increase in the values of the apparent bimolecular rate constants (Table 4 and Fig. 4). For the F295A mutant this value is 130 fold higher than the value for wild type AChE and 1.5 times higher than that of BChE. In fact comparison of the apparent bimolecular rate constants for F295A, F295L, F297A, F297V and F295L/F297V mutants with the corresponding value for BChE shows that the main difference in the catalytic efficiency between AChE and BChE towards BCh can be traced to a difference in the side chain of a single residue - F295.

Although residue F338 appears to participate in the stabilization of both the noncovalent and the covalent complexes (Table 4), the effects of its replacement is similar for ATC, PTC and BTC . Therefore it appears that this residue does not contribute to specificity for the alkyl group of the acyl moiety (we note that in HuBChE the analogous position to F338 of HuAChE is also a phenylalanine).

Plasticity of the Active Center and Substrate Specificity: Conformational changes in the active center of AChE induced by inhibitors or even by the natural substrate have been invoked in the past to account for the complex kinetic behavior of the enzyme (Quinn, 1987). It was suggested that, at least for the neutral substrates, an induced - fit conformation change of AChE occurs after substrate binding but before chemical catalysis (Rosenberry, 1975). In addition, allosteric regulation of AChE activity by ligand binding to an anionic site(s) physically removed from the active site was suggested (Changeux, 1966). Allosteric changes were shown experimentally by measurements of emission maxima shifts for fluorescent alkyl

phosphonates attached to the active site serine (Berman *et al.*, 1981). Thus, the concept that AChE possesses conformational flexibility of catalytic significance is not new, however demonstration of this plasticity through the individual motions of participating residues is only beginning to emerge.

In a previous study we have proposed that substrate inhibition operates via a sequence of changes leading to the motion of residue Y337, induced by substrate binding to the peripheral anionic site (Shafferman *et al.*, 1992b). Residue Y337, together with residues W86, F338 and F297, is also involved in stabilizing the complex of HuAChE with the inhibitors edrophonium and BW284C51 (Tables 2 and unpublished results). Stabilization of these interactions with inhibitors by Y337 is probably achieved through stacking interactions of the aromatic moieties of the inhibitors. Residue W86 should function in accommodating the charged tetra-alkylammonium group of edrophonium and BW284C51 (Table 2 and unpublished results) in a way similar to that in the HuAChE - ATC adduct. To account for both the interaction of the cationic head with W86 and the stacking interaction with Y337, our model suggests relative motions of the two residues out of their original position in the unoccupied enzyme (Fig. 7). In fact, for TcAChE- edrophonium complex in the solid state reorientation of F330 (analogous to HuAChE Y337) was observed (Sussman *et. al.*, 1992).

As mentioned in the preceding sections, movements of aromatic residues in the active site center were also implicated in stabilization of covalent enzyme - substrate adducts and in determination of substrate specificity. The contribution of W86 to the stabilization of the covalent adducts for TB and TPA probably involves motion of the side chain of this residue. The feasibility of such motion was shown by molecular modelling for the adducts with uncharged substrates (Fig. 5c) as well as for the unoccupied enzyme (Fig. 7). Motion of residue F338 was suggested as a part of the conformational adjustment in the active center, for accommodation of the aryl moiety of PNPA (Fig. 5d). Accommodation of TPA involves slight motions of F337 and F338 apart from that of W86. Movement of F297 was suggested by molecular modelling of the HuAChE - BTC adduct (Fig. 6a). Thus, the plasticity of the active site center , exemplified here through the motions of aromatic residues W86, F297, Y337, and F338 is an intrinsic element of the HuAChE active center dynamics, and is directly involved in determining substrate specificity for both the noncovalent and for the covalent adducts.

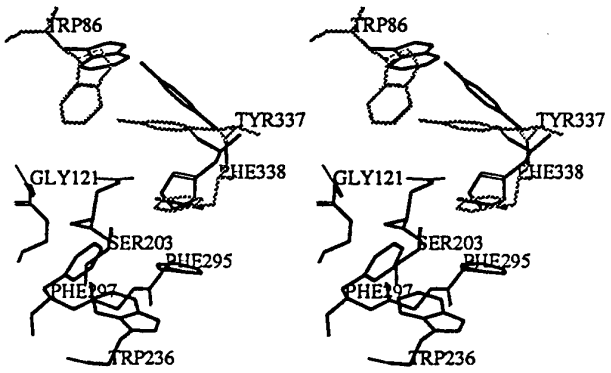

Fig. 7 Stereo view of probable conformational changes for selected aromatic residues in HuAChE active center. The span of motion between two conformational states (marked by heavy and light lines) depicts the range of possible movement for residues W86, Y337 and F338 depending on the nature of the substrate or inhibitor accommodated in the active center or on the binding of ligands to the peripheral anionic site (see text for details).

A Possible "Cross-Talk" Between the Peripheral Anionic Site and the Active Center W86: The conformational flexibility of W86 side chain described above may also be related to the observed resistance of the W86A mutant to inhibition by the peripheral anionic site ligand propidium. Compared to the wild type enzyme the hydrolysis of ATC by W86A mutant is almost completely refractive to inhibition by propidium. Moreover, for hydrolysis of TB and PNPA we find that the W86A mutant is not only resistant to inhibition but that hydrolysis is actually accelerated by propidium. Certain active center ligands were reported (Barnett and Rosenberry, 1977) to accelerate catalysis but to our knowledge this is the first report of acceleration of hydrolysis of AChE substrates by a peripheral anionic site ligand. These observations are quite surprising in view of the location of W86A deep inside in the active site gorge, 15Å away from the surface of the enzyme. To account for this and other results presented here we propose a functional cross-talk between W86 and residue W286 which constitutes part of the peripheral anionic site (Shafferman et. al. 1992b,c and Table 3).

In this cross-talk between W286 and W86 we assume that the conformational state of W86 depends on the interaction of ligands with peripheral anionic site . In view of the architecture of the active site gorge this inhibitor induced conformational state should effect differently the various substrates. Thus PNPA which, as discussed above, has a minimal interaction with W86 in the wild type enzyme should be less efficiently inhibited by propidium and a nonlinear inhibition pattern is expected as is indeed the case (Fig 3). Also consistent with this idea is the observation that inhibition of TB hydrolysis becomes nonlinear in both W86A and W286A mutants while it is linear in the wild type enzyme. In these cases there is no efficient coupling between W286 and W86, and the TB ternary complexes may proceed to the acyl enzyme, in spite of the presence of propidium. From the kinetic behavior of the various mutants with ATC, TB and PNPA in the presence of propidium, we may therefore conclude that a functional cross-talk operates whereby the differential state of occupation of the peripheral anionic site induces distinct conformations of W86 in the active center. This conclusion is also consistent with spectroscopic studies by Berman *et al.*, (1981), and Berman and Nowak (1992) that demonstrated that occupation of the peripheral anionic site affects the conformation of the active center (see also Sections III, IV and V).

In summary the dissection of the HuAChE active center by site directed mutagenesis begins to unravel a complex array of interactions that modulate the activity of the enzyme. We have

identified several aromatic amino acids that determine substrate specificity for binding of the alcoholic and the acyl parts in the active center and manifested their potential involvement in the dynamic nature of the catalysis. The built-in flexibility of the aromatic side chains in the active center can be one of the major elements in the catalytic efficiency of AChE. We have previously suggested (Shafferman *et al.*, 1992b) that substrate inhibition is modulated by cross-talk between the periphery and the active center through D74 and Y341 as well as other aromatic residues along the active site gorge terminating in Y337. Another manifestation of the cross-talk between the periphery and the active center, suggested here , terminates in W86 and again affects the activity of the enzyme. The sensitivity of the residues on the surface and the plasticity of the active center are probably the result of evolutionary design aimed to confer optimal catalytic activity under a wide variety of conditions that are characteristic for the operation of AChE in the synaptic cleft.

III. Identification of Residues Constituting the Peripheral Anionic Subsite in HuAChE.

INTRODUCTION

Acetylcholinesterase (AChE) exhibits a remarkable capacity to bind structurally diverse cationic ligands. Some of these ligands bind at the active center while others associate with a peripheral anionic site (PAS), remote from the active center (for reviews see Hucho *et al.*, 1991; Massoulie *et al.*, 1993). Allosteric modulation of AChE catalytic activity, through binding to the PAS, was first suggested by Changeux (1966) and further substantiated by numerous studies: Roufogalis and Quist (1972), Rosenberry and Bernhard (1972), Taylor and Lappi (1975) and Berman *et al.*, (1981). While the mechanism for such modulation is yet unknown, the PAS is considered to be the target for the dramatic effects exerted, on AChE catalytic activity, by various ligands, metal cations and most notably high concentrations of substrate. The resolution of the enzyme structure, by x - ray crystallography (Sussman *et al.*, 1991), did not yield any clues as to the mechanism of the allosteric effect but rather rendered it more enigmatic by placing the active site within a narrow gorge about 20Å away from the periphery.

The functional significance of PAS is a controversial issue. It was implicated in the catalytic pathway of acetylcholine (ACh) hydrolysis (Haas *et al.*, 1992), in ionic strength monitoring (Berman and Nowak, 1992) and in substrate inhibition (Radic *et al.*, 1991). A decrease in affinity for a selective PAS ligand (propidium) and a concomitant loss of substrate inhibition, were observed for certain human AChE mutants (Shafferman *et al.*, 1992b,c).

Although PAS ligands, which include gallamine, d-tubocurarine, decamethonium and propidium, bind in a mutually exclusive manner, their modes of inhibition of catalysis are not equivalent and appear to depend upon the structure of the ligand (Roufogalis and Quist, 1972; Rosenberry, 1975). Determination of the structural parameters affecting ligand-affinity for the PAS can have important implications for the design of anti - AChE drugs. A number of such drugs are under clinical trials (Giacobini *et al.*, 1988) while additional AChE inhibitors are investigated as a possible treatment for Alzheimer's disease (Han *et al.*, 1992).

Site directed labelling (Weise *et al.*, 1990) and mutagenesis studies (Shafferman *et al.*,

1992b,c; Ordentlich *et al.*, 1993a) allow for an approximate localization of PAS at or near the rim of the active center 'gorge'. Such topography is compatible with the suggestion that bisquaternary ligands, typified by decamethonium, bind to the enzyme by bridging the active and the peripheral sites (Krupka, 1966).

For further characterization of the residues participating in binding of PAS ligands, we employ here site directed mutagenesis, molecular modeling techniques and fluorescence binding studies, together with examination of the kinetic behavior of the muteins toward the various PAS inhibitors. This multidisciplinary approach generates information pertaining to the topography of the complexes of HuAChE with the classical PAS ligands propidium, decamethonium, the highly specific AChE inhibitor BW284C51 and the active center ligands edrophonium (Fig. 1) and hexamethonium. In this study, we identify some of the major structural elements of the PAS array, we demonstrate that alternative elements participate in interaction with various ligands and provide further insight into the "cross-talk" (Shafferman *et al.*,1992b,c; Ordentlich *et al.*, 1993a) between PAS and the active center .

METHODS

Mutagenesis of Recombinant HuAChE and Construction of Expression Vectors- Mutagenesis of AChE was performed by DNA cassette replacement into a series of HuAChE sequence variants which conserve the wild type coding specificity (Soreq *et al.*, 1990), but carry new unique restriction sites (Velan *et al.*,1991a; Kronman *et al.*, 1992; Shafferman *et al.*, 1992a). Generation of mutants D74N(*Asp-72*), W86A(*Trp-84*), W286A(*Trp-279*), F295A(*Phe-288*), F297A(*Phe-290*) Y337A, Y337F(*Phe-330*), F338A(*Phe-331*) and Y341A(*Tyr-334*) was described previously (Shafferman *et al.*, 1992a,b; Ordentlich *et al.* 1993a). Substitution of residues Tyr-72(*Tyr-70*) and Tyr-124(*Tyr-121*) was carried out by replacement of the *AccI-NruI* and the *NruI-NarI* DNA fragments of the AChE-w4 variant (Shafferman *et al.*, 1992a) with synthetic DNA duplexes, respectively. Likewise substitution of Glu-285(*Glu-278*) was carried out by replacement of the *MluI-PmlI* DNA fragment of the HuAChE-w7 variant with a synthetic DNA duplex. In the synthetic DNA-duplexes the TAT and TAC codons of Tyr-72 and Tyr-124 respectively, as well as the

GAA codon of Glu-285, were all changed to the GCC-Ala codon. Multiple site mutants were generated by using either synthetic DNA duplexes (E285A/W286A) or by relying on previously generated single mutants, using the unique restriction sites: *BstEII*, *Bsu36I* and *NruI* in the appropriate AChE cDNA variants. All the synthetic DNA oligodeoxynucleotides were prepared using the automatic Applied Biosystems DNA synthesizer. The sequences of all new clones were verified by the dideoxy sequencing method (USB sequenase kit). The rHuAChE cDNA mutants were expressed in tripartite vectors which allows expression of the *cat* reporter gene and the *neo* selection marker (Kronman *et al.*, 1992, Shafferman *et al.*, 1992a).

Transient Transfection, Preparation and Quantitation of AChE and its Mutants- Human embryonal 293 cells were transfected with various purified plasmids using the calcium phosphate method. Transient transfection was carried out as described previously (Shafferman *et al.*, 1992 a,b) and stably transfected colony-pools (Velan *et al.*, 1991b) were generated by G418 selection. Efficiency of transfection was monitored and normalized by levels of co-expressed CAT (chloramphenicol acetyl transferase) activity (Kronman *et al.*, 1992). The various AChE polypeptides secreted into the medium were quantified by activity (see below) and by AChE-protein determination relying on specific enzyme linked immunosorbent assays (ELISA) (Shafferman *et al.*, 1992a). For fluorescence studies which required purified wild type HuAChE and the W286A mutants, we generated a stable 293 clone cell line expressing high levels of HuAChE W286A as described previously for the wild type recombinant HuAChE (Kronman *et al.* 1992). Crude preparations of HuAChE and of the W286A mutant polypeptide (~20mg) were collected from several liters of supernatant of cells propagated on multitrays (Lazar *et al.*, 1994). The wild type and the mutant enzymes were purified as described previously (Kronman *et al.*, 1992) except that for the W286A mutant two cycles of purifications on the procainamide affinity chromatography were required and a low ionic strength elution buffer (1mM sodium phosphate pH 8.0) was used.

Substrates and Inhibitors- All kinetic studies reported here were carried out with acetylthiocholine iodide (ATC) (Sigma) as substrate. The inhibitors: 3,8 diamino-5-(3'-trimethylammonium)propyl-6-phenyl phenanthridinium diiodide (propidium), ethyl(m-

phenyl)-pentane-3-one (BW284C51) (Fig. 1), 1,10-bis(trimethylammonium) decane (decamethonium) and 1,6-bis(trimethyl-ammonium) hexane (hexamethonium) were all purchased from Sigma.

Determination of AChE Activity and Analysis of Kinetic Data- AChE activity with ATC was assayed according to Ellman *et al.,* (1961). Standard assays were performed in the presence of 0.1 mg/ml BSA, 0.3mM DTNB (5,5'-dithiobis(2-nitrobenzoic acid)) 5mM or 50mM sodium-phosphate buffer pH-8.0 and varying substrate (ATC) concentrations. The assays were carried out at 27°C and monitored by a Thermomax microplate reader (Molecular Devices). Michaelis-Menten constant (Km) and the apparent first order rate constant- k_{cat} values ,were determined as described before (Shafferman *et al.,* 1992a,b). Kinetic data from inhibition studies were analyzed according to a combination of the kinetic treatment developed by Barnet and Rosenberry (1977) , Berman and Leonard (1990) and as described recently by Ordentlich *et al.,* (1993). This analysis yielded values for Ki and Ksi, the competitive and noncompetitive inhibition constants respectively, for each of the HuAChE molecules with the different ligands tested. Since the present study is mainly involved with the enzyme ligand complexes, only values of the competitive inhibition component are displayed.

Structure Analysis and Molecular Graphics- Building and analysis of the three dimensional models was performed on a Silicon Graphics workstation IRIS 70/GT using SYBYL modeling software (Tripos Inc.). Construction of models for the HuAChE adduct and the enzyme-inhibitor complexes was based upon the model structure of the enzyme obtained by comparative modeling (Barak *et al.*, 1992) based on the x-ray structure of TcAChE (Sussman *et al.*, 1991). Such modelling is feasible since the homology between the amino acid sequences of the two enzymes is 74% and the degree of conservation in the 34 amino acids, comprising the active site gorge, is even higher (97% homology, 85% identity, see Cygler *et al.,* 1993). For enzyme-inhibitor complexes, the initial models were constructed by manual docking of the ligand into the active site gorge using the following guidelines:

a. The cationic head of the active center ligands is accommodated by the anionic subsite - Trp-86 (Ordentlich *et al.*, 1993a). b. The PAS includes residue Trp-286 (Weise *et al.*, 1990; Shafferman *et al.*, 1992b,c). c. The alkyl portions of decamethonium and hexamethonium are oriented along the walls of the gorge so that they can be accommodated by the free as well as

the phosphonylated enzyme (Berman and Decker, 1986). The resulting structures were optimized by molecular mechanics using the MAXMIN force field (and AMBER charge parameters for the enzyme) and zone refined by the ANNEAL procedure (both included in SYBYL). Zone refinement included 35 amino acids within the active site gorge and in close vicinity. Final structures of HuAChE-inhibitor complexes were derived by iterative refinement based on results from inhibition studies of various mutants with the respective ligands.

RESULTS and DISCUSSION

Selection of Inhibitors and Mutants : To evaluate the effects of structural modifications of the enzyme on ligand binding, several types of reversible inhibitors were used. Propidium was included as an exclusive PAS ligand (Taylor and Lappi, 1975). The bisquaternary ligands decamethonium and BW284C51, that span the distance between the active center and PAS (Krupka ,1966; Hodge *et al.*, 1992), were used to map their interactions with residues along the active center ' gorge' . Hexamethonium which is an active center bisquaternary ligand, too short to reach the PAS (Lullmann *et al.*, 1971), was included since its alkyl chain is expected to be subject to some of the interactions of the alkyl moiety of decamethonium. For comparison we have also included the cationic active center ligand edrophonium.

Recently we have characterized by mutagenesis and kinetic studies , the binding sites of the active center and proposed a structure for the tetrahedral intermediate of ACh-HuAChE in which the quaternary ammonium group is accommodated by interaction with Trp-86 (Ordentlich *et al.*, 1993a) . This structure served as a starting point for the construction of preliminary models for the HuAChE-inhibitor complexes (see methods). From these preliminary models it appeared that the cationic moiety of the various PAS ligands could be involved in interactions with residues Tyr-72, Asp-74, Tyr-124, Trp-286 and Tyr-341, near the rim of the gorge . Replacement of residues Trp-286 , Asp-74 and Tyr-341 were shown recently to affect the IC_{50} values of PAS ligands towards the corresponding HuAChE mutants (Shafferman *et al.*, 1992b,c). The aromatic rings of residues Tyr-72 and Tyr-124 flank the indole portion of Trp-286 and can interact with charged groups juxtaposed against this moiety. Glu-285, a highly conserved amino acid in cholinesterases is the only negatively charged

residue in the PAS peptide identified by Weise *et al.*, 1990 and therefore could be a potential component of the PAS array. To examine possible synergistic effects between the various putative PAS residues, we generated some double and triple mutants of residues at positions 72, 124, 285, and 286. Analysis of HuAChE mutants, of amino acids located at the periphery, was complemented by analysis of mutants at residues: Trp-86, Phe-295, Phe-297, Tyr-337 and Phe-338 shown previously (Shafferman *et al.*, 1992b,c; Ordentlich *et al.*, 1993a) to participate in active center interactions.

Kinetic Study of the Catalytic Activity and Inhibition of HuAChE Mutants :

Catalytic activity of the mutants: The Michaelis-Menten constants (Km), apparent catalytic first order rate constants (k_{cat}) and apparent bimolecular rate constants ($k_{app}=k_{cat}/Km$) for all the mutants used in this study are listed in Table 6. For single site mutants, the most significant changes in the kinetic parameters relative to the wild type enzyme, were observed for mutations at residues Trp-86, Phe-297 and Asp-74 (Table 6). Trp-86 and Phe-297 were recently shown to be constituents of the anionic subsite and part of the acyl pocket, respectively (Ordentlich *et al.*, 1993a). Asp-74 appears to be the only residue, located at the rim of the 'gorge', having a substantial effect on catalytic properties. Mutation of Asp-74 resulted in a 9-fold decrease in k_{app} relative to the wild type enzyme (Table 6). Less pronounced but yet significant effect on k_{app} was observed for substitution of Tyr-341. Single as well as multiple replacements of the aromatic amino acids Tyr-72, Tyr-124 and Trp-286, lining the upper part of the 'gorge', had only a small effect on the values of Km and k_{cat}. Nevertheless, triple mutants including replacements of both Glu-285 and Trp-286 exhibited 6-7 fold reduction in the apparent bimolecular rate constant. Taken together, the results demonstrate that mutations involving only the *aromatic* residues at the rim of the 'gorge' appear to have a minor effect on the overall structure and the integrity of the catalytic machinery of HuAChE. Therefore, inhibition patterns of these HuAChE mutants by the various inhibitors, should reflect predominantly the structural modifications of the enzyme-inhibitor complexes, induced by the specific mutations of the aromatic residues.

Effects of mutation on inhibition by the active center and PAS ligands: Inhibition constants for HuAChE mutants by the active center ligands edrophonium and hexamethonium were determined (Table 7). As could be expected replacements of most of the tested residues, located near the rim of the active site 'gorge', have a minor effect on the inhibitory activity of

edrophonium. The most notable exception is Asp-74, replacement of which by Asn results in 5-fold increased resistance to inhibition by this ligand, substantiating the previously reported value of IC_{50} (Shafferman *et al.* , 1992b). A smaller effect (two-fold increase in Ki) was observed upon substitution of Tyr-124 or Tyr-341. On the other hand, substitution of residues Trp-86 and Tyr-337 (Table 7) or Glu-202 (not shown), located at the active center, clearly affect the inhibitory activity of edrophonium. The effects of these replacements on the interactions with the active center ligand edrophonium, were discussed elsewhere (Shafferman *et al.* 1992b; Ordentlich *et al.*, 1993a).

The active center ligand hexamethonium is also susceptible to replacement of HuAChE residues which are expected to interact with the cationic head of the inhibitor in the active center. This is demonstrated by the 720 fold increase in Ki resulting from replacement of Trp-86 by alanine. However , unlike the case of edrophonium, replacement of Tyr-337 by alanine appears to enhance affinity towards the enzyme by a factor of 2. Still within the active center, replacement of Phe-297 resulted in a substantial increase (17-fold) in Ki for hexamethonium which was not observed for edrophonium. This effect may be due to specific interactions of Phe-297 with the hydrocarbon chain, as demonstrated for its function in the acyl pocket (Ordentlich *et al.*, 1993a; Vellom *et al.*, 1993), as well as with the second quaternary nitrogen. Pronounced effects on inhibition by hexamethonium were also observed for mutation of residues at the top of the gorge (Table 7). Substitution of Asp-74 resulted in a 10-fold increase in Ki, in analogy to the effect observed for edrophonium. However unlike the case of edrophonium, replacement of Glu-285 resulted in a 7-fold increase in Ki. This effect is surprising since the distance of this residue from the quaternary ammonium groups of the ligand (~10Å; see Fig. 8c) precludes direct interaction. It is possible therefore, that the effect of mutation at position 285 reflects an indirect overall conformational change around and within the upper part of the 'gorge'.

Inhibition of the HuAChE mutants by the PAS ligand propidium, is significantly affected by replacement of certain residues near the rim of the active site 'gorge' (Table 7). The most remarkable increase (~10-fold) in resistance to propidium is exhibited by replacement of Trp-286. Other single mutants, with the exception of the Y124A, display increased resistance to inhibition varying between 2 to 6-fold . Examination of the inhibition behavior of multiple mutants suggests a synergistic effect between Trp-286 and its neighboring residues. Namely , the sum of the free energy contributions to ligand binding, estimated from single site mutants,

Table 6: Kinetic constants for ATC hydrolysis by HuAChE and its PAS mutants

HuAChEs	Km (mM)	kcat ($x10^{-5}xmin^{-1}$)	kapp[a] ($M^{-1}x10^{-8}xmin^{-1}$)
Wild Type	0.12	4.2	35.0
Mutations at rim and top of 'gorge'			
Y72A	0.13	3.8	29.2
D74 N	0.60	2.5	4.2
Y124A	0.25	2.5	10.0
E285A	0.28	3.8	13.6
W286A	0.20	3.2	16.0
Y341A	0.30	2.5	8.3
Y72A/Y124A	0.07	2.5	35.7
Y72A/E285A	0.24	4.0	16.7
Y72A/W286A	0.30	4.2	14.0
E285A/W286A	0.35	4.4	12.6
Y72A/E285A/W286A	0.30	2.0	6.7
Y124A/E285A/W286A	0.28	1.4	5.0
Mutations down the 'gorge' near active center			
W86A	93.0	0.8	0.009
F295A	0.13	3.0	23.0
F297A	0.31	1.2	3.9
Y337F	0.16	4.0	25.0
Y337A	0.10	1.0	10.0
F338A	0.14	1.7	12.1

[a] kapp = kcat/Km

does not account for the reduced ligand affinity observed in the multiple site mutants. This can be exemplified in the double mutation E285A/W286A which increases resistance to propidium inhibition 95 fold, while the corresponding single mutants display only 5-fold and 10-fold increase, respectively. The other double and triple mutants: Y72A/W286A, Y72A/E285A/W286A and Y124A/E285A/W286A exhibit a comparable resistance to inhibition by propidium, which is over 100-fold higher than for the wild type enzyme. This synergism is consistent with the notion that the aromatic residues, centered around Trp-286, constitute a binding pocket for propidium . The increased resistance to inhibition by propidium of the mutant E285A, may be due to conformational modifications as suggested for hexamethonium. Howèver, since propidium and hexamethonium are not likely to bind to the same site, the replacement of Glu-285 may also affect the stability of the propidium complex in a different way. The carboxylate of Glu-285 is located behind the indole moiety of Trp-286. Since the latter probably participates in the stabilization of the enzyme - propidium complex via stacking with the phenanthridine moiety (see model of HuAChE-propidium complex - Fig. 8d), the proximal negative charge may enhance this interaction by polarization of the π-electron system (Burley and Petsko,1988). Binding of propidium is refractive to most substitutions at the active center except for that of Trp-86. The effect of replacement of Trp-86, located 15Å from the entrance to the active site 'gorge', has been rationalized previously in terms of allosteric interaction between PAS and Trp-86 (Ordentlich *et al.*, 1993a). Comparison of the inhibitory activity of propidium vs its binding to certain PAS mutants is presented in Section V.

The interactions of bisquaternary ligands decamethonium and BW284C51, with the various mutants, are affected by structural modifications at both the active center and the rim of the active site 'gorge' . This can be expected since these bisquaternary ligands bridge the distance between the periphery and the active center (Krupka ,1966) . Indeed, examination of the data in Table 7 indicates that *any* mutant exhibiting resistance to inhibition by either the active site ligand edrophonium or the PAS ligand propidium, also show resistance to inhibition by BW284C51 and decamethonium. As was the case for edrophonium and hexamethonium, the dominant interaction of the bisquaternary ligands at the active center is that with Trp-86, indicated by the high Ki values for the mutant W86A . The affinity for BW284C51 is lowered by replacement of Tyr-337 by Ala (but not by Phe), whereas an opposite effect is observed for decamethonium (Table 7). Such difference was also observed for edrophonium vs hexamethonium and is in good agreement with the structural similarity patterns of

edrophonium to BW284C51 and of decamethonium to hexamethonium. Furthermore, as for the case of edrophonium, the differential effect of Y337A and Y337F on Ki for BW284C51 reflects the contribution of the aromatic-aromatic interaction of the residue at position 337 with the aryl moiety of the ligand (Table 7).

Replacement of Trp-286, Asp-74 and Tyr-341, at the rim of the active site' gorge,' has a major effect on the stability of the enzyme - ligand complexes of the two bisquaternary inhibitors, whereas the effect of mutation of other residues in this region (Tyr-72, Tyr-124 and Glu-285), is less pronounced (Table 7). The Ki values for inhibition of the D74N mutant either by decamethonium or by BW284C51, were two orders of magnitude higher than those for the wild type enzyme. However, Asp-74 is unique in its capacity to influence events taking place at both the active center and the PAS, as can be seen from the effect of its replacement on k_{app} of catalysis (Table 6) as well as on inhibition by active center (edrophonium) and PAS (propidium) ligands (Table 7). Thus, the pronounced effect of Asp-74 substitution, on inhibition by bisquaternary ligands, may be attributed to the combined influence of the mutation on both sites, substantiating its proposed role in signal transduction from the periphery to the active center (Shafferman *et al.*, 1992b).

As in the case of propidium, certain multiple mutants display synergistic effects of resistance to inhibition by the two bisquaternary PAS ligands . Inhibition patterns of the multiple mutants by these ligands, reflect also the structural difference of these inhibitors. The higher affinity of BW284C51 for HuAChE, which probably results from interactions with its aromatic moieties, should also be more sensitive to structural modifications of the PAS binding domain. This is evident from the relative resistance to inhibition of the multiple mutants of aromatic residues (cf. Y72A/Y124A and Y72A/W286A), to inhibition by BW284C51 vs decamethonium (Table 7). In conclusion, the fact that three structurally different cationic moieties, present in propidium, decamethonium and BW284C51, are affected by residues at the enzyme exterior centered around Trp-286, supports the assignment of that region as the peripheral anionic site.

Molecular Modeling of HuAchE-Inhibitor Complexes: Modeling of the non-covalent complexes of HuAchE with active center ligands and PAS inhibitors was carried out as described in Methods. The final models for all HuAchE-inhibitor complexes studied, together with that of the HuAChE-ACh adduct (Shafferman *et al.*, 1992b), are depicted in Fig. 8. The

Table 7: The competitive inhibition constants of HuAChE and its active center and PAS mutants with active center, peripheral and bifunctional bisquaternary ligands

HuAChEs	Inhibition Constant (Ki)				
	Propidium[a] (μM)	Decamethonium[b] (μM)	BW284C51[b] (nM)	Hexamethonium[c] (mM)	Edrophonium[c] (μM)
Wild Type	1.4	6	10	0.2	0.75
Mutations at rim and top of 'gorge'					
Y72A	5.3	13	22	0.35	0.3
D74 N	7.8	850	2450	2.0	3.5
Y124A	1.2	12	17	0.4	1.5
E285A	6.5	26	21	1.3	0.8
W286A	14.3	41	121	0.3	0.6
Y341A	3.4	57	322	0.4	2.0
Y72A/Y124A	7	22	355	0.2	0.2
Y72A/E285A	14	370	140	2.2	0.6
Y72A/W286A	103	81	1290	1.0	0.6
E285A/W286A	133	280	2220	1.8	0.6
Y72A/E285A/W286A	138	340	3870	3.3	0.6
Y124A/E285A/W286A	110	790	3500	2.1	0.6
Mutations down the 'gorge' near active center					
W86A	870	90000	40000	144.6	[>150]
F295A	0.9	0.8	3.5	0.3	0.4
F297A	4.7	64	5	3.5	0.7
Y337F	0.9	5.2	10.7	0.2	0.75
Y337A	0.9	0.9	51	0.08	5.7
F338A	1.5	19	10	0.4	0.8

[a] peripheral site ligand; [b] bisquaternary ligands; [c] active center ligands.

basic features of each model and its correspondence to the kinetic data for inhibition, are described in this section.

Model of HuAChE-Edrophonium complex: Edrophonium was initially docked into the active center by superimposing its quaternary ammonium group on the equivalent moiety in the HuAChE-ACh adduct (Fig. 8a; Shafferman *et al.*, 1992b,c). Manual adjustment of the aryl moiety was followed by energy optimization (see Methods). In the resulting structure (Fig. 8b) the quaternary nitrogen methyl groups are within ~3.5Å from the centroid of the Trp-86 indole ring, and the quaternary nitrogen within 4.4Å from Cε2-Tyr-337. The phenyl moiety of edrophonium is within aromatic-aromatic interaction distance from aromatic side chain of Tyr-337 (5.6Å between centroids, 4.5Å edge to face). The 3-hydroxyl substituent of edrophonium is within H - bond distance from Oγ– S203 and from Nε-H447 (not shown).

The increased resistance to inhibition by the D74A and Y341A mutants cannot be directly explained by this model as these residues are remote (11Å and 8Å respectively) from the quaternary nitrogen. This observation is discussed below and may be a reflection of the involvement of Asp-74 and Tyr-341 in the cross-talk between the periphery and the active center (Shafferman *et al.*, 1992b,c; Ordentlich *et al.*, 1993).

Our model which was optimized according to the kinetic data presented above, is in good agreement with structure-activity studies of edrophonium analogues (Wilson and Quan 1958) and with findings from x-ray studies of edrophonium-TcAChE crystals (Sussman *et al.*, 1992).

Model of HuAChE-Propidium complex. The initial model for the HuAChE-propidium complex was based on our previous kinetic studies (Shafferman *et al.*, 1992b,c), identifying Trp-286 and Asp-74 as residues affecting inhibition by propidium and assuming a stacking interaction between the indole ring of Trp-286 and the phenanthridine moiety of propidium. The adjustment of propidium involves sliding of the phenanthridine moiety in parallel to the plane of Trp-286 indole ring. Further refinement of the model was based on the effects of substitution of Tyr-72, Tyr-124, Tyr-338, Tyr-337, Tyr-341, Phe-295 and Phe-297 on inhibition by propidium. In the refined model (Fig. 8d) the side chain of residue Trp-286 was rotated towards the phenanthridine moiety of propidium ($\chi1$=112°, $\chi2$= -55° vs. -66° and 135° in the free enzyme). The bulky aminophenanthridine moiety could be subject to numerous

aromatic-aromatic and charge-charge interactions, with residues vicinal to Trp-286 including Tyr-72 and Tyr-124. Of these three aromatic residues Trp-286 has the most pronounced contribution to binding. This is consistent with the relative resistance (compared to wild type) to inhibition of the double mutant Y72A/Y124A (5-fold), as opposed to the hundred-fold increase in Ki for double or triple mutants that include replacement of Trp-286. The aromatic side chains of residues Tyr-72 and Tyr-124 in the model are rotated from their respective positions in the free enzyme and are within charge-charge interaction distance from the aniline nitrogen of propidium. The aryl ring of residue Tyr-72 also participates in weak aromatic-aromatic interaction with the phenanthridine moiety (~4Å edge to edge) as well as with neighboring aromatic residues. Energy optimization of the model does not affect appreciably the conformation of the phenanthridinium moiety of propidium although the distortion obtained here may be somewhat exaggerated due to the force field employed. Similar lack of planarity, in an analogous aromatic ring system, was observed in the x-ray structure of phenanthrene. The proposed model is consistent with binding studies of decidium and hexidium (Berman *et al.*, 1987) which suggested that the phenanthridine moieties of the two ligands do not associate with identical regions of the enzyme structure, yet their interactions contribute equally to the binding energy. The aniline nitrogen of propidium is within H-bond distance from the carboxylate of Asp-74 (2.8Å from Oδ1) following adjustment of the position of its side chain (χ1=-56° χ2=82° vs. -161° and -96° in the free enzyme). According to this model, the carboxylate of residue Glu-285 is too far (>7Å) from the phenanthridine moiety to allow for a direct interaction with propidium. As already mentioned, the participation of Glu-285 in stabilization of the propidium complex may operate via polarizing effect on the indole π-electrons of Trp-286 (Burley and Petsko,1988), or through maintaining the integrity of the structural domain that includes Trp-286 and its neighboring aromatic residues lining the active site 'gorge'. Other interactions predicted by the model are also in agreement with the kinetic data for most of the HuAChE mutants. The alkyl substituents of the quaternary nitrogen of propidium are within hydrophobic interaction distance from the aromatic moieties of residues proximal to the active center: Phe-297, Tyr-337 and Phe-338 (3.5-4Å). Indeed, replacement of Phe-297 affected Ki values (3 fold). As already noted, Trp-86 is located 9Å away from this quaternary nitrogen, yet the W86A mutant is refractive to inhibition by propidium (Ordentlich *et al.*, 1993a).

Model of HuAChE-BW284C51 complex. The energetically optimized structure of BW284C51 was docked into the active center of HuAChE by superimposing one of its ammonium aryl groups on the equivalent moiety in the edrophonium complex. Due to the inherent relative rigidity of BW284C51, optimization of the initial model resulted in minor adjustments to the ligand structure and to the HuAChE residues constituting the ligand binding pocket. In the final model (Fig. 8e) , the ammonium group projecting from the active site 'gorge' is within charge-charge interaction distance from the carboxylate of Asp-74 and the phenolic oxygens of Tyr-341 and Tyr-72. The phenyl moiety (adjacent to this ammonium group) is stabilized by aromatic-aromatic interactions with the side chain of Tyr-341 (edge to edge distance of 4.4Å) which was rotated from its original position (χ1=-114°, χ2=-61° vs. -64° and 63° in the free enzyme). The same BW284C51 phenyl moiety is also stabilized by aromatic-aromatic interactions (face to edge,4.7Å intra-centroid separation) with the side chain of Trp-286 that was rotated towards the ligand (χ1= -114°, χ2= -56° vs. -66° and 134° in the free enzyme).

The tight fit between the ligand and its binding pocket, suggested by the model, is in agreement with the extent of the synergistic effect of multiple mutations of residues at the rim of the 'gorge'. The model also predicts a steric hindrance due to the proximity of the carbonyl oxygen and the aromatic rings of Phe-295 and Phe-297. This is consistent with the observed increase in affinity for BW284C51 following replacement of either Phe-295 or Phe-297 by the less bulky residue alanine. The effect of replacement of Glu-285 on BW284C51, can be rationalized in analogy to its effect on propidium.

Model of HuAChE-decamethonium and HuAChE-hexamethonium complexes . Similarly to the construction of the molecular model for the complex of the bisquaternary ligand BW284C51, one of the quaternary nitrogens of decamethonium was positioned in analogy to that of edrophonium . The alkyl chain was grown tracing the shape of the active center 'gorge'. Due to the flexibility of decamethonium, multiple plausible orientations for the second charged group were observed. Only two of these structures (A and B in Fig. 9) were in agreement with the kinetic data of inhibition for the HuAchE mutants. These two structures of the HuAChE-decamethonium complex are of comparable energy and may therefore exist in equilibrium. Their interconversion proceeds through rotation about bonds C7-C8 and C9-C10 of the inhibitor.

In structure A (Fig. 8f, Fig. 9A), Trp-286 is the main interaction locus for the quaternary ammonium group. Two of the ammonium methyl groups are located within ~3.8Å away from

Fig. 8. Molecular models of HuAChE-inhibitor complexes (Opposite page). Only the amino acids mutated in this study are displayed and hydrogen atoms are omitted for clarity. The backbone of the ligands are marked by a heavy line and the volume occupied by each ligand - by dot surface. All complexes are displayed in an orientation identical to that of the HuAChE-ACh adduct displayed in panel (**a**) (the entrance to the 'gorge' is marked by an arrow). Complexes of the active center selective ligands, which occupy the lower part of the 'gorge', are displayed in panel (**b**) - edrophonium and panel (**c**) - hexamethonium. Complex of the PAS selective ligand propidium, which is confined to the upper part of the 'gorge' is displayed in panel (**d**). Complexes with bisquaternary ligands, bridging the active center and PAS, are displayed in panel (**e**) - BW284C51 and panel (**f**) - decamethonium.

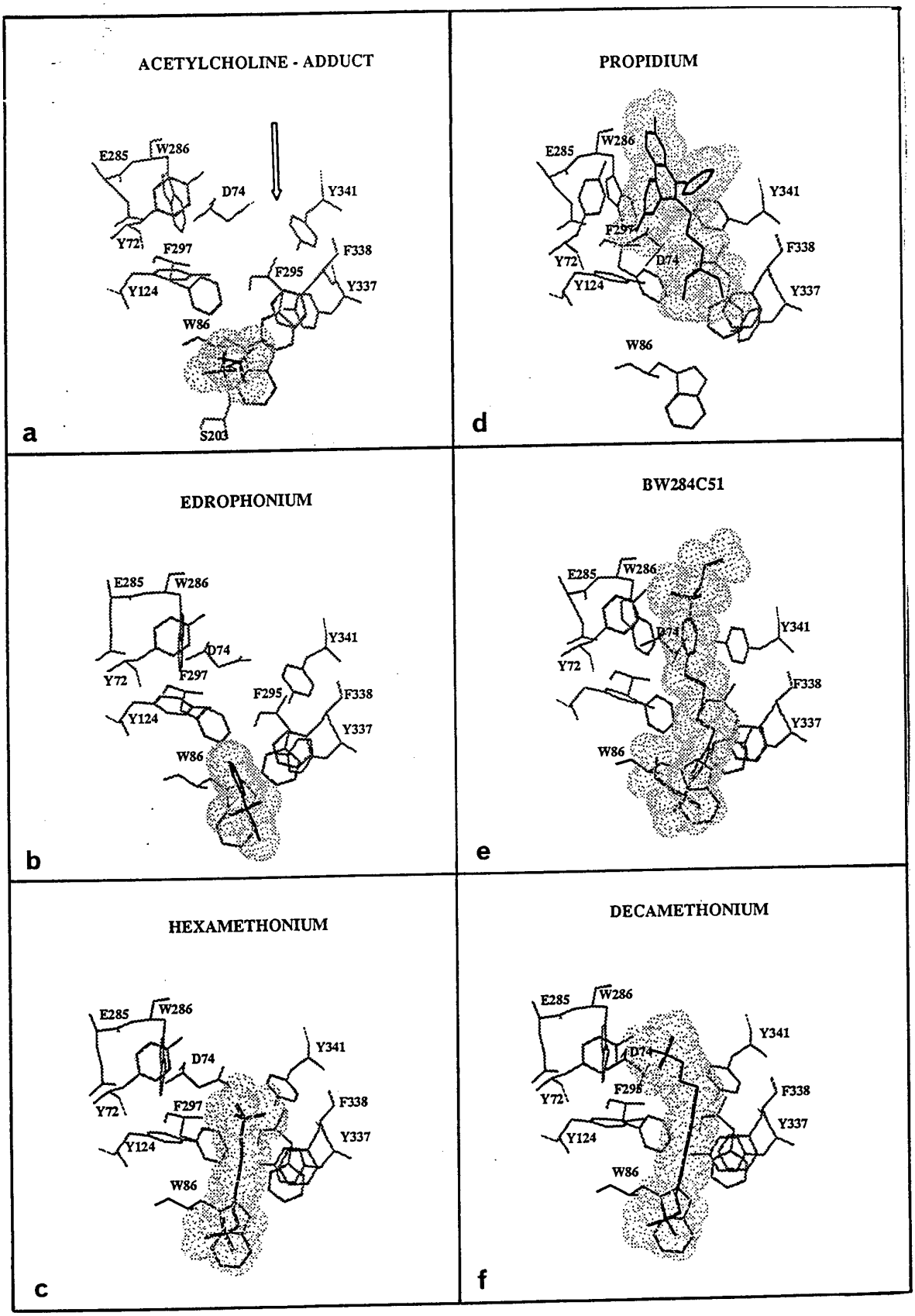
ACETYLCHOLINE - ADDUCT
E285
W286
D74
Y341
Y72
F297
F338
F295
Y124
Y337
W86
S203
a
PROPIDIUM
E285
W286
Y341
F297
F338
Y72
D74
Y124
Y337
W86
d
EDROPHONIUM
E285
W286
Y341
D74
Y72
F297
F295
F338
Y124
Y337
W86
b
BW284C51
E285
W286
D74
Y341
Y72
F338
Y337
W86
e
HEXAMETHONIUM
E285
W286
Y341
D74
Y72
F297
F338
Y337
Y124
W86
c
DECAMETHONIUM
E285
W286
Y341
D74
Y72
F338
Y337
Y124
W86
f

the centroid of the indole ring (π-cation interaction). The adjacent side chains do not undergo major movements with the exception of the sidechain of Asp-74, which rotated downwards from its position in the free enzyme ($\chi 1$=-67°, $\chi 2$= -100° vs. -161° and -96°). Still, the distance of Asp-74 carboxylate from the quaternary nitrogen remains relatively large (6.6Å). Residue Tyr-341, in this structure, is not within interaction distance from the quaternary nitrogen. The model implies that the aromatic residues Tyr-72 and Tyr-124, may contribute to stabilization of structure A via weak charge-charge interactions. Thus, structure A is in accordance with the kinetic observations for the Trp-286 mutant but does not provide an explanation for the observed effects of replacement of both Asp-74 and Tyr-341. An explanation for the latter is provided by structure B (Fig. 9B) which implicates Tyr-341 together with Asp-74, as the main interaction locus for the quaternary nitrogen. In structure B the ammonium methyl groups are within 4.1Å from the centroid of the aryl moiety of Tyr-341 (π-cation interaction), which was rotated ($\chi 1$=-72°, $\chi 2$=-21° vs. -63° and 63° in the free enzyme), while maintaining H-bond distance from the carboxylate of Asp-74 (2.4Å). This quaternary nitrogen is within ~6Å from Trp-286. Unlike structure A, the side chain of Asp-74 does not rotate from its original position and may contribute to the complex stabilization by charge-charge interaction (3.9Å from the quaternary nitrogen). The phenolic oxygen of residue Tyr-72 is within charge-charge interaction distance from the quaternary nitrogen (4.3Å) and one of the quaternary methyl groups is within 3.5Å from the phenyl ring of this residue. In this structure, no specific interaction for residue Tyr-124 was observed.

In both structures A and B, no specific interactions with the ligand are observed for residues Phe-295, Phe-297, Tyr-338, Tyr-337 and Glu-285 thus none of the models can directly account for the change in inhibition by decamethonium observed upon their substitution.

The molecular model for the hexamethonium complex (Fig. 8c), was constructed like that of decamethonium. The first quaternary nitrogen of hexamethonium is stabilized by π-cation interaction with the indole moiety of Trp-86 and interacts with Glu-202 (not shown). No significant interaction was observed with Asp-74 (5.3Å from the proximal quaternary nitrogen) thus its effect on inhibition cannot be directly accounted for by this model and is most likely to be a consequence of its involvement in allosteric effects (Shafferman *et al.*, 1992b and as discussed later). Stabilization of the quaternary nitrogen include: charge-charge interaction with the phenolic oxygen of Tyr-124 (3.7Å from the quaternary nitrogen) and π-cation interaction with the aromatic moiety of Tyr-341. The model is in agreement with the effects of

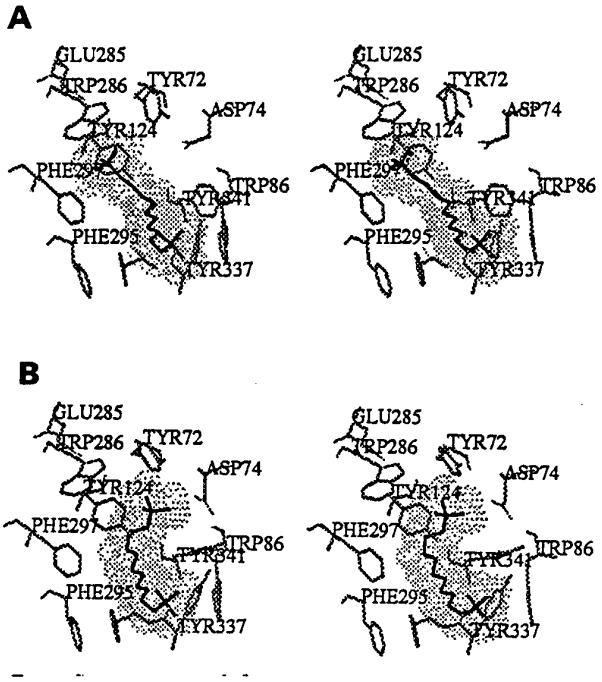

Fig. 9. Stereo views of the two proposed conformers of the HuAChE-decamethonium complex. Only the amino acids mutated in this study are displayed and hydrogen atoms are omitted for clarity. The ligand is marked by heavy line and its volume - by a dot surface. Alternative stabilization of the quaternary ammonium group of decamethonium proximal to PAS, by π-cation interaction with : **a.** the indole ring of Trp-286 (structure A); or **b.** The aromatic moiety of Tyr-341 (structure B). Orientation of the HuAChE-decamethonium-complex shown in Fig. 8f, is identical to structure A. See text for more details on interactions of decamethonium with the different residues in the active site gorge.

substitution of residues at the rim of the gorge however, as was the case for decamethonium, it does not provide an explanation for interactions of the ligand with residues Tyr-337, Tyr-338, Phe-295 and Phe-297. Thus, using the shorter ligand hexamethonium did not result in a better definition of the interactions in the vicinity of the active center. However this model together with the kinetic data for inhibition of E285A by hexamethonium, strongly suggest that Glu-285 which is within 10Å from the quaternary nitrogen, plays an important role in maintaining the structural integrity of the upper domain of the 'gorge' adjacent to residue Trp-286.

Functional Degeneracy of HuAChE Peripheral Anionic Binding Sites: Analysis of the results from inhibition studies of the HuAChE muteins with PAS selective inhibitors and of the molecular models of enzyme - inhibitor complexes, reveals that PAS is not a single binding site. The data suggest that each of the inhibitors examined binds to PAS in a distinct manner and that the nature and extent of participation of the individual residues is ligand dependent. This divergence of binding sites within the PAS array can be exemplified through comparative examination of the interaction modes of propidium, BW284C51 and decamethonium with specific residues of HuAChE.

In the HuAChE-propidium complex, the indole ring of Trp-286 is involved in a stacking interaction with the positively charged aromatic moiety of propidium and is an essential element of binding. This is evident from the direct measurements of propidium binding to the wild type and W286A enzymes as well as from inhibition studies (Table 7) demonstrating that double mutations which do not include Trp-286, have a limited effect on inhibition by propidium. The indole ring of Trp-286 interacts also with BW284C51. However in this case, the interaction appears to be of the aromatic-aromatic edge to face type (Burley and Petsko, 1988; Fig. 8e) rather than stacking interaction. Of the two possible conformations of the HuAChE-decamethonium complex (Fig. 9), one appears to include a π-cation (McCurdy *et al.*, 1992) stabilizing interaction of the quaternary nitrogen with the Trp-286 indole group (Fig. 8f, Fig. 9A). Thus, the indole moiety of Trp-286 displays a range of interaction modes including stacking, aromatic-aromatic and π-cation attractions. The π-electron system of the Trp-286 indole moiety may be polarized by the adjacent carboxylate of Glu-285, enhancing the stabilizing effect of all the interaction modes mentioned here.

Stabilization through π-cation interaction was observed for the other conformation of decamethonium (structure B, Fig. 9B), as well as for the BW284C51 (Fig. 8e) complexes,

with the aromatic moiety of Tyr-341. In the latter complex, aromatic-aromatic interactions with this side chain,were also observed.

Residue Asp-74 interacts with an aniline nitrogen of propidium probably through H-bonding since this nitrogen is unlikely to bear a positive charge. On the other hand, Asp-74 appears to be involved in charge-charge interactions in the HuAChE complexes with the two bisquaternary inhibitors. In the BW284C51 complex, the aromatic ammonium group of the ligand is oriented across the entrance to the active center 'gorge,' placing the quaternary nitrogen within 4Å from the carboxylate of Asp-74. Similar juxtaposition of the quaternary nitrogen and the carboxylate was observed for conformer B of the HuAChE-decamethonium complex.

Thus, charting of the ligand stabilizing interactions in the three HuAChE complexes, delineates parts of the amino acid array comprising the PAS. Elements of this array line the rim of the active site 'gorge' and include Trp-286 and a cluster of vicinal residues (Tyr-72, Tyr-124, Glu-285) as well as residues Asp-74 and Tyr-341 located on the other side of the 'gorge' entrance. This array has sufficient flexibility to accommodate structurally distinct ligands by employing alternative elements to form the appropriate binding sites, thereby creating different peripheral anionic sites which are functionally degenerate. Such accommodation implies also a conformational mobility for the elements of the PAS array, in agreement with their location at or close to the enzyme surface. A common feature of these sites is a core comprising of residues Trp-286 and Asp-74.

The influence of Asp-74 substitution, on inhibition by both peripheral site and active center specific ligands and in particular its striking effect on ligands bridging the two sites, is consistent with its proposed role (Shafferman *et al.*, 1992b) in the relay of allosteric signals from the periphery. Such involvement of Asp-74 was also inferred from the marked influence of its replacement on substrate inhibition (Shafferman *et al.*, 1992b). Interestingly, replacement of residues Tyr-72, Tyr-124, Trp-286, Glu-285 and Tyr-341 generates AChE molecules in which substrate inhibition is affected to about the same extent as the inhibition constants for PAS ligands (up to 10-fold). Yet, unlike for inhibition by PAS ligands, no synergistic effects on substrate inhibition were observed, for the multiple mutants studied herein (unpublished results). This may indicate that the substrate interacts at multiple locations within the PAS array. Since the molecular size of the substrate is much smaller than that of the PAS inhibitors, its interactions are more localized and therefore less affected by changes of the PAS architecture

that result in the synergistic effects. Existence of two binding loci within this array, were suggested above for the quaternary ammonium group of decamethonium, which structurally resembles the cationic head of the substrate.

In addition to the effects of Asp74 we recently suggested that coupling between residues Trp-286 at the periphery and Trp-86 at the active center plays an important role in allosteric modulation of AChE activity (Ordentlich *et al.*, 1993a). This conclusion is further supported here by the considerably higher relative resistance, of W86A to inhibition by bisqaternary ligands, capable of bridging the two tryptophan residues (Fig. 8e, Fig. 8f, Table 7), as compared to that by hexamethonium (Fig. 8c, Table 7) interacting exclusively with Trp-86. In conclusion, the observed functional degeneracy at the periphery of HuAChE, may be instrumental in the allosteric modulation of catalytic activity effected by binding to PAS (Changeux 1966; Berman *et al.*, 1981; Quinn 1987) and implies an important role for the common core residues Asp-74 and Trp-286, in transmission of these effects.

IV. Contribution of Aromatic Moieties in the Active Center to Catalysis and Allosteric Modulation Via the Peripheral Anionic Subsite

INTRODUCTION

The recently resolved 3D structure of *Torpedo californica* AChE (TcAChE) revealed a deep and narrow 'gorge', which penetrates halfway into the enzyme and contains the catalytic site at about 4Å from its base (Sussman *et al.*, 1991). In addition, the structure reveals two remarkable features of the enzyme which may bear upon its catalytic efficiency. One of these is the uneven overall distribution of negative charge giving rise to a large electrostatic dipole, aligned with the axis of the active site gorge, that could draw the positively charged substrate down the gorge to the active center (Ripoll *et al.*, 1993). However, it was recently shown, by septuple replacement of negatively charged amino acids, that electrostatic attraction does not contribute to the catalytic rate of the enzyme (Shafferman *et al.*, 1994). The second striking feature of the enzyme is related to the 14 aromatic residues that contribute to the lining of the active site gorge. Most of these residues are highly conserved in enzymes from different species (for sequence compilation see Gentry and Doctor, 1991; Massoulie *et al.*, 1993). This complex array of aromatic residues was hypothesized to provide a guidance mechanism facilitating a two-dimensional diffusion of ACh to the active site (Sussman *et al.*, 1991), to be involved in substrate accommodation and to participate in allosteric modulation of catalysis (Shafferman *et al.*, 1992b; Ordentlich *et al.*, 1993a; Barak *et al.*, 1994). Chemical affinity labelling (Weise *et al.*, 1990), x-ray structure of TcAChE and of TcAChE - ligand complexes (Sussman *et al.*, 1991; Harel *et al.*, 1993), site directed mutagenesis and molecular modeling (Barak *et al.*, 1992; Shafferman *et al.*, 1992a,b; Ordentlich *et al.*, 1993a; Vellom *et al.*, 1993; Radic *et al.*, 1993; Barak *et al.*, 1994; Gnat *et al.*, 1994; Taylor, and Radic, 1994) elucidated some aspects of the functional role of 9 of the 14 aromatic amino acids. Residues Phe-295(*288*) and Phe-297(*290*) determine specificity for phosphylating agents (Barak *et al.*, 1992; Fournier *et al.*, 1993) and for the acyl moiety of the substrate (Harel *et al.*, 1993; Ordentlich *et al.*, 1993a; Vellom *et al.*, 1993). The hydrophobic site for the alcoholic portion of the covalent adduct (tetrahedral intermediate) includes residues Trp-86(*84*), Tyr-337(*330*) and Phe-

338(*331*), which operate through nonpolar and/or stacking interactions, depending on the substrate (Ordentlich *et al.,* 1993a). Residues Tyr-72(*70*), Tyr-124(*121*), Trp-286(*279*) and Tyr-341(*334*) are localized at or near the rim of the active center gorge and together with Asp-74(*72*) constitute the peripheral anionic subsite(s) in AChE (Weise *et al.,* 1990; Shafferman *et al.,* 1992a; Radic *et al.,* 1993; Barak *et al.,* 1994; Radic *et al.,* 1994). Binding of ligands to the peripheral sites was suggested to modulate the AChE catalytic activity through conformational changes in the active center (Changeux, 1966; Shafferman *et al.,* 1992b;Ordentlich *et al.,* 1993a).

Residue Trp-86(*84*) was recently shown to be essential for interaction of AChE with the quaternary ammonium moiety of choline as well as of active center inhibitors (Weise *et al.*, 1990; Sussman *et al.*, 1991; Shafferman *et al.,* 1992a,b; Ordentlich *et al.,* 1993a; Harel *et al.,* 1993) and was therefore suggested to be a main element of the classical 'anionic subsite' of the enzyme. The structure of this subsite and the nature of its interactions with quaternary ammonium groups is a matter of a longstanding controversy. One opinion, argued on the basis of the alleged presence of multiple negative charges in the active center, that the 'anionic subsite' is a true anionic locus (Quinn ,1987). The opposite view based on the structure - activity studies with charged and noncharged substrates and inhibitors suggested that the 'anionic subsite' is in fact a trimethyl site, binding the ligands through hydrophobic interactions (Hassan *et al.*, 1980; Cohen *et al.*, 1984) or dispersive forces (Nair *et al.*, 1994).

In this study we investigate in depth the constitution and function of the 'anionic subsite' of HuAChE through replacement of residue Trp-86 by aromatic or charged amino acids and through substitution of additional residues projecting into the gorge cavity such as Tyr-337 and the highly conserved Glu-202 and Tyr-133. Guided by the catalytic properties of the mutated enzymes, their interactions with reversible and irreversible inhibitors and by molecular modeling, we conclude that the stabilization of charged ligands at the active center does not appear to be mediated by true ionic interactions but rather through cation - aromatic interactions with the residue at position 86. The functional conformation of the "anionic subsite" Trp-86, which is critical to the overall catalytic efficiency, is achieved through aromatic - aromatic interactions with residue Tyr-133. We also provide evidence, consistent with the notion, that the hydroxyl group of Tyr-133 participates, through hydrogen bonding, in maintaining the functional integrity of the active center.

METHODS

Mutagenesis of Recombinant HuAChE and Construction of Expression Vectors- Mutagenesis of AChE was performed by DNA cassette replacement into a series of HuAChE sequence variants which conserve the wild type (Soreq *et al.*, 1990) coding specificity, but carry new unique restriction sites (Shafferman *et al.*, 1992a). Generation of mutants W86A(W*84*), Y337A(F*330*) and Y337F was described previously (Shafferman *et al.*, 1992b). The W86E(*84*) and W86F(*84*) mutated HuAChEs were formed by replacement of the *AccI - NarI* DNA fragment of the pAChEw4 (Shafferman *et al.*, 1992a) variant with synthetic duplexes carrying the mutated codons GAG(Glu) or TTC(Phe). Generation of mutations Y133A(*130*) and Y133F(*130*) was carried out by replacement of the *NarI-XhoI* DNA fragment of the pAChEw4 variant with synthetic DNA duplexes carrying the mutated codons GCC(Ala) or TTC(Phe). All the synthetic DNA oligodeoxynucleotides were prepared using the automatic Applied Biosystems DNA synthesizer. The sequences of all new clones were verified by the dideoxy sequencing method (USB sequenase kit). The rHuAChE cDNA mutants were expressed in tripartite vectors which allow expression of the *cat* reporter gene and the *neo* selection marker (Kronman *et al.*, 1992, Shafferman *et al.*, 1992a).

Transient Transfection, Preparation and Quantitation of AChE and its Mutants- Human embryonal kidney 293 cells were transfected with various purified plasmids using the calcium phosphate method. Transient transfection was carried out as described previously (Velan *et al.*, 1991a; Shafferman *et al.*, 1992 a,b) and efficiency of transfection was normalized by levels of co-expressed CAT (chloramphenicol acetyl transferase) activity. The various AChE polypeptides secreted into the medium were quantified by AChE-protein determination relying on the various specific enzyme linked immunosorbent assays (Shafferman *et al.*, 1992a).

Substrates and Inhibitors- Acetylthiocholine iodide (ATC), 5:5'-dithiobis (2-nitrobenzoic acid) (DTNB), ethyl(m-hydroxy-phenyl)-dimethylammonium chloride (edrophonium), 3,8 diamino-5-3'-(trimethylammonium)propyl-6-phenyl phenanthridinium iodide (propidium), 1,10-bis(trimethylammonium) decane (decamethonium) and diisopropyl phosphorofluoridate (DFP) were all purchased from Sigma. 3,3-Dimethylbutyl thioacetate

(TB) was synthesized and purified as described previously (see Section II).

Determination of HuAChE Activity and Analysis of Kinetic Data- Catalytic activity of the recombinant HuAChE and its mutant derivatives collected from transiently or stably transfected cells were assayed according to Ellman *et al.*, (1961). Assays were performed in the presence of 0.1 mg/ml BSA, 0.3mM DTNB (5,5'-dithiobis(2-nitrobenzoic acid) in 5mM or 50mM sodium-phosphate buffer pH-8.0 and varying ATC (0.01-0.6mM) concentrations. The assays were carried out at 27°C and monitored by a Thermomax microplate reader (Molecular Devices). Michaelis-Menten constant (Km) and the apparent first order rate constant (kcat) values, were determined as described before (Shafferman *et al.*, 1992a,b). The apparent bimolecular rate constants (kapp) were calculated from the ratio kcat/Km.

Kinetic data for inhibition by edrophonium, decamethonium and propidium were analyzed as described previously (Ordentlich *et al.*, 1993a) according to the kinetic treatment developed by Barnet and Rosenberry (1977) and Berman and Leonard (1990) for the following reaction scheme:

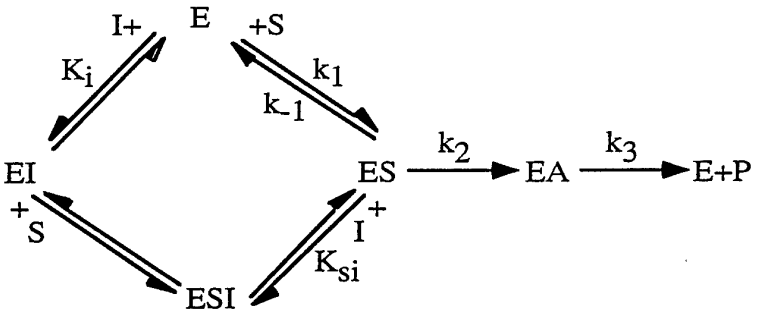

This scheme is consistent with the linear mixed inhibition patterns observed for all the cases reported here. Ki is the competitive inhibition constant and Ksi the noncompetitive inhibition constant. A kinetic solution for the dependence of the reciprocal rate on the inverse concentration of substrate is provided in equation 1. The slopes of the double reciprocal plots of rate versus substrate concentration allow derivation of Ki while the intercepts the calculation of Ksi. This is accomplished by reploting the relative slopes and intercepts, in the presence or absence of inhibitor, against the inhibitor concentration.The reciprocal of the slopes of these replots yield the values of Ki and Ksi.

(1)

$$\frac{1}{V} = \frac{1}{Vm}\left[\frac{k_{cat}}{k_2}\left(1+\frac{[I]}{K_{si}}\right) + k_{app}\left(1+\frac{[I]}{K_i}\right)\cdot\frac{1}{[S]}\right]$$

Phosphorylation experiments were carried out using at least four different concentrations of DFP with two concentrations of enzyme, and the residual enzymatic activity (E) at various times was monitored. The apparent bimolecular phosphorylation constants (ki), determined under pseudo - first order conditions, were computed from the plot of slopes of ln(E) vs. time at different inhibitor concentrations.

Structure Analysis and Molecular Graphics- Building and analysis of the three dimensional models was performed on a Silicon Graphics workstation IRIS 70/GT using SYBYL modeling software (Tripos Inc.). Construction of models for the HuAChE and the mutated enzymes, was based upon the model structure of the enzyme obtained by comparative modeling (Barak *et al.*, 1992) from the x-ray structure of TcAChE (Sussman *et al.*, 1991). Examination of the conformational mobility of residue Trp-86(*84*) side chain in the wild type enzyme included an initial search within the acceptable values of χ_1 and χ_2 followed by structural optimization of the most probable conformers. The two lowest energy structures were considered as representing the alternative conformational states of Trp-86(*84*). Similar search was carried out for models of Y133F(*130*) and Y133A(*130*) mutants. Energy optimizations were carried out by zone refinement including amino acids that either line the active site gorge or are vicinal to residue Tyr-133 (33 residues).

RESULTS

The Functional Consequences of Replacement of Residue Trp-86 in HuAChE by Aromatic and Aliphatic Amino Acids.

The significance of residue Trp-86 in HuAChE for interaction with the charged substrate was already demonstrated by the over 660 - fold increase in the Km value for ATC in the W86A mutant as well as by the over 100 - fold increase of the inhibition constant (Ki) for the active

center inhibitor edrophonium (Ordentlich *et al.*, 1993a). On the basis of these observations we proposed that the noncovalent complex of the charged substrate is stabilized through cation - aromatic interactions. To further examine this hypothesis additional modifications of the side chain at position 86 were made by replacement of Trp-86 by phenylalanine and by glutamic acid. If our hypothesis is valid then the replacement of the indole moiety at position 86 by another aromatic group - phenyl should have a minor effect on the Michaelis - Menten constant (Km) for ATC and none for its noncharged isostere TB. In addition, the values of kcat for both substrates should not be affected by this mutation. Indeed, results presented in Table 8 show that the kinetic values for hydrolysis of ATC and TB by the W86F enzyme are similar to those of the wild type enzyme except for the small increase in the Km value for ATC (6 -fold). On the other hand replacement of Trp-86 by a charged aliphatic residue (W86E) resulted in over 600-fold increase of the Km value for ATC but had no significant effect on the corresponding value for TB. Like the replacement of Trp-86 by alanine, substitution by glutamate results in a moderate decrease in kcat for both ATC and TB (10-fold and 8-fold respectively). The moderate effects of the W86A and W86E mutations on the turnover numbers (kcat) suggests that residue Trp-86 is not essential for the acylation - deacylation steps of the catalytic reaction. The differential effect of residue at position 86 on the reactivity towards charged and noncharged ligands was corroborated also by testing the various Trp-86 mutants with the irreversible noncharged inhibitor DFP and with the two classical reversible quaternary ligands edrophonium and decamethonium (Fig. 1). Like in the case of TB, the bimolecular rate constants of phosphorylation of W86F, W86E and W86A enzymes are similar to the corresponding rate constant of the wild type enzyme exhibiting at most a 6-fold decrease (Table 9). On the other hand, for the charged inhibitors, edrophonium (Fig. 1) and decamethonium, the substitution of Trp-86 by aliphatic residues results in a substantial decrease in affinity (Table 9). Thus, for concentration of edrophonium as high as 45mM no inhibition could be observed. This suggests that replacement of the indole moiety by either acidic or neutral aliphatic side chain brings about an estimated 100,000-fold decrease in binding affinity of edrophonium. The same pattern is observed for the bisquaternary ligand decamethonium, however the magnitude of the change is somewhat lower: ca. 10,000 fold higher than wild type : from a Ki value of 6μM in the wild type enzyme to 50mM and 90mM for the W86E and W86A mutated HuAChEs respectively. The noncompetitive component of inhibition (Ksi) of

Table 8: Kinetic constants for ATC and TB hydrolysis by HuAChE and its W86, Y133, Y337 and E202 mutant derivatives.

HuAChEs	ATC			TB		
	K_m (mM)	k_{cat} ($x10^{-5}$ min^{-1})	k_{app}[a] ($x10^{-8}M^{-1}$ min^{-1})	K_m (mM)	k_{cat} ($x10^{-5}$ min^{-1})	k_{app}[a] ($x10^{-8}M^{-1}$ min^{-1})
Wild Type	0.14	4.0	28.5	0.30	0.55	1.8
W86F	0.8	2.1	2.6	0.30	0.47	1.6
W86E	90	0.4	0.0044	0.36	0.07	0.2
W86A	94	0.8	0.0086	0.44	0.18	0.4
Y133F	0.48	2.0	4.2	0.24	0.05	0.2
Y133A	12.8	0.5	0.038	-[b]	-[b]	-[b]
Y337F	0.16	4.0	25.0	0.33	1.3	3.9
Y337A	0.10	1.0	10.0	0.20	0.2	1.0
E202Q	0.35	0.75	2.1	0.23	0.1	0.4

Values represent mean of triplicate determinations with standard deviation not exceeding 20%. The correlation coefficient of the linear plots were at least 0.95. [a] The apparent bimolecular rate constant (k_{app}) was calculated from the ratio of k_{cat}/K_m.. [b] No detectable reactivity was observed for Y133A enzyme even at a protein concentration of 20µg/ml therefore the expected k_{app} value for this mutated enzyme is at least 200-fold lower than that for wild type.

Table 9: Inhibition constants of quaternary ammonium ligands and bimolecular phosphorylation rate constants of HuAChE and its W86, Y133, Y337 and E202 mutant derivatives.

	Inhibition constants (μM)						(x10-4 M-1 min-1)
	Edrophonium		Propidium		Decamethonium		DFP
HuAChEs	K_i	K_{si}	K_i	K_{si}	K_i	K_{si}	k_i
Wild Type	0.6	4.8	0.6	0.9	6.0	5.7	14
W86F	38.0	128	3.2	122	500	-[d]	14
W86E	(>45000)[a]	-[b]	250	261	51000	120000	4
W86A	(>45000)[a]	-[b]	870	13.5	90000	30000	2.6
Y133F	18.0	111	1.5	6.4[c]	15.0	-[d]	1.4
Y133A	780	180	110	92	15000	32000[c]	0.034
Y337F	0.7	4.6	0.9	1.8	5.2	0.5	40
Y337A	5.7	21	0.9	3.7	0.9	3.9	3.1
E202Q	12.8	83.4	1.2	1.4[c]	33.5	163	0.2

Values represent mean of triplicate determinations with standard deviation not exceeding 20%. The correlation coefficient of the linear plots were at least 0.95. [a] Values in parentheses refer to the highest concentration of edrophonium (45mM) used, yet this concentration was still insufficient to cause detectable inhibition of activity. [b] K_{si} values could not be extracted. [c] The correlation coefficient of the linear plots were below 0.9. [d] Ri slope was close to zero and the computed non-competitive K_{si} value is too large to be of significance.

these enzymes by decamethonium appears to change in a similar manner to that observed for the competitive component : an increase in Ksi from 5.7μM in the wild type HuAChE to 120mM and 30mM for W86E and W86A enzymes respectively. We note that substitution at position 86 of the indole group by a phenyl moiety results in a relatively moderate decrease in affinity (60-80-fold) for the charged reversible inhibitors (Table 9). These results demonstrate that the classical 'anionic subsite' has a predominantly aromatic character. Such conclusion is also supported by the finding that replacement of Glu-202, which is the only acidic residue proximal to the active site, by glutamine resulted in moderate and nonselective decrease of catalytic activity towards ATC and TB (14-fold and 4-fold respectively). Furthermore, the consequence of the mutation E202Q, on the rate of phosphorylation (ki) by DFP, is by far more pronounced than that resulting from any replacement of Trp-86 (Table 9). The about 5-fold decrease in the value of ki due to replacement of Trp-86 by an aliphatic residue is consistent with the conclusion that Trp-86 does not interact with neutral agents reacting at the active site Ser203. On the other hand, the 50-fold decrease in the DFP phosphorylation rate, due to replacement of Glu-202, signifies the involvement of this residue in the hydrolytic reaction as has been also reported for mouse AChE (Radic *et al.*, 1992).

A further indication of the distinct characteristics of HuAChE enzymes, carrying aliphatic residues at position 86, is the marked decrease in affinity of the W86A and W86E mutants towards the peripheral site inhibitor propidium (Fig. 10; Table 9). This inhibitor, which binds to amino acids at the entrance to the gorge, is too short to interact with residues at position 86 at the active center (in the propidium - AChE complex the tetraalkyl ammonium group of propidium is 9Å away from Trp-86; Barak *et al.*, 1994). Yet, replacements of Trp-86 by aliphatic residues generate enzymes which are highly resistant to inhibition by propidium (420 and 1450-fold increase in the competitive inhibition constants for W86E and W86A HuAChE enzymes respectively relative to the wild type enzyme) (Fig. 10 and Table 9). On the other hand, the W86F enzyme shows only a 5-fold increase of Ki for propidium relative to the wild type enzyme (Table 9). The behavior of the W86A and W86E HuAChEs towards propidium may provide some clues to yet another role of aromatic residues at position 86 such as the previously proposed "cross - talk" between the periphery and the active center (Ordentlich *et al.*, 1993a; Barak *et al.*, 1994 and discussion).

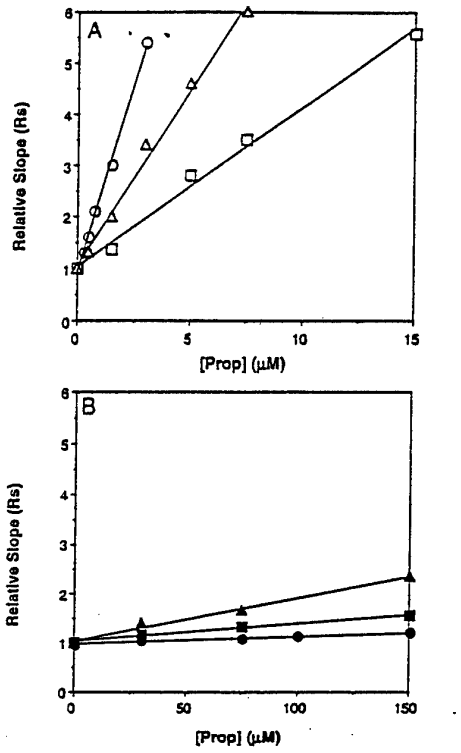

Fig. 10 Dependence of relative slopes (Rs) on propidium concentrations used for inhibition of ATC hydrolysis by the various HuAChE enzymes. The values of Rs = 1+(1/Ki)[I] were determined from the slopes of the double reciprocal plots according to Eq. 1 (see Methods) utilizing 0.02-25mM of ATC. A. wild type HuAChE (O), Y133F (Δ) and W86F (□) mutated HuAChEs. B. Y133A (▲), W86E (■) and W86A (●) mutated HuAChEs. Note that propidium concentrations in panel B are about 10-fold higher than those in panel A.

Effects of Substitutions of the Active Center Residue Tyr-133 on Reactivity of the Resulting HuAChE Enzymes.

The possible functional importance of Tyr-133 is suggested both by virtue of the evolutionary constraint on the conservation of this residue in all ChEs (Gentry and Doctor, 1991; Massoulie *et al.,* 1993) and by its unique location proximal to residue Trp-86 (Fig. 11, 12A). In addition, molecular modeling suggests that Tyr-133 may participate in hydrogen bond interactions in the active center (Ordentlich *et al.,* 1993b and Fig. 11; see also Section IX). To evaluate the possible role of the hydroxyl moiety in such interactions as well as the potential structural role of the aromatic moiety of Tyr-133, we replaced the tyrosine by phenylalanine and by alanine, and analyzed the effects of these substitutions on the catalytic activity. For comparative purposes, we also included in this study the Y337F and Y337A mutated HuAChEs (Tables 8, 9). The Tyr-337 residue is located on the opposite side of to Trp-86, relative to Tyr-133 (Fig. 12A) and like the latter its side chain projects into the gorge cavity. In contrast to the minor effect of replacement of Tyr-337 by phenylalanine, an analogous replacement at position 133 yielded an enzyme that is 7-fold less efficient (kapp) than the wild type HuAChE in hydrolysis of either ATC or TB (Table 8). The affinity of the Y133F enzyme towards the peripheral site specific ligand - propidium is comparable to that of the wild type HuAChE (Table 9) as could be expected from the location of its binding locus at the entrance to the gorge (more than 10Å away from Tyr-133, Barak *et al.*, 1994). Similarly the interaction of the Y133F mutated enzyme with the bisquaternary ligand decamethonium, which bridges the peripheral and the active center binding sites, shows a minimal change (less than 3-fold) in the value of Ki as compared to the wild type enzyme (Table 9). It was therefore quite surprising that the specific active center inhibitor edrophonium exhibited a 30-fold decrease in affinity relative to the wild type enzyme (Table 9). The molecular modeling analysis of the Y133F enzyme complexes, described below, provides a rationale for the differential behavior of the two quaternary ligands decamethonium and edrophonium, on the basis of the effect of this mutation on the orientation of Glu-202. This explanation is consistent with the proposed involvement of the hydroxyl group of Tyr-133 in the hydrogen bond network (Fig. 11; Ordentlich *et al.*, 1993b) and could also account for the decrease in kcat for hydrolysis of ATC and TB or for the 10-fold decrease in the phosphorylation rate constant of the Y133F enzyme by DFP (Table 9).

The outcome of the replacement of Tyr-133 by alanine is by far more dramatic than that

resulting from its replacement by phenylalanine. For the Y133A HuAChE, we observed a 90-fold increase in Km, relative to the wild type enzyme, for ATC (Table 8). To date, out of the 80 HuAChE residues analyzed by mutagenesis, the effect of Tyr-133 substitution on the Km is second only to that of Trp-86 replacement by alanine or glutamate. In addition, replacement of Tyr-133 by alanine resulted in 8-fold reduction of kcat, similar to the 5-fold decrease in the corresponding rate observed for W86A enzyme. The combined effects on Km and kcat are reflected in a 760-fold reduction in kapp for ATC in the HuAChE Y133A enzyme, comparable to the 3400-fold decrease for hydrolysis of the same substrate in the W86A HuAChE (Table 8). The observed similarity in kinetic parameters for ATC hydrolysis, and especially in Km, of W86A and of Y133A HuAChE enzymes (but not for the W86F or the Y133F HuAChEs) may imply that these two aromatic residues, are involved in stabilization of the enzyme-substrate complex. However unlike the differential effect of mutation W86A on the hydrolysis of ATC versus TB, mutation Y133A results in a marked reduction in catalytic activity for both substrates (Table 8). It therefore appears that replacement of Tyr-133 by alanine has more profound consequences on the integrity of the active center than the analogous replacement of Trp-86. This assumption is also supported by comparison of the reactivities of the Y133A enzyme towards the noncharged and charged inhibitors. As can be seen in Table 9, substitution of Tyr-133 by alanine results in almost 400-fold reduction in the phosphorylation rate by DFP, similar to the decrease in kapp for ATC . It is also noteworthy that the change in the apparent bimolecular rate constants for phosphorylation by DFP usually parallels that of the kapp for hydrolysis of TB by any of the mutated HuAChEs tested (Tables 8, 9). If a similar reduction in reaction rate is assumed for catalysis of TB by the Y133A enzyme the expected value of kapp should be below the background readings in our system which explains our inability to measure hydrolysis of TB by the Y133A mutant. Like the replacements of Trp86 by aliphatic residues also substitution of Tyr133 by alanine, but not phenylalanine, results in marked resistance to inhibition by peripheral ligands such as decamethonium or propidium (Table 9, Fig 10).

The limited effect of substitution of Tyr-337 by alanine or phenylalanine, relative to the wild type enzyme, is in accordance with the observation that of the three residues studied Trp-86, Tyr-133 and Tyr-337, the latter is the least conserved among ChEs and is replaced by alanine and phenylalanine in BChE and TcAChE, respectively (Gentry and Doctor, 1991; Massoulie *et al.,* 1993).

Molecular Modeling of the Various Mutants and their Complexes with ATC and with Reversible Quaternary Ligands

According to the crystal structures of TcAChE complexes with edrophonium and decamethonium (Harel *et al.*, 1993) and the models of the corresponding HuAChE complexes (Barak *et al.*, 1994) the positions of the quaternary groups of the two ligands, adjacent to the indole moiety of Trp-86, are practically equivalent. The positional equivalence of the quaternary groups, in the complexes of both ligands implies that nearly optimal juxtaposition with the Trp-86 indole moiety has been achieved. Thus, modeling of complexes of edrophonium with HuAChE enzymes mutated at positions 86 and 133, together with the measured reactivities of the corresponding mutants towards ATC and edrophonium, may provide insight as to the particular roles of Trp-86 and Tyr-133 in catalysis. Moreover, the HuAChE - edrophonium complex may serve a template for modeling of the Michaelis - Menten complex of ATC since the position of the quaternary group for the latter appears to be strongly dependent upon the presence of Trp-86.

Modeling of the W86F and Y133F HuAChE enzymes and their edrophonium and decamethonium complexes : Models of the W86F and Y133F HuAChE enzymes were obtained from the HuAChE model (Barak *et al.*, 1992) by replacing the appropriate side chains, adjusting their geometry and optimizing the resulting structure as described before (Ordentlich *et al.*, 1993a; Barak *et al.*, 1994). The resulting model of W86F mutated enzyme is very similar to that of the wild type enzyme, including the overlapping positions of the aromatic moieties at position 86. Only minor shifts in residues Tyr-419 and Trp-430, adjacent to residue at position 86, could be observed. The only notable change in the model of Y133F mutant, relative to that of the wild type, is a moderate conformational modification of the side chain of Glu-202 and a shift of the water positioned originally between Tyr-133, Glu-202 and Gly-120.

Edrophonium and decamethonium were docked into the active center of W86F and Y133F enzymes according to their positions in the complexes with the wild type enzyme (Barak *et al.*, 1994). In the optimized structures of the enzyme complexes, the positions of the quaternary groups of the ligands, relative to phenylalanine-86 in W86F enzyme (see Fig.13B) and to tryptophane-86 in Y133F enzyme (not shown) are very similar and correspond closely to the

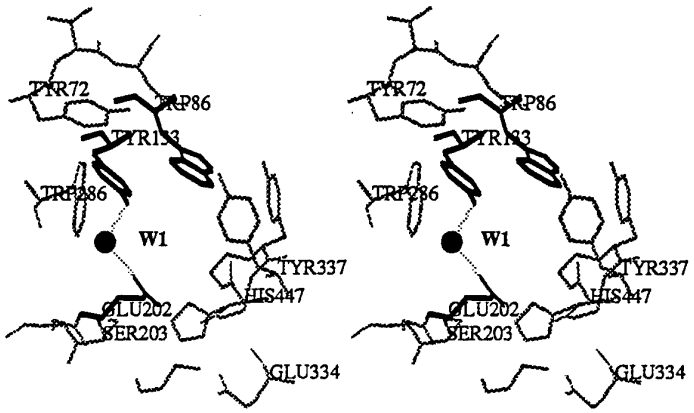

Fig. 11 Stereo view of the HuAChE active center demonstrating the hydrogen - bond interaction between residues Tyr-133 and Glu-202 through a water molecule. The position of water molecule W1 in the model of HuAChE is assumed to be similar to that of water-4 (HETATM - 4297; PDB1ACE.ENT) in the x - ray structure of TcAChE [distances: O^{η}(Tyr133)-O(W1) 2.50Å; O^{ε}(Glu-202)-O(W1) 3.01Å]. This interaction is a part of a hydrogen - bond network spanning the cross section of the active site gorge of HuAChE (Ordentlich *et al.*, 1993b). Other residues depicted in the figure are: the catalytic triad Ser-203, His447 and Glu-334; Trp-86 (shown in heavy line), Tyr-337, and the peripheral anionic subsite residues Tyr-72 and Trp-286 at the entrance to the active site gorge.

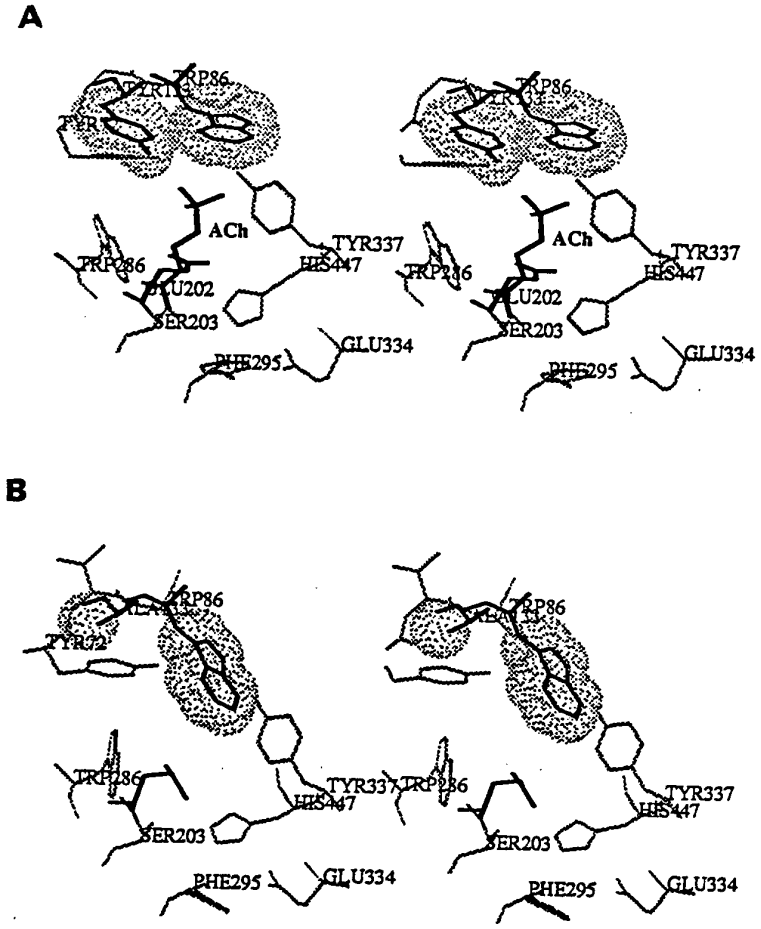

Fig. 12 Stereo view of the most stable positions of the indole moiety of Trp-86 in the active center of wild type and Tyr-133Ala mutated HuAChEs. The most stable conformer of the Trp-86 side chain is depicted for each type of enzyme. Proximity of the side chains, of residues at positions 86 and 133, is illustrated by van der Waals surfaces. The position of the quaternary ammonium group of the substrate ATC, relative to the aromatic ring of Trp-86 is depicted in its noncovalent complex with the wild type HuAChE in panel A. **A.** The displayed conformer of Trp-86 side chain in wild type HuAChE (χ_1=-56.3°; χ_2=108.2°) is more stable by 0.48 kcal/mole than the second most stable conformer which is analogous to that shown in panel B (χ_1=-65.9; χ_2=1.72°). **B.** The displayed conformer of Trp-86 side chain in Y133A (χ_1=-57.7°; χ_2=107.0°) is more stable by 1.65 kcal/mole than the next stable conformer analogous to that displayed in panel A (χ_1=-68.5°; χ_2=4.6°). Note that in the conformation displayed in panel B the indole moiety of Trp-86 should interfere with binding at the active center.

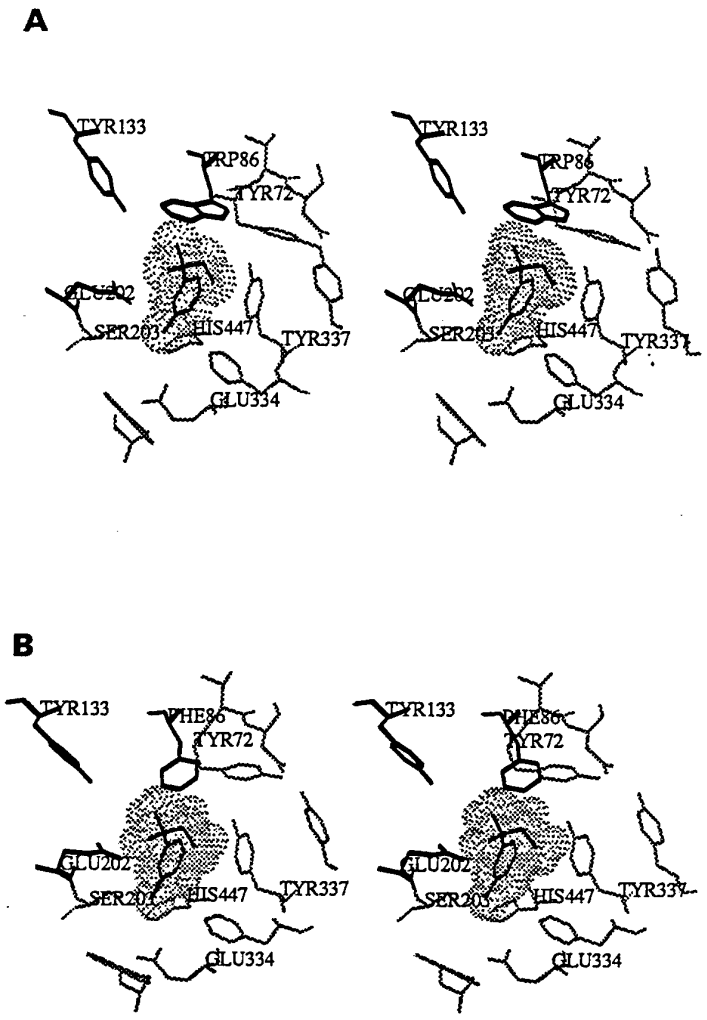

Fig. 13 Stereo views of edrophonium complexes with the wild type HuAChE and the W86F enzyme. The ligand, residues Tyr-133, Glu-202 and amino acid at position 86 are marked by a heavy line. The volume of the ligand is marked by dot surface. Note the distinct interactions of each of the three structural moieties of the ligand: the quaternary group is facing the aromatic ring of residue at position 86; the edge of the ligand aromatic moiety is wedged between the carboxylate oxygens of Glu-202; the hydroxyl group is within hydrogen - bond distance from O^{γ}–Ser-203 and $N^{\varepsilon 2}$-His-447. **A**. HuAChE- edrophonium complex. **B**. W86F HuAChE- edrophonium complex.

wild type complexes (see Fig. 13A for HuAChE-edrophonium complex). Thus, the cation - π interaction of the quaternary ammonium group with the aromatic substituent at position 86 is maintained by phenylalanine, although the interaction energy is lower than that for tryptophane. The aromatic group of the latter is π-excessive and contains an extended π-electron system which is therefore more negative and polarizable than that of benzene (Remers, 1971; the SYBYL force field reproduces a more favorable interactions of tetramethyl ammonium ion with indole than with phenyl moieties however it is not specifically parametrized to allow for quantitative estimations of such differences). The more favorable cation - π interaction of edrophonium or decamethonium with indole than with phenyl at position 86, may account for the 60 and 80-fold increase of the inhibition constant ($\Delta\Delta G$= 2.44 kcal/mole and 2.65 kcal/mole respectively), for these ligands in W86F HuAChE relative to the wild type enzyme.

The equivalent positions of the quaternary groups in Y133F HuAChE and in the wild type enzyme complexes indicate that the ligands do not interact directly with the aryl moiety of Y133 (Fig. 12A, 13A). Therefore, the 30-fold increase of the Ki value for inhibition of Y133F by edrophonium, relative to the wild type enzyme, is probably due to an indirect effect of Tyr-133 replacement, affecting the conformation of other active center residues. We note that the carboxylate of Glu-202 in the wild type enzyme is in a more favorable position to interact with the aromatic group of edrophonium. In the model of Y133F - decamethonium complex (not shown) no appreciable differences with respect to the model of the wild type enzyme complex (Barak *et al.*, 1994) could be observed .

Modeling of ATC complexes with HuAChE and W86F mutant : Construction of the HuAChE - ACh noncovalent (Michaelis Menten) complex started with superposition of the ACh quaternary ammonium group on the equivalent moiety in the HuAChE - edrophonium complex. In the all trans conformation of ACh the carbonyl oxygen was positioned within interaction distance from the amide nitrogens of the oxyanion hole (Gly-121, Gly-122), bringing the terminal methyl group into the acyl pocket (Phe295, Phe297). In the final structure the O^{γ}–Ser-203 is within hydrogen- bond distance (2.95Å) from the alkoxy oxygen of ACh (Fig. 12A). Similar docking of ACh into the model of W86F HuAChE results in a structure which is equivalent to that of the complex with the wild type enzyme.

Modeling of the Y133A HuAChE enzyme : As already mentioned, residue Tyr-133 does not appear to interact directly with the ligands in HuAChE complexes with ATC, edrophonium or decamethonium. Therefore, it is quite striking that the Y133A mutation had such dramatic effects on the various aspects of the enzyme chemical reactivity including catalytic activity towards charged and noncharged substrates as well as covalent and noncovalent inhibitors. Molecular modeling provides insight into these surprising results by investigating the effect of elimination of aromatic residue from position 133 on the conformation of other residues at the active center. Examination of molecular models shows that replacement of residue Tyr-133 by alanine induces an altered conformation of Trp-86 in which the indole moiety is rotated by over 100° (around χ_2) from its position in the wild type enzyme (Fig 13B). On the other hand, replacement of Tyr-133 by phenylalanine had only a small effect on the expected conformational mobility of residue Trp-86 and resembles that of wild type. The conformational transition introduced by replacement of Tyr-133 by alanine places the Trp-86 indole group across the gorge obstructing the access to the active site. Therefore, this energetically favored conformation (1.6 kcal/mole) for the Y133A HuAChE mutant (Fig. 12B) should interfere with any ligand interacting with the active center.

DISCUSSION

How is the Quaternary Ammonium Moiety of AChE Ligands Stabilized in the Active Center ?

Early studies of the rate of hydrolysis of various charged and noncharged substrates as well as the observed ability of tetraalkylammonium derivatives to inhibit AChE in a pH dependent manner, have led to the hypothesis that the active center contains a quaternary ammonium binding subsite (for reviews see Rosenberry, 1975; Quinn, 1987; Massoulie, *et al.*,1993). Wilson (1952) postulated that this subsite is predominantly involved in ionic interactions and therefore should be regarded as the "anionic subsite". An alternative view negated the ionic character of this site and suggested it to be essentially nonpolar in character, accommodating the charged ammonium groups through either ion - induced dipole or through van der Waals interactions (O'Brien, 1971; Hassan *et al.*, 1980; Nair *et al.*, 1994).

These opposing views regarding the nature of the classical "anionic subsite" which were

based mainly on structural and mechanistic assumptions may now be reevaluated relying on the molecular structure of AChE and on modern techniques for site directed manipulation of the enzyme structure. Examination of the x - ray structure of TcAChE (Sussman *et al.*, 1991) and the derived model of HuAChE (Barak *et al.*, 1992), reveals that the only negatively charged residue vicinal to the catalytic serine is Glu-202. The two other acidic residues: Asp-74 and Glu-450, located within the active site gorge, are 15.1Å and 8.9Å away from residue Ser-203 respectively (measured from $O^{\varepsilon 2}$-Glu-450 or $O^{\delta 2}$-Asp-74 to O^{γ}-Ser-203) and are therefore unlikely to participate in interactions of the "anionic subsite". From the kinetic data in Table 8 it is evident that substitution of Glu-202 by the neutral residue glutamine has a comparable effect on catalysis for both ATC and its noncharged isostere TB, suggesting that residue Glu-202 has no specific role in stabilizing positively charged substrates and therefore is not a part of the "anionic subsite". On the other hand, recent kinetic data (reviewed by Taylor and Radic, 1994) indicates that the negative charge at position 202 plays an important role in the acylation step of the catalytic reaction (Radic *et al.*, 1992;Shafferman *et al.*, 1992b) as well as in phosphylation, carbamoylation (Radic *et al.*, 1992; Ordentlich *et al.*, 1993b), aging (Ordentlich *et al.*, 1993b; Saxena *et al.*, 1993) and for interactions with noncovalent ligands (Radic *et al.*, 1992; Shafferman *et al.*, 1992b).

Unlike the indiscriminate effect on catalysis due to replacement of Glu-202, substitutions at position 86 affect differentially the hydrolytic activity towards charged and noncharged substrates (Table 8). While the wild type enzyme is 20-fold more active towards ATC than towards TB, the HuAChE mutants carrying aliphatic residues at position 86 show 50-fold higher reactivity for TB. This reversal of selectivity towards the sterically identical noncharged substrate, and the fact that kinetic parameters for TB are only marginally affected by the various mutations, is a clear manifestation of the existence of a functional "anionic subsite" and of the role of residue Trp-86 in this subsite. The effect of substitution of Trp-86 by non-aromatic residues suggests a role for this position in stabilizing the Michaelis Menten complexes of HuAChE with charged substrates. Such conclusion is also supported by : a. the lack of measurable affinity of W86A and W86E mutants towards the charged active center inhibitor edrophonium; b. the 8500 and 15000-fold increase, relative to the wild type enzyme, in Ki value for decamethonium in the W86A and W86E enzymes respectively; c. the hundred fold higher affinity of W86F HuAChE towards edrophonium or decamethonium, compared to either the W86A or the W86E enzymes (Table 9). In marked contrast, the nature of residue at

position 86 has only a marginal contribution to the activity of HuAChE towards noncharged substrates like TB or noncharged inhibitors like DFP. Taken together these observations imply also that in the Michaelis Menten complexes, the orientations of the trimethyl ammonium and the 3,3-dimethylbutyl groups, of ATC and TB respectively, are not equivalent relative to residue Trp-86. The topographical distinction between trimethyl and trimethylammonium sites, was also suggested by Berman and Decker (1986) on the basis of the differential affinity of the covalent adducts of AChE with isosteric charged and noncharged methylphosphonates, towards the fluorescent ligand decidium. The contrasting suggestions, regarding the "anionic subsite" as a common trimethyl binding site (Cohen *et al* 1984; Cohen *et al.*, 1985) or a common locus for dispersion interactions (Nair *et al.*, 1994), cannot be reconciled with either the differential effects of substitutions at position 86 of HuAChE or the results of Berman and Decker (1986).

Accommodation of the quaternary ammonium groups of AChE ligands by the indole moiety of residue Trp86 is an additional example of interactions between organic cations and protein aromatic residues, the importance of which is recently becoming recognized as major contributors to molecular recognition. The stabilizing interaction involves the positive charge and the electron-rich face of an aromatic ring. Such cation - π interactions were investigated both theoretically (Gao *et al.*, 1993; Kearney *et al.*, 1993) and experimentally, using several synthetic host molecules (Dougherty and Stauffer 1990; McCurdy *et al.*, 1992; Garel *et al.*, 1993). The nature of the interactions is predominantly electrostatic involving ion - dipole, ion - quadruple and ion - induced dipole (Schneider, 1991, McCurdy *et al.*, 1992). Analysis of protein structures shows that protonated amines interact favorably with aromatic groups (Burley and Petsko, 1988). The crystal structures of TcAChE complexes with edrophonium and decamethonium (Harel *et al.*, 1993) and that of the Fab McPC603-phosphocholine complex (Satow *et al.*, 1986) demonstrate interactions of quaternary ammonium moieties with tryptophan and tyrosine residues. Mutagenesis, NMR and fluorescence binding studies indicate that aromatic moieties are important determinants in binding of quaternary amines to nicotinic and muscarinic ACh receptors (Galzi *et al.*, 1991; Wess, 1993; Fraenkel *et al.*, 1990) as well as to the peripheral anionic sites of AChE (Ordentlich *et al.*, 1993a; Radic *et al.*, 1993; Barak *et al.*, 1994).

In conclusion, results from site directed mutagenesis of HuAChE and from x - ray crystallography of TcAChE (Sussman *et al.*, 1991) and its complexes (Harel *et al.*, 1993)

provide a compelling evidence for the presence of a specific locus - "anionic subsite". This site stabilizes the quaternary ammonium groups of substrates and other ligands through cation-aromatic interactions mainly with residue Trp86, rather than through ionic interactions.

The Dual Role of Tyr-133 in Maintaining the Functional Integrity of the Active Center

Although molecular model of the mutant Y133F enzyme suggests only minor changes, as compared to the wild type enzyme, mainly in orientation of Glu-202, kinetic results indicate that removal of the hydroxyl group, at position 133, affects both hydrolytic activity and affinity towards edrophonium. Such effects are compatible with the proposed participation of the hydroxyl group of Tyr-133 in a hydrogen - bond network (Ordentlich *et al.*, 1993b) that maintains the proper orientation of the carboxylate of Glu-202. Indeed, substitution of Tyr-133 by phenylalanine affects catalysis almost to the same extent as replacement of Glu-202 by glutamine (Table 8). This parallelism, in behavior of the Y133F and E202Q enzymes, is not limited to hydrolytic activity towards substrates but is observed also for phosphorylation of the respective mutants by DFP or with their comparable decrease in affinity towards the active center inhibitors edrophonium and decamethonium (Table 9). In the HuAChE - edrophonium complex the edge of the aromatic moiety of the inhibitor is wedged between the two negatively charged O^{ε}-Glu-202 (Fig. 13A) and thus can participate in charge - quadruple interactions (Burley and Petsko, 1988). The nature of these interactions obviously depends on the exact positioning of the carboxylate with respect to the ligand. It is worth noting that in decamethonium, which unlike edrophonium cannot participate in such interactions, the Y133F and E202Q enzymes show only 2-5-fold decrease of affinity relative to the wild type enzyme. Thus, it appears that the main role of the hydroxyl group of Tyr-133 is in providing the exact juxtaposition of the Glu-202 carboxylate, relative to the elements of the active site. Such positioning may be important in stabilizing the evolving transition states of acylation and other covalent reactions of the catalytic serine like phosphylation and carbamoylation.

Replacement of residue Y133 by alanine produces enzyme severely impaired in its reactivity towards substrates and inhibitors (Tables 8, 9). This may be interpreted to suggest that Tyr-133 is a key element in stabilization of the complexes with the various ligands however the corresponding models show that residue at position 133 does not interact directly with any of the substrates or inhibitors examined here. Therefore, the altered reactivity of Y133A probably

originates from modification of the active center induced by the replacement at position 133. On the other hand such modification affects mainly the noncovalent binding of substrates and inhibitors since Y133A mutant is still a very efficient catalyst of ATC hydrolysis with kcat only 8-fold lower than that of the wild type enzyme, suggesting that the catalytic machinery has been only slightly affected. A possible characterization of the modification of the active center in the Y133A enzyme is provided by the molecular model according to which removal of the aromatic group from position 133 induces rotation of the Trp-86 side chain placing the indole moiety across the active site gorge (Fig. 12B). In this conformation the indole is stabilized by interactions with other residues lining the wall of the gorge and consequently obstructing the access of substrates and other ligands to the active site of the enzyme. Finally, the particular way of maintaining the proper geometry of the quaternary ammonium binding subsite, through aromatic - aromatic interactions, may not be unique to AChE. Clusters of aromatic residues have been implicated, by site directed mutagenesis and molecular modeling, in the putative binding sites of receptors for ACh and other monoamine neurotransmitters, suggesting that aromatic - aromatic interactions can be instrumental in binding of ammonium ions in a variety of macromolecular systems (Hibert *et al.*, 1993).

Possible Functional Significance of Two Conformational States of Trp-86

Molecular models of the wild type, Y133F and Y133A enzymes reveal that the side chain of residue Trp-86 can occupy two conformational states: one that is functional as the "anionic subsite" while the other occludes the active center and should reduce catalytic efficiency (Fig. 14). This effect on catalytic activity, due to the alternation between the two conformational states of a single residue, raises the intriguing possibility that the enzyme actually utilizes this structural flexibility to adjust its catalytic efficiency.

One of the more elusive features of AChE reactivity is the allosteric modulation (Changeux 1966) of the catalytic activity following ligand binding to the peripheral sites on the enzyme surface. In the past, evidence was presented that such peripheral site ligands, including the natural substrate, or other chemical stimuli present in the synaptic cleft such as bivalent cations (Ca^{+2}, Mg^{+2}) affect the conformation of the active center (Radic *et al.*, 1991; Berman and Nowak, 1992). Furthermore, allosteric modulation of AChE activity was demonstrated only for charged substrates and inhibitors. Since we have demonstrated the role of Trp-86 in the binding of charged substrate and its potential conformational mobility, it is possible that

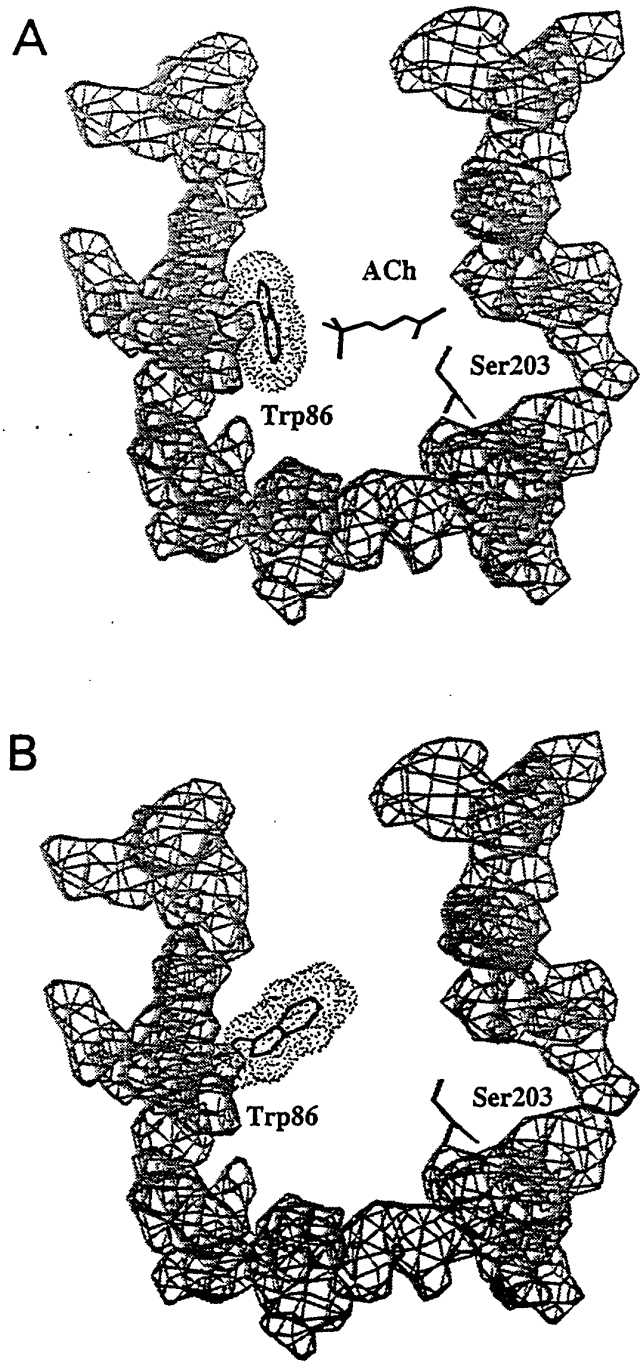

Fig. 14 Proposed accessibility of the HuAChE active center in the two conformational states of residue Trp-86. A side view cross - section of the active site gorge is represented by volume contours of the amino acids lining its walls. The volume of Trp-86 side chain is marked by dot surface and the side chain of Ser-203 marks the position of the active site. **A**. The functional conformation of Trp-86. The substrate ACh can access the active site and orient its quaternary ammonium for favorable interaction with the indole moiety ("anionic site"). **B**.The blocking conformation of Trp-86. The side chain is positioned across the gorge obstructing access of substrates and other ligands to the active site. Transition between state A and B is proposed to be induced in response to binding of ligands to the peripheral anionic site at the entrance to the active site gorge.

motion of this residue, induced by an allosteric signal on the surface, abolishes the "anionic subsite" and at the same time blocks the access to the active site (Fig. 14). Such mechanism of allosteric modulation of AChE provides a ready explanation for the baffling inhibition patterns of W86E, W86A and Y133A HuAChE enzymes, by the peripheral site ligand propidium compared to the marginal effects in the W86F and Y133F HuAChEs. Accordingly, the resistance of W86A and W86E enzymes to inhibition is simply due to the absence of a bulky residue, suitable for blocking the access to the active site, in these mutated HuAChEs. In the Y133A enzyme (but not in the Y133F HuAChE) the conformation of Trp-86 blocking the active center (Fig. 12B) is present prior to the exposure to propidium and therefore only a minor inhibitory effect due to addition of propidium can be expected. In both cases propidium binding to the peripheral anionic site, at the entrance to the active site gorge, should be hardly affected. Indeed, preliminary results from fluorescence binding studies of propidium with purified W86A mutated HuAChE appear to support this prediction.

Although the conformational flexibility of Trp-86 and its effects on the catalytic activity provide a possible mechanism for the "cross - talk" between the peripheral sites and the active center, the relay path of the allosteric signal is still unclear. Clues to a possible way for signalling the incidence of binding at the periphery to the active center and for inducing motion of Trp-86, can be found in the fact that the central binding element of the peripheral site - Asp-74, which was also implicated in the "cross - talk" mechanism (Shafferman *et al.*, 1992b), as well as Trp-86 are part of the sequence comprising the small cysteine loop (Cys-69-Cys-96). It is conceivable that external stimuli affecting Asp-74 might alter somewhat the position of this loop relative to the rest of the structure, separating the indole moiety of Trp-86 from the aromatic ring of Tyr-133 and thus inducing the conformational transition of the side chain of Trp-86 that obstructs the active site. The potential flexibility of the TcAChE small cysteine loop was indeed suggested by molecular dynamics studies (Axelsen *et al.*, 1994). Accordingly, one may design selective structural modifications within this loop, concomitant with other changes of residues in the active center gorge, and utilize various molecular probes to further explore this putative mechanism of signal transduction that modulates the enzymatic activity of AChE.

V. Allosteric Modulation of Acetylcholinesterase Activity by Peripheral Ligands Involves a Conformational Transition of the Anionic Subsite.

INTRODUCTION

One of the more intriguing features of acetylcholinesterase (AChE) reactivity is the modulation of its catalytic activity following ligand binding to peripheral site (PAS) at the enzyme surface (Changeux, 1966; Hucho *et al.*, 1991; see also Section III). The significance of such modulation for the enzymatic function is probably in adjusting the catalytic activity to the rapid fluctuations in the concentration of neurotransmitter and other charged species, like cations Ca^{++}, Mg^{++} and Na^{+}, in the synaptic cleft (Berman and Nowak, 1992). While evidence exists that peripheral site ligands affect the conformation of the active center (Berman *et al.*, 1981; Taylor and Radic, 1994), implying an allosteric effect, direct evidence is still lacking and the actual mechanism of this modulation is yet unknown. The resolution of the enzyme structure by x-ray crystallography (Sussman *et al.*, 1991), did not yield any clues as to this mechanism but rather rendered it more enigmatic by placing the active site within a narrow 'gorge' about 20Å away from the periphery.

Site directed labelling (Weise *et al.*, 1990), mutagenesis studies and molecular modeling (Shafferman *et al.*, 1992a,b; Ordentlich *et al.*, 1993a; Radic *et al.*, 1993; Barak *et al.*, 1994) allow for the identification and localization of the PAS residues at the protein surface and near the rim of the active center gorge. These include aromatic residues Tyr72, Tyr124, Trp286 and Tyr341 that together with the acidic residue Asp74 constitute an array of partially overlapping but distinct binding sites (Barak *et al.*, 1994) capable of binding structurally diverse ligands like propidium, gallamine or fasciculin (Rosenberry, 1975; Quinn, 1987; Radic *et al.*, 1994). The relative locations of the active center and the PAS, in the molecular model of HuAChE (Barak *et al.*, 1992; based on the x - ray structure of *Torpedo Californica* acetylcholinesterase - TcAChE), are consistent with the suggestion that bisquaternary ligands, typified by decamethonium, bind to the enzyme by bridging the two sites (Harel *et al.*, 1993; Barak *et al.*, 1994). The location of PAS, relative to the gorge entrance, implies also that association of AChE with the prototypical PAS ligand propidium, may affect the access of substrates to the

active center by either physical obstruction or charge repulsion imparted by the cationic ligand (Taylor and Radic, 1994). Thus, the way by which PAS specific ligands like propidium exert their inhibitory effects is not yet clear.

The nearly equal affinities of propidium towards free and phosphylated TcAChE (Taylor and Lappi, 1975), indicates that modifications at the active site do not affect the binding properties of PAS. In addition, the failure of reversible active center inhibitors like edrophonium or N-methyl acridinium to displace propidium has been regarded as evidence for formation of ternary complexes (Taylor and Radic, 1994). On the other hand HuAChE mutant enzymes, in which the anionic subsite at the active center was altered by replacement of either residue Trp86 or the adjacent residue Tyr133 (both of which are about 15Å away from the PAS) by alanine, are practically refractory to inhibition by propidium (Ordentlich *et a*l., 1993; Ordentlich *et al* ., 1995). These findings imply that either the binding affinity of propidium to PAS has been indirectly affected by these replacements or that the allosterically induced conformational changes in the active center that abolish catalytic activity, are no longer possible. The first alternative is compatible with the notion that physical blocking of the active site gorge, by the PAS ligand, contributes to the inhibitory activity of propidium. Such a conclusion is also consistent with the molecular model of HuAChE - propidium complex (Barak *et al.*, 1994) in which the ligand obstructs the access to the active site. On the other hand, inhibition through conformational flexibility of the side chain of residue Trp86 is consistent with the differential catalytic activities of the W86A and Y133A enzymes towards the charged substrate ATC and its noncharged isostere TB, relative to the wild type HuAChE (Ordentlich *et al.*, 1993; Ordentlich *et al.*, 1995).

In this study we further investigate the role of the active center residues Trp86 and Tyr133 in the inhibition of HuAChE catalytic activity, through ligand association with the PAS. We provide evidence that the affinity of W86A enzyme for propidium is close to that of the wild type HuAChE suggesting that the inhibitory effect of propidium is not a direct consequence of its association with the PAS. We demonstrate that the reactivity properties of the double mutant W86A/Y133A of HuAChE are consistent with the notion that conformational transition of residue Trp86 constitutes the structural response to the occupation of the PAS. Finally, we propose that the conformational state of Trp86 is governed by the dynamic behavior of the cysteine loop (Cys69 - Cys96) on the protein surface and that this mobility plays an important role in the mechanism of the allosteric effect in AChE.

METHODS

Mutagenesis of Recombinant HuAChE and Construction of Expression Vectors- Mutagenesis of AChE was performed by DNA cassette replacement into a series of HuAChE sequence variants which conserve the wild type (Soreq *et al.*, 1990) coding specificity, but carry new unique restriction sites (Shafferman *et al.*, 1992a). Generation of mutants W86A(W*84*), D74N*(72)*, Y133A(*130*), Y133F(*130*), Y341A*(334)*, and W286A*(279)* was described previously (Shafferman *et al.*, 1992b; Ordentlich *et al.*, 1995). The double mutant W86A/Y133A HuAChE was formed by substituting the *Eco* RV - *Esp* I fragment and the *Esp* I - *Bst* EII fragment of the human *ache* DNA with the respective fragments of the W86A and Y133A mutant DNAs. All the synthetic DNA oligodeoxynucleotides were prepared using an Applied Biosystems DNA synthesizer. The sequences of all new clones were verified by the dideoxy sequencing method (USB sequenase kit). The rHuAChE cDNA mutants were expressed in tripartite vectors which allow expression of the *cat* reporter gene and the *neo* selection marker (Kronman *et al.*, 1992, Shafferman *et al.*, 1992a).

Establishment of Stably Expressing Cell Pools and High Expressor Cell Clones Human embryonal kidney 293 cells were transfected by the calcium phosphate method as described previously (Kronman *et al.*, 1992). Following overnight incubation in the transfection mix, cells were refed with DMEM containing 10% ChE depleted FCS (PAT) after which the cells were incubated for an additional 48 h at 37°C in the presence of 5% CO_2. Transient expression levels of the various rHuAChE mutants was determined by AChE activity measurement complemented by specific enzyme - linked immunoadsorbent assay (ELISA; Shafferman *et al.*, 1992a). The latter allows assessment of AChE production by mutants in which enzymatic activity is impaired under normal conditions.

Cells in which stable integration of the plasmid has occurred were selected by exposure to G418 for a period of 3-4 weeks. In a typical experiment 100-200 stable G418 resistant cell colonies were formed. To assist confluent pool formation, cell colonies were trypsinized and allowed to resettle in the cell culture dish. Stably transfected cell pools were assayed for enzyme activity and protein mass (ELISA). Individual clones of the rHuAChE mutants Y72A, D74N W86A, Y133A, W286A, Y341A and Y72A/W286A were isolated by limiting dilution of the

stable pool cells followed by seeding onto 96-well microtiter plates. The arising cell clones (usually between 200-500 per AChE type) were subjected to screening procedures. In accordance with the data gathered at the transient expression phase and from the stable cell pools, the method of screening for high - producer clones was adopted. In all cases the selected high - producer clones displayed enzyme secretion level higher than 1 μg per 10^6 cells during 24 h period. In the cases of W286A and Y72A/W286A, especially high levels of secreted enzymes were observed (10-25 μg/10^6 cells/24 h).

Purification of HuAChE Enzymes - The crude HuAChE enzymes were purified by affinity chromatography on monoclonal antibody AE-1 (Fambrough *et al.*, 1982) coupled to Sepharose. Activation of Sepharose CL-4B was carried out according to Wilchek and Miron (1982). Purified AE-1 monoclonal antibodies were coupled to the activated Sepharose at a ratio of 15mg McAB/gram wet resin. The enzyme binding capacity of the column was 0.5-1.5 mg enzyme/ml gel. Following elution by 4M $MgCl_2$ in 1M glycine buffer pH 6.0, the purified enzyme was dialyzed, concentrated by 70% ammonium sulfate precipitation, resuspended in 10mM phosphate buffer pH 8.0 and dialyzed against either 10mM phosphate buffer pH 8.0 or 1mM Tris HCl buffer pH 8.0.

Substrates and Inhibitors- Acetylthiocholine iodide (ATC), 5:5'-dithiobis (2-nitrobenzoic acid) (DTNB), 3,8 diamino-5-3'-(trimethylammonium)propyl-6-phenyl phenanthridinium iodide (propidium), 1,5-bis(4-allyldimethylammoniumphenyl)pentan - 3-one dibromide (BW284C51), p-nitrophenyl diethyl phosphate (paraoxon) and diisopropyl phosphorofluoridate (DFP) were all purchased from Sigma. 3,3-Dimethylbutyl thioacetate (TB) was synthesized and purified as described previously (see Section II).

Determination of HuAChE Activity and Analysis of Kinetic Data- Catalytic activity of the recombinant HuAChE and its mutant derivatives collected from transiently or stably transfected cells were assayed according to Ellman *et al.*, (1961). Assays were performed in the presence of 0.1 mg/ml BSA, 0.3mM DTNB [5,5'-dithiobis(2-nitrobenzoic acid)] in 5mM or 50mM sodium-phosphate buffer pH 8.0 and varying ATC (0.01-0.6mM) concentrations. The assays were carried out at 27°C and monitored by a Thermomax microplate reader (Molecular Devices). Michaelis-Menten constants (Km) and the apparent first order rate

constants (kcat), were determined as described before (Shafferman *et al.*, 1992a,b). The apparent bimolecular rate constants (kapp) were calculated from the ratio kcat/Km.

Kinetic data for inhibition by propidium and determination of the competitive inhibition constants (Ki) were derived as described previously (Ordentlich *et al.*, 1993a; Ordentlich *et al.*, 1995) according to the kinetic treatment developed by Barnet and Rosenberry (1977) and Berman and Leonard (1990).

The apparent bimolecular rate constants for the irreversible inhibition of HuAChE enzymes by organophosphonates DFP and paraoxon (ki) were determined as described in Section VIII.

Equilibrium Fluorescence Titrations - Equilibrium titrations of purified W86A, D74N, Y133A, Y341A and Y72A/W286A enzymes with propidium were carried out essentially as described before (Taylor *et al.*, 1974; Taylor and Lappi, 1975). A SLM 500 spectrofluorometer was used to monitor ligand fluorescence at 625 nm, upon excitation at 535 nm. All fluorescence titrations were performed at 1 mM sodium phosphate buffer pH 8.0, at 25±0.2°C. Dissociation constants (K_D) were obtained from Scatchard plots. The concentrations of free (P_f) and bound (P_b) propidium are obtained from the following relations (Mooser *et al.*, 1972):

$$[P_f] = (I_o - \alpha'[P_o])/(\gamma - \gamma') \qquad [Pb] = [P_o] - [P_f]$$

where Io is the observed fluorescence intensity, $[P_o]$ is the total concentration of propidium and γ and γ' are fluorescence proportionality coefficients of free and bound propidium respectively (Taylor *et al.*, 1974). The coefficient γ' is evaluated from the initial limiting slope of the fluorescence titration curve where the concentration of the enzyme is much higher than that of propidium. In all cases, except except for one of the mutants, a saturable profile of the fluorescence titration curves was obtained. The contribution of nonspecific binding was estimated from fluorescence titration of the wild type enzyme in presence of 10-fold molar excess of the nonfluorescent PAS ligand BW284C51.

Generation of Alternative Conformations of HuAChE by Molecular Simulations
All simulations were performed on a SUN-Sparc 10 workstation using the AMBER 4.01 suite of programs with all-atom parameter set (Pearlman *et al.*, 1991). Characterization and visual examination of the molecular structures were done using the molecular modeling package SYBYL 6.03 (Tripos 1994) running on IRIS 4D/70GT workstation. The starting conformation

of the enzyme was the HuAChE model (Barak *et al.*, 1992). The cysteine loop (Cys69-Cys96) as well as the active center gorge were solvated by adding a spherical cap of water (using the SOL option in AMBER, a total of 691 molecules were added). The cap waters were restrained by soft half-harmonic potential to avoid evaporation without affecting the protein movement. The HuAChE residues included in the simulation (using the belly option in AMBER) comprised of the cysteine loop (Cys69-Cys96) as well as residues in or around the active site gorge (a total of 96 residues). The simulation protocol consisted of a. initial solvent relaxation followed by minimization of the entire structure (Laughton, 1994); b. gradual heating to 1000°K (at the rate of 50°K/3ps) and a production run of molecular dynamics carried out for 60ps, with weak coupling to a temperature bath (Björkstén *et al.*, 1991); c. from different starting points along this trajectory the system was cooled down to 300°K (at a rate of 50°K/3ps; Brünger and Krukowski, 1990); d. structural stability of the resulting structures was assessed via a molecular dynamics run at 300°K for 50ps, followed by averaging of the structures (using the MDANAL module of AMBER) and minimization.

RESULTS

Effects of Peripheral and Active Center Anionic Site Mutations on Inhibition and Binding by Propidium.

Recently several residues, at the rim of the AChE active site gorge, were identified as constituents of the PAS array, participating in interactions with a variety of PAS ligands (Shafferman *et al.*, 1992a,b; Radic *et al.*, 1993; Barak *et al.*, 1994). The molecular model of the HuAChE - propidium complex, constructed according to these studies, indicates that the inhibitor does not interact with the active center residues Trp86 and Tyr133 (the tetraalkylammonium group of the ligand is 9Å away from Trp86; Barak *et al.*, 1994). However, replacement of these residues by aliphatic amino acids resulted in enzymes almost refractory to inhibition by propidium. It was therefore suggested that the aromatic residue at position 86 is involved in the inhibitory process through allosteric interactions with the periphery (Barak *et al.*, 1994; Ordentlich *et al.*, 1995). In order to gain a better understanding of the way propidium exerts its allosteric inhibitory activity, we have studied the binding profiles of propidium to selected HuAChE enzyme derivatives. The experimental method

utilizes the spectroscopic characteristics of propidium which upon complexation with AChE shows a significant red shift in its absorption spectrum concomitant with fluorescent enhancement (Taylor *et al.*, 1974). These properties were used in the past (Taylor and Lappi, 1975; Berman *et al.*, 1981; Radic *et al.*, 1991) to demonstrate a correspondence between the kinetic value of the inhibition constant (Ki) and the value of the dissociation constant (K_D) for interaction of propidium with TcAChE.

Titrations were performed on HuAChE enzymes carrying replacement of residues at either the active center or the PAS and compared to the wild type enzyme. Since such titrations require purified enzymes in relatively large quantities, we generated stable 293 clone cell lines expressing constitutively high levels of the various HuAChE mutants. The screening for high producer cell clones of W286A, D74N, Y341A, and Y72A/W286A enzymes was possible through quantitative measurements of the catalytic activity, while those expressing the relatively unreactive W86A and Y133A enzymes through quantitative immunological assays (ELISA). Since most of the mutants were not bound to the procainamide - affinity columns, which are usually employed for rHuAChE purification (Kronman *et al.*, 1992), an alternative affinity column was developed, based on monoclonal antibodies (AE1) as described in the Methods section.

The concentrations of purified enzymes used in the fluorescence titrations with propidium were in the range of 0.6 - $2.0 \cdot 10^{-6}$ mole equivalent of HuAChE monomeric subunit. With the exception of the double mutant Y72A/W286A, the concentrations of the enzyme used corresponded within ±5% to the concentrations derived from the inflection points in the fluorescence titration curves (Taylor *et al.*, 1974). This stoichiometric ratio is clearly demonstrated in the Scatchard plots (Fig.15), again with the exception of the double mutant (Fig. 15F). We note that in the case of Y72A/W286A enzyme saturation of binding was not observed in the fluorescence titration curve, even at high propidium concentrations (up to 8mM) and from the corresponding Scatchard plot it appears that the value of K_D is at least 10-fold higher than that of the wild type enzyme. Results similar to those for the double mutant were obtained in control experiments where fluorescence titrations of the wild type enzyme were carried out in presence of saturating concentrations of the PAS bisquaternary ligand BW284C51, which should effectively compete out the specific binding of propidium to the PAS. The propidium fluorescence enhancement, under such conditions, was therefore regarded as nonspecific binding and it determined the upper limit of the method for evaluation

of the dissociation constants.

To evaluate the correlation between propidium inhibitory activity and its affinity towards the various HuAChE enzymes, inhibition experiments were carried out at ionic strength similar to that used for the binding studies. Resulting values of the inhibition constants Ki (Table 10) are an order of magnitude lower than those evaluated previously at higher buffer concentration (Barak *et al.*, 1994). The average K_D value for the wild type HuAChE (0.26μM) is similar to the values reported for TcAChE (0.1-0.37μM) under similar ionic strength conditions (1mM Tris buffer, pH=8; Taylor *et al.*, 1974; Taylor and Lappi, 1975; Radic *et al.*, 1991), and is in excellent agreement with the corresponding value of Ki (Table 10). It may be noted that the values of dissociation constants K_D, determined for TcAChE at high ionic strength (3.4-4.7μM; Berman *et al.*, 1987, Berman and Leonard, 1992) are about an order of magnitude higher. This behavior is consistent with the effect of ionic strength on the values of inhibition constants Ki and indicates the electrostatic nature of interaction of the positively charged ligand with the negative electrostatic field of the enzyme surface.

Examination of the corresponding values of K_D and Ki for the HuAChE enzymes reveals a clear distinction between the behavior of enzymes carrying replacements at the PAS and those enzymes mutated at the active center (positions 86 and 133). For the D74N and Y341A mutant HuAChEs, the minor effects on inhibition constants Ki, relative to the wild type HuAChE, are reflected by comparable changes in the values of K_D. In the case of W286A the 10-fold increase in Ki corresponds to the 4-fold increase in the value of K_D. The 170-fold increase in the value of Ki, for the double mutant Y72A/W286A, is again in complete accordance with our inability to measure high K_D values by the fluorescence titration method. Although suggested many times in the past, the identity of the locus interacting with propidium, at the AChE surface, was never before established by a direct measurement. The variation of the K_D values, for HuAChE enzymes carrying replacements at the periphery, demonstrates that residues Trp286, Tyr72 and Asp74 indeed constitute the binding site of propidium. Furthermore, the correspondence of the respective K_D and Ki values, for these HuAChE enzymes, demonstrates that the changes in the inhibitory activity of propidium are a direct outcome of an altered binding to the PAS. The aromatic residues, at positions 72, 124 and 286, were also identified recently as constituents of the binding site for fasciculin (Radic *et al.*, 1994), a PAS specific ligand competitive with propidium.

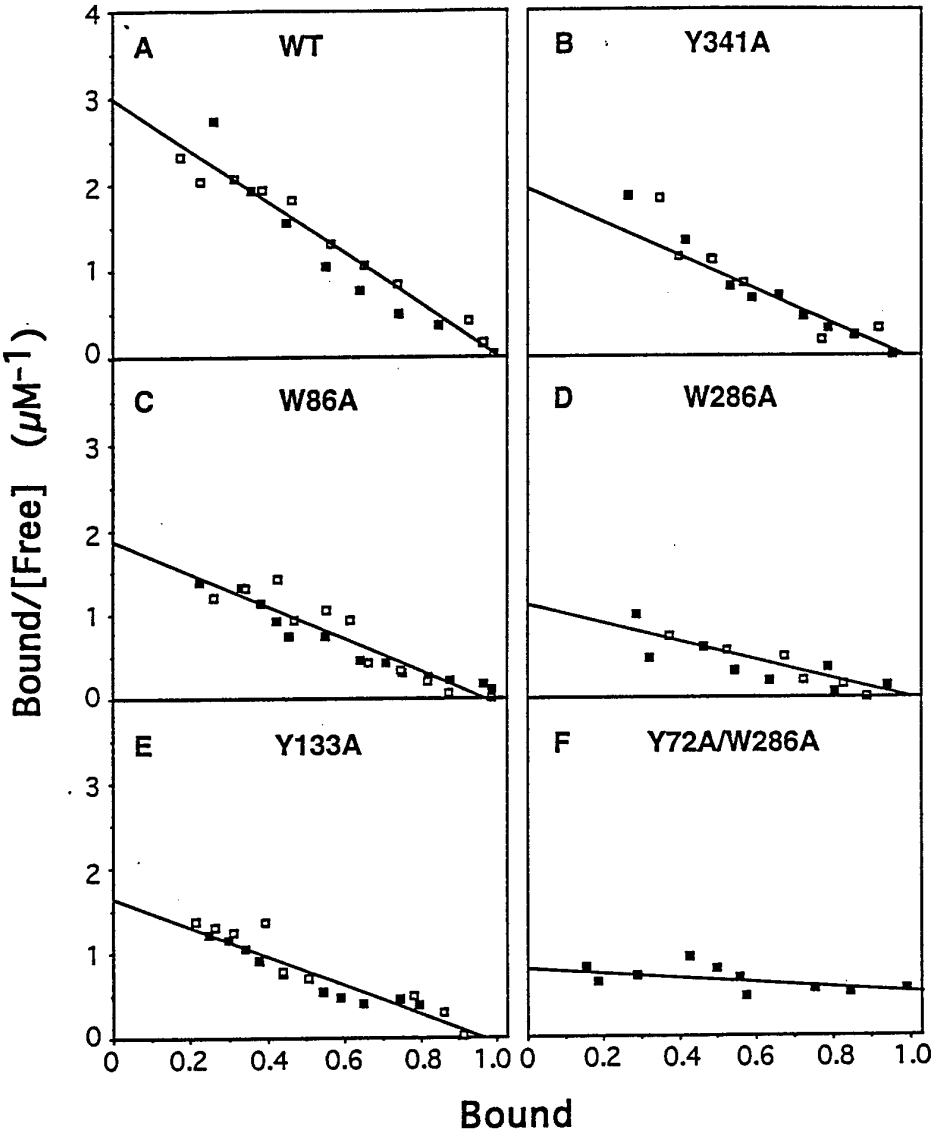

Figure 15: Scatchard plots of propidium association with wild type HuAChE and some of its derivatives. The enzyme identity and the concentrations of enzyme subunits used in the titrations are shown in the corresponding panels. For the double mutant Y72A/W286A (panel F), titration at the lower enzyme concentration did not exhibit measurable binding and was identical to that measured for the wild type enzyme in presence of excess BW284C51. Enzyme concentration range: empty squares (0.6-0.8μM); full squares (1.6-2.0μM).

In contrast with the good correspondence between K_D and Ki values observed for the HuAChE PAS mutants, for the HuAChE enzymes carrying replacements at the active center, the values of K_D are similar to that of the wild type HuAChE (less than 2-fold increase). Yet Ki values are 350-fold (for W86A) and 25-fold (for Y133A) higher than that for the wild type enzyme. Consequently, these results demonstrate that the resistance of the active center mutants W86A and Y133A to inhibition by propidium *is not a result of reduced binding but rather of an impaired inhibition mechanism.*

Effects of Replacement of Trp86 and Tyr133 on Reactivity Towards Organophosphates

Replacement of Tyr133 by alanine, but not by phenylalanine, was shown to compromise the reactivity of the corresponding HuAChE towards both charged and noncharged substrates (Ordentlich *et al.*, 1995). We have recently suggested that such reduced reactivity is due to a conformational transition of residue Trp86 in the active center, of the Y133A HuAChE mutant enzyme, resulting in destabilization of the initial noncovalent complexes with substrates (Ordentlich *et al.*, 1995). A similar transition was invoked with respect to the mechanism of inhibition induced by binding of propidium (Ordentlich *et al.*, 1995). To further investigate this putative mechanism we studied in detail the reactions of organophosphate covalent inhibitors with HuAChE enzymes carrying mutations at positions 86 and 133. The organophosphate inhibitors DFP and paraoxon, associate with AChE through formation of transient noncovalent complexes, followed by covalent attachment to the catalytic serine resulting in stable tetrahedral adducts. These reactions are analogous to the acylation step in AChE reaction with substrates and therefore should be similarly affected by structural changes in the active center. Treatment of the irreversible inhibition kinetic data, according to method by Hart and O'Brien (1973; Method B - see Section VIII), allows to evaluate the dissociation constants (K_d) of the initial noncovalent complexes EPX as well as the phosphorylation rate constants k_2 (see Scheme 1 Section VIII). Since in this method the K_d values are calculated from the apparent bimolecular rate constant of inhibition ($ki^B = k_2/K_d$), we confirmed these values by an alternative method (Method A, see Section VIII) where the bimolecular rates were determined under pseudo - first order conditions with respect to the inhibitor concentrations. Kinetics of phosphorylation reactions was studied for the wild type, Y133A, Y133F and

W86A HuAChE enzymes. According to our model the affinity of the Y133A enzyme towards the organophosphate derivatives should be much lower (higher values of K_d) compared to either that of the wild type HuAChE or to those of Y133F and W86A enzymes.

The values of bimolecular inhibition rate constants ki^A and ki^B for either DFP or paraoxon (Section VIII - Tables 16-18), as determined by the two independent methods, are very similar. This similarity corroborates the reliability of the values for K_d and k_2 derived from ki^B. Examination of the K_d values for the HuAChE enzymes shows as predicted, that while W86A and Y133F exhibit nearly wild type like affinity towards DFP, that of Y133A is 25-fold lower. An even more dramatic increase of the K_d value for Y133A HuAChE is observed in the case of paraoxon (517-fold). However, in this case, the respective K_d values are also somewhat higher for both W86A and Y133F (15-fold and 6-fold respectively), indicating that for paraoxon the steric requirements during complex formation with the enzyme are more stringent. The values of phosphorylation rate constants k_2 show little variation irrespective of the inhibitor or the HuAChE enzyme tested. The most notable deviation from the wild type HuAChE value is the 7-fold decrease of k_2 for the phosphorylation of Y133A enzyme by DFP. This finding suggests equivalent orientation of the inhibitor, relative to the nucleophilic serine, in the noncovalent complexes with the HuAChE enzymes.

The reactivity patterns for Y133A and Y133F enzymes towards organophosphates confirm our predictions and are consistent with the molecular models of Y133A and Y133F mutants (Ordentlich *et al.,* 1995). According to these models the only major difference, distinguishing the Y133A mutant from Y133F or the wild type enzymes, is the altered conformation of residue Trp86 in the active center.

Reactivity of the HuAChE Double Mutant W86A/Y133A Towards Charged and Noncharged Substrates

If as we propose, the main effect of replacing Tyr133 by alanine is steric occlusion of the active center through conformational transition of Trp86, it should be prevented by removal of the bulky indole side chain from position 86 in the Y133A mutant. In addition, the resulting double mutant HuAChE would lack the anionic subsite in the active center.

Indeed, generation of the W86A/Y133A enzyme and evaluation of its hydrolytic activity demonstrates that like the W86A enzyme, the double mutant is not active towards the charged substrate ATC (Table 11). Furthermore, the W86A/Y133A enzyme exhibits hydrolytic activity

towards the noncharged substrate TB with Km value similar to that of the wild type enzyme (Table 11). Thus, the reactivity pattern of the double mutant W86A/Y133A is clearly distinct from that of the Y133A enzyme for which no reactivity towards TB could be observed. It is interesting to note that the double replacement, at positions 86 and 133, has a substantial effect on the catalytic machinery as manifested by the 100-fold decrease of the kcat value, relative to the wild type HuAChE (Table 11). In part, this may be related to the removal of the H - bond acceptor moiety from position 133 since the corresponding kcat for the Y133F enzyme is 10-fold lower (Ordentlich *et al.*, 1995). Thus, the W86A/Y133A enzyme appears to exhibit binding characteristics, that discriminate between charged and noncharged ligands, resembling that of the W86A HuAChE. The fact that substitution of Trp86 by alanine within the Y133A enzyme *restores* the catalytic activity towards TB and in particular that the value of Km, of the W86A/Y133A mutant, is similar to that of the wild type enzyme, is consistent with the notion that Trp86 is indeed involved in restricting the access to the active center of the Y133A HuAChE. This is further demonstrated in the increase of Kd values for the organophosphate inhibitors, in the case of the Y133A enzyme.

Alternative conformations of the cysteine loop (Cys69-Cys96) in HuAChE

Residue Trp86 as well as Asp74, which is an important constituent of the PAS (Barak *et al.*, 1994), are part of the sequence comprising the cysteine loop (Cys69-Cys96). The notion that conformational mobility of residue Trp86 may be coupled to the occupation of the PAS, through rearrangement of this loop (Ordentlich *et al.*, 1995) prompted us to examine its conformational mobility. The conformational properties of the cysteine loop (Cys69-Cys96) in HuAChE were assessed by simulated annealing. Analysis of the several structures, resulting from the simulation protocol (see Methods), shows that the loop can assume a range of similar conformations that are different from that of the initial HuAChE model. One of these conformations is shown in Figure 16. The results indicate that: a) the cysteine loop (Cys69-Cys96) is the most mobile part of the structure; b) the observed conformational changes affect the positioning of Trp86 abolishing its function as the "anionic" locus in the active center; and most significantly c) the enhanced mobility is always confined to the same loop segment, although the simulated conformational changes cannot be classified as a rigid body motion.

Table 10: Dissociation constants and competitive inhibition constants of propidium for HuAChE and various PAS and W86 mutant derivatives

HuAChEs	K_D (μM)[a]	K_i (μM)[b]
Wild type	0.26 ± 0.07[c]	0.20 ± 0.02
W86A	0.48 ± 0.20	70 ± 35
Y133A	0.47 ± 0.17	5.0 ± 2.5
D74N	0.42 ± 0.24	0.83 ± 0.07
Y341A	0.30 ± 0.14	0.60 ± 0.10
W286A	1.00 ± 0.16[d]	2.15 ± 0.15
Y72A/W286A	≥ 3.1[e]	35 ± 5.0

[a] Values calculated from Scatchard plots of six independent measurements at different concentrations of catalytic subunits (0.6 - 2.0μM); ± refer to standard deviations).
[b] Values represent mean of triplicate determinations.
[c] Value in agreement with that reported by Barak *et al.*, 1994.
[d] Reported by Barak *et al.*, 1994.
[e] This lower limit value corresponds closely to that obtained for the wild type HuAChE in presence of large excess of the PAS ligand BW284C51 (see text).

Table 11: Kinetic constants for ATC and TB hydrolysis by W86A/Y133A HuAChEs compared to enzymes substituted at positions 86 and 133[a]

HuAChEs	K_m (mM)		k_{cat} (x10^{-5}min^{-1})	
	ATC	TB	ATC	TB
Wild Type[b]	0.14	0.30	4.0	0.55
Y133A[b]	26.0	-[c]	0.4	-[c]
W86A[b]	93.0	0.55	0.8	0.18
W86A/Y133A	-[c]	0.07	-[c]	0.005

[a] Values represent mean of triplicate determinations with standard deviation not exceeding 20%.
[b] Values correspond closely to those reported by Ordentlich *et al.*, 1993 and Ordentlich et al., 1995.
[c] Activity could not be detected.

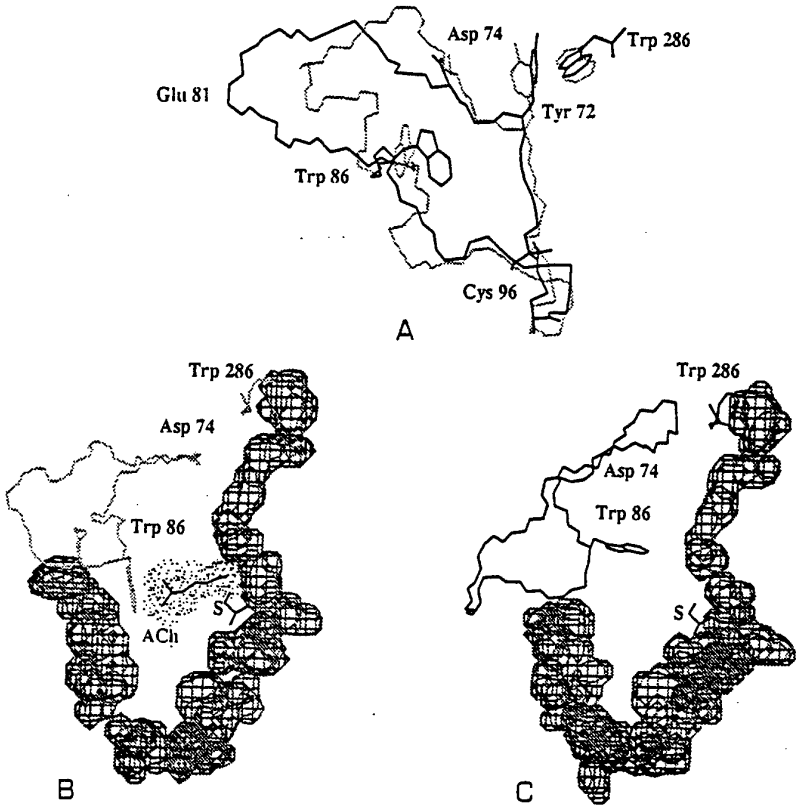

Figure 16 :Relation of the conformational state of residue Trp86 to the overall conformation of the cystein loop (Cys69-Cys96) and its effect on accessibility of the HuAChE active center. **A** - Superposition of the conformation derived from x-ray structure of AChE (light line) and a representative computed alternative conformation (heavy line) of the loop obtained from simulated annealing of HuAChE (Ariel *et al.*, in preparation). Note that the major movement occurs in the stretch spanning 16 aminoacids from Asp74 to Arg90. The position of the indole moiety of Trp86 relative to the active site gorge is provided in panels B and C, where a side view cross - section of the gorge is represented by volume contours along with the respective conformation of the loop. **B** - The functional conformation of Trp86, allowing the substrate ACh (shown with its van der Waals volume) to access the active center and interact favorably with the indole moiety (anionic site). S denotes the location of the active site Ser203. **C** - Nonfunctional conformation of Trp86, blocking access of substrates and other ligands (e.g. DFP, paraoxon etc.) to the active center.

DISCUSSION

How Does Propidium Inhibit HuAChE?

The molecular mechanism of allosteric modulation of AChE activity, following ligand binding to peripheral sites, has been a subject of considerable interest ever since proposed almost 30 years ago (Changeux; 1966) . Early studies established that structurally diverse ligands like propidium, tubocurarine and gallamine can occupy binding sites which are distinct from the active site, all eliciting similar but not identical changes in the active center (Berman *et al.*, 1981). These changes were associated with the inhibitory effects on AChE catalytic activity and were analyzed in terms of two state models whereby the ligands alter the distribution between reactive and unreactive conformations of the enzyme (Pattison and Bernhard, 1978; Tomlinson *et al.*, 1980). Recently, the involvement of specific residues in the binding sites array, referred collectively as PAS, has been suggested by site directed mutagenesis and kinetic studies of inhibition by PAS - specific ligands as well as by x - ray crystallography (Shafferman *et al.*, 1992a; Radic *et al.*, 1993; Harel *et al.*, 1993; Barak *et al.*, 1994). Elements of this array are located at or near the rim of the active site gorge and include Trp286 and a cluster of vicinal residues (Tyr72, Tyr124 and Glu285) as well as residues Asp74 and Tyr341 located on the other side of the gorge entrance. A common feature of these sites is a core comprising of residues Trp286 and Asp74 (Shafferman *et al.*, 1992a; Barak *et al.*, 1994). The propidium fluorescence titration experiments of D74N, W286A, Y341A and Y72A/W286A HuAChE enzymes reported here (Fig. 15), demonstrate the correlation between affinities towards the modified PAS sites and the inhibitory activity (Table 10). This correlation provides a direct evidence that inhibition by propidium results from a specific binding to a single PAS site and is consistent with the proposed molecular model of the HuAChE - propidium complex (Barak *et al.*, 1994). On the other hand, neither the value of K_D, from fluorescence titration experiments, nor the molecular model is consistent with the previously observed resistance of W86A HuAChE towards inhibition by propidium (Ordentlich *et al.*, 1993; Table 10). To account for this discrepancy, the inhibition characteristics of W86A HuAChE together with the conformational flexibility of the Trp86 side chain,were interpreted as indication of a functional "cross - talk" between the periphery and the active center whereby the conformational state of Trp86 depends on the interaction of ligands with the remote PAS

(Ordentlich *et al.*, 1995). An alternative explanation can be offered, in which propidium interacts directly with Trp86. This is inconsistent with the relative affinities of propidium and of its decamethylene homolog decidium, towards the AChE - pyrenebutyl methylphosphonate adduct (Berman *et al.*, 1987). The affinity of decidium, which interacts with both the active center and the PAS, towards the free AChE is 100-fold higher than towards the adduct. Yet propidium was shown, in that study, to bind with equivalent affinity to both the adduct and the free AChE. This comparison demonstrates that affinity towards decidium, but not towards propidium, is affected by steric occlusion of the active center by the bulky phosphonate moiety, indicating that propidium indeed does not interact with the active center residue Trp86. This conclusion is further supported by the failure of reversible active center ligands like edrophonium and N-methyl acridinium to displace propidium (Taylor and Radic, 1994).

Due to the location of the PAS, near the rim of the active site gorge, the bound ligand may hinder the access of substrates to the active center by physical obstruction of the gorge entrance and/or by charge repulsion imparted by the association of the cationic ligand. While this suggestion is consistent with the molecular model of propidium - HuAChE complex in which the gorge entrance is indeed blocked by the ligand (Barak *et al.*, 1994), it is not supported by the available experimental data, pertaining inhibition of AChE by propidium and other reactivity characteristics of the enzyme. The rate of phosphonylation of AChE, by noncharged methylphosphonates, is only marginally affected by addition of saturating concentration of propidium (Berman and Leonard, 1990). In addition, AChE complexed with the slowly dissociating PAS ligand fasciculin, can still react with the phosphorylating agent DFP (Marchot *et al.*, 1993). Finally, as indicated by the corresponding value of K_D, binding of propidium does not affect significantly the reactivity of W86A enzyme towards charged and noncharged substrates, although the location of the bound ligand relative to the gorge entrance should resemble that of the wild type HuAChE complex. Thus it appears that steric obstruction of the inward path for substrates and inhibitors does not contribute in a major way to the inhibitory effect of propidium. Finally the lack of effect of propidium on reactivity of the W86A HuAChE towards ATC indicates also that charge repulsion is of no consequence to the propidium inhibitory mechanism. This conclusion is also supported by the reported reactivities of AChEs, chemically labelled at the PAS by charged reagents (Haas *et al.*, 1992; Duran *et al.*, 1994), towards ATC.

The Role of Residue Trp86 in Allosteric Modulation of HuAChE Reactivity

As suggested recently, on the basis of molecular modeling of the wild type, the W86F and the W86A enzymes, the side chain of Trp86 can occupy two conformational states: one that is functional as the anionic subsite while the other occludes the active center and should reduce catalytic activity (Ordentlich *et al.*, 1995). Induction of conformational change of Trp86 by occupation of the PAS is consistent with our results as well as with the report regarding the spectral changes induced in the pyrenebutyl phosphonate - AChE adduct that arise from occupation of the PAS (Berman *et al.*, 1981). The increase in the polarizability of the pyrenebutyl environment was interpreted as resulting from torsional movements of aromatic side chains. These studies imply not only that the conformational change of Trp86 is coupled to binding of PAS ligand but also that such change can be induced irrespective of the state of occupation of the active center.

We proposed (Ordentlich *et al.*, 1995) that the involvement of residue Trp86 in the allosteric mechanism of full or partial inhibition of the enzyme, is apparently through destabilization of the noncovalent complexes which are formed, in the active center, following the initial enzyme - ligand encounter. The reactivity properties of the Y133A and Y133F enzymes and in particular those of the double mutant W86A/Y133A HuAChE, appear to support this hypothesis. The affinity of Y133A HuAChE towards ATC is considerably reduced, relative to the wild type enzyme, as is evident from the 185-fold respective increase in the value of Km. In addition, this enzyme is refractory to inhibition by the active center ligand edrophonium (Ordentlich *et al.*, 1995). If this decrease in affinity results from steric occlusion of the active center, a similar effect could be expected for the noncharged substrates and inhibitors. Indeed, the bimolecular rate constants of phosphorylation of the Y133A enzyme (but not of the Y133F or W86A enzymes) by two organophosphate derivatives DFP and paraoxon are 170 and 805-fold lower respectively, compared to those of the wild type enzyme, while corresponding values of the dissociation constants of the noncovalent complexes (K_d) are 23 and 517-fold higher. Thus, the reduced reactivity of Y133A towards noncharged ligands is largely due to the relative destabilization of the initial noncovalent complexes.

Since altered conformation of the Trp86 side chain is the only major difference between the modeled structures of Y133A and the wild type HuAChE, it could be expected that other structural elements of the active center should not contribute significantly to such interference.

In this case, one could expect that removal of the bulky residue from position-86, in both the Y133A enzyme and the HuAChE - propidium complex, should relieve the steric occlusion at the active center and restore reactivity towards noncharged, but not towards charged, ligands. Such expectation is borne out by both the observed behavior of the W86A - propidium complex towards TB (Ordentlich *et al.*, 1993) and reactivity of the W86A and W86A/Y133A enzymes towards this substrate (Table 11, Km values similar to that of the wild type enzyme). Although the conformational flexibility of Trp86 and its effects on the catalytic activity provide a very plausible mechanism for the "cross - talk" between the peripheral sites and the active center, the relay path of the allosteric signal is still unclear. Clues to a possible way for signalling the incidence of binding at the periphery to the active center and for inducing motion of Trp86, can be found in the fact that the central binding element of the peripheral site - Asp74, which was also implicated in the "cross - talk" mechanism (Shafferman *et al.*, 1992b), is part of the sequence comprising the cysteine loop (Cys69-Cys96) (see Fig. 16A) which also includes Trp86. It is possible that the alternative conformation of Trp86 is not a result of a local motion of the indole moiety but rather a part of a larger conformational change involving the entire cysteine loop (Cys69-Cys96). This loop, which constitutes the thin portion of the gorge wall in AChE, is a structurally conserved element (variable length loop $L_{b3,2}$; Cygler *et al.*, 1993) in the lipase/esterase family of proteins sharing the α/β hydrolase fold (Ollis *et al.*, 1992). In lipases from various sources, conformational flexibility of the corresponding loops was implicated in the mechanisms of interfacial activation and substrate accommodation. Moreover, participation of surface loops in conformational changes, upon association with substrates or inhibitors, has been observed in a wide variety of biochemical systems (Kempner 1993; Gerstein *et al.*, 1994). The possible participation of the cysteine loop (Cys69-Cys96) of AChE in some sort of conformational adjustment is suggested both by virtue of the evolutionary constraint on the conservation of this structural motif in the lipase/esterase family (Ollis *et al.*, 1992) and by the x - ray structure of TcAChE which indicates that such adjustment may be essential for the enzymatic activity (Axelsen *et al.*, 1994). The crystallographic dimensions of the active site gorge (Sussman *et al.*, 1991) should preclude the access of ACh or larger ligands, like THA (Harel *et al.*, 1993), to the active center *in contrast* to the experimental evidence. Furthermore, according to the model of HuAChE - propidium complex (Barak *et al.*, 1994), built on the basis of these x - ray results, occupation of the PAS by either propidium or fasciculin, should block the gorge entrance, again in contrast to

experimental observations (Radic *et al.*, 1994). Indeed, molecular dynamics simulations of TcAChE (Axelsen *et al.*, 1994) as well as our preliminary results from simulated annealing suggest that the structure of unliganded enzyme differs from that observed in x- ray crystallography (Fig. 16). It is possible that the crystallographic structure may represent the ligand bound enzyme since it remains virtually unchanged in complexes with edrophonium and THA (Harel *et al.*, 1993; Axelsen *et al.*, 1994). In conclusion, it appears that AChE can exist in at least two conformational states differing with respect to the shape and dimensions of the entrance to the active site gorge. Interaction with charged substrates or active center inhibitors will stabilize the catalytically functional state, as reflected in the x-ray structure (Sussman *et al.*, 1991 and Fig. 16B), while association with PAS ligands such as propidium may shift the equilibrium in the direction of a nonfunctional state (Fig. 16C). Although the extent of structural difference between the functional and the nonfunctional states is not known, kinetic studies and molecular dynamics simulations (Ariel *et al.*, in preparation) suggest that the main difference, in the architecture of the active center, is in the conformational state of residue Trp86. From structural analogies to other enzymes of the lipase/esterase family and from molecular dynamics simulations it appears that the surface loop $L_{b3,2}$ is one of the most mobile structural motifs in AChE and that this mobility constitutes part of the transition between the reactive and the nonreactive states. Thus, the relay path of the allosteric signal, in the cross - talk between the periphery and the active center, may comprise of shifting the *natural* equilibrium between the different conformational states of the cysteine loop (Cys69-Cys96) in AChE.

VI. Surface Charge does not Contribute to Catalytic Efficiency of AChE.

INTRODUCTION

Electrostatic fields around the surface of proteins are believed to play an important role in molecular recognition and binding due to the long - range nature of the Coulombic potential (Sharp and Honig, 1990). For enzyme - charged substrate encounter two types of effects are possible: the enzyme charge distribution may influence the nonspecific collision rate for substrate with any part of the enzyme surface or it may steer the substrate to a particular area of the enzyme surface, altering the probability of enzyme - substrate complex formation (Sines *et al.,* 1990). Electrostatic attraction was implicated as a part of the initial nonspecific encounter followed by a two dimensional diffusion towards the binding site (Calef and Deutch, 1983). The effect of electrostatic steering was shown to enhance the catalytic rates of superoxide dismutase with superoxide ion (Tainer *et al.,* 1983; Allison *et al.,* 1988; Davis *et al.,* 1991) and of triose phosphate isomerase with glyceraldehyde 3-phosphate (Blacklow *et al.,* 1988; Luty *et al.,* 1993). On the other hand, global charge - charge interactions do not appear to contribute to the association of dihydrofolate reductase with folate or NADPH since, although the net charge of enzymes from different sources varies from +3 to -10, they display equivalent catalytic activity (Bajorath *et al.,* 1991). Thus the contribution of the electrostatic properties of an enzyme to its catalytic activity has to be evaluated for each particular enzyme.

Acetylcholinesterase (AChE), is an extremely efficient enzyme, believed to operate at, or near the diffusion control limit (Quinn, 1987). Amino acid sequences of AChEs from different sources (Doctor *et al.,* 1990; Massoulie *et al.,* 1993) indicates that these enzymes carry a net negative charge ranging from of -11e up to -14e. Early estimates from studies of ionic strength dependence on association rates with N-methyl acridinium and acetylthiocholine, led to the conclusion that electrostatic attraction is a driving force for rapid binding of acetylcholine (ACh) to AChE (Nolte *et al.,* 1980; Quinn, 1987). Recently, it was shown that in the structure of *Torpedo californica* AChE (TcAChE; Sussman *et al.,* 1991) an uneven spatial charge distribution results in a negative electrostatic potential extending roughly over half of the

protein surface and a strong directionality of electric field along the axis of the active center gorge (Ripoll *et al.,* 1993). These electrostatic properties were proposed to play an important role in attracting the positively charged substrate, acetylcholine, and in steering it towards and into the active center gorge of the enzyme (Tan *et al.,* 1993; Ripoll *et al.,* 1993). The implicit assumption in these proposals is that the catalytic bimolecular rate constant is diffusion limited (Davis *et al.,* 1991), however the actually measured bimolecular rate constants of various AChEs are about an order of magnitude lower than the expected rates of diffusion controlled reactions (10^7-$10^8 M^{-1}s^{-1}$ vs 10^8-$10^9 M^{-1}s^{-1}$; Fersht, 1985) and furthermore, they do not exhibit the expected linear dependence on medium viscosity (Hasinoff, 1982; Bazeliansky *et al.,* 1986). In addition, the observed dependence of the bimolecular rate on the molal volume of the various substrates, suggests an involvement of at least one chemical step in determination of the overall catalytic rate (Hassan *et al.,* 1980; Cohen *et al.,* 1984). Finally the Km values for the charged substrate acetylthiocholine (ATC) and for its isosteric uncharged analog, 3,3-dimethyl butylacetate (TB), are within a factor of two, suggesting that the initial encounter rate is charge independent (Ordentlich *et al.,* 1993a).

In order to further investigate the proposed contribution of electrostatic attraction to the rate of catalytic activity of AChE, we have generated mutants of human-AChE (HuAChE) in which up to seven of the surface negative charges, located near the rim of the active site gorge, were neutralized. While such substitutions was shown to have dramatic effects on the electrostatic potential, no major effects on the reactivity towards various substrates or a reversible inhibitor were observed, suggesting that neither electrostatic attraction nor electrostatic steering by the surface charges, contribute significantly to the catalytic properties of AChE.

METHODS

Mutagenesis of Recombinant HuAChE and Construction of Expression Vectors- Mutagenesis of AChE was performed by DNA cassette replacement into a series of HuAChE sequence variants which conserve the wild type coding specificity (Soreq *et al.*, 1990), but carry new unique restriction sites (Velan *et al.*,1991a; Kronman *et al.*, 1992; Shafferman *et al.*, 1992a). Generation of mutants E84Q, D349N and E285A was described previously (Shafferman *et al.*, 1992a,b; Barak *et al.* 1994). Substitution of other residues was

carried out through replacement of the following DNA fragments of pACHE-w7 by synthetic DNA duplexes: Glu292 on *MluI-NarI* , Glu358 on *NarI-BglII* and Glu389 or Asp390 on *BglII-Bsu36I.* The Glu codons were replaced either by a GCC-Ala or CAG-Gln and Asp codons by AAC-Asn. Multiple site mutants were generated by using either the synthetic DNA duplexes for generation of the D349N/E358Q and E389Q/D390N mutants or by rearrangement of the appropriate DNA fragments from the single site mutants: E84Q, E285A, E292A, D349N, E358Q, E389Q and D390N, relying on the unique restriction sites: *BstEII, PmlI, NarI* and *BglII.* All the synthetic DNA oligodeoxynucleotides were prepared using the automatic Applied Biosystems DNA synthesizer. The sequences of all new clones were verified by the dideoxy sequencing method (USB sequenase kit). The rHuAChE cDNA mutants were expressed in bipartite vectors which allows expression of the *cat* reporter gene (Shafferman *et al.*, 1992a).

Transient Transfection, Preparation and Quantitation of AChE and its Mutants- Human embryonal kidney 293 cells were transfected with various purified plasmids using the calcium phosphate method. Transient transfection was carried out as described previously (Velan *et al.*, 1991a; Shafferman *et al.,* 1992 a,b) and efficiency of transfection was normalized by levels of co-expressed CAT (chloramphenicol acetyl transferase) activity (Kronman *et al.*, 1992). Recombinant HuAChEs expressed in 293 cells are secreted into the growth medium as soluble T - type homo - oligomers (composed mainly of dimers;, Velan *et al.,* 1991b, Velan *et al.,* 1993). The various secreted AChE polypeptides were quantified by AChE-protein determination relying on specific enzyme linked immunosorbent assays (ELISA) (Shafferman *et al.,* 1992a) and by active site titrations (Ordentlich *et al* , 1993b) using the organophosphonate MEPQ (Levy and Ashani, 1986). Enzyme quantitation by these two methods were in good agreement (±10%).

Substrates and Inhibitors- Acetylthiocholine iodide (ATC), 5:5'-dithiobis (2-nitrobenzoic acid) (DTNB), ethyl(m-hydroxy-phenyl)-dimethylammonium chloride (edrophonium) were purchased from Sigma. S - 3,3 - dimethylbutyl thioacetate - $CH_3C(O)SC_2H_4C(CH_3)_3$ - (TB), synthesized and purified as described previously (see Section II), was a gift of Dr. Y.Segal. Purified 7-(methylethoxyphospho-phinylloxy)-1-methylquinolinium iodide (MEPQ) was a gift from Dr. Y. Ashani.

Determination of HuAChE Activity and Analysis of Kinetic Data- Recombinant HuAChE and its mutant derivatives collected from transient transfections were dialyzed extensively against 5mM Tris-buffer pH-8.0. Catalytic activity of the AChEs was assayed according to Ellman *et al.*, (1961). Assays were performed in the presence of 0.1 mg/ml BSA, 0.3mM DTNB (5,5'-dithiobis(2-nitrobenzoic acid)) and appropriate ionic strength (NaCl concentrations from 0 to 1.0M) in 5mM Tris-buffer pH-8.0, and varying concentrations (0.01-0.6mM) of the substrates ATC or TB. The assays were carried out at 27°C and monitored by a Thermomax microplate reader (Molecular Devices). Michaelis-Menten constant (Km) and the apparent first order rate constant (kcat) values, were determined as described before (Shafferman *et al.*, 1992a,b). The apparent bimolecular rate constants (k_{app}) were calculated from the ratio kcat/Km. Kinetic data from inhibition studies were analyzed according to the kinetic treatment described recently by Ordentlich *et al.*, (1993a).

Structure Analysis and Molecular Graphics- Building and analysis of the three dimensional models was performed on a Silicon Graphics workstation IRIS 70/GT using SYBYL modeling software (Tripos Inc.). Construction of models for the HuAChE and the mutated enzymes, was based upon the model structure of the enzyme obtained by comparative modeling (Barak *et al.*, 1992) based on the x-ray structure of TcAChE (Sussman *et al.*, 1991). The relative positions of acidic and basic residues on the HuAChE surface were determined from the z- coordinate of the respective C_α atoms, by positioning a frame of reference at the center of the enzyme, with the origin at C_β atom of residue Glu202 and defining an arbitrary axis along the gorge as the z-direction. A point, at z = 20Å, is regarded as a reference point for estimation of distances of the various residues from the entrance of the active site gorge (Fig. 17). The x,y plane divides the structure into two parts referred to as "northern" and "southern" hemispheres. The simulated mutants were constructed from the model coordinates by replacing the acidic amino acid sidechain with the neutral sidechain. The electrostatic potentials, of HuAChE enzymes, were calculated by using the program GRASP (Nicholls and Honig, College of Physicians and Surgeons , Columbia University New York), that includes routines for a numerical solution of the Poisson - Boltzmann equation. Values of dielectric constants for the solvent and the protein interior, were set as 80 and 4 respectively. Contribution of the ionic strength of the medium was not included. A set of united-atom point charges from the program

AMBER (Weiner *et al.,* 1986) was assigned to the protein atoms. The electrostatic potentials were displayed as isopotential surfaces at -1kT/e, where k is the Boltzmann constant, T is the temperature (°K) and e is the charge of electron.

RESULTS

Contribution of Specific Charged Residues on the HuAChE Surface to the Electrostatic Potential and Selection of Mutants

The model structure of HuAChE contains 55 acidic amino acids. Except for Asp74, Glu202, Glu334 and Glu450, which are located within the active site gorge, all these negatively charged residues are unevenly distributed on the protein surface. There is a marked preponderance of acidic residues in the "northern" hemisphere (see methods), giving rise to a negative electrostatic potential that extends over most of the protein surface. Similar electrostatic properties were reported for TcAChE (Ripoll et al., 1993). Since this potential is apparently due to the effect of the overall charge distribution rather than the effect of specific residues (Soman *et al.,* 1989), its cancellation should be possible through removal of a sufficient number of negative charges from the surface. The effect of neutralization of the negatively charged amino acids on the electrostatic potential extending over the entrance to the active site gorge was examined for various combinations of the 15 acidic residues located in the "northern" hemisphere 11Å above an arbitrarily defined center (C_β of Glu202; see methods and Fig. 17). The electrostatic potential of the various simulated HuAChE mutant enzymes, was calculated by GRASP, and displayed at the -1kT/e contour. A gradual shrinking of the electrostatic potential, over the "northern" hemisphere, corresponding to the progressive reduction of the surface negative charge was observed (cf. Fig. 18). Replacement of the five residues Glu84, Glu285, Glu292, Asp349, and Glu358, which roughly encircle the gorge entrance, had a major effect on the contours of the electrostatic potential of selected mutants (Fig. 18, bottom left). For hexa or hepta mutants, which include additional acidic residues, there is already no significant electrostatic potential (>-1kT/e) above the rim of the active site gorge area and therefore, additional replacements appeared unnecessary. As noted before (Ripoll *et al.,* 1993) the four acidic residues located within the gorge (Asp74, Glu202, Glu334 and Glu450) do not appear to contribute to the electrostatic potential over the molecular surface

as is demonstrated in the penta and more so in the hepta simulated mutants (Fig. 18).

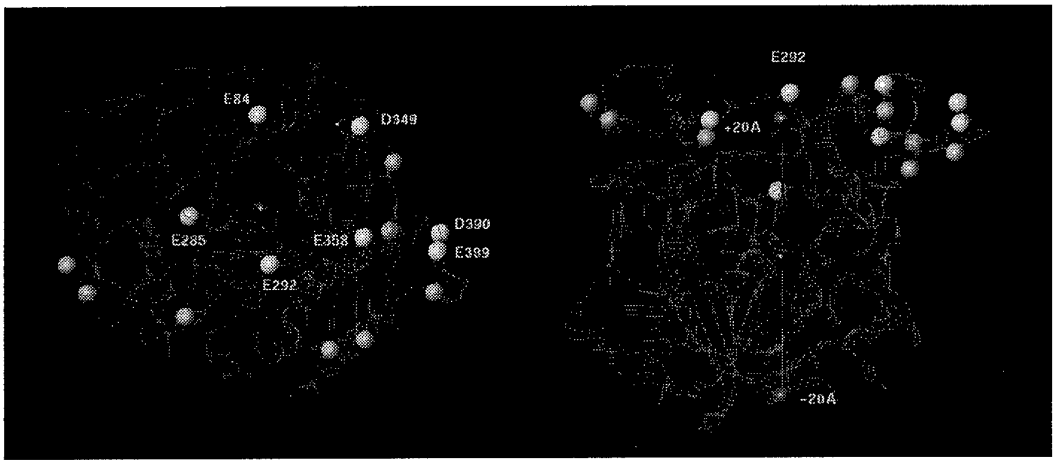

Fig. 17 Distribution of acidic amino acids in the upper part (z>11Å) of the "northern" hemisphere of HuAChE. The protein backbone is represented as a ribbon. The spheres represent: position of C_α atoms of acidic residues replaced, in this study (light grey); position of C_α atoms of additional acidic residues (grey); reference points at z = ±20Å (dark grey) and the point of origin (assigned to C_β of Glu202, almost black). This section of the "northern" hemisphere contains also 12 basic residues (not shown).Reference point at +20Å represents the approximate center of the entrance to the active site gorge. Orientation in x,y-plane (Left), provides a view in the direction of the gorge axis. The semicircular arrangement of residues Glu84, Asp349, Glu358, Glu292 and Glu285, around the midpoint of the gorge entrance is illustrated. The respective distances, of these residues, from the active center (C_α of amino acid – C_β of Glu202), are: 16.705Å; 25.644Å; 29.422Å; 25.150Å; 22.505Å. Orientation in y,z- plane (Right) illustrates the cross section of the protein slice containing the mutated acidic residues. Positions of residues Glu358 and Glu292 (3.669Å and 2.612Å above the midpoint of the gorge entrance) and residue Glu84 (8.832Å below the midpoint), define the thickness of this slice.

According to the above calculations we selected to study mutants of HuAChE containing replacements of the five acidic residues (Glu84, Glu285, Glu292, Asp349, and Glu358) vicinal to the active site gorge. Two additional acidic amino acids Glu389 and Asp390, further removed from the gorge entrance (Fig. 17), were selected in order to ascertain the absence of nonspecific effects of the replacements on the catalytic activity of the mutated enzymes. Although single replacement of each of these acidic residues, was not expected, to alter appreciably the electrostatic properties of the mutants, their generation was required for

determining their possible indirect effects on the catalytic rate. Indirect effects such as conformational changes affecting enzyme stability (Matthews, 1993), or allosteric modulation of the active center could mask the specific contribution of the electrostatic attraction and complicate the interpretation of kinetic data. This was one of the reasons for not including in the analysis replacement of residue Asp74, which is located in the upper part of the gorge, since it was previously shown to affect allosterically the conformation of both the periphery and the active center (Shafferman *et.al.,* 1992b; Neville *et al.,* 1992; Radic *et al.,* 1993). None of the single site mutations of the seven selected amino acids had a major effect on the catalytic properties of the resulting enzymes (Tables 12, 13). Therefore, we proceeded to modify gradually the surface charge of HuAChE by expressing enzymes with multiple replacements of the above seven acidic residues. Thirteen HuAChE mutants containing multiple substitutions ranging from two up to seven amino acids were constructed (Table 12). Several double, triple, quadruple and quintuple charge replacements were carried out in order to assess possible effects of different combinations of equal charge modifications on kinetic parameters of catalytic activity.

Reactivity of HuAChE Mutants Towards Substrates and a Reversible Inhibitor

The catalytic activity of the single and multiple site HuAChE mutants was examined, using the charged substrate ATC and its isosteric noncharged analog TB. These two acetates differ in that the trimethylammonium moiety is replaced by a t-butyl group and should therefore allow examination of the net effect of charge on the catalytic properties of the mutated enzymes (Ordentlich *et al.,* 1993a). In all the 20 mutants examined no effect on kinetic parameters, of catalytic activity towards TB, was observed (Table 12). Therefore the changes in surface charges are of no consequence to the catalytic properties of the HuAChE.

Examination of the kinetic parameters, of the single site HuAChE mutants, for hydrolysis of ATC (Table 13), shows that most of them have practically equal reactivities to that of the wild type enzyme. No effect on the apparent first order rate constant kcat, relative to the wild type HuAChE, was observed in all the seven single site mutants. With respect to Km (Michaelis Menten constant) values, only in the cases of the single site mutants E84Q and

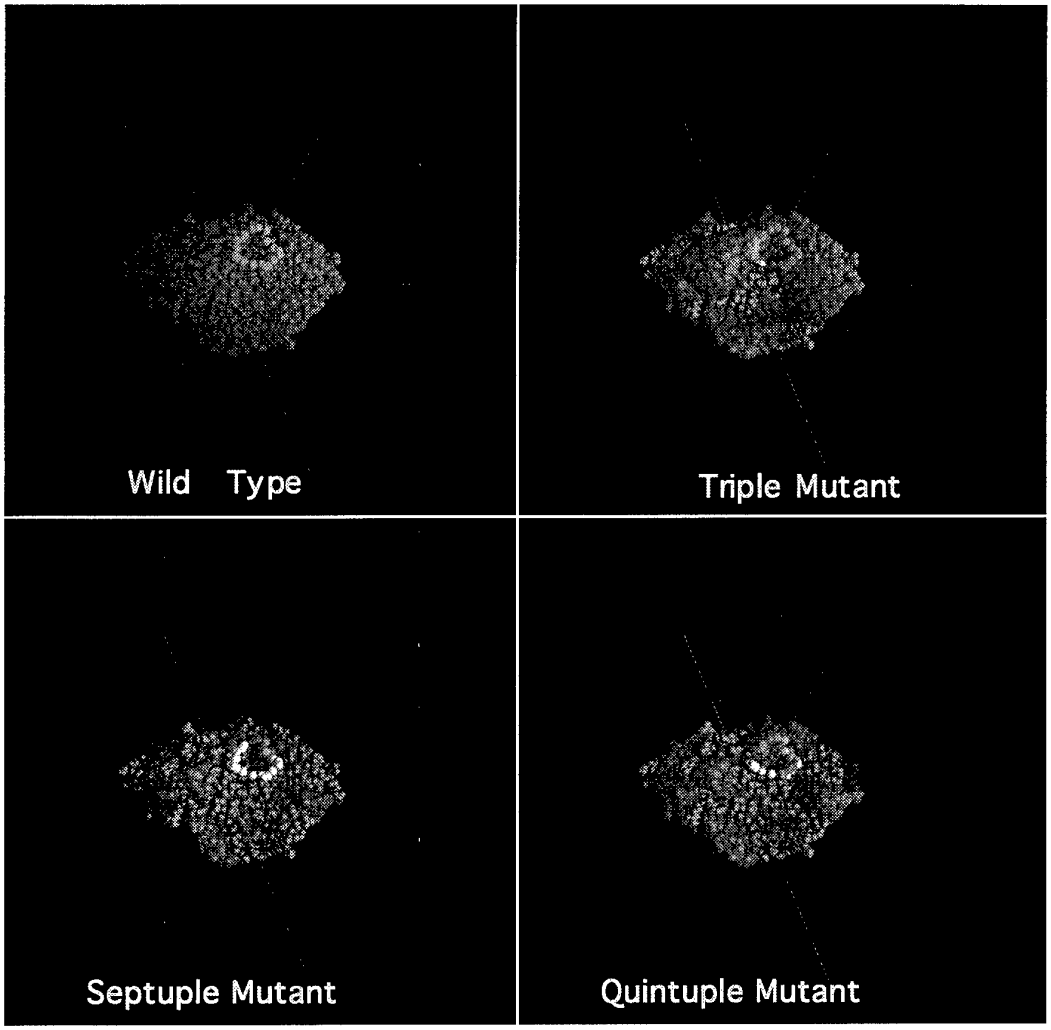

Fig. 18 Spacefilling models of HuAChE and selected mutants with superimposed negative electrostatic isopotential surfaces. The transluscent surfaces corresponds to the isopotential contours -1kT/e for each of the different HuAChE derivatives. Portions of the protein surface (displayed as grey coloured balls) covered by the negative potential ,are slightly darker as compared to the uncovered areas. The rim of the active site gorge is outlined as a white ring. All the structures are oriented in the same way with the z-axis aligned with the gorge axis
Wild type HuAChE (Upper Left), triple mutant - E84Q/D349N/E358Q (Upper Right), quintuple mutant - E84Q/E285A/E292A/D349N/E358Q (Lower Right) and septuple mutant-E84Q/E285A/E292A/D349N/E358Q/E389Q/D390N (LowerLeft).

E285A, a two fold increase, relative to the wild type enzyme, was observed. Reactivities of the multiple site mutants towards ATC display patterns similar to these manifested by the single site mutants (Table 13). Thus, in no case is an appreciable difference in values of kcat observed for all the 13 multiple mutants tested. Furthermore, in all the multiple site mutants no effect on Km was observed except for those carrying replacement of Glu84 and/or Asp285. Notably, irrespective of the number of other amino acid replacements, the increase in values of Km (2-3 - fold) always reflects the particular contribution of Glu84 and Asp285 as observed in the single site mutants. The effect of replacing both Glu84 and Glu285 in the same molecule, is neither synergistic nor additive suggesting that these replacements induce a similar structural effect. It therefore appears that the small effects, are not related to the modification of the overall electrostatic properties but rather to some subtle local conformational variations, induced by replacements at positions 84 and 285, which appear to affect the noncovalent complex formation of the charged substrate ATC.

For further investigation of this possibility, the kinetics of inhibition of the various mutants was studied, using edrophonium - a charged, reversible active center AChE ligand. Edrophonium was shown, by site directed mutagenesis (Shafferman *et al.,* 1992a) and recently by x - ray crystallography (Harel *et al.,* 1993), to interact with regions of the active center similar to those binding the charged substrate ATC. However unlike the Km value, inhibition constant Ki is a true measure of the ratio kon/koff and therefore a better indicator of changes affecting the noncovalent complexation process. As observed for Km values for ATC, the values of Ki are practically equal for all of the tested mutants except for those carrying replacement of Glu84 and/or Glu285. Moreover, the extent of the change in Ki values, relative to the wild type, resembles that of Km and does not exceed 2-4 - fold. These findings further support the interpretation regarding the localized conformational changes induced by replacements at positions 84 and 285, and general conclusion regarding the lack of contribution of surface charges to the formation of enzyme - ligand complex.

Effect of Ionic Strength of the Medium on Kinetic Parameters: The observed activity of the wild type HuAChE and the various mutants towards ATC and TB, at two ionic strengths, is summarized in Tables 12, 13. As expected for the noncharged substrate TB, no effect of the ionic strength on the kinetic parameters of wild type or any of the mutant enzymes

Table 12: Kinetic constants of hydrolysis of TB by HuAChE and selected surface charge HuAChE mutants at ionic strength of 5 and 150 mM.

AChE Type	K_m (x10^{4}M)		k_{cat} (x10^{-5}xmin^{-1})		k_{app} (x10^{-8}M^{-1}xmin^{-1})	
	I=150	I=5	I=150	I=5	I=150	I=5
WT	2.8±0.4	2.6±0.3	0.50±0.08	0.46±0.07	1.8±0.3	1.8±0.3
E84Q	2.8±0.4	2.3±0.2	0.44±0.07	0.43±0.06	1.6±0.2	1.9±0.3
E292A	2.8±0.4	2.8±0.5	0.48±0.07	0.44±0.07	1.7±0.3	1.6±0.2
E285A	2.6±0.4	2.3±0.3	0.50±0.08	0.42±0.06	1.9±0.3	1.8±0.3
D349N	2.5±0.4	2.2±0.3	0.44±0.07	0.40±0.05	1.8±0.3	1.8±0.3
E358Q	2.5±0.3	2.3±0.4	0.50±0.08	0.45±0.07	2.0±0.4	2.0±0.3
E389Q	2.4±0.3	2.1±0.3	0.50±0.08	0.43±0.06	2.0±0.3	2.0±0.3
D390N	2.4±0.3	2.4±0.4	0.50±0.08	0.46±0.07	2.0±0.3	1.9±0.3
E84Q/E292A	3.2±0.5	2.3±0.3	0.53±0.90	0.45±0.07	1.7±0.2	2.0±0.3
D349N/E358Q	2.4±0.4	2.0±0.3	0.43±0.07	0.38±0.06	1.8±0.3	1.9±0.3
E389Q/D390N	2.4±0.4	2.4±0.4	0.50±0.08	0.40±0.05	2.0±0.3	1.7±0.2
E84Q/D349N/E358Q	2.6±0.5	2.9±0.5	0.43±0.06	0.48±0.07	1.7±0.3	1.7±0.3
E292A/D349N/E358Q	2.5±0.4	2.6±0.4	0.40±0.06	0.47±0.07	1.6±0.2	1.8±0.3
E292A/E389Q/D390N	2.4±0.4	2.5±0.4	0.44±0.06	0.46±0.06	1.8±0.3	1.8±0.3
E84Q/E292A/D349N/E358Q	2.2±0.5	2.6±0.3	0.41±0.06	0.46±0.06	1.9±0.2	1.8±0.3
D349N/E358Q/E389Q/D390N	2.4±0.4	2.4±0.4	0.42±0.06	0.49±0.08	1.8±0.3	2.0±0.3
E84Q/E285A /E292A/D349N/E358Q	2.9±0.6	2.2±0.3	0.50±0.08	0.40±0.06	1.7±0.3	1.8±0.3
E84Q/D349N/E358Q/E389Q/D390N	2.9±0.5	2.3±0.4	0.47±0.07	0.42±0.05	1.6±0.3	1.8±0.3
E292A/D349N/E358Q/E389Q/D390N	2.7±0.5	2.5±0.4	0.50±0.07	0.47±0.07	1.9±0.3	1.9±0.3
E84Q/E292A /D349N/E358Q/E389Q/D390N	2.6±0.4	2.0±0.3	0.41±0.06	0.42±0.06	1.6±0.2	2.1±0.3
E84Q/E285A /E292A/D349N/E358Q/E389Q/D390N	2.6±0.4	2.2±0.3	0.50±0.07	0.44±0.06	1.9±0.3	2.0±0.3

Values are average of 3 to 5 independent experiments; ± standard error.

Table 13. Kinetic constants and edrophonium inhibition constants for hydrolysis of ATC by HuAChE and selected surface charge HuAChE mutants at ionic strength of 5 and 150 mM.

AChE Type	K_m ($\times 10^4$M)		k_{cat} ($\times 10^{-5}$ x min^{-1})		k_{app} ($\times 10^{-8}$M^{-1}xmin^{-1})		Edrophonium Ki ($\times 10^6$M)
	I=150	I=5	I=150	I=5	I=150	I=5	I=150
WT	1.4±0.2	0.8±0.1	4.0±0.6	4.0±0.6	29.0±4.4	52.2±7.8	0.50±0.08 (0.32±0.05)[a]
E84Q	2.7±0.4	1.5±0.2	4.0±0.6	4.0±0.6	15.0±2.3	27.0±3.7	1.20±0.20
E292A	1.6±0.2	0.9±0.1	4.1±0.6	4.2±0.6	26.0±3.9	46.8±6.4	0.50±0.08
E285A	3.0±0.4	1.7±0.3	4.0±0.6	4.0±0.6	13.3±2.0	24.0±3.6	1.00±0.15
D349N	1.7±0.2	1.0±0.1	4.4±0.7	3.9±0.5	26.0±4.0	39.0±5.8	0.60±0.09
E358Q	1.6±0.2	0.8±0.1	4.0±0.6	3.6±0.5	25.0±3.8	45.0±6.8	0.50±0.08
E389Q	1.4±0.2	0.7±0.1	4.0±0.6	3.7±0.6	29.0±4.3	52.8±7.9	0.90±0.14
D390N	1.4±0.2	0.7±0.1	4.0±0.6	3.6±0.5	29.0±4.4	51.5±7.1	0.70±0.10
E84Q/E292A	3.3±0.5	1.8±0.3	3.9±0.6	3.8±0.6	12.0±1.8	21.6±3.0	1.50±0.20
D349N/E358Q	1.4±0.2	0.8±0.1	4.2±0.7	3.8±0.6	30.0±4.5	47.2±7.1	0.90±0.14
E389Q/D390N	1.4±0.2	0.7±0.1	3.9±0.6	3.5±0.5	28.0±4.2	50.4±7.6	0.70±0.11
E84Q/D349N/E358Q	3.4±0.5	2.0±0.3	4.1±0.6	4.3±0.7	12.0±1.9	21.6±2.9	1.80±0.30
E292A/D349N/E358Q	1.6±0.3	0.9±0.1	4.0±0.6	4.0±0.5	25.0±3.6	45.0±6.8	0.80±0.12
E292A/E389Q/D390N	1.2±0.2	0.7±0.1	4.2±0.6	3.7±0.5	35.0±5.3	52.8±8.2	0.60±0.10
E84Q/E292A/D349N/E358Q	3.5±0.5	2.0±0.3	4.4±0.7	3.9±0.6	12.6±1.9	19.5±2.5	1.60±0.24
D349N/E358Q/E389Q/D390N	1.3±0.2	0.7±0.1	4.3±0.6	3.6±0.5	33.0±5.0	50.0±7.5	0.80±0.12
E84Q/E285A /E292A/D349N/E358Q	3.9±0.6	2.1±0.3	4.1±0.6	4.0±0.6	10.5±1.6	18.9±2.6	1.70±0.25
E84Q/D349N/E358Q/E389Q/D390N	2.9±0.4	1.6±0.2	3.9±0.6	3.6±0.5	13.4±2.0	22.2±3.3	1.70±0.24
E292A/D349N/E358Q/E389Q/D390N	1.6±0.2	0.9±0.1	4.3±0.7	4.0±0.7	27.0±4.0	44.4±6.2	0.70±0.11
E84Q/E292A /D349N/E358Q/E389Q/D390N	3.5±0.5	1.9±0.3	4.3±0.6	3.9±0.6	12.3±1.8	20.5±2.8	1.70±0.26
E84Q/E285A /E292A/D349N/E358Q/E389Q/D390N	3.5±0.5	1.9±0.3	4.3±0.7	3.8±0.6	12.3±1.9	20.0±2.5	1.90±0.28 (1.40±0.20)[a]

[a] Inhibition constant at ionic strength of 5 mM. Values are average of 3 to 5 independent experiments; ± standard error.

was observed. For ATC hydrolysis, values of kcat are unaffected while values of Km show a very moderate increase with increasing ionic strength. A detailed analysis, over a wide range of ionic strength, with the mutants containing 6 or 7 acidic residue replacements shows dependence pattern of the apparent bimolecular rate constant (kapp) similar to that observed for the wild type enzyme, over a wide range of ionic strengths (Fig. 19). For these two mutants, the slopes of log kapp vs square root of ionic strength ($I^{1/2}$), at the linear range (2-250mM), are almost identical to that of the wild type enzyme (for higher ionic strengths, the expected deviation from linearity is again observed for both the mutants and the wild type

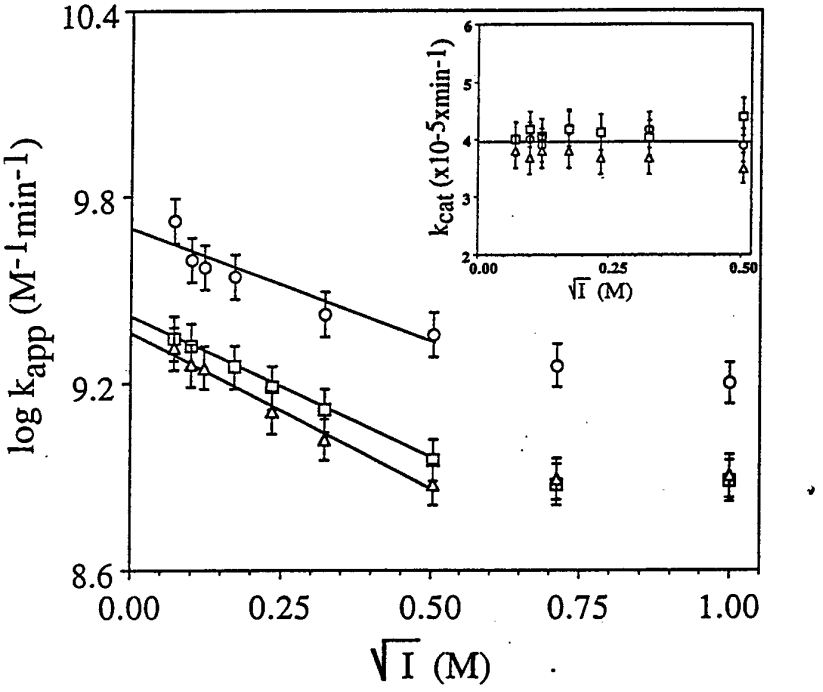

Fig 19. Dependence of kinetic constants of HuAChE and selected mutants on ionic strength. The bimolecular rate constant (kapp) was calculated from the ratio of values for kcat and Km. Inset depicts the dependence of the first order rate constant of catalysis (kcat) on ionic strength. The values are average of three independent experiments. Bars represent standard errors.
O Wild type HuAChE; □ sextuple mutant - E84Q/E292A/D349N/E358Q/E389Q/D390N; Δ septuple mutant - E84Q/E285A/E292A/D349N/E358Q/E389Q/D390N

enzyme). The values of kcat, for the wild type and all the mutants examined, are not dependent on the ionic strength (Table 13; Fig. 19 inset). Similar dependence of the kinetic parameters on ionic strength was noted previously for native AChE from electric eel (Nolte *et al.*, 1980) or for TcAChE (Berman and Leonard, 1990). Thus, the effect of ionic strength on Km values is not related to the polar interactions, during the initial enzyme-substrate encounter, since it is moderate and constant irrespective of the electrostatic properties of the various HuAChE enzyme molecules.

DISCUSSION

The structures of acetylcholinesterases are characterized by a high net negative charge (e.g. -11e for HuAChE; -12e for bovine AChE or -14e for TcAChE) and by asymmetrical distribution of acidic and basic amino acids on the protein surface, with excess acidic residues in the "northern" hemisphere (Fig. 17). This uneven charge distribution appears to be a general feature of the cholinesterases, conserved even in butyrylcholinesterases (BuChE), although their overall net charges are much lower than those of AChEs (e.g. -3e for human BuChE; +1e for rabbit BuChE). Conservation of an excess negative charge, in the vicinity of the entrance to the active site gorge, taken together with the fact that the natural substrates bear a positive charge, may suggest that the electrostatic properties are a part of an evolutionary design for optimization of the catalytic efficiency of cholinesterases. Indeed, recent evaluation of the possible effects due to the shape of TcAChE and its charge distribution, on the diffusion controlled rate of enzyme-substrate encounter by numerical brownian dynamics simulation, suggested an over 80 - fold rate enhancement (Tan *et al.*, 1993). According to this simulation, most of the enhancement (over 40 - fold) is due to electrostatic attraction, while a further minor effect could be attributed to electrostatic steering effects. Consequently, the uneven surface charge distribution and the resulting electrostatic potential, extending over the 'northern" hemisphere of AChEs, was proposed to contribute to the high catalytic efficiency of these enzymes (Ripoll *et al.*, 1993; Tan *et al.*, 1993).

This hypothesis was initially tested through simulated modulation of the charge distribution, in the "northern" hemisphere of HuAChE, and examination of the effects on the electrostatic potential as an indicator of the enzyme capacity for electrostatic attraction. Four out of the eleven acidic amino acids that constitute the net negative charge of the enzyme, are located

within the active site gorge and do not contribute significantly to the electrostatic potential above the surface . Neutralization of remaining 7, or even 6 negative surface charges, practically abolishes the negative electrostatic potential over most of the "northern" hemisphere (Fig. 18). Moreover, the direction of the electric field, which in the wild type is aligned along the active site gorge axis, as observed also for TcAChE (Ripoll *et al.,* 1993), changes by ~20° away from the z-axis. It was therefore expected that an actual neutralization of the surface negative charges should affect the bimolecular rate constant of the enzyme - substrate reaction, provided it does depend on electrostatic attraction. This was examined, through generation of 20 HuAChE enzymes, mutated in up to seven acidic amino acids, vicinal to the rim of the active site gorge. In marked contrast to the shrinking of the electrostatic potential (Fig. 18), the kinetic constants for reactivity of the mutants towards charged substrate and inhibitor are practically invariant (Table 13), indicating that the electrostatic attraction does not contribute to the reaction rates.

Minor variation in the values of Km for ATC, can be attributed to local effects of specific mutations of glutamates at positions 84 and 285. These replacements had a similar effect on the Ki values of the reversible inhibitor edrophonium, underscoring the relation of these substitutions to the stability of the noncovalent enzyme -charged ligand complex. The subtle nature of these effects is further demonstrated by the invariance of the kinetic data, for reactivity of the HuAChE mutants towards TB. Replacement at position 285 was already shown to moderately affect the binding of an active center ligand (Barak *et al.,* 1994). Effects due to replacement of Glu84 may be attributed to its relative proximity to the active center (Fig. 17).

The values of the apparent first order rate constant of catalysis (kcat) of both ATC and TB are invariant for all the HuAChE mutants and are not sensitive to the ionic strength of the medium (Tables 12, 13 and Fig. 19 inset). This finding indicates that the active sites of the various mutants are effectively shielded from surface charges. Furthermore, it suggests that long-range electrostatic interactions, due to the surface charges of AChE, do not participate in stabilization of transition states in the catalytic process. Such shielding effect was proposed in order to account for the identity of catalytic mechanisms in two trypsin isozymes differing in their net charge by 12.5e (Soman *et al.,* 1989). In another study, a small but significant contribution, of electrostatic interactions with surface charges, to stabilization of the catalytic transition state, was observed for subtilisin BPN' (Jackson and Fersht, 1993). The

expectation, that such stabilization may be particularly important for enzymes which have a very asymmetric surface charge distribution, is not realized in the case of AChE.

Ligands binding to the AChE surface show a pronounced dependence on ionic strength (Taylor and Lappi, 1975; Berman and Decker, 1986). A much weaker effect of ionic strength is observed for edrophonium and ATC (Table 13, Fig. 19). Moreover, the effect is constant, irrespective of the net surface charge of HuAChE and its various mutants (Fig. 19), indicating that the observed dependence of kapp on the ionic strength, is not related to the rate of the initial enzyme-substrate encounter. Similar dependence of kinetic parameters for AChE catalysis on ionic strength was observed previously for eel AChE (Nolte *et al.,* 1980) and for TcAChE (Leonard and Berman, 1990). The relative invariance of kapp values, over a wide range of NaCl concentrations, led Leonard and Berman (1990) to suggest that an electrostatic sensing mechanism is involved in preserving the enzymatic activity under a variety of physiological conditions. On the other hand, our results seem to indicate that such sensing mechanism is unnecessary since ionic composition of the medium has no significant effect on reactivity of the various mutant HuAChE enzymes with very different electrostatic characteristics.

The lack of contribution of electrostatic attraction to the catalytic rate, together with the nature of its dependence on ionic strength suggest that the rate of enzyme - substrate reaction is not diffusion controlled. Such conclusion is consistent with the lack of correlation of the catalytic rate with the charge of the substrate (e.g. the two charged substrates with trimethyl- and methylamino ß-substituents differ by more than 330 - fold in their respective catalytic rates, Quinn, 1987). Furthermore, AChE activity appears to correlate with molal volumes and hydrophobic properties of the substrates (Cohen *et al.,* 1984). According to this study, the noncatalytic hydrolysis of TB is about 40 - fold slower than that of ATC. However the value of the bimolecular rate constant, for the catalytic hydrolysis of TB (kapp, Table 12), is likewise about 30 - fold lower than the corresponding value for ATC (kapp extrapolated to zero ionic strength, Fig. 19). Consequently, the normalized catalytic power (ratio of catalytic and noncatalytic hydrolysis rates) of AChE is almost equal, for ATC and TB, suggesting similar enzyme - substrate encounter rates for both cases. Such result is incompatible with the notion that AChE catalytic rate is diffusion controlled since the effects of electrostatic interactions should have become apparent in the case of ATC.

Our results, showing unequivocally the lack of contribution of electrostatic attraction to AChE

catalytic properties, underscore the enigma of the uneven charge distribution, conserved throughout the cholinesterase family. It is possible that the electrostatic attraction in aqueous solutions is cryptic while in the viscous milieu of the synaptic cleft it becomes operational. Alternatively, the uneven charge distribution may be related to the noncatalytic functions of cholinesterases related to non - synaptic neuronal function (Greenfield, 1984, 1992), development of the nervous system (Layer, 1992) or cell adhesion (Massoulie *et al.*, 1993). While the catalytic power of AChE is not related to the electrostatic properties of its surface, the enzyme is still one of the most efficient natural catalysts (Quinn, 1987). The secret of its catalytic efficiency is probably the combination of the unique organization of the catalytic subsites (Shafferman *et al.*, 1992a,b; Ordentlich *et al.*, 1993a,b; Vellom *et al.*, 1993; Radic *et al.*, 1993; Loewenstein *et al.*, 1993; Barak *et al.*, 1994) within the active site gorge and may be unraveled through further structure -function studies of the elements constituting the intricate architecture of its active center .

VII. Product Clearance in Catalysis by AChE: Is There Evidence for the "Back Door" Subsite?

INTRODUCTION

Acetylcholinesterase (AChE) plays a key role in cholinergic neurotransmission by rapid hydrolysis of acetylcholine (ACh; Rosenberry, 1975; Massoulie *et al.*, 1993; Taylor and Radic, 1994). The recently solved crystal structure of AChE from *Torpedo californica* AChE (TcAChE) reveals a deep and narrow gorge, penetrating halfway into the enzyme, and containing the catalytic site about 4Å from its base (Sussman *et al.*, 1991). Modeling studies indicate that this structure is maintained in other cholinesterases (Harel *et al.*, 1992; Millard and Broomfield, 1992) including HuAChE (Barak *et al.*, 1992) . The residue composition and the fold of the enzyme give rise to an inward electrostatic field, which was assumed to facilitate the diffusion of the positively charged substrate down the gorge (Ripoll *et al.*, 1993; Tan *et al.*, 1993). The active center interacts with ACh through several subsites including the catalytic triad (Ser203*(200)*, His447*(440)* , Glu334*(327)*; Sussman *et al.*, 1991; Gibney *et al.*, 1990; Shafferman *et al.*, 1992a,b), the oxyanion hole (Gly121(*119*), Gly122(*120*), Ala204(*201*); Sussman *et al.*, 1991 and Section II), the acyl pocket (Phe295 (*288*) and Phe297(*290*); Harel *et al.*, 1992; Vellom *et al.*, 1993; Ordentlich *et al.*, 1993a) and the "anionic" subsite (Trp86(*84*); Ordentlich *et al.*, 1993a; Kreienkamp *et al.*, 1991; Shafferman *et al.*, 1992c) . The indole portion of Trp86(84) binds, through π - cation interactions, the quaternary ammonium groups of substrate and active center inhibitors (Ordentlich *et al.*, 1993a; Harel *et al.*, 1993 and Sections III, IV). While this indole moiety points into the gorge, the main chain of Trp86(*84*) is close to the protein surface (Ripoll *et al.*, 1993). Structural as well as mutagenesis studies do not explain how the positively charged reaction product - choline is cleared from the deep gorge rapidly enough to maintain a turnover rate of $4.0 \times 10^5 min^{-1}$ for this enzyme. Recently, an exit path was suggested in TcAChE (Ripoll *et al.*, 1993) involving conformational changes of Trp*84* and the adjacent Met*83* forming a "back door" channel for escape of the enzymatic reaction products. The "back door" mechanism was speculated to rely on either local conformational transitions of these two residues, or on larger movements involving the

disulfide - linked Ω loop (residues *67 - 94)*. In fact, a molecular dynamics simulation of TcAChE (Gilson *et al.*, 1994) revealed transient opening of a short channel, through a thin wall of the active site, near Trp*84* , which involves motions of residues Trp*84,* Val*129* and Glu*441*. This putative channel is large enough to allow passage of water molecules and was further suggested as an exit path for larger molecules (Gilson *et al.*, 1994).

The "back door" hypothesis implies that the anionic subsite residue Trp86(*84*) is also a "gate keeper" of the alternative exit, operating through "shutter like" motions (Gilson *et al.*, 1994). Therefore, its replacement by alanine may be expected to facilitate the "back door" opening, allowing for a faster product clearance and increasing the apparent bimolecular rate constant (kapp) of hydrolysis by the enzyme. However, previous studies (Ordentlich *et al.*, 1993a) of the HuAChE W86A mutant indicate that the value of kapp for the noncharged substrate, is actually somewhat lower than that of the wild type and thus appear to be inconsistent with the "back door" hypothesis. Yet, since the proposed hypothesis offers a straightforward means for product clearance in acetylcholinesterase, we decided to investigate this mechanism by mutating additional residues which could be implicated in formation of the putative back door channel.

METHODS

Mutagenesis of Recombinant HuAChE and Construction of Expression Vectors- Mutagenesis of AChE was performed by DNA cassette replacement (Shafferman *et al.,* 1992a) and involved substitution by synthetic DNA duplexes of the following fragments in pACHEw4: *AccI-NruI* for E84Q and *NarI-XhoI* for D131N, V132A and V132K. The Glu codon was replaced by CAG-Gln codon, Asp codon by AAC-Asn and the Val codon by GCC-Ala or AAG-Lys codons. The sequences of all new clones were verified by the dideoxy sequencing method (USB sequenase kit). The rHuAChE cDNA mutants were expressed in bipartite vectors which allows expression of the *cat* reporter gene. Human embryonal kidney (HEK) 293 cells were transfected with various purified plasmids as described previously (Kronman *et al.,* 1992 ; Shafferman *et al.*, 1992a). The various AChE polypeptides secreted into the medium were quantified by AChE-protein determination relying on specific ELISAs and by active site titrations (Velan *et al.*, 1991a; Ordentlich *et al.,* 1993b). Enzyme quantitation by these two methods were in good agreement (±10%).

Transient Transfection, Preparation and Quantitation of AChE and its Mutants- Human embryonal kidney 293 cells were transfected with various purified plasmids using the calcium phosphate method. Transient transfection was carried out as described previously (Velan *et al.*, 1991a; Shafferman *et al.*, 1992 a,b) and efficiency of transfection was normalized by levels of co-expressed CAT (chloramphenicol acetyl transferase) activity. The various AChE polypeptides secreted into the medium (containing 10% AChE-depleted serum) were quantified by AChE-protein determination relying on specific ELISA (Shafferman *et al.*, 1992a). Concentrations of wild type and mutated HuAChE enzymes secreted to the medium varied between 40-120 nanogram/ml (approximately 1-3 picomole/ml of catalytic subunits).

Substrates and Inhibitors- Acetylthiocholine iodide (ATC), 5:5'-dithiobis (2-nitrobenzoic acid) (DTNB), ethyl(m-hydroxy-phenyl)-dimethylammonium chloride (edrophonium), were all purchased from Sigma. S-3,3-dimethylbutyl thioacetate (TB) was synthesized as described before (see Section II).

Determination of HuAChE Activity and Analysis of Kinetic Data- Catalytic activity of the recombinant HuAChE and its mutant derivatives collected from transient transfections were assayed according to Ellman *et al.*, (1961). Assays were performed with ~10^{-10}M enzymes (total volume 0.1ml) in growth medium in the presence of 0.1 mg/ml BSA, 0.3mM DTNB (5,5'-dithiobis(2-nitrobenzoic acid) in 50mM sodium-phosphate buffer pH-8.0 and varying ATC (0.01-25mM) concentrations. The assays were carried out at 27°C and monitored by a Thermomax microplate reader (Molecular Devices) and corrected for background readings using medium collected from mock transfected cells. Michaelis-Menten constant (Km) and the apparent first order rate constant (kcat) values, were determined as described before (Shafferman *et al.*, 1992a,b). The apparent bimolecular rate constants (kapp) were calculated from the ratio kcat/Km. Kinetic data from inhibition studies were analyzed according to the kinetic treatment recently described by Ordentlich *et al.*, (1993a).

Structure Analysis and Molecular Graphics- Building and analysis of the three dimensional models was performed on a Silicon Graphics workstation IRIS 70/GT using SYBYL modeling software (Tripos Inc.). Construction of models for the HuAChE and the

mutated enzymes, was based upon the model structure of the enzyme obtained by comparative modeling (Barak *et al.*, 1992) from the x-ray structure of TcAChE (Sussman *et al.*, 1991). Models of the adducts of HuAChE mutants with ACh, were constructed by replacing the appropriate side chain, in the model of HuAChE - ACh adduct (Ordentlich *et al.*, 1993a), and optimization of the resulting structure with MAXIMIN2 (SYBYL 6.0, Tripos Inc., St. Louis) using the TRIPOS force field and Kollman all - atom charges for the enzyme (Weiner *et al.*, 1986). Zone refinement was performed on 49 residues, including amino acids comprising the active site gorge and the surface cavity above the plane of Trp86 indole moiety.

RESULTS AND DISCUSSION

According to the molecular model of HuAChE (Barak *et al.*, 1992) the residues flanking the outer opening of the "back door", are located within a cavity in the protein surface, and the rim of this cavity is lined by several acidic residues. This suggests that the outward diffusion of choline through the "back door", should be impeded by an electrostatic field. In order to modify the electrostatic and structural characteristics of this cavity, HuAChE mutants carrying single substitutions of amino acids Glu84(*82*), Asp131(*128*) and Val132(*129*), located at the enzyme surface, were chosen for study. Specifically, HuAChE mutants D131N and E84Q were evaluated in order to assess the effects of modified negative electrostatic field at the exit of the "back door", while mutant V132A was generated in order to minimize steric hindrance and thereby facilitate movement through the putative "back door". Finally, replacement of Val132(*129*) by Lys was intended to introduce a positive charge and to increase the steric crowding inside the cavity (see Fig. 20b,c). Such a mutation was also suggested by Gilson *et al.*. (1994), as a test for the "back door" hypothesis, since according to their model the positive group of the lysine could be positioned between Met*83*, Glu*445* and Asp*128*, effectively sealing the exit in TcAChE. Indeed, in the HuAChE V132K mutant, modeling of the side chain conformation of Lys132(*129*) indicated that it extends on the surface across the cavity, with the ε – amino group actually forming a salt bridge with the carboxylate of Glu452(*445*) (see Fig. 20b).

The kinetic constants of catalytic hydrolysis of ATC and its noncharged isostere TB, for all the HuAChE mutants described above, are summarized in Table 14. The "back door" hypothesis

implies that replacement of the "gate keeper" residue Trp86(*84*) by alanine should facilitate opening of the channel (see Fig. 20d), allowing for a faster product clearance and consequently an increase in the apparent bimolecular rate (kapp) of the enzyme. As described previously (Ordentlich *et al.*, 1993a) residue Trp86, constitutes the "anionic subsite" in the active center. This is evident from the modest effects of mutation W86A on kinetic parameters for the TB in contrast to those observed for ATC (Table 14). It follows that the expected rate enhancement due to substitution of Trp86 should be observed for hydrolysis of TB, but not for ATC, since the interaction of the latter with the mutated enzyme is impaired.

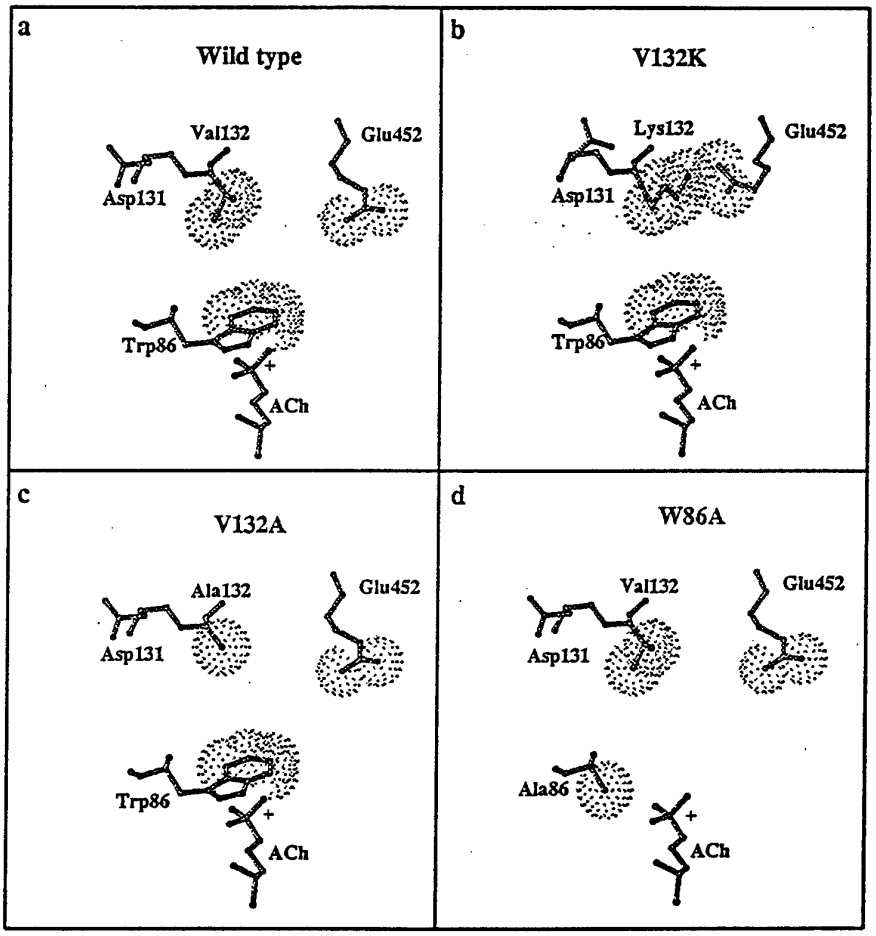

Figure 20: Relative orientations of residues along the hypothetical path of the "back door" of HuAChEs and it mutants. Molecular models depict the HuAChE-ACh tetrahedral intermediates (Ordentlich ,1993a). Hydrogen atoms are omitted for clarity. Comparison of panels (a) and (b) shows that replacement of Val132 by Lys affects the conformation of both Asp131 (a. χ_1=-65.1; χ_2=-61.9, b. χ_1=160.1; χ_2=85.5) and Glu452 (a. χ_1=54.7; χ_2=-161.6; χ_3=-141.6, b. χ_1=-67.2; χ_2=-84.5; χ_3=-144.8). Replacements of Val132 or Trp86 by Ala (panels (c) and (d)) do not precipitate major movements of the acidic residues. Van der Waals surfaces of the side chains, protruding into the path of the putative "back door", allow for visual comparison of changes in steric crowding due to residue replacement.

This prediction is obviously not supported by the kinetic measurements with TB which actually indicate a slight decrease in values of kcat and kapp for the HuAChE W86A mutant. The apparent first order rate constants for hydrolysis of ATC and its noncharged isostere TB, for all the other HuAChE mutants (E84Q, D131N, V132A and V132K) are quite similar to those determined for the wild type enzyme. This invariance in the turnover rates for the mutated HuAChE enzymes, and in particular for the mutant V132K, strongly suggests that the "back door" is not a route for clearance for the enzymatic reaction products. The only substantial deviation from the wild type behavior, is the 6 - fold increase of the Km value of ATC, but not of TB, for the mutant V132K. Since the relative destabilization of the enzyme - substrate complex is particular to the charged substrate, it appears that replacement of Val132 by lysine does not induce major conformational changes but is rather related to a local effect on the anionic subsite - Trp86(*84*). Structural changes in the HuAChE mutants, affecting the interaction capacity of residue Trp86(*84*), can be probed by measurement of the respective inhibition constants of the active center reversible inhibitor - edrophonium. The importance of the Trp86(*84*) indole moiety in the interaction of the edrophonium quaternary ammonium group with the enzyme, was well established by chemical affinity (Kreienkamp *et al.*,1991), site directed mutagenesis (Ordentlich *et al.*, 1993a; Barak *et al.*, 1994) and by x - ray crystallography (Harel *et al.*,1993). As expected inhibition of hydrolysis of ATC and TB by edrophonium, for mutants E84Q, D131N and V132A resemble that for the wild type. On the other hand the inhibition constants (Ki) for the mutant V132K are 54 and 150 fold higher for ATC and TB respectively (Table 15). Since the geometry of the active center in the V132K HuAChE mutant is not affected (see results for TB hydrolysis, Table 14) the increase in Ki values is most likely a consequence of impaired interaction of the inhibitor with residue Trp86 (Table 15). These results on edrophonium inhibition are qualitatively similar to those precipitated by replacement of Trp86 by alanine (Tables14, 15). In conclusion the kinetic data for edrophonium further support the assignment of the effect on Km for ATC in mutant V132K, to the local effects on Trp86. This conclusion is also consistent with the molecular model which places the positive group of lysine-132 about 8Å away from the plane of the indole ring of this tryptophane (Fig. 20b).

Table 14: Kinetic constants for ATC and TB hydrolysis by HuAChE and its putative "back door" mutants

HuAChEs	ATC			TB		
	K_m mM	k_{cat} x10^{-5}min^{-1}	k_{app}[a] x10^{-8}M^{-1}min^{-1}	K_m mM	k_{cat} x10^{-5}min^{-1}	k_{app}[a] x10^{-8}M^{-1}min^{-1}
Wild type	0.14 ± 0.01	4.0 ± 0.5	28.6	0.30 ± 0.06	0.55 ± 0.1	1.8
W86A	94 ± 15	0.8 ± 0.1	0.0086	0.44 ± 0.07	0.18 ± 0.014	0.4
E84Q	0.27 ± 0.03	4.0 ± 0.6	14.8	0.30 ± 0.06	0.50 ± 0.1	1.7
D131N	0.14 ± 0.01	3.9 ± 0.4	28.0	0.30 ± 0.05	0.55 ± 0.1	1.8
V132A	0.12 ± 0.01	3.4 ± 0.4	28.3	0.21 ± 0.03	0.58 ± 0.09	2.8
V132K	0.90 ± 0.14	2.2 ± 0.5	2.4	0.35 ± 0.05	0.30 ± 0.04	0.9

[a] The apparent bimolecular rate constant (k_{app}) was calculated from the ratio of k_{cat}/K_m. Values are the average of at least three independent measurements ±S.E.

Table 15: Competitive inhibition constants of HuAChE and its putative "back door" mutants with the active center ligand edrophonium

HuAChEs	Inhibition constant (Ki) (μM) ATC	TB
Wild type	0.7 ± 0.1	0.6 ± 0.1
W86A	(>45000)[a]	(>45000)[a]
E84Q	1.2 ± 0.1	1.0 ± 0.1
D131N	1.0 ± 0.2	2.1 ± 0.3
V132A	1.2 ± 0.1	1.2 ± 0.1
V132K	38.0 ± 4.0	90 ± 20

[a] Values in parentheses refer to the highest concentration of edrophonium (45 mM) used, yet this concentration was still insufficient to cause detectable inhibition of activity. Values are the average of at least three independent measurements, ± S.E..

Notwithstanding its origin, the marked reduction in affinity of the HuAChE V132K mutant to edrophonium is incompatible with the exit of this ligand through the "back door". Actually, sealing of the putative exit path in the V132K mutant, should have decreased the rate constant of product release (k_{off}) and thus should have decreased rather than increased the inhibition constant for edrophonium.

In summary, kinetic studies with HuAChE mutants carrying replacements of some of the major elements implicated in channel forming movements: Trp86(*84*) - at the bottom of the channel, Val132(*129*) - near its exit, as well as mutations of charged residues Glu84 and Asp131 flanking the putative channel exit, do not support the idea that such channel is of functional significance in catalysis. The reported results leave unresolved the original question of how the positively charged choline is removed from the gorge, against the direction of the electrostatic field. However, recent findings suggest that at the stage of product clearance, the diffusion rate of choline is not sensitive to the electrostatic field since major modifications of the electrostatic properties in HuAChE enzymes have no effect on catalytic activity (Shafferman *et al.,* 1994). These observations raise the possibility that product clearance, from the active site gorge, is less prohibitive than initially suspected. Furthermore, one could speculate that binding of substrate to the active center induces an allosteric effect which opens the gorge and thus facilitates product release.The possible involvement of allosteric effects in modulation of AChE activity is well documented (Changeux, 1966) and was recently shown to involve a "cross - talk" between aromatic residues at the periphery and residues Trp86(84) and Tyr337(330) at the active center (Shafferman *et al.,* 1992b; Ordentlich *et al.,* 1993a). In fact, recent findings, from molecular dynamics simulations of TcAChE, indicate that presence of quaternary ammonium species within the active site gorge affects its geometry and shape (Axelsen *et al.*, 1994). The hypothesis of substrate/product induced opening of the gorge can be explored by comparative molecular dynamics simulations of the enzyme - substrate complexes vs the free enzyme. This could provide an insight for further experimentation designed to elucidate the mechanisms involved in diffusion into and out of the active center gorge of AChE.

VIII. Determination of Amino Acids in The Active Center of Human AChE Affecting Reactivity Toward Phosphorylating Agents

INTRODUCTION

Acetylcholinesterase (AChE, EC 3.1.1.7) is among the most efficient enzymes, with a turnover number of over 10^4 sec^{-1} (Quinn, 1987). Its catalytic power and the high reactivity towards organophosphorus inhibitors are believed to be determined by the unique architecture of the AChE active center, consisting of several subsites. Resolution of the 3D structure of *Torpedo* AChE (Sussman *et al.*, 1991), site directed mutagenesis and molecular modeling together with kinetic studies of the AChE muteins with substrates and reversible inhibitors (Gibney *et al.*, 1990; Velan *et al.*, 1991a,b; Shafferman *et al.*, 1992a,b,c; Shafferman *et al.*, 1993; Vellom *et al.*, 1993; Ordentlich *et al.*, 1993a,b; 1995; Radic *et al.*,1992,1993; Barak *et al.*, 1994; Kronman *et al.*, 1994; Gnatt *et al.*, 1994; for recent review see also Taylor and Radic, 1994) are beginning to unveil the functional role of the various active center subsites in the reactivity characteristics of the enzyme: a) the esteratic site containing the active site serine; b) the "anionic subsite"-Trp-86(*84*); c) the hydrophobic site for the alkoxy leaving group of the substrate includes residues Trp-86(*84*), Tyr-337(*330*) and Phe-338(*331*); and d) the acyl pocket - Phe-295(*288*) and Phe-297(*290*). Apart from the esteratic subsite, the main contribution of these active center components to the catalytic activity appears to be in the stabilization of the Michaelis-Menten complexes, since most of the structural perturbations of the active center hardly affect the rate of the nucleophilic step (Ordentlich *et al.*, 1993a). In these complexes, the trigonal geometry of the substrates and their limited structural variety allow only partial mapping of the specific interactions with the other elements of the active center. In addition, the Michaelis-Menten constants (Km) only approximate the true dissociation constants of the noncovalent complexes. The saturation phenomena demonstrated for inhibition of AChE by a variety of organophosphorus compounds indicate the intermediacy

of a noncovalent complex in the phosphylation process. Formation of such Michaelis complexes, in the AChE active center (analogous to the Michaelis-Menten complexes), is followed by nucleophilic reaction of the catalytic serine resulting in stable tetrahedral adducts (Aldridge and Reiner, 1972; Main, 1976). In these reactions, the tetrahedral configuration of the organophosphorus inhibitors affords an additional dimension in probing the spatial organization of the AChE active center. Furthermore, since in phosphylation a process analogous to deacylation does not occur (or takes place very slowly), the dissociation constant of the enzyme-organophosphate Michaelis complex can be kinetically estimated, provided no other enzyme-inhibitor complexes are formed (e.g. interaction with the peripheral anionic site, Friboulet *et al* ., 1990) . In the past most of the structure-activity studies of organophosphate inhibitors were interpreted in terms of the covalent adduct's stabilization (Jarv, 1984; Benschop and de Jong, 1988; Barak *et al.,* 1992). The contribution of the Michaelis complex formation was omitted mainly due to the lack of structural information essential for definition of the inhibitor binding sites. On the other hand, the reactivity and stereoselectivity of AChE towards various organophosphate derivatives are critically dependent upon the nature of the groups surrounding the tetrahedral phosphorus (Berman and Leonard 1989).

In the present study, we further explore the functional architecture of AChE active center and the reactivity characteristics of the enzyme by means of site directed mutagenesis and kinetic studies with three different organophosphate derivatives. Symmetrically substituted phosphate inhibitors have been used in order to avoid chirality at the phosphorus which would complicate the kinetic analysis. Phosphates bearing different substituents allowed to probe both the hydrophobic interactions of the alkoxy moieties with the binding environment of the active center and the effects of different leaving groups on the reactivity of AChE. We show that unlike the case of substrates, the unique organization of the active center contributes predominantly to the formation of the enzyme-organophosphate Michaelis complexes and that stabilization of these complexes is the major determinant of AChE reactivity toward organophosphorus inhibitors.

METHODS

Substrates and Inhibitors- Acetylthiocholine iodide (ATC) and 5:5'-dithiobis (2-nitrobenzoic acid) (DTNB) were purchased from Sigma. The organophosphate inhibitors (Fig. 21): diisopropyl phosphorofluoridate (DFP) and p-nitrophenyl diethyl phosphate (paraoxon) were purchased from Sigma while diethyl phosphorofluoridate (DEFP) was prepared according to the procedure by Saunders and Stacy (1948).

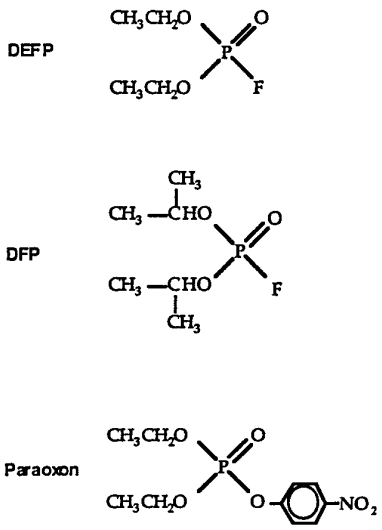

Fig. 21: Chemical formulae of organophosphates used: DFP, DEFP and paraoxon

Recombinant HuAChE and its Mutants - Expression of recombinant HuAChE and its mutants in a human embryonal kidney derived 293 cell line (Shafferman *et al.*, 1992a; Velan *et al.*, 1991a; Kronman *et al.*, 1992), and generation of all the mutants was described previously (Shafferman *et al.*, 1992a,b,c; Ordentlich *et al.*, 1993a,b; Ordentlich *et al.*, 1995). Stable recombinant cell clones expressing high levels of each of the mutants were established according to the procedure described previously (Kronman *et al.*, 1992).

Kinetic Studies and Analysis of Data - AChE activity was assayed according to Ellman *et al.* (1961) (in the presence of 0.1 mg/ml BSA, 0.3mM DTNB 50mM sodium-phosphate buffer pH-8.0 and various concentrations of ATC), carried out at 27°C and monitored by a Thermomax microplate reader (Molecular Devices). The apparent bimolecular

rate constants for the irreversible inhibition of HuAChE enzymes by organophosphonates DFP, DEFP and paraoxon (k_i) were determined by two methods:

Method A. Phosphylation experiments were carried out in at least 4 different concentrations of organophosphorus inhibitor (PX, see schemes 1, 2). The overall inhibitor concentration range was 10^{-8}-10^{-6}M, and for an individual enzyme the concentration span was about a factor of 10. In the first procedure, enzyme residual activity (E) was monitored at various times. The apparent bimolecular phosphylation rate constants (k_i^A) determined under pseudo-first order conditions (scheme 1) were computed from the plot of slopes of ln(E) vs time at different inhibitor concentrations. Rate constants under second order conditions were determined from plots of $\ln\{E/[PX_0 - (E_0 - E)]\}$ versus time.

scheme 1:

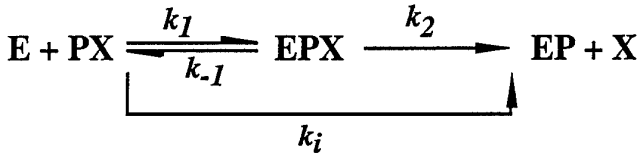

Method B. Determination of the bimolecular rate constants for phosphorylation (k_i^B) was carried out following the double - reciprocal method of Hart and O'Brien (1973). Apart from bimolecular rate constants this method allows to evaluate the apparent dissociation constant for the enzyme-inhibitor Michaelis complex (EPX; $K_d = k_{-1}/k_1$) and the phosphorylation rate constant of the reaction (k_2, see scheme 2).

scheme 2::

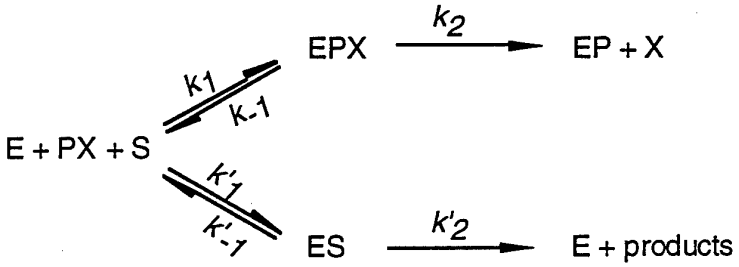

The enzyme is reacted simultaneously with an excess of inhibitor and of substrate that ensure a pseudo first order conditions with respect to both reactions. The kinetic data were analyzed according to the reaction depicted in scheme 2. A typical progressive inhibition curve is shown

in Fig. 22. Slopes of the tangents at each 20 sec. were obtained as part of fitting cubic spline curve through the experimental points (Rogers and Adams, 1990). Semi-logarithmic plots of these slopes against time resulted in linear correlations for all the concentrations of the inhibitors used. The slopes (Δlnv/Δt) were determined by linear regression (Fig. 22). These values are related to the kinetic parameters of the inhibition process according to the following expression:

Equation 1:

$$\frac{1}{k_{obs}} = \frac{K_d}{k_2} \frac{1}{[PX](1-\alpha)} + \frac{1}{k_2} \qquad \alpha = \frac{[S]}{K_m + [S]}$$

Plotting $\Delta t/\Delta lnv$ against $1/[PX](1-\alpha)$ yields the ratio K_d/k_2 and $1/k_2$ as the slope and the ordinate intercept respectively (Fig. 22C).

While in method A inhibitor concentrations fulfilled the condition $[PX] << K_d$, in method B inhibitor concentrations for most enzymes were in the range of $0.3K_d$ up to $10K_d$. In these experiments, for all enzymes except for the case of W86A, saturating concentrations of substrate (e.g. [ATC]/Km>3.5) were used.

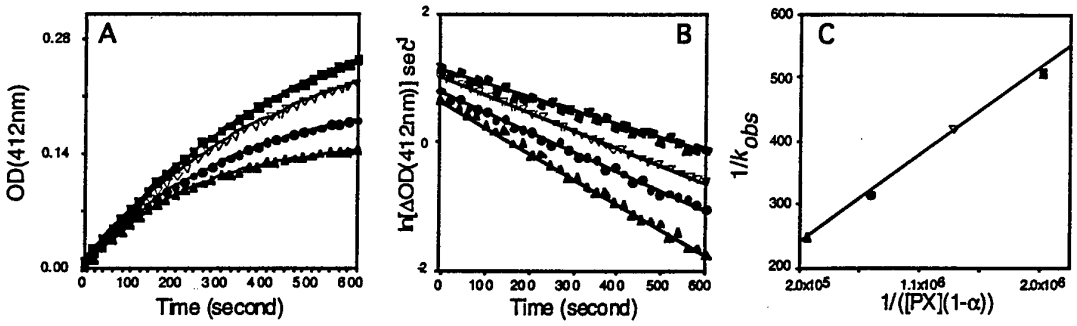

Figure 22: Progressive inhibition curves and derivation of the kinetic parameters for phosphorylation of HuAChE by paraoxon in presence of substrate (Method B). **A** - time course of hydrolysis of ATC in presence of paraoxon. **B** - linear time dependence of the slopes (ln ΔOD - equivalent to lnv) of the progressive inhibition curves shown in panel A. The slopes (Δlnv/Δt) of these plots yield the values of k_{obs} for the corresponding concentrations of inhibitor. **C** - double reciprocal plot of k_{obs} vs inhibitor concentration corrected for the presence of substrate ($1-\alpha$). The plot allows to derive the ratio K_d/k_2 and $1/k_2$ from the slope and the intercept respectively.

Molecular Modeling - Building and optimization of three-dimensional models of the HuAChE-organophosphate Michaelis complexes were performed on a Silicon Graphics workstation IRIS 70/GT using SYBYL modeling software (Tripos Inc.).The initial models were constructed by manual docking of the ligands into the active site gorge using the following guidelines: a. The alkoxy substituents were placed into the acyl pocket with the oxygen positioned according to the location of the methyl group in the model of HuAChE-ATC tetrahedral intermediate (Ordentlich *et al.*, 1993a). b. The P=O bond was positioned in a way that minimizes the distance P-O$^{\gamma}$–Ser-203 and that of the phosphoryl oxygen to amide nitrogens of residues Gly-121, Gly-122 and Ala-204. The resulting structures were optimized by molecular mechanics using the MAXMIN force field (and AMBER charge parameters for the enzyme) and zone refined, including 127 amino acids (15 Å substructure sphere around Ser-203). Optimization of the initial models included restriction of the distance between the phosphorus and O$^{\gamma}$– Ser-203 to 2.8Å, which was relieved in the subsequent refinement.

RESULTS

Selection of Organophosphate Inhibitors and HuAChE Mutants for Study : For both the Michaelis complex and the tetrahedral adduct we assume that the positioning of the phosphoryl moiety in the AChE active center is determined by the orientation of the P=O bond and by the P-O$^{\gamma}$-Ser203 distance. Therefore, the interactions of the phosphate inhibitor with the elements of its binding site are mainly through the alkoxy substituents and the leaving group. Such interactions can be studied by using diisopropyl phosphorofluoridate (DFP) and diethyl phosphorofluoridate (DEFP), which share the same leaving group (fluor) versus p-nitrophenyl diethyl phosphate (paraoxon) in which the leaving group is p-nitrophenoxy (Fig. 21). Similarly, DEFP and paraoxon, having the same alkoxy moieties are compared to DFP. Selection of mutants for this study was guided by previous mapping of the active center which identified residues constituting the functional subsites for interaction with substrates and presumably also with covalent inhibitors. These residues include: Tyr-337, Phe-338 which are part of the hydrophobic alkoxy site, Trp-86 - the "anionic" subsite (Ordentlich *et al.*, 1993a; 1995), Glu-450, Glu-202 and Tyr-133 key elements maintaining the functional architecture of

the active center (Ordentlich *et al.,* 1993b; Ordentlich *et al.,* 1995) and Phe-295 and Phe-297 that confer specificity of the acyl pocket (Fournier *et al.*, 1992; Harel *et al.,* 1992a,b; Vellom *et al.,* 1993; Ordentlich *et al.,* 1993a; Gnatt *et al.*, 1994).

Kinetic Analysis of Interaction of HuAChE Enzymes : Elucidation of the specific HuAChE-inhibitor interactions in the Michaelis complex and during the subsequent nucleophilic process is essential for understanding the reactivity of AChE toward phosphate derivatives. Towards this goal, the apparent bimolecular rate constants for the irreversible inhibition of the HuAChE enzymes were determined under experimental conditions (in the presence of substrate) that allow the evaluation of the apparent dissociation constants (K_d) as well as the phosphorylation rate constants k_2 (Hart and O'Brien, 1973; see scheme 2). Since in this method the apparent bimolecular rate constants of inhibition ($k_i^B=k_2/K_d$, Method B, see Methods) are determined using high concentrations of inhibitor, the calculated values of K_d may include contributions from other possible enzyme-inhibitor complexation processes and consequently may not correspond to the dissociation constants of the Michaelis complexes. Therefore, it was important to confirm the values of k_i by an alternative procedure (Method A) in which much lower inhibitor concentrations could be used ($[PX]<<K_d$) and where k_{obs} becomes insensitive to k_2 (Gray and Duggleby, 1989; Kovach, 1991). Under these conditions, the values of k_i^A are determined directly from the residual enzymatic activity after various periods of exposure to the inhibitor and in all cases a linear correlation of k_{obs} versus inhibitor concentration was observed. This indicates that the reaction involves a single enzyme-inhibitor equilibrium which is presumably the Michaelis complex (Aldridge and Reiner 1972).

The combination of the two methods allowed examination of the k_i values over a thousand fold range of inhibitor concentrations. At the lower end of the range k_{obs} approximates $k_i/[PX]$ while at the high concentrations k_{obs} approaches the limiting value of k_2. For most HuAChE enzymes, an excellent correlation between the bimolecular rate constant values determined by the two methods was observed. This correlation of k_i values, extending over 3 orders of magnitude, is linear irrespective of the nature of mutation or inhibitor with slopes approaching unity (0.945, 0.987 and 0.999 for DFP, DEFP and paraoxon respectively, see Fig. 23). The single HuAChE enzyme which consistently deviates from these correlations is Y337F. However, for reasons not clear to us, an outstanding standard deviation in determinations of

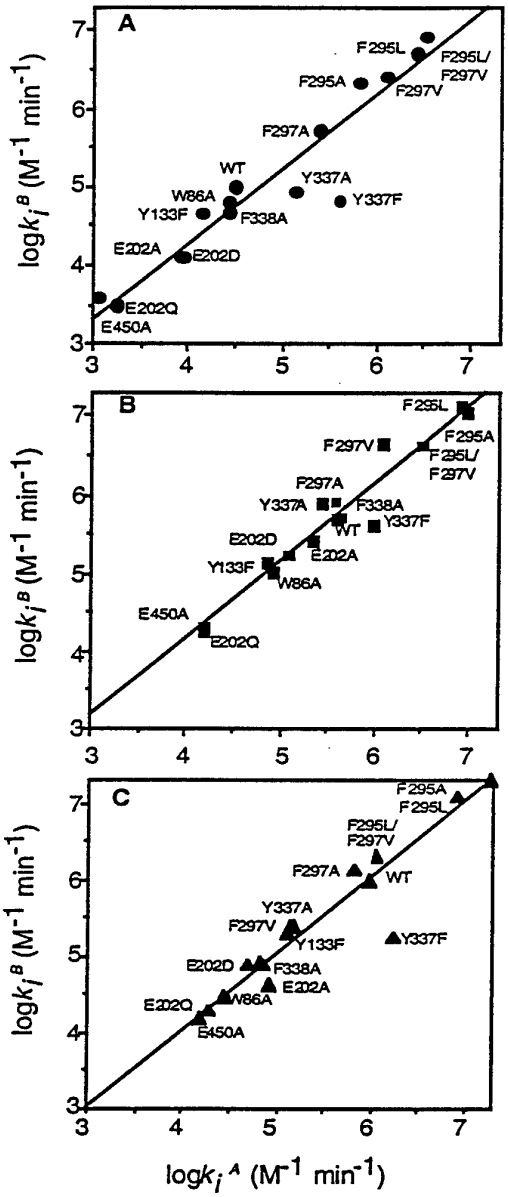

Fig. 23: Correlation of the bimolecular rate constants of phosphorylation for different HuAChE enzymes determined in absence (k_i^A) and in presence (k_i^B) of substrate. A. Correlation for DFP (slope = 0.945; r=0.925); **B.** Correlation for DEFP (slope = 0.987; r = 0.964); **C.** Correlation for paraoxon (slope = 0.999; r = 0.913)

k_i^A was also observed in this case. In the $\log k_i^A$ versus $\log k_i^B$ plots (Fig. 23) three major clusters of HuAChE enzymes can be defined. Interestingly, these three clusters correspond to the division according to the functional subsites in the HuAChE active center: mutants of the acyl pocket (F295A, F295L, F297A, F297V and F295L/F297V) exhibiting the highest k_i values of all the mutants tested; the alkoxy pocket (W86A, Y337A, Y337F and F338A) with k_i values close to that of the wild type enzyme; the H-bond network (E202A, E202D, E202Q, E450A and Y133F) with k_i values consistently lower as compared to the wild type enzyme. We note that within each cluster some variations of the k_i values can be observed, indicating a direct effect of the mutation on the interactions with the inhibitor. The considerable variability of the k_i values, reported for AChEs from different species (e.g. for paraoxon the reported range was 1.8 - 0.02$\mu M^{-1}min^{-1}$; Wang and Murphy 1982), probably originates from subtle structural changes similar to those described here. On the other hand, the ki values for the wild type HuAChE are in good agreement with those reported for primates and some other mammalian AChEs. For inhibition of monkey AChE by paraoxon and DFP, the k_i values are $1.22x10^6M^{-1}min^{-1}$ and $3.3x10^4M^{-1}min^{-1}$ respectively (Wang and Murphy, 1982).

The inhibitor concentrations used in the kinetic measurements of phosphorylation, according to method B, were for most mutants in the range of 0.3-10-fold or higher of the K_d value of the respective HuAChE enzyme derivative. Kinetic measurements (method B) for all the HuAChE mutants, except for the W86A enzyme, were carried out at saturating levels of substrate (e.g. [ATC]/Km>3.5). In the case of W86A such levels of substrate concentration are precluded by the high value of Km (Ordentlich *et al.*, 1993a) and therefore the corresponding K_d and k_2 values should be regarded as tentative. The calculated values of k_2 for the HuAChE enzymes are low compared to those reported by Hart and O'Brien (1973) and by Main and Iverson (1966) for the bovine erythrocyte and eel AChEs respectively. However many of the more recent studies report values closer to those obtained by us (Liu and Tsou 1986; Kemp and Wallace 1990). In particular, inhibition studies of mouse AChE mutants by paraoxon resulted in k_2 values in the range of 3.4 - $1.8min^{-1}$ (Radic *et al.*, 1995) while inhibition of *Torpedo californica* AChE mutants by DFP yielded k_2 values in the range of 0.3-$1.6min^{-1}$ (Radic *et al.*, 1992). Notably, the rate constants of the chemical transition from the enzyme-phosphate Michaelis complex to the phosphorylated enzyme (k_2) varied within a narrow range for almost all the various HuAChE enzymes (Fig. 24).

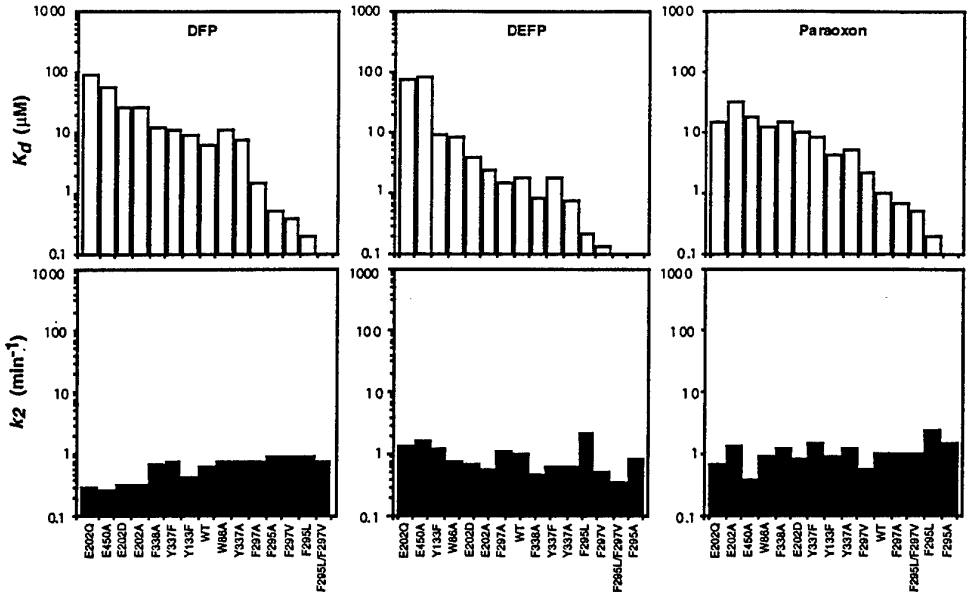

Fig. 24: Effects of mutations at the HuAChE active center on the values of the dissociation constants K_d and the phosphorylation rate constants k_2. The figure illustrates that for a given organophosphate the variability in K_d extends over a factor 1000 while that in k_2 does not exceed factor 4.

The relative invariance of k_2 values, irrespective of the enzyme source or the structure of organophosphorus inhibitors, has been already observed in several cases (Main and Iverson, 1966; Andersen *et al.*, 1977; Forsberg and Puu, 1984; Grey and Dawson 1987; Kemp and Wallace 1990). In the present study the limited variability of the k_2 values is evident for a series of enzymes differing *only* in a single or in one case a double replacement of residues at the active center. This may suggest that perturbations of the active center architecture affect mainly the enzyme affinity towards organophosphate inhibitors as demonstrated in the variability of the dissociation constant (K_d) values over a range of 3 orders of magnitude for each of the inhibitors (Fig. 24).

Effect of Mutation of Acyl pocket Residues on Interactions with Various Organophosphates: Two phenylalanine residues at positions 295 and 297 were implicated in accommodation of the acyl moieties of various substrates, by site directed mutagenesis (Vellom *et al.,* 1993; Ordentlich *et al.,* 1993a), by molecular modelling of HuAChE (Ordentlich *et al.,* 1993a) and of TcAChE (Harel *et al.,* 1992) and by comparison to BuChE (Gnatt *et al.,* 1994). We substituted these phenylalanine residues by less bulky amino acids and studied the kinetics of inhibition for the following enzymes: F295A, F295L, F297A, F297V and F295L/F297V (Table 16). Replacements by alanine remove steric hinderance in the HuAChE acyl pocket while introduction of valine at position 295 or leucine at position 297, follows the corresponding occupation (Lockridge *et al.,* 1987) of these positions in BuChE . In general, replacements at the acyl pocket enhance the reactivity towards the organophosphate inhibitors although some differences related to the inhibitor structure can be observed (Table 16). Replacement of Phe-295 by alanine brings a larger decrease in the values of K_d as compared to the one observed for its replacement by valine, suggesting that phenylalanine at position 295 restricts the accommodation of the ethoxy group at the acyl pocket. Removal of the bulky group from position 297 (F297A) has no effect on the affinity towards DEFP while, introduction of valine (F297V) improves the accommodation of the inhibitor. This observation is somewhat surprising in view of the prediction from previous molecular modeling (Barak *et al.*, 1992; Ordentlich *et al.,* 1993a) which implicated *both* residues Phe-295 and Phe-297 in steric interference with groups larger than methyl.

The pattern of effects due to replacements at positions 295 and 297 on the affinities towards DFP is somewhat different from DEFP, reflecting the influence of the bulkier alkoxy group. Steric hindrance due to Phe-297 is evident from the increase in affinity of DFP compared to DEFP in the F297A enzyme. In addition the hydrophobic interactions in both F295L and F297V are more pronounced in the case of DFP. Both DFP and DEFP show enhanced affinities towards the double mutant F295L/F297V, however the effect in case of DFP is more pronounced indicating again the larger contribution of hydrophobic interactions. As could be expected from the identity of their alkoxy groups, the pattern of affinity changes for paraoxon follows that of DEFP with respect to replacements of Phe-295. However the lack of affinity enhancement of the double mutant F295L/F297V towards paraoxon may be related to the difference in leaving groups. Unlike the fluorine in DFP and DEFP, the leaving group in

Table 16: Effect of mutation of acyl pocket residues on interactions with various organophospates.

	HuAChEs	k_i A ($x10^{-4}$ M^{-1} min^{-1})	k_i B ($x10^{-4}$ M^{-1} min^{-1})	K_d (μM)	k_2 (min^{-1})
DFP	WT	14 ± 1	10.0 ± 0.2	6.0 ± 0.3	0.60 ± 0.02
	F295A	65 ± 14	220 ± 12	0.50 ± 0.07	1.0 ± 0.1
	F295L	264 ± 21	500 ± 32	0.20 ± 0.07	0.94 ± 0.3
	F297A	25 ± 9	48 ± 4	1.5 ± 0.4	0.7 ± 0.2
	F297V	123 ± 10	250 ± 16	0.37 ± 0.08	0.92 ± 0.15
	F295L/F297V	340 ± 40	810 ± 65	0.10 ± 0.02	0.8 ± 0.1
DEFP	WT	40 ± 2	50 ± 2	1.9 ± 0.3	1.0 ± 0.1
	F295A	830 ± 300	1450 ± 70	0.06 ± 0.01	0.8 ± 0.1
	F295L	940 ± 180	1060 ± 175	0.22 ± 0.05	2.3 ± 0.6
	F297A	40 ± 8	90 ± 14	1.4 ± 0.5	1.2 ± 0.3
	F297V	126 ± 2	426 ± 26	0.13 ± 0.02	0.54 ± 0.06
	F295L/F297V	310 ± 55	400 ± 80	0.09 ± 0.03	0.35 ± 0.05
Paraoxon	WT	97 ± 2	100 ± 1	0.98 ± 0.02	1.00 ± 0.01
	F295A	1800 ± 220	3080 ± 490	0.05 ± 0.02	1.5 ± 0.3
	F295L	800 ± 80	1240 ± 15	0.20 ± 0.02	2.3 ± 0.2
	F297A	68 ± 4	134 ± 10	0.73 ± 0.24	1.0 ± 0.3
	F297V	14 ± 1	25 ± 1	2.2 ± 0.8	0.54 ± 0.18
	F295L/F297V	117 ± 22	200 ± 16	0.5 ± 0.1	1.0 ± 0.1

The apparent bimolecular rate constant k_i A was determined using method A while k_i B, K_d and k_2 were determined using method B (see 'Methods').

The following Km (mM) values were used for determination of α parameter (equation 1) : Wild Type 0.14, F295A 0.13, F295L 0.27, F297A 0.43, F297V 1.20, F297L/F297V 0.40.

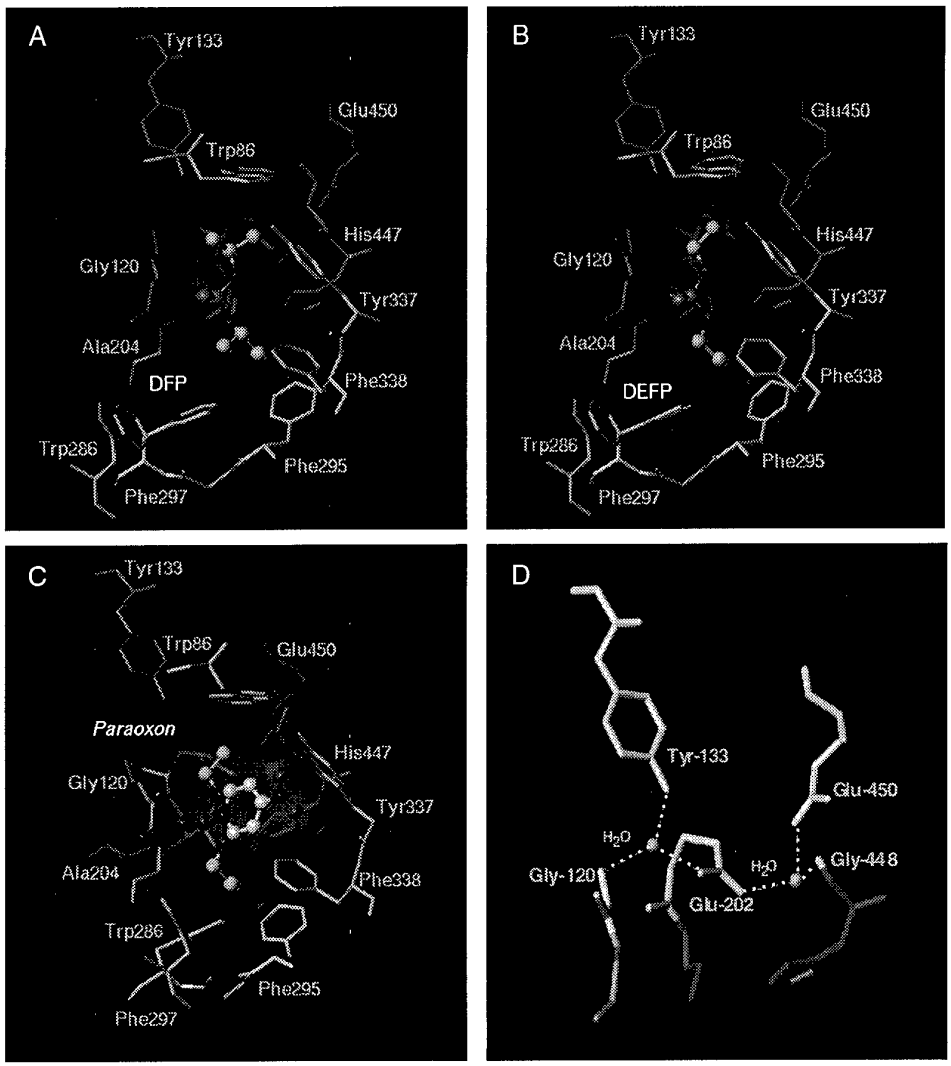

Fig. 25: HuAChE Michaelis complexes with organophosphate inhibitors and the H-bond network in the HuAChE active center. Residues desplayed represent the acyl pocket: Phe295 and Phe297; the alkoxy pocket: Tyr337 and Phe338; and the "anionic" subsite: Trp86. The ligands are depicted as balls and sticks. The volume occupied by the ligand is shown as a semi-transparent solid shape. Residues Glu-202 and the catalytic Ser-203 can be seen behind the ligand. For all the Michaelis complexes the distances phosphorus - Oγ-Ser-203 are equivalent (3.45Å). Note also the near equivalent distances of the phosphoryl oxygen (P=O) from H-bond donors of the oxyanion hole (Glu-121, Glu-122 and Ala-204). **A**. HuAChE-DFP complex; distances P=O - N-amide of Gly-121, Gly- 122 and Ala-204 (2.44, 2.82 and 3.84 Å respectively); distances of the isopropoxy methyl from aromatic Cζ - Phe-297 and Cε1 - Phe-295 (3.30 and 3.10 Å respectively). **B**. HuAChE-DEFP complex; distances P=O - N-amide of Gly-121, Gly-122 and Ala-204 (2.48, 2.72 and 3.90 Å respectively); distances of the ethoxy methyl from aromatic Cζ - Phe-297 and Cε1 - Phe-295 (3.56 and 2.98 Å respectively). **C.** HuAChE-paraoxon complex; distances P=O - N-amide of Gly-121, Gly-122 and Ala-204 (2.44, 2.69 and 3.80Å respectively); distances of the ethoxy methyl from aromatic Cζ - Phe-297 and Cε1 - Phe-295 (3.60 and 2.98 Å respectively); distance of paraoxon nitro oxygen - Oη–Tyr-337 (2.80 Å); distances of paraoxon aromatic C_2 and C_3 - Cζ-Phe-338 (3.60 and 3.44 Å respectively). **D**. The proposed hydrogen-bond network across the active center of HuAChE, bridging three of the loops which bear respectively the oxyanion hole (Gly-121, Gly-122), the catalytic Ser-203 and the catalytic His-447. The H - bond distances, marked by dashed lines, between the active center water molecules and relevant residues within the network are: N(G121)-O(H_2O) 2.58 Å; O(Y133)-O(H_2O) 2.50 Å; O(E202)-O(H_2O) 3.01 Å; O(E450)-O(H_2O) 2.80 Å; O(E202)-O(H_2O) 2.36 Å; N(G441)-O(H_2O) 3.07 Å.

paraoxon is capable of forming specific interactions with elements of the active center that restricts its ability to optimally adjust the positioning of the alkoxy group in the acyl pocket (compare Fig. 25A,B to Fig. 25C) .

Effect of Mutation of Alkoxy Pocket Residues on Interactions with Various Organophosphates: The aromatic residues Trp-86, Tyr-337 and Phe-338 define a hydrophobic alkoxy pocket for the alkoxy leaving group of the substrates (Ordentlich *et al.*, 1993a). The extent to which any of these residues interact with the substrates depends upon the charge of the substrate leaving group. As shown previously for ATC (Ordentlich *et al.*, 1993a; 1995), the contribution of Trp-86, the anionic subsite, is of paramount importance for stabilization of the charged tetraalkyl nitrogen while for the noncharged isosteric substrate TB the hydrophobic interactions with Tyr-337 and Phe-338 appear to be more significant. One can assume that the same binding pocket can accommodate one of the phosphate alkoxy moieties. However, due to the tetrahedral geometry of the phosphate it is expected to interact with additional elements in the active center and the juxtaposition of the alkoxy moiety versus the aromatic side chains of Trp-86, Tyr-337 and Phe-338 should be somewhat different than for the noncharged substrates such as TB. The affinity of paraoxon towards the W86A enzyme is 12-fold lower than that for the wild type HuAChE (Table 17).

This effect can be attributed mainly to the nature of the paraoxon leaving group since no comparable effects were observed for the corresponding affinities of DEFP and DFP (compare Fig. 25A,B to Fig. 25C). Affinity towards paraoxon is also sensitive to replacement of Phe-338 by alanine (17-fold lower than that of the wild type enzyme). Again, no such effect is observed for either DEFP or DFP suggesting a specific participation of the p-nitrophenyl group in interaction with Phe-338. Involvement of Phe-338 in aromatic-aromatic interaction was reported previously for the p-nitrophenyl acetate hydrolysis by HuAChE enzymes (Ordentlich *et al.*, 1993a).

The affinities of both DFP and DEFP are not sensitive to replacements at position 337 by either phenylalanine or alanine. The comparable reduction in affinity of paraoxon towards Y337A and Y337F enzymes indicates that the main contribution to the stabilization of the complex is due to the hydroxyl group of Tyr-337 and not due to its aromatic moiety. The picture emerging from

Table 17: Effect of mutation of alkoxy pocket residues on interactions with various organophosphates.

	HuAChE	k_i A ($x10^{-4}$ M^{-1} min^{-1})	k_i B ($x10^{-4}$ M^{-1} min^{-1})	K_d (μM)	k_2 (min^{-1})
DFP	WT	14 ± 1	10.0 ± 0.2	6.0 ± 0.3	0.60 ± 0.02
	W86A	2.6 ± 0.1	6.5 ± 0.1	11.3 ± 0.5	0.73 ± 0.02
	Y337A	3.0 ± 0.2	10.0 ± 0.5	7.3 ± 1.4	0.7 ± 0.1
	Y337F	40 ± 10	7.7 ± 0.8	11 ± 5	0.8 ± 0.3
	F338A	2.6 ± 0.2	5.4 ± 0.1	12 ± 1	0.7 ± 0.1
DEFP	WT	40 ± 2	50 ± 2	1.9 ± 0.3	1.0 ± 0.1
	W86A	9 ± 1	10.5 ± 0.3	8.0 ± 3.2	0.8 ± 0.3
	Y337A	27 ± 4	78 ± 2	0.75 ± 0.14	0.6 ± 0.02
	Y337F	99 ± 15	37 ± 4	1.8 ± 0.5	0.7 ± 0.1
	F338A	45 ± 5	64 ± 1	0.80 ± 0.04	0.5 ± 0.01
Paraoxon	WT	97 ± 2	100 ± 1	0.98 ± 0.02	1.00 ± 0.01
	W86A	5.0 ± 0.7	7.5 ± 0.2	11.7 ± 1.8	0.9 ± 0.2
	Y337A	14.4 ± 1.4	24 ± 1	4.9 ± 0.6	1.2 ± 0.1
	Y337F	180 ± 54	17 ± 1	9 ± 3	1.4 ± 0.4
	F338A	7.0 ± 0.6	7.2 ± 0.3	16.7 ± 2.4	1.2 ± 0.1

The apparent bimolecular rate constant k_i A was determined using method A while k_i B, K_d and k_2 were determined using method B (see 'Methods').

The following Km values (mM) were used for determination of α parameter (equation 1) : Wild Type 0.14, W86A 94, Y337A 0.10, Y337F 0.16, F338A 0.24.

these results is that the extent of participation of residues Trp-86, Tyr-337 and Phe-338 in accommodation of the phosphate alkoxy moiety depends mainly upon the nature of the leaving group. The p-nitrophenyl moiety of paraoxon is unlikely to interact directly with all the three aromatic residues and its indirect effect is probably due to restrictions imposed on the possible reorientation of the inhibitor in the active center (compare the relative binding environment for the leaving groups of DEFP - Fig. 25B and paraoxon - Fig. 25C).

Although residue Tyr-133 is adjacent to Trp-86, molecular models (Ordentlich *et al.*, 1995) indicate that it does not interact directly with the alkoxy moieties of substrates or organiophosphates.The reported major reduction in reactivity of the Y133A enzyme toward organophosphates was explained by steric obstruction of the alkoxy pocket (Ordentlich *et al.*, 1995). The effect of replacement of Tyr-133 by phenylalanine, on the affinities towards all the phosphate inhibitors studied, is less pronounced and not uniform with respect to the different inhibitors. While the respective affinities for paraoxon and DEFP decrease about 5-fold, the affinity for DFP is hardly affected. The participation of the hydroxyl group of Tyr-133 in the H-bond network (Fig. 25D) maintaining the relative position of the Glu-202 carboxylate, in the HuAChE active center, has been suggested before (Ordentlich *et al.*, 1993b). Thus the decrease in affinity of Y133F mutant enzyme towards paraoxon and DEFP could be attributed to the somewhat altered architecture of the active center due to the disruption of this H-bond network.

Effect of Mutation of H-bond Network Residues on Interactions with Various Organophosphates: The H-bond network in the HuAChE active center was suggested (Ordentlich *et al.*, 1993b) to include two of the three buried acidic residues (Glu-202 and Glu-450), two water molecules which correspond to solvent molecules in the structure of TcAChE (Sussman *et al.*, 1991), Tyr-133 and the backbone amide oxygens of Gly-122 and Gly-448 (Fig. 25D). Replacement of each of the acidic residues (Glu-202 and Glu-450) affected the catalytic activity of the resulting enzymes towards both charged and noncharged substrates (Ordentlich *et al.*, 1993b). This effect was attributed to reorganization of the active center upon replacement of the carboxylates with noncharged moieties. In the case of phosphate inhibitors, replacement of Glu-450 by alanine, resulted in a substantial decrease of the affinities towards paraoxon and DEFP (18 and 42-fold respectively; Table 18).

Table 18: Effect of mutation of H-bond network residues on interactions with various organophosphates.

	HuAChEs	k_i A ($x10^{-4}$ M^{-1} min^{-1})	k_i B ($x10^{-4}$ M^{-1} min^{-1})	K_d (μM)	k_2 (min^{-1})
DFP	WT	14 ±1	10.0 ±0.2	6.0 ±0.3	0.60 ±0.02
	Y133F	1.4 ±0.1	4.6 ±0.1	9.0 ±0.4	0.40 ±0.01
	E202A	0.9 ±0.1	1.3 ±0.1	25.3 ±0.7	0.30 ±0.01
	E202D	0.8 ±0.1	1.3 ±0.1	25.3 ±1.5	0.30 ±0.01
	E202Q	0.18 ±0.06	0.30 ±0.06	90 ±16	0.30 ±0.02
	E450A	0.09 ±0.03	0.5 ±0.1	53 ±15	0.30 ±0.04
DEFP	WT	40 ±2	50 ±1.6	1.9 ±0.3	1.0 ±0.1
	Y133F	7.7 ±0.5	14 ±2	9 ±4	1.2 ±0.4
	E202A	22.3 ±1.6	25 ±1	2.3 ±0.5	0.6 ±0.1
	E202D	12.5 ±1.5	17 ±2	3.9 ±0.1	0.7 ±0.1
	E202Q	1.5 ±0.6	1.8 ±0.1	75 ±12	1.3 ±0.2
	E450A	1.5 ±0.6	2.1 ±0.2	80 ±15	1.7 ±0.5
Paraoxon	WT	97 ±2	100 ±1	0.98 ±0.02	1.00 ±0.01
	Y133F	13 ±1	20.5 ±0.7	4.3 ±0.5	0.9 ±0.1
	E202A	8.3 ±0.2	4.3 ±0.1	30 ±10	1.3 ±0.4
	E202D	6.8 ±1.2	8.2 ±0.1	10 ±1	0.80 ±0.07
	E202Q	2.8 ±0.5	4.7 ±0.2	14 ±1	0.70 ±0.01
	E450A	1.9 ±0.7	2.4 ±0.4	18 ± 8	0.4 ±0.1

The apparent bimolecular rate constant k_i A was determined using method A while k_i B, K_d and k_2 were determined using method B (see 'Methods').

The following Km values (mM) were used for determination of α parameter (equation 1) : Wild Type 0.14, Y133F 0.48, E202A 0.44, E202D 0.30, E202Q 0.35, E450A 0.35.

A similar pattern of effects was observed for E202Q, however while Glu-202 is adjacent to the catalytic serine (Ser203), residue Glu-450 is 9 Å away. Replacement of Glu-202 by alanine or by aspartic acid produce only minor effects on the respective affinities towards DFP and DEFP, but for paraoxon the decrease in affinities is more substantial (30 and 10-fold, respectively). Quite surprisingly, the most pronounced effect on affinity is observed for E202Q for which the steric perturbation is minimal. These results indicate that the effects due to replacement of Glu-202, are not related only to charge since E202A and E202D show comparable affinities for the phosphate inhibitors.

DISCUSSION

Interactions of Organophosphates with the Acyl Pocket

Early investigations of AChE and BuChE active center topologies, based on structure-activity studies of several series of substrates and organophosphorus inhibitors, indicated specific binding pockets for the acyl and the alkoxy groups of the substrate (Jarv, 1984). In addition, these studies suggested that the distinct sizes of the AChE and BuChE acyl pockets are the main structural difference in the ligand binding environments of the two enzymes . Molecular modeling of this subsite in HuAChE (Barak *et al.*, 1992), based on the x-ray structure of TcAChE (Sussman *et al.*, 1991), equally implicated residues Phe-295 and Phe-297 in conferring selectivity for ATC by restricting the dimensions of the acyl pocket (Harel *et al.*, 1992; Ordentlich *et al.*, 1993a). However, measurements of Km values of HuAChE enzymes for ATC and BTC (butyrylthiocholine; Ordentlich *et al.*, 1993a; Hosea *et al.*, 1995) revealed that while replacements at position 297 had only a minor effect on selectivity, those at position 295 lowered the Km value for BTC even below that of BuChE. The absence of similar effects on kcat signified that replacements at position 295 relieve steric interference mainly in the noncovalent (Michaelis Menten) complex of BTC.

The observed similarity of the overall effects of residue replacements at the acyl pocket, on the values of Km for substrates and K_d for phosphates, provides an important insight into the organization of the respective Michaelis complexes, indicating that the acyl pocket serves indeed a analogous purpose in both cases. However, due to the added dimensionality of the

phosphates, variations in the K_d values reveal additional effects of the acyl pocket structural modifications. These are exemplified by the opposite effects on affinity , due to replacement of Phe-295 by alanine versus leucine, toward the ethoxy and isopropoxy substituted phosphates, indicating the interplay between the steric and the hydrophobic interactions in the acyl pocket. Replacement of Phe-297 by valine stabilizes the complex of DEFP while it destabilizes that of paraoxon. This difference may signify the influence of the leaving group since in the DEFP complex the enzyme-ligand assembly can readjust without affecting the relative juxtaposition of its P=O bond relative to the active site serine and the oxyanion hole. Such plasticity is less likely in case of paraoxon due to the additional specific interactions of the p-nitrophenoxy moiety which prevents the repositioning of the alkoxy group in the acyl pocket (compare the model of Michaelis complex of paraoxon to that of DEFP, Fig. 25C and 25B respectively).

The equivalence of the binding subsites for the substrate acyl moiety and for the phosphate alkoxy group can be further demonstrated by comparing the relative reactivity of the F295L/F297V HuAChE towards DFP, to that of BuChE (in which the native acyl pocket configuration is leucine/valine). The bimolecular rate constant of DFP phosphorylation (k_i) for the F295L/F297V is 80-fold higher than that for the wild type HuAChE (Table 16) and likewise the corresponding rate constant for BuChE is 110-fold higher than that for AChE (Main and Iverson, 1966). In addition, the reactivity of the F295L/F297V double mutant of HuAChE toward paraoxon is very similar to that of the wild type enzyme (Table 16) and to that of BuChE (Aldridge and Reiner, 1972). For the acylation reaction, the functional equivalence of the acyl pocket subsites in the F295L/F297V HuAChE and in BuChE was already demonstrated through the similarity (less than 2-fold) of the bimolecular rate constants for butyrylthiocholine hydrolysis by the two enzymes (Ordentlich *et al.*, 1993a).

The emerging picture, concerning the roles of residues Phe-295 and Phe-297 as the determinants of specificity in the HuAChE active center, is that they form a pocket which can accommodate substituents of ligands for which the primary locus of interaction is the active site of the enzyme. In case of ATC accommodation of the methyl group in this pocket together with the oxyanion hole orient the molecule in plane for the incipient nucleophilic attack (Fournier *et al.*, 1992; Harel *et al.*, 1992; Vellom *et al.*, 1993; Ordentlich *et al.*, 1993a; Gnatt *et al.*, 1994; Hosea *et al.*, 1995). In a similar way, interaction of this subsite with organophosphates helps to orient the molecules for the in-line attack by the catalytic serine. In both cases the respective substituent is projected towards Phe-295 and therefore the corresponding complexes are more

sensitive to the volume of residue at this position. Steric interactions with residue at 297 become important for branched alkoxy substituents which present larger volume to the acyl pocket (see Fig. 25A-C).

Accommodation of the Phosphate Leaving Group in the Alkoxy Pocket

Like the case of the acyl pocket, the involvement of the substrate alkoxy binding pocket in accommodation of organophosphate inhibitors appears to be confined to the stabilization of the Michaelis complexes, since replacements of residues associated with this pocket had no effect on the phosphorylation rate constants k_2 (Table 17). Only marginal effects could be observed, upon replacement of the aromatic residues Trp-86, Tyr-337 or Phe-338, on the stability of complexes with DFP and DEFP underscoring the nonspecific nature of the hydrophobic interactions of the alkyl moieties with the enzyme surface. Such absence of contributions due to specific residues was already observed in the cases of noncharged substrates TB and propylacetate (Ordentlich *et al.*, 1993a). A somewhat more pronounced dependence on the structure of the alkoxy pocket is evident in the case of paraoxon. However, most of these effects appear to originate from interactions with the p-nitrophenoxy leaving group (e.g. compare the effects of replacements at positions 337 and 338 on values of K_d for DEFP and paraoxon, Table 17). Molecular modeling (Fig. 25C) of paraoxon Michaelis complexes with the corresponding HuAChE enzymes (Y337A, Y337F and Y338A) demonstrates that the effects of replacement of the aromatic residue at position 338 or the H-bond donating function at position 337, on the complex stability is due to interactions with the p-nitrophenyl moiety. Furthermore, the model shows that these interactions induce a somewhat different position of the ethoxy moiety, compared to the DEFP complex, bringing it closer to the indole ring of Trp-86 (Fig. 25B-C). This proximity, together with the already mentioned limited plasticity of paraoxon complexes is consistent with the larger decrease in affinity of the W86A enzyme toward paraoxon than toward DEFP. In complexes of DEFP and DFP the corresponding fluoro leaving group does not appear to interact with elements of the alkoxy pocket.

Interaction of the p-nitrophenoxy leaving group with residue Phe-338 has already been demonstrated for the tetrahedral intermediate of p-nitrophenyl acetate (Ordentlich *et al.*, 1993a). However, the absence of effect due to residue Tyr-337 indicates that the position of the p-nitrophenoxy moiety in the tetrahedral conjugates of p-nitrophenyl acetate and paraoxon are somewhat different. In addition, since for these two conjugates the positioning of the

appropriate substituent in the acyl pocket appears to be equivalent, the locations of the other oxy- substituents (ethoxy group in paraoxon or Ser203 in case of p-nitrophenyl acetate) have to be quite different. The potential multiplicity of the alkoxy pocket binding elements raises the possibility that both the alkoxy substituent and certain leaving groups are accommodated by this subsite. Thus, it appears that the interactions of AChE with the tetrahedral organophosphate mimic only partially those of enzyme-substrate tetrahedral intermediate and by analogy those with the transition state of the acylation by carboxylates.

Affinity of HuAChE Towards Organophosphates is a Major Determinant of its Overall Reactivity in the Phosphorylation Process

The most consistent characteristics of the HuAChE enzymes reactivity pattern toward the organophosphates studied here is that structural variations in both the enzyme and the inhibitor affect mainly the stability of the Michaelis complexes. While replacements of selected residues in HuAChE brought about changes of about 2,000-fold in the K_d values, the corresponding phosphorylation rate constants (k_2) remained essentially unchanged (Fig. 24). Although observations regarding the limited variability of k_2 have been reported for AChEs from numerous sources, including bovine erythrocytes, electric eel, monkey, catfish or frog brain (Wang and Murphy 1982; Forsberg and Puu, 1984; Kemp and Wallace, 1990), it is the first study in which this reactivity characteristics of AChE has been systematically examined in a series of enzymes with limited and well defined structural differences. Furthermore the relative invariance of k_2 was also reported for various organophosphorus inhibitors, using different experimental techniques, including stop flow methods (Forsberg and Puu, 1984; Gray and Davson, 1987; Ryu *et al.*, 1991). Possible rationalization of these observation is that while the affinity is influenced by the spatial complementarity of the organophosphorus inhibitor with the AChE active center binding environment, the nucleophilic reaction rate is dependent mainly on the nucleophilicity of the catalytic serine and the electronic properties of the phosphoryl moiety, as has been also suggested by others (Kemp and Wallace, 1990). In addition, perturbation of the H-bond network in HuAChE active center, through replacement of the participating residues Tyr-133, Glu-202 or Glu-450 does not significantly affect the rate constants of the phosphorylation step (Table 18). Such limited effect on the k_2 values indicates that for the organophosphates tested here, the nucleophilic reaction at the phosphorus is not very sensitive to the altered architecture of the active center. Since the same perturbations of the H-bond

network were shown to affect the rate constants of the catalytic process (Ordentlich *et al.*, 1993b) we may conclude that the participation of the active center molecular environment in facilitating the formation of covalent bonds is probably different for acylation by carboxyl and by phosphoryl esters.

IX. Engineering Resistance to 'Aging' of Phosphylated Human Acetylcholinesterase

INTRODUCTION

Cholinesterases (ChEs) are readily phosphylated (the comprehensive term "phosphyl" is adopted from Bourne and Williams 1984 for all tetravalent P electrophilic groups) , at the active site serine, by a variety of organophosphonates and organophosphates (OP) (Aldrich and Reiner 1972; Taylor 1990). The OP-ChEs conjugates then undergo postinhibitory processes, the nature and extent of which depend upon the structure of the inhibitor and the particular enzyme studied. Spontaneous reactivation, through displacement of the phosphyl moiety (Scheme 1) from the active site, is usually very slow (Main 1976) however the enzyme can be reactivated by various oxime nucleophiles (Re in Scheme 1) (Aldrich and Reiner 1972; Froede and Wilson 1971). In certain cases such reactivation is thwarted due to a concomitant unimolecular process termed aging (Aldrich and Reiner 1972; Hobbinger 1955). It was proposed that this process consists of through alkyl - oxygen bond scission resulting in a formal negative charge in the OP - ChEs conjugate (see Scheme 1) (Michel *et al.*, 1967, Berman and Decker 1986). The aged OP-conjugate is refractive to reactivation (Michel *et al.*, 1967, Gray 1984) and thus renders treatment, following intoxication with certain OP insecticides or nerve gas agents, extremely difficult (Glickman *et al.*, 1984).

Scheme 1:

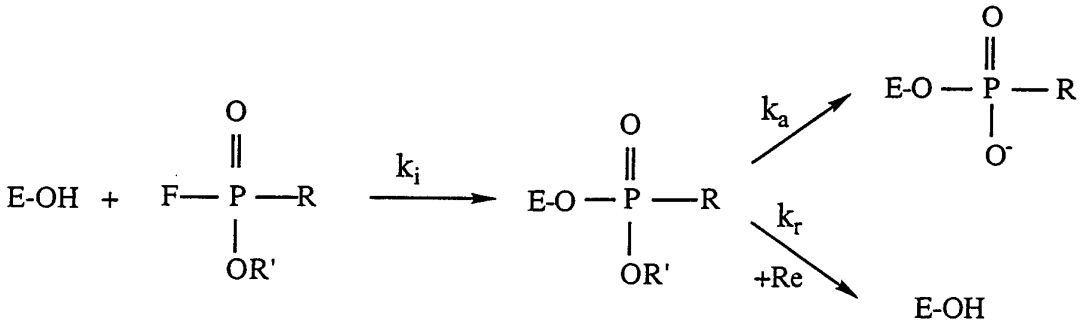

Although the aging process is understood on the basis of carbonium ion mechanism (Benschop and Keijer 1966) and depends on the phosphorus stereochemistry in the conjugates (Berman and Decker 1989), the role of the enzyme environment in facilitating the process is not well

understood. In general, the catalysis of aging is particularly efficient in ChEs compared to OP - conjugates with other serine hydrolases (Van der Drift *et al.*, 1985; Grunwald *et al.*, 1989), indicating a specific involvement of residues vicinal to the phosphyl moiety in the ChEs active center.

Recently we have generated a large number of recombinant human acetylcholinesterase (HuAChE) mutants and identified amino acids important for maintaining the structural integrity of the enzyme (Velan *et al.*, 1991b; Shafferman *et al.*, 1992a) as well as residues involved in catalysis and in interactions with various substrates and reversible inhibitors (Shafferman *et al.*, 1992b,c; Ordentlich *et al.*, 1993; see also section VIII). In these studies, active center residues comprising the catalytic triad, the anionic subsite and the acyl pocket, as well as residues of the peripheral anionic subsites were identified. Here we report on the extension of this approach to gain insight into reactions with irreversible OP inhibitors and the subsequent postinhibitory processes.

Comparison of reaction rates of inhibition and aging of selected active center HuAChE mutants and the wild type enzyme reveals key residues involved in the generation and stabilization of the negatively charged E-P-O^- conjugate.

METHODS

Substrates and Inhibitors- Acetylthiocholine iodide (ATC), 5:5'-dithiobis (2-nitrobenzoic acid) (DTNB), diisopropyl phosphorofluoridate (DFP) were purchased from Sigma. S - 3,3 - dimethylbutyl thioacetate ($CH_3C(O)SC_2H_4C(CH_3)_3$ - TB) was synthesized and purified as described previously (see Section II).Purified pinacolyl methylphosphonofluoridate (soman) was a gift from Dr.Y.Segall; 7-(methylethoxyphosphophinylloxy)-1-methylquinolinium iodide (MEPQ) a gift from Dr.Y.Ashani; and 1-(2-hydroxyiminomethylpyridinium)-1-(4-carboxyimino-pyridinium) dimethylether dichloride (HI-6) was a gift from Dr. G.Amitai.

Recombinant HuAChE and its Mutants - Expression of recombinant HuAChE and its mutants in a human embryonal kidney derived 293 cell line, was described previously (Shafferman *et al.*, 1992a; Velan *et al.*, 1991a; Kronman *et al.*, 1992). Generation of mutants E202Q(*E199*) (Amino acids and numbers in parentheses refer to the position of analogous

residues in Torpedo AChE (TcAChE) according to the recommended nomenclature: Massoulie *et al.*, 1992) and Y337A(F*330*) and F338A(*F331*) were described previously (Ordentlich *et al.*, 1993). Substitution of residue E450(*E443*) was carried out by replacement of the *BstBI-BamHI* DNA fragment of the AChE-w3 variant (Shafferman *et al.*, 1992a) with synthetic DNA duplexes carrying the GCC(Ala) codon. Construction of Y133F was described in section IV. Stable recombinant cell clones expressing high levels of each of the mutants were established according to the procedure described previously (Kronman *et al.*, 1992). The resulting recombinant clones were propagated in multitray systems (Lazar *et al.*, 1994). The secreted enzymes in the cell supernatant (2-6 liters) were purified (over 90% purity) by affinity chromatography as described previously (Kronman *et al.*, 1992).

Kinetic Studies and Analysis of Data - AChE activity was assayed according to Ellman *et al.* (1961) (in the presence of 0.1 mg/ml BSA, 0.3mM DTNB 50mM sodium-phosphate buffer pH-8.0), carried out at 27°C and monitored by a Thermomax microplate reader (Molecular Devices). Michaelis-Menten constant (Km) values were obtained from the double reciprocal Lineweaver Burk plots and k_{cat} calculations were based on ELISA quantitations (Shafferman *et al.*, 1992b) as well as on determination of active site concentration by MEPQ titrations (Velan *et al.*, 1991b; Levy and Ashani 1986) (see Fig. 27). Phosphylation experiments were carried out in at least 4 different concentrations of OP-inhibitor (I) and two concentrations of enzyme, and enzyme residual activity (E) at various times was monitored. The apparent bimolecular phosphylation rate constants (ki - scheme 1) determined under pseudo-first order conditions were computed from the plot of slopes of ln(E) vs time at different inhibitor concentrations. Rate constants under second order conditions were determined from plots of $\ln\{E/[I_o-(E_o-E)]\}$ versus time. In aging experiments the initial OP-conjugates were obtained under conditions where $ki[I_o] >> ka$ (see scheme 1) and with over 98% inhibition of the initial enzyme activity. The reactivatable (non-aged OP-conjugate) fraction was determined by reactivation with HI-6 under conditions where kr[Re]>ka (scheme 1). The excess OP-inhibitor was removed either by column filtration (Sephadex, G15) or by 100 fold dilution, prior to reactivation. The activity of the reactivated enzyme (Er) was routinely corrected for the inhibitory effect of the reactivator (De Jong and Kossen (1985)). The first order rate constants of aging, ka, were determined from the slopes of ln(Er) vs. time.

RESULTS

Selection of OP Inhibitors and HuAChE Mutants for Study : The OP inhibitors chosen for this study represent two important classes of extensively studied agents (Main (1976)): diisopropyl phosphorofluoridate (DFP) and pinacolyl methylphosphonofluoridate (soman). Both of these OP inhibitors result in OP - ChEs conjugates that undergo aging (Aldrich and Reiner 1972). For the selection of mutants we were guided by molecular models of OP - HuAChE adducts (Barak *et al.*, 1992), based on the x - ray structure of TcAChE (Sussman *et al.*, 1991) and on structures of OP - conjugates of chymotrypsin (Harel *et al.*, 1991). Initially, residues Y337 and E202 were selected since the main focus of this study is the evaluation of interactions of the active center residues with the initial phosphyl moiety and in particular with the alkyl leaving group and the resulting P-O^- moiety in the aged conjugate (Fig. 26). The models suggest that amino acid Y337 and F338 are vicinal to the isopropyl (DFP) or the pinacolyl (soman) groups of the phosphyl moieties of the corresponding OP - HuAChE conjugates and residue E202 is proximal to the scissible O - alkyl bond. Indeed, Qian and Kovach (1993) proposed recently that E202 may be involved in stabilization of the evolving carbonium ion during the dealkylation process. In addition to mutation in these two residues, we included in the study HuAChE mutated at position 450. Residue E450 and Y133 are remote from the phosphyl moiety but as revealed during this study may consitute elements of the H-bond network and affect the positioning of E202 in the active center (see Fig. 28 and discussion).

Effect of Mutation on Hydrolysis of Charged and Uncharged Substrates : The five HuAChE mutants Y337A, F388A, E202Q, Y133A and E450A were compared with respect to their efficiency in catalyzing the hydrolysis of acetylthiocholine (ATC) and its uncharged isostere S-3,3-dimethylbutyl thioacetate (TB). As shown previously (Ordentlich *et al.*, 1993), replacement of the aromatic residue Y337 and F338 had only a marginal effect on the kinetic parameters (Km and kcat) for the two substrates (Table 19) while the corresponding values for hydrolysis of ATC catalyzed by E202Q HuAChE (Shafferman *et al.*, 1992c), or of the corresponding mutation E199Q in TcAChE (Radic *et al.*, (1992)), differ significantly from those of the wild type enzyme. We now demonstrate that this decrease in catalytic efficiency of E202Q is observed also for the noncharged substrate TB (Table 19). This indicates that the

effect of replacement of E202 of HuAChE on catalysis is not solely due to electrostatic interactions with the substrate. Interestingly, a similar pattern of reduction of the catalytic parameters, for both ATC and TB, is observed when residue E450, and Y133 which are remote from the active site, is replaced by alanine (Table 19).

Interaction of HuAChE Mutants with Irreversible OP Inhibitors: To determine the effects of mutations on the stoichiometry of the inhibition reaction of the various AChEs by the OP inhibitors the recombinant enzymes were titrated with different concentrations of soman and MEPQ. The organophosphonate MEPQ is a potent OP-inhibitor of AChEs, commonly

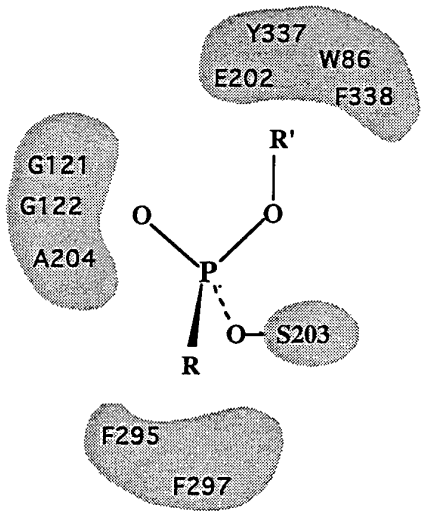

Fig. 26. Schematic presentation of the OP - HuAChE conjugate.
Residue domains within interaction distances (Barak *et al.*, 1992)) from the phosphorus substituents are displayed, as well as the catalytic site serine 203.

Table 19. Comparison of kinetic constants for ATC and TB hydrolysis by HuAChE and selected H-bond network and alkoxy pocket mutants.

HuAChEs	ATC			TB		
	K_m (mM)	k_{cat} (x10-5xmin-1)	k_{app}[a] (x10-8 M-1xmin-1)	K_m (mM)	k_{cat} (x10-5xmin-1)	k_{app}[a] (x10-8 M-1xmin-1)
Wild Type	0.13 ± 0.015	3.7 ± 0.3	28.5	0.28 ± 0.08	0.5 ± 0.1	1.8
Y337A	0.10 ± 0.01	1.0 ± 0.1	10.0	0.20 ± 0.03	0.2 ± 0.05	1.0
F338A	0.30 ± 0.03	1.7 ± 0.1	5.7	0.30 ± 0.04	0.13 ± 0.03	0.43
Y133F	0.48 ± 0.08	2.0 ± 0.2	4.2	0.24 ± 0.03	0.05 ± 0.01	0.2
E202Q	0.35 ± 0.04	0.75 ± 0.15	2.1	0.23 ± 0.03	0.1 ± 0.04	0.43
E450A	0.35 ± 0.04	0.10 ± 0.02	0.3	0.20 ± 0.04	0.006 ± 0.001	0.03

[a] The apparent bimolecular rate constant (k_{app}) was calculated from the ratio of k_{cat}/K_m.

used as titrant for standardization of concentration of AChE active sites (Levy and Ashani 1986). As shown in Fig. 27 the wild type enzyme and the mutants examined show the expected 1:1 stoichiometry in reactions with MEPQ. The concentrations of the active site subunits, determined by this method, are in good agreement (±10%) with results obtained from the quantitative immunological (ELISA) assays. Furthermore, under similar experimental conditions, the titration studies demonstrate that for soman 1:2 stoichiometry is obtained for the wild type enzyme as well as for the mutants examined. Due to the chirality of the phosphorous in soman, this OP-inhibitor is known to exhibit a marked stereoselectivity in reactions with AChE from various sources (Benshop and De Jong 1988), including recombinant HuAChE (Velan *et al.*, 1991b). Thus, the HuAChE mutants studied appear to retain the stereoselectivity towards soman diastereomers.

The actual bimolecular reaction rates of phosphylation of HuAChE and its mutants, by DFP and soman, were determined under either pseudo first order or second order conditions (Table 20). For the wild type enzyme the rates obtained for DFP and soman are in agreement with values published previously for different AChEs (Gray and Dawson 1987; Benschop *et al.*, 1984; Andersen *et al.*, 1977). It appears that replacement of Y337 or F388 by alanine had a minimal effect on the bimolecular rate constants of inhibition. On the other hand, replacement of E202 by glutamine resulted in a marked decrease of the phosphylation rates. Radic *et al.*, have recently reported similar effects for the reactivity of an analogous mutant of TcAChE (E199Q) with DFP (Radic *et al.*, 1992). Again, as for the acylation process, we find that the effect of replacement of E450 on the rates of phosphylation (Table 20), parallels that of E202 substitution. It is worth noting that despite the marked decrease in the rates of phosphylation of the HuAChE E202Q , Y133F and E450A mutants, the relative reactivity of DFP and soman with each mutant resemble that observed for the wild type enzyme.

Examination of the process of aging through measurements of the enzyme residual activity (De Jong and Kossen 1985) was carried out with the potent oxime reactivator HI-6 (Roussaux and Dua 1989). Under the experimental conditions used, we were able to achieve substantial regeneration of enzymatic activity, even for the pinacolyl methylphosphonyl derivative of the wild type HuAChE which proceeds very rapidly towards the nonreactivatable (aged) enzyme. It appears that reactivation of OP conjugates with the wild type HuAChE and Y337A enzymes proceeds at comparable rates while for the E202Q and E450A mutants, reactivation is slower (data not shown).

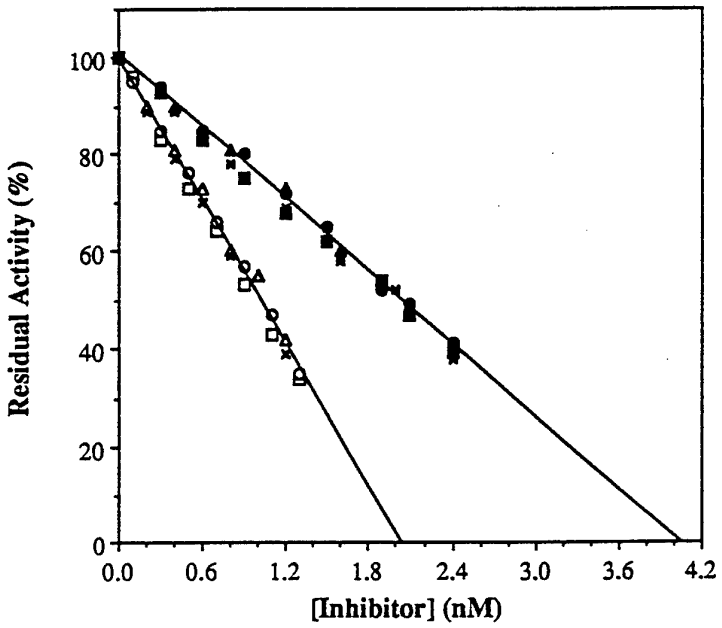

Fig. 27. Active site titration of HuAChE and its mutants with soman and MEPQ.

In all titration experiments the concentration of the catalytic subunits of HuAChE and its mutants was approximately 0.12 μg/ml as determined by ELISA. The residual activity was determined after 30 and 60 minutes incubation (27^{0}C) with soman (WT (■), Y337A (●), E202Q (▲) and E450A (+)) and MEPQ (WT (❑), Y337A (○), E202Q (Δ) and E450A (x)). The intercepts for zero activity were determined by extrapolation and the values of active site concentration were approximately 2.05x10^{-12} moles/ml for MEPQ and twice as high for soman titration (see text).

Table 20: Rate constants of phosphylation (k_i) and aging (k_a) of HuAChE and selected H-bond network and alkoxy pocket mutants.

HuAChEs	k_i ($x10^{-4}xM^{-1}xmin^{-1}$)		k_a ($x10^{3}xmin^{-1}$)
	DFP[a]	soman[b]	soman[c]
Wild Type	9.6 ± 0.5 (1.0)	8600 ± 1970 (1.0)	91 ± 12 (1.0)
Y337A	3.1 ± 0.2 (0.32)	2950 ± 636 (0.34)	180 ± 64 (2.0)
F338A	2.6 ± 0.2 (0.27)	9000 ± 3000 (1.0)	0.7 ± 0.4 (0.0077)
Y133F	1.4 ± 0.1 (0.15)	250 ± 30 (0.03)	4.0 ± 0.9 (0.044)
E202Q	0.18 ± 0.06 (0.019)	312 ± 100 (0.036)	0.58 ± 0.06 (0.0064)
E450A	0.085 ± 0.03 (0.009)	120 ± 20 (0.014)	3.4 ± 0.18 (0.037)

The correlation coefficients of the corresponding linear plots were at least 0.95. Values represent mean of at least 3 independent experiments. Numbers in parenthesis represent the values relative to the wild type.
[a] Concentration range of DFP : for wild type, F338A and Y337A $5x10^{-7}$ - $3x10^{-6}$ M and for Y133F, E202Q and E450A $5x10^{-6}$ - $7.5x10^{-5}$M. [b] Concentration range of soman : for wild type, F338A and Y337A $4x10^{-10}$ - $1.4x10^{-8}$M and for Y133F, E202Q and E450A $1.4x10^{-8}$ - $2.8x10^{-7}$M. [c] All enzymes were 95-98% inhibited by soman and reactivated at various times by HI-6 (1- 5 $x10^{-4}$ M).

The first order rate constant for aging of the diisopropyl phosphoryl derivative of HuAChE was determined to be $3.5 \cdot 10^{-4} min^{-1}$. This value is 260 fold lower than that for the corresponding pinacolyl methylphosphonyl derivative (Table 20), and in good agreement with values published for the same OP-conjugates in other AChEs (De Jong and Kossen 1985; Benschop *et al.*, 1984) . For the diisopropyl phosphoryl derivatives of E202Q, Y133F and E450A HuAChE's the rates of aging appear to be very slow and not measurable under the experimental conditions used. Consequently, there is no experimental evidence that the aging process occurs in these cases. For the pinacolyl methylphosphonyl derivative of the Y337A, the first order rate constant for aging is similar to that of the wild type enzyme while the corresponding values for F338A, E202Q, Y133F and E450A are 150, 150 , 25 and 30 fold lower respectively. If we assume a similar decrease in the rate of aging for the diisopropyl phosphoryl derivatives of E202Q, Y133F and E450A, then we could expect a half life of several days for these processes. It is therefore not surprising that no aging could be observed with DFP - conjugates of these mutants.

DISCUSSION

Molecular modeling studies of HuAChE and its phosphonylated conjugates implicated several residues, at the active center, in stabilizing the initial OP conjugate (Fig. 26) and in facilitating the subsequent aging process. These residues include the catalytic triad (S203, H447 and E334), the oxyanion hole (G121, G122 and A204), the pockets accommodating the alkoxy groups (W86, Y337 and F338, and residues which constitute the acyl pocket for ACh F295 and F297) as well as E202 which is proximal to the P-O-C linkage. The participation of most of these residues in the analogous process of acylation was recently demonstrated experimentally, by site directed mutagenesis (Shafferman *et al.*, 1992a,b,c; Radic *et al.*, 1992; Vellom *et al.*, 1993). The kinetic studies reported here suggest that in phosphylation and even in the dealkylation of the OP conjugates of HuAChE, residue Y337 appears to have a minimal contribution. On the other hand replacement of E202 by a neutral residue results in 30-150 fold reduction in the bimolecular rate constant of phosphylation and the first order rate constant of aging.

Based on modeling studies of soman - TcAChE adduct it was proposed by Qian and Kovach that the carboxylate of E199 (equivalent to E202 in HuAChE) would be within interaction

distance from the positive charge on the chiral carbon, thereby facilitating the detachment of the alkyl group by means of electrostatic interactions (Qian and Kovach 1993). However it should be emphasized that substitution of E202 by glutamine has pleiotropic effects of comparable magnitude on catalytic activity towards both charged and noncharged substrates (Table 19), on substrate inhibition (Shafferman *et al.*, 1992c; Radic *et al.*, 1992)), on interactions with reversible inhibitors (Shafferman *et al.*, 1992b; Radic *et al.*, 1992) as well as on the rates of phosphylation by DFP and soman (Table 20).

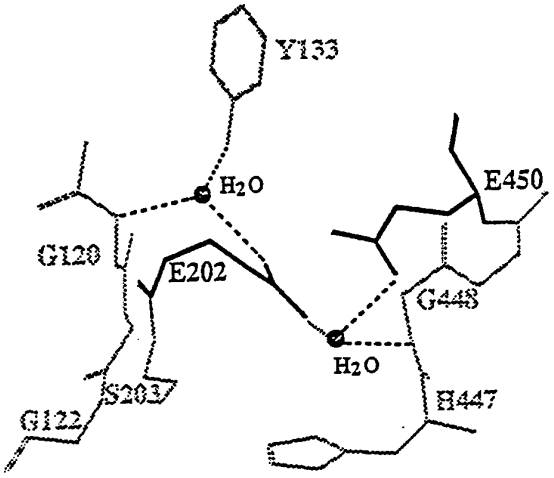

Fig. 28 Involvement of residues E202, Y133 and E450 in the hydrogen bond network across the active center of HuAChE.
The positions of water molecules in the model of the HuAChE are assumed to be equivalent to those in the x - ray structure of TcAChE [Sussman *et al.*, 1991). Segments of the two backbone stretches, spanned by the H -bond network, are displayed. The separation of the two backbone segments determines the relative orientation of the oxyanion hole (G121, G122) and the catalytic triad (H447). The distances within the network , marked by broken lines, are as follows: N(G121) - O(H_2O) 2.58Å; O(Y133) - O(H_2O) 2.50Å; O(E202) - O(H_2O) 3.01Å; O(E450) - O(H_2O) 2.80Å; O(E202) - O(H_2O) 2.36Å; N(G441) - O(H_2O) 3.07Å. (See also figures 11 and 25).

These observations are therefore consistent with our previous suggestion (Shafferman *et al.*, 1992b,c) that replacement of E202 probably disrupts the *overall* spacial organization of the active center. Nevertheless this conformational change is not sufficient to abolish the stereoselectivity of the E202Q mutant for the soman diastereomers (Fig. 27). Some clues as to how residue E202 could play such a role in maintaining the architecture of the active center is again provided from the studies by Sussman *et al.*, (1991) on the x-ray structure of TcAChE (see also section IV). As shown in Fig. 28, the carboxyl group of E202 is a central element in a network of hydrogen bonds that spans the crossection of the active center gorge. This array bridges two AChE backbone segments one of which contains the residues constituting the oxyanion hole while the other includes the catalytic triad histidine (H447). In this array, residue E202 is bound, via water molecule, to residue E450 and tyrosine 133 . Therefore, although E450 is quite remote from the active site (distances of 9.72Å from Oγ–S203), it is expected that substitution of E450 by alanine and of Y133 by phenyalanine would be as disruptive to the hydrogen bond network as is the replacement of E202 by the neutral residue glutamine. In accordance with this prediction, the E450A and Y133F HuAChE mutants exhibited reduced reactivity towards the substrates ATC and TB, or towards the OP inhibitors DFP and soman, in a similar manner to that observed for the mutant E202Q. Furthermore the OP conjugates of both E202Q and E450A and Y133F mutants exhibit marked resistance to aging. A common mechanistic element, in these diverse processes, is a protonation step. This protonation can be mediated by the imidazole moiety of the catalytic triad histidine 447, and it is reasonable to assume that the appropriate positioning of H447 is achieved (Fig. 28) via the hydrogen bond network involving E202-water-E450 alignment in the active center.

Finally in addition to understanding some of the basic aspects of the mechanism of catalysis, phosphylation and aging, the findings reported here have practical implications. Since aging is an irreversible process leading to a nonreactivatable enzyme the demonstrated ability to engineer ChEs resistant to aging should be advantageous with respect to the proposed utility of such biomolecules for treatment against OP insecticide poisoning or decontamination of environmentally harmful OP agents. In this respect the mutation at position 338 is most promising since unlike mutations in the H-bond network (E202, E450 and Y133) where the reactivity toward the OP-agent is markedly dimnished in the F338A enzyme only the aging process has been affected.

X. Large Scale Production of Recombinant HuAChE in Human Cell Lines 293

INTRODUCTION

Expression of recombinant cholinesterases may provide a way to obtain large quantities of these enzymes, for analysis or for therapeutic purposes and could also generate wealth of information on their structure and function. Human BChE and AChE cDNA have been expressed in a bacterial system (*Escherichia coli*). The crude enzyme was devoid of activity, yet low yields of active BChE were regenerated when the product was exposed to denaturing and renaturing conditions (Masson *et al.*, 1992). A recombinant monomeric HuAChE was expressed in *E. coli* (Fisher *et al.*, 1993) to a level of 10% of total bacterial protein and accumulated in the form of inclusion body aggregates. Solubilization of the inclusion bodies followed by folding and oxidation procedures, resulted in partial regeneration of molecules with authentic AChE activity. This bacterial HuAChE was cleared rapidly (within minutes) from the blood stream of injected mice. This phenomenon may be due to the lack of polypeptide glycosylation in bacteria (see glycosylation below) or to the instability of the monomeric forms of AChE (Velan *et al.*, 1991b). *Drosophila* AChE and the T subunit of TcAChE have been expressed in *Spodoptera* insect cells infected with recombinant baculovirus (MacPhee-Quigley *et al.*, 1988; Cerutti *et al.*, 1991; Radic *et al.*, 1992). Although these systems allow production of milligram quantities of recombinant glycoproteins, they frequently are of lower molecular weights than the natural mammalian products, probably because of incomplete N-linked oligosaccharide processing (Lin *et al.*, 1985; Jacobs *et al.*,;1985; Steiner *et al.*,;1988; Imai *et al.*, 1990). Cholinesterases have been expressed in *Xenopus* oocytes (Soreq and Seidman, 1992) microinjected with natural mRNAs (Soreq *et al.*, 1982; Randall, 1991) or with cloned mRNAs (Dreyfus *et al.*, 1989; Fournier *et al.*, 1992). The cDNAs for TcAChE subunits of types T and H have been transiently expressed in COS cells (Gibney *et al.*, 1990; Duval *et al.*, 1992). Wild type or mutated T subunits of human AChE have been transiently expressed in the 293 human kidney (HEK) cell line (Velan *et al.*, 1991a,b; Shafferman *et al.*, 1992a,b). The expression plasmids transfected into the 293 cells also included the coding sequence of chloramphenicol acetyl-transferase (CAT) and a neomycin resistance (*neo*) marker, so that the efficiency of protein synthesis could be monitored and

selection of stable clones producing high amounts of AChE, can be achieved (Kronman *et al.*, 1992). The 293 HEK cell line was also used to express the mouse T subunit (Randall, 1991; Vellom *et al.*, 1993).

Detailed analyses of the biochemical, pharmacological, and structural (e.g x-ray) properties of mammalian- especially human-, butyryl- or acetylcholinesterase have been hampered by the lack of adequate sources for substantial amounts of homogeneous soluble enzyme. The systems described above: the bacterial, the insect-baculovirus and some mammalian systems could allow production of sufficient amounts of enzyme. However except for the mammalian system, all the others are either deficient or limited in their post-translation modifications bioprocesses and thus, as mentioned earlier, their products may be defective (reviewed by Goochee *et al.*, 1991). Using multicistronic vectors for expression of rHuAChE we have isolated several stable human 293 cell lines which produce and secrete high levels of human AChE (approx. 10 mg/10^9 cells/day) (Kronman *et al.*, 1992; Velan *et al.*, 1993). To the best of our knowledge these engineered cell lines have a production potential exceeding by at least 1000 fold any other known AChE producing mammalian cell line and have attained among the highest production levels reported for recombinant proteins (Conners *et al.*, 1988; Goto *et al.*, 1988; Friedman *et al.*, 1989; Hendricks *et al.*, 1989; Walls *et al.*, 1989; Yan *et al.*, 1989 ; Filbin and Tennekoon, 1990). Thorough analysis of the post translation process involved in the biosynthesis of HuAChE by the 293 recombinant cells indicated very efficient assembly of monomeric subunits into dimeric forms as well as consensus terminal glycosylation of the oligosaccharide side chains (Kerem *et al* .,1993).

Large-scale growth of 293 HEK cells has been limited in the past because of difficulties in growing 293 cells on currently available anchorage-dependent cultivation systems like roller bottles and microcarrier cultures (Robert *et al.*, 1991). We have developed several propagation systems for the recombinant 293-cells and achieved system productivities of 4-10mg AChE/L/day during a production period of 8 days in either a surface propagator (multitray system), or in a fixed-bed reactor (polyurethane macroporous sponges). Similar rates of production, but for longer periods of up to 28 days, were achieved in microcarrier cultures (Lazar *et al.*, 1994). The rHuAChE produced under all growth conditions is uniform in its catalytic properties, yet partial degradation of the oligomeric forms of the enzyme in aged cultures, was noted (Lazar *et al.*, 1994).

Unlike previous sections this one is more technical and is written as an update report intended to summarize the production process and yields of the recombinant enzyme produced during the last 18 months.

METHODS

Cell Culture : The AChE-producing cells used in these studies, are cloned recombinant human embryonal kidney 293 cells (Kronman *et al.*. 1992). The cell culture medium for stock cells was Iscove's modified Dulbecco's medium (IMDM, Sigma, USA), supplemented with 10% fetal bovine serum (FBS, Beth Haemek, Israel), and 100 units/ml each of penicillin and streptomycin (Teva, Israel). Cells were maintained in culture by serial trypsinizations in plastic tissue culture flasks. Cells were counted after trypsinization using a hemocytometer. Viability was assessed by trypan-blue stain exclusion (Paterson, 1979). Cells grown on MC could not be removed efficiently by enzymatic treatment for counting. For these cultures, the nuclei staining method was applied (Sanford *et al.*, 1951). Bench-scale cell growth was performed with medium containing a modified FBS in which the intrinsic AChE was removed by procainamide-sepharose affinity chromatography (PAT-FBS), (Shafferman *et al.*, 1992b).

Multitray System :A standard multitray unit (Nunc, Denmark) comprises ten chambers, each having a surface area of 600 cm^2, fixed together vertically and supplied with interconnecting channels. Cells were inoculated at a concentration of $3x10^8$ cells/2 L IMDM supplemented with 10% PAT-FBS. Culture medium was replaced every 48 hr starting at the third day after inoculation (Lazar *et al.*, 1994).

Microcarrier Cultures: Cells were cultured on 4 g/L DEAE-cellulose beads (Servacel, Serva, Germany). Cells were inoculated at a concentration of 3-5 x 10^5 cells/ml in MC systems based either on a hanging magnetic bar (Bellco-type), or on a stirring rod (Techne-system). Scaling up of MC cultures was performed in a 4 liter Celligen bioreactor (New Brunswick Scientific, USA) (Lazar *et. al.*, 1994). DO was controlled by sparging a mixture of oxygen, air, and nitrogen. The pH was controlled by gassing CO_2 or addition of a 7.5% Na_2HCO_3 solution into the reactor (Reuveny, 1986).

AChE Activity : AChE was determined by the colorimetric method of Ellman *et al.* (1961). The reaction mixture contained 0.5 mM acetylthiocholine, 50 mM Na-phosphate buffer, pH 8.0, 0.1 mg/mL bovine serum albumin (BSA), and 0.3 mM 5:5'-dithiobis (2-nitrobenzoic acid, DTNB). The assay was performed at 27^{0}C. The reaction was monitored by recording the increase in absorbance at 410 nm in a microplate reader (Dynatech, MR5000, USA). One unit of AChE is defined as the amount of enzyme hydrolyzing 1 umol of acetylthiocholine per minute. The specific activity of purified AChE is 6000 units/mg protein (Kronman et. al. 1992). Specific productivity is defined as AChE units/10^6 cells/day. System productivity is defined as AChE units/liter culture/day.

Purification of Recombinant HuAChE: Recombinant human AChE was purified from the high AChE producer cell lines on procainamide-sepharose affinity columns (Ralston *et al.*, 1985). Cell culture supernatants were concentrated and dialyzed by ultrafiltration (Minitan System, 100K cutoff membranes). Dialysis buffer was 10mM Na-phosphate buffer pH 8.0. The concentrated enzyme solution was adsorbed to the procainamide-sepharose 4B column (3000 units per ml resin) which was then rinsed with 50 mM Na-phosphate buffer pH 8.0/1mM EDTA and again with 50 mM Na-phosphate buffer pH 8.0/0.4M NaCl/1mM EDTA. Enzyme elution was performed with decamethonium (0.15 M) in 50 mM Na-phosphate buffer pH 8.0/1 mM EDTA. Further purification was achieved on a second procainamide column as above. Purified enzyme was dialyzed against 50mM Na-phosphate buffer pH 8.0 and concentrated by ultrafiltration (Minitan, 30 K cutoff membrane).

RESULTS and DISCUSSION

Production of rHuAChE in Cell Culture in a MC Bioreactor and Multitrays- On the basis of improved cell growth and AChE production, Servacel MC in a 4 L Celligen bioreactor were used to propagate the recombinant 293 cells (cell line 293-R11 (C33-20-B4-2C4) Kronman *et al.*, 1992). Culture medium was replaced every 2-3 days at the initial growing phase, and daily as the cells entered the maintenance phase starting at day 16. Cell growth and AChE production was carried out for a period of 32 days. High densities of 1-1.5x10^7 cells/ml were achieved after 16 days in culture. AChE production increased with cell growth and reached high levels of 6-10 mg/L/day. The controlled environment in the

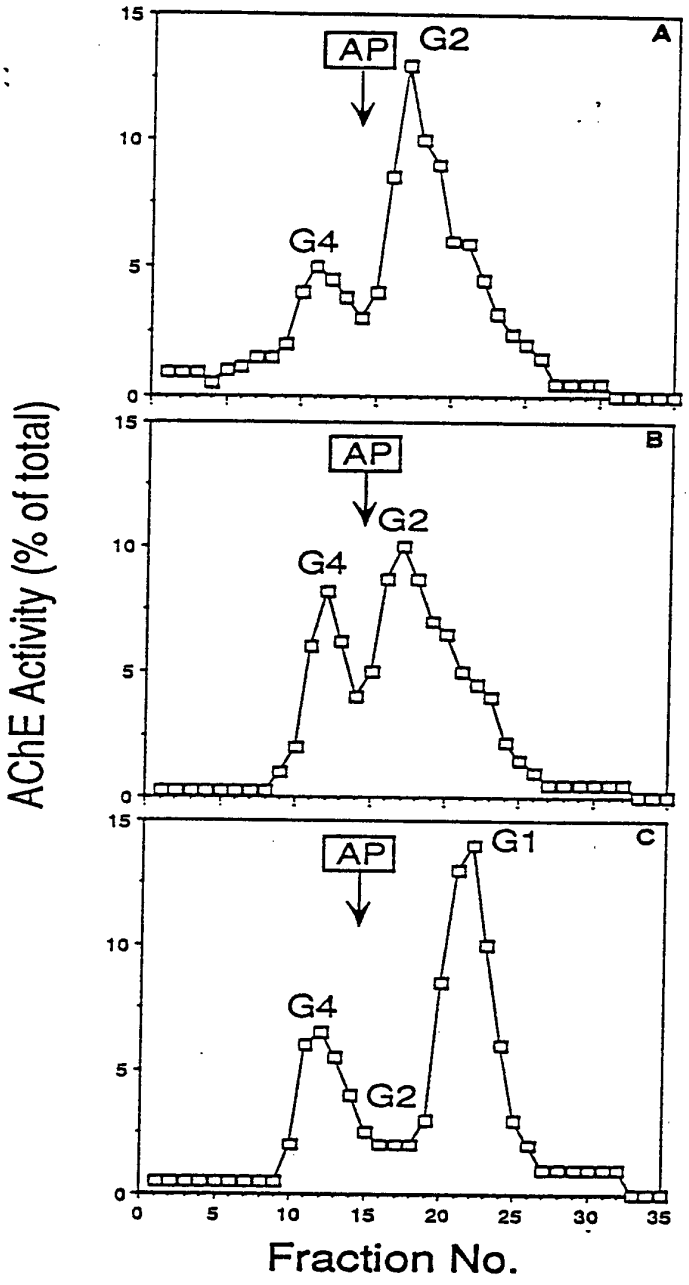

Fig. 29. Sucrose gradient profiles of various pools of medium containing recombinant HuAChE collected from the microcarrier large scale production system. A. Enriched for dimers (G2) of recombinant HuAChE (up to 10 days in culture) B. Enriched for dimers and tetramers (G4) of recombinant HuAChE (14-17 days in culture). C. Enriched for monomers (G1) and tetramers of recombinant HuAChE (25-32 days in culture).

bioreactor together with the daily medium change helped to maintain the high cell level and the high system productivity for long culture period. However, the specific cell productivity decreased by 5-10 fold as the size of the aggregates increased. In addition, as the culture aged (after the 20th day), accumulation of cell-derived protease activity was detected by sucrose gradients analysis, causing partial degradation of the oligomeric forms of the enzyme. Diffusional limitations of nutrients to the center of the clumps may affect the enzyme production and reduce the cell productivity, as well as, induce proteolytic activity as the clumps grow in size (Lind *et al.*, 1991). Nevertheless, the relatively high system productivity together with long culture time provided sufficient quantities of enzyme for the various research goals.

We collected over 100 liter liters of medium containing 6-10mg/liter of rHuAChE (a total of up to 0.5g of rHuAChE product). Cultures from various stages of production were pooled : a. enriched for dimers b.enriched for dimers and monomers c. enriched for tetramers and monomers (Fig 29). About 500mg from these pools was supplied to Drs. Sussman and Dr. Silman of the Weizman Institute to evaluate possibilities of preparation of crystals for x-ray analysis. This aspect of the research is still in progress, however it appears that conditions were identified to overcome separation of the proteolytic activity that led to degradation of the enzyme during purification on size columns. Another part of the supernatant material was purified at IIBR and yielded a few hundred of milligrams rHuAChE of 95% pure enzyme. A large portion of this purified preparation was again used for evaluating crystallization conditions at Sussman's lab. The same preparation as well as additional preparations from multitrays were used for pharmacological studies and as reference material for studies in our lab and other labs throughout the world (e.g H.Soreq Hebrew Univ. Israel ; C. Broomfield EREDC U.S.Army; B.P. Doctor WRAIR U.S.Army; D.Queen Iowa Univ. U.S; T.Rosenbbery Case Western U.S; P.Masson in CRSSA France; S.Greenfield Oxford U.K).

In addition to the above we have prepared during the research stable clones of selected mutants of rHuAChE. Usually a few liters of each clone were collected and used to prepare purified material.

XI. N-Glycosylation of HuAChE: Effects on Activity Stability and Biosynthesis

INTRODUCTION

Post-translational glycosylation can affect the biological activity of proteins, their transport towards the cell surface and the stabilization of their functional conformation (Gibson *et al.*, 1979; Dube *et al.*, 1988; Semenkovich *et al.*, 1990; Matzuk *et al.*, 1989). The acetylcholinesterases (AChE), whose main function is termination of acetylcholine induced nerve impulse transmissions at cholinergic synapses, are multimeric glycosylated ectoenzymes. AChEs are polymorphic in their quaternary structure (Massoulie *et al.,* 1993; Chatonnet and Lockridge, 1989; Taylor 1991), and like the related butyrylcholinesterases (BuChE), carry varying amounts of carbohydrate side chains attached to their core polypeptides (Liao *et al.*, 1991; Liao *et al.*, 1992; Treskatis *et al.*, 1992). These carbohydrates are primarily Asn-linked side chains as indicated by their susceptibility to specific sugar-hydrolases (Liao *et al.*, 1992; Kronman *et al.*, 1992) and by their selective affinity for lectins (Rotundo, 1988; Kerem *et al.*, 1993).

Cholinesterase sequences display several potential N-glycosylation signals (Asn-X-Ser/Thr), yet the number and location of these signals are not well conserved throughout the cholinesterase family. Human butyrylcholinesterase has nine potential sites (Lockridge *et al.*, 1987; Prody *et al.*, 1987), *Torpedo californica* AChE has four sites (Schumacher *et al.*, 1986), and the bovine enzyme has five sites (Doctor *et al.*, 1990). The human AChE (HuAChE) sequence (Soreq *et al.*, 1990), as well as the mouse and rat AChE (Rachinsky *et al.*, 1990; Legay *et al.*, 1993) display only three potential Asn-linked glycosylation sites, located at positions 265(*258*) , 350(*343*) and 464(*457*) (number in parentheses corresponds to the analogous TcAChE position, according to nomenclature recommendations in Massoulie *et al.*, 1992). These three N-glycosylation sites are conserved in all mammalian cholinesterases sequenced to date (Gentry and Doctor, 1991) and may represent a core of N-glycosylation targets required for their function.

The role of N-glycosylation in cholinesterases is not fully understood. In the vertebrate cholinesterases, catalytic polypetides with different glycosylation patterns were isolated from

different tissues, (Bon *et al.*, 1987; Liao *et al.*, 1992; Treskatis *et al.*, 1992). At least in one case, this variation was associated with differences in catalytic properties (Meflah *et al.*, 1984). In *Drosophila* AChE, on the other hand, mutagenesis of each one of the five potential N glycosylation signals (none of which corresponds to sites conserved in mammalia; Hall and Spierer, 1986) yielded enzyme molecules with wild type activity (Mutero and Fournier, 1992).

Here we try to examine the role of the carbohydrate side-chains in cholinesterase function by site-directed mutagenesis of rHuAChE employing an optimized expression system for production of secreted enzyme (Velan *et al.*, 1991a; Kronman *et al.*, 1992). This system is based on multipartite plasmids, carrying the human *ache* cDNA under control of the cytomegalovirus immediate early promoter-enhancer, which are transfected into human embryonal 293 kidney cells. To allow for stable and continuous expression, the vectors carry the *neo* selector gene under the control of the H2Ld promoter. The use of the low efficiency promoter H2Ld (Kronman *et al.*, 1992), assures selection of clones in which chromosomal integrations at transcriptionally active sites has occured. These systems proved to be instrumental in identifying amino acid residues involved in catalytic activity, folding, post translational processing and secretion of HuAChE (Shafferman *et al.*, 1992 a,b; Velan *et al.*, 1991b; Kerem *et al.*, 1993; Ordentlich *et al.*, 1993). In this study we analyze HuAChE polypeptides in which single or multiple N-glycosylation signals have been mutated, and examine the biosynthesis, stability and catalytic activity of the mutant enzymes.

METHODS

Construction of Expression Vectors for AChE and AChE Mutants : Tripartite vectors (Fig 30B), expressing the human *ache* cDNA (Shafferman *et al.*, 1992a) the *cat* reporter gene (Gorman *et al.*, 1982) and the selection marker *neo* (Southern and Berg, 1982) were generated as outlined previously (Kronman *et al.*, 1992). Mutagenesis was performed by DNA cassette replacement into a series of HuAChE sequence variants (Soreq *et al.*, 1990) which conserve the wild type amino acids, but carry new unique restriction sites. The cDNA spanning the asparagine targeted for mutagenesis was excised by cutting at the nearest restriction sites on the appropriate AChE cDNA variant and then replaced with a synthetic DNA

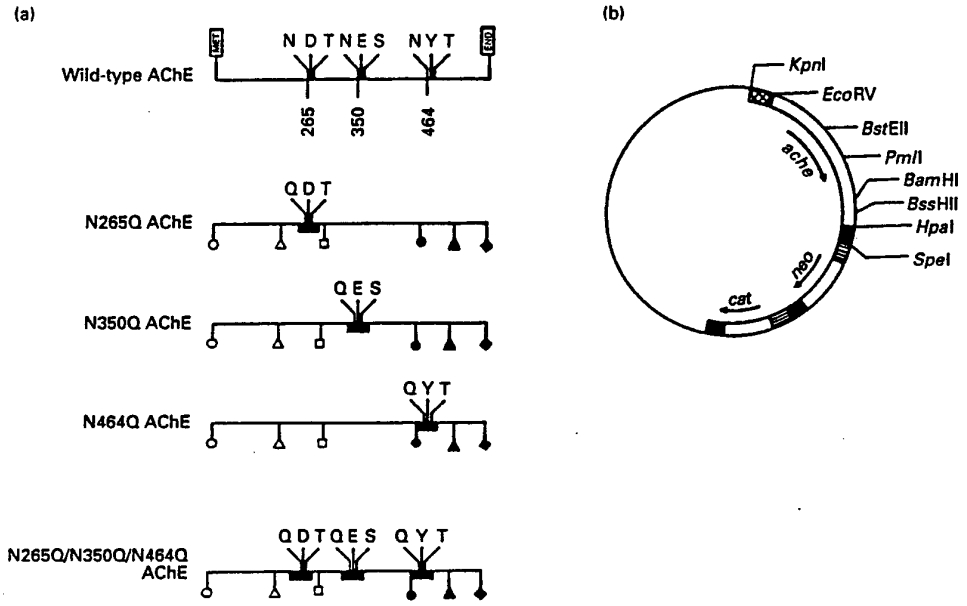

Fig. 30 - Strategy for generation of AChE mutant devoid of potential glycosylation sites.

A. - N-glycosylation signals targeted for mutagenesis are presented in the top line (positions of asparagines are denoted), followed by three lines depicting single substitution mutants. Double (not shown) and triple (fourth line) substitution mutants were generated from these by ligating DNA fragments carrying the individual mutations. Unique restriction sites used for these constructions were *Eco*RV (open circle), *Bst*EII (open triangle), *Pml*I (closed square), *Bam*HI (closed circle), *Bss*HII (closed triangle) and *Hpa*I (closed diamond).

B. - The prototype tripartite vector used for expression of wild type and mutagenized rHuAChEs. The three elements comprising the vector are: the *ache* gene controlled by the cytomegalovirus immediate early promoter/enhancer (grid); the *neo* gene controlled by the $H2L^d$ histocompatibility antigen promoter (vertical stripes) and the *cat* gene controlled by the SV40 early promoter/enhancer (horizontal stripes).

duplex carrying the mutated codon. Detailed maps of the different human *ache* variants which express wild type polypeptides are presented in Shafferman *et al.*, (1992a). The N464Q mutant was generated by replacement of the *BamHI- BamHI* fragment of the native HuAChE cDNA. The distal *BamHI* site is eliminated upon ligation since the GGG codon of Gly-487 was replaced by GGC in the synthetic DNA duplex . The N350Q mutant was generated by substituting the *NarI-BglII* fragment of the human *ache* variant Ew5. The N265Q mutant was generated by replacement of a *SalI-MluI* DNA fragment in the *ache* variant Ew7 (Ew7 is a derivative of Ew5 in which new *SalI* and *MluI* sites were engineered at codons 246/247 and 275/276 respectively). All Asn codons in the putative N-glycosylation sites were replaced by the CAG codon of Gln. Synthetic DNA oligodeoxynucleotides were prepared using the automated Applied Biosystems DNA synthesizer, and sequences of all cloned synthetic DNAs were verified by the dideoxy sequencing method (USB sequenase kit).

Multiple substitution mutants were generated by cloning DNA fragments carrying the individual mutations into the tripartite vectors (Fig 30B). The DNA fragments used were: *BstEII* - *PmlI* fragment for the N265Q substitution, *PmlI- BamHI* fragment for the N350Q substitution and *BamHI-HpaI* DNA fragment for the N450Q substitution (Fig. 30A).

Transfection of Cells: CsCl purified plasmid preparations were used to transfect human embryonal 293 kidney cells as previously described (Shafferman *et al.*, 1992a). At least two different clone isolates were tested for each plasmid construct. Transient transfection was carried on as previously described (Velan *et al.*, 1991a). 24 hours after transfection, cells were transferred to medium (2ml per a 100mm plate) containing 10% AChE depleted serum (Shafferman *et al.*, 1992a) and incubated for 48 hours. Medium was collected, and assayed for AChE, medium of mock transfected 293 cells served as control. Cell lysates were assayed for intracellular AChE and CAT activity (Gorman *et al.*, 1982). Stably transfected isolated clones or pooled clones (ca. 50 clones per pool) were generated by G418 selection as previously described (Kronman *et al.*, 1992).

Analysis of rHuAChE Mutants : AChE activity in medium of transfected cells was assayed according to Ellman *et al.*, (1961). Standard assays were performed in the presence of 0.5mM acetylthiocholine, 50mM Na-phosphate buffer pH 8.0, 0.1 mg/ml BSA and 0.3 mM 5:5'-dithiobis(2-nitrobenzoic acid) (DTNB). The assay was carried out at 27^{0}C and monitored

by a Thermomax microplate reader (Molecular Devices). AChE-protein mass was determined by ELISA based on polyclonal antibodies to native rHuAChE (Shafferman *et al.*, 1992a). This quantitation was confirmed, whenever ACHE quantities were sufficient, by immunoblots developed with conformation-independent anti peptide-rHuAChE (see below). Activity levels as well as AChE-protein levels of the individual mutants (average of four transfections) were calculated by normalization to CAT activity as described in detail previously (Shafferman *et al.*, 1992a). In mutants secreting low levels of AChE, cell growth medium samples were concentrated 10 fold by vacuum, prior to quantitation.

Km values of the AChE mutants for acetylthiocholine were obtained from the Lineweaver Burk plots and k_{cat} calculations were based on the polyclonal-ELISA quantitations. Interaction of the various mutants with AChE-specific inhibitors was monitored by comparing IC50 values (inhibitor concentration causing 50% reduction in catalytic activity) to those of WT enzyme as described previously (Shafferman *et al.*, 1992b). Both, the peripheral anionic-site ligand - propidium, and the active-site inhibitor -edrophonium were employed. In addition, we have included the two bisquaternary inhibitors decamethonium and BW284C51 which bridge the peripheral site and the active center of the enzyme (for review see Hucho *et al.*, 1991).

Sucrose Density Gradient Centrifugation : Analytical sucrose gradient centrifugation was performed on 5-25% sucrose gradients containing 50 mM Na-phosphate buffer pH-8.0 . Centrifugation was carried out in an SW41 Ti rotor (Beckman) for 22 hrs at 36.000 rpm, at 4^{0}C. 0.3ml fractions were collected and assayed for AChE activity.

Visualization of AChE in SDS-PAGE : rHuAChE was immunoprecipitated from cell growth medium with rabbit anti-rHuAChE antibodies bound to Sepharose as previously described (Kerem *et al.*, 1993). Immunoadsorption was carried out for 2 h at room temperature, immunoprecipitates were eluted from the Sepharose beads by 30 min incubation with Laemmli's sample buffer at room temperature. Immunoprecipitated AChE was subjected to SDS PAGE (Laemmli, 1970) at reducing conditions and electroblotted onto nitrocellulose filters. Immunoblots were developed by immunostaining with rabbit antibodies directed to bacteria derived HuAChE polypeptides (Velan *et al.*, 1991b).

Metabolic Labeling and Immunoprecipitation of Proteins : Cells were preincubated for 1 h in methionine-free Dulbecco's modified Eagle's medium supplemented with 10% AChE-depleted fetal calf serum. Cells were then labeled for 1/2 h with [^{35}S] methionine (200 μCi/ml;1000 Ci/mmol; Amersham) and chased in methionine-containing medium supplemented with 20 μg/ml Aprotinin (Sigma). At various chase periods, culture media were collected and cells were washed and then lysed. Cell lysis was performed using a modification of previously described procedures (Amitay *et al.*, 1991; Weitz and Proia, 1992). Lysis buffer consisting of 50mM Tris-HCl pH 7.4, 150mM NaCl, 1% sodium deoxycholate, 1% SDS, 1% Nonidet P-40, 20 μg/ml aprotinin and 0.1M iodoacetamide (freshly dissolved) was added to cells (1ml buffer /~10^6 cells). Lysates were boiled for 5 min, cooled to room temperature, cleared by 15 min centrifugation at 16000g and then diluted 1:4 in lysis buffer, to which 10mg/ml BSA were added (iodoacetamide was deleted).

AChE was immunoprecipitated from cleared cell lysates and media with rabbit anti-rHuAChE antibodies (Shafferman *et al.*, 1992a) followed by precipitation with protein-A bacterial adsorbent (Biomakor, Israel) as described previously (Amitay *et al.*, 1991).

RESULTS AND DISCUSSION

Generation of Glycosylation-Impaired AChE Mutants : Each one of the three N-glycosylation signals of the HuAChE catalytic subunit was rendered non-functional by DNA-cassette replacement mutagenesis (Fig. 30A). The respective Asn codons were replaced by Gln codons to generate the three AChE mutants N265Q, N350Q and N464Q (CAG, the most commonly occurring Gln codon in the HuAChE cDNA was used in all replacements). These single mutants were then used to engineer the double mutants [N265Q/N350Q], [N265Q/N464Q], [N350Q/N464Q] and the triple mutant [N265Q/N350Q/N464Q] which is devoid of any potential N glycosylation sites. All forms were integrated into multipartite expression vectors (Fig 30B) and used for transient or stable transfections of 293 cells.

The effect of elimination of potential N-glycosylation signals on glycosylation level was analyzed by SDS-PAGE of secreted AChE mutant enzymes, derived from isolated clones (see below) of stably transfected cells (Fig 31). Elimination of each one of the individual

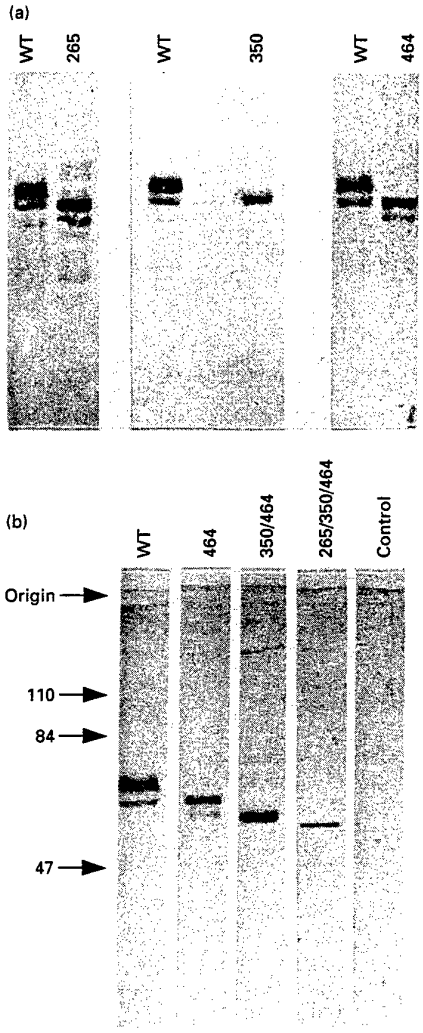

Fig 31. The effect of elimination of N-glycosylation signals on the electrophoretic mobility of rHuAChE.
Wild-type (WT) rHuAChE and the various glycosylation-site mutants (designated by position of the mutated asparagines) were immunoprecipitated by specific antibodies from growth medium of stably-transfected cell lines. Supernatant of non-transfected 293 cells served as control. Samples were obtained from clone pools or selected clones secreting 0.2-3 U/ml WT rHuAChE or mutant rHuAChE. The relative amount of AChE in the various preparation is not a direct reflection of the production efficiency of the specific mutant, but rather of the production level of the individual cell clone used. Immunoprecipitates of individual single site mutants (A) as well as multiple-site mutants (B) were subjected to SDS-PAGE at reducing conditions together with WT immunoprecipitates. AChE was electroblotted onto nitrocellulose and visualized by immunostaining as described in "Methods". Migration of prestained molecular weight markers (Bio-Rad marker kit) is indicated by arrows.

glycosylation sites at positions 265, 350 and 464, resulted in a decrease in the apparent molecular weight of the HuAChE polypeptide as visualized by blotting and immunostaining (Fig. 31A). Accordingly, enzyme molecules with two mutations migrated faster than the single mutants, and the AChE subunit in which all three N-glycosylation signals were mutated migrated even faster (Fig. 31B), forming a faint sharp band resembling N-glycanase treated wild-type AChE molecule (Kronman *et al.*, 1992). These results indicate that all three Asn-X-Ser signals of HuAChE are actually glycosylated, and agree with the 3-dimensional model of HuAChE (Barak *et al.*, 1992) which maps the three relevant asparagine moieties on the outer surface of the molecule (Fig 32). The migration patterns depicted in Fig. 31 suggest that size heterogeneity characteristic of WT recombinant HuAChE (Kronman *et al.*, 1992) originates from partial occupancy of one of the three glycosylation signals. The fast-migrating minor band of the WT enzyme comigrates with the major band of the single site glycosylation mutants, and the fast migrating band of the single N glycosylation site mutants comigrates with the major band of double-site mutant. Comparison between migration patterns of the various mutants (Fig 31) could also suggest that the major target for this partial glycosylation is Asn-350, since only N350Q mutants lack the accompanying fast-migrating minor band observed in the other single-site mutants.

Elimination of N-glycosylation sites did not interfere with the ability of AChE subunits to form sulfhydryl-linked dimers, as reflected in sucrose gradient sedimentation analysis (Fig. 33). It appears, therefore, that the oligosaccharide side-chains do not affect the structural elements which hold together the two subunits of the AChE homodimer. Indeed, none of the N-glycosylation sites is in close proximity (HuAChE 3-dimensional model, Barak *et al.*, 1992) to helices αF'3 and αH which form the four helix bundle, suggested by Sussman *et al.*, (1991) to function in dimerization of TcAChE.

N-glycosylation is Required for Efficient Production of rHuAChE by Transfected Cells : The effects of N-glycosylation on the levels of AChE production was examined in 293 cells, transiently transfected with vectors expressing WT and mutant enzyme. Amounts of AChE secreted into the cell growth medium were monitored by activity measurements as well as by ELISA quantitation of AChE-polypeptide mass (normalized to levels of the coexpressed CAT; Shafferman *et al.*, 1992a). Results obtained by these two independent assay systems indicate that elimination of N-glycosylation sites has a pronounced

Table 21: Secretion levels of HuAChE by cells transfected with N-glycosylation site mutants.

HuAChE type	HuAChE activity[a]		HuAChE production[b]	
	mU	% of WT	ng	% of WT
WT	840 ± 110	100	128 ± 22	100
N265Q	160 ± 17	19	30 ± 4	23
N350Q	118 ± 18	14	32 ± 3	25
N464Q	235 ± 25	27	38 ± 6	29
N265Q/N464Q	17 ± 3	2	3 ± 1	2
N265Q/N350Q	18 ± 2	2	3.5 ± 1.5	3
N350Q/N464Q	17 ± 2	2	5 ± 2	4
N265Q/N350Q/N464Q[c]	3 ± 0.4	0.35	0.8 ± 0.4	0.6

[a] Enzyme activity (mU) recovered from cell supernatant of a 100mm culture plate 48h posttransfection. Values are CAT-normalized (Shafferman *et al.*, 1992a) and represent the average of quadruplicate transfections.

[b] Enzyme polypeptide (ng) recovered from cell supernatant of a 100mm culture plate 48h post transfection was determined by ELISA, values are CAT-normalized as above.

[c] Values for the triple mutant were measured in 10 fold concentrated culture supernatant

effect on the levels of HuAChE secreted by the cells (Table 21). The decrease in yields of HuAChE was proportional to the number of available N glycosylation sites. Elimination of a single site, two sites and all three sites resulted in secreted enzyme yields of 20-30%, 2-4% and about 0.5% respectively (Table 21). Thus, N-glycosylation at each of the three sites appears to be important for efficient production of secreted HuAChE by the recombinant 293 cells. One cannot overlook the possibility that the reduction in production level reflects protein instability brought about by the Asn to Gln substitutions *per se*. Nevertheless, when Asn-265 was substituted to a residue with minimal spatial requirements - Ala, the N265A mutant displayed the same phenotype as the N265Q mutant (80% decrease in enzyme secretion, relative to WT). Furthermore, we note that all three mutated asparagines map to the exposed surface of the folded-polypeptide (Fig. 32) and are probably not essential for maintaining the molecular fold (Alber *et al.*, 1987; Lim *et al.*, 1992; Shafferman *et al.*, 1992a). The pronounced influence of N-glycosylation on the production of rHuAChE is in contrast to observations made with glycosylation impaired *Drosophila* AChE in an Xenopus oocytes expression system (Mutero and Fournier, 1992). Nevertheless, rHuAChE behaves like other eukaryotic glycoproteins, in which aberrations in post translational glycosylation lead to impaired biosynthesis (Dorner *et al.*, 1987; Machamer and Rose, 1988; Matzuk and Boime, 1988; Trifft *et al.*, 1992; Weitz and Proia, 1992).

Secretion-Incompetent Molecules are Formed in Cells Producing HuAChE Glycosylation Mutants : Analysis of the events leading to the low production of AChE by glycosylation-impaired mutants relied on intracellular chase of metabolically labeled molecules. To this end, we decided to generate stable cell clones expressing the various HuAChE N-glycosylation mutants. While stable clones expressing the single site glycosylation mutants were quite readily obtained, producer clones for multiple site mutants could be established only for the double mutant [N350Q/N464Q].

Pulse-chase experiments performed with the stable clones indicate that glycosylation affects the secretion pathway of rHuAChE. In the WT-enzyme, the majority of the newly synthesized AChE polypeptides were secreted from the cells within 6 h, and were recovered efficiently in the medium (Fig. 34, left panel), in accordance with previous observations (Kerem *et al.*,1993). In the double-site mutant [N350Q/N464Q], only a small fraction of the labeled

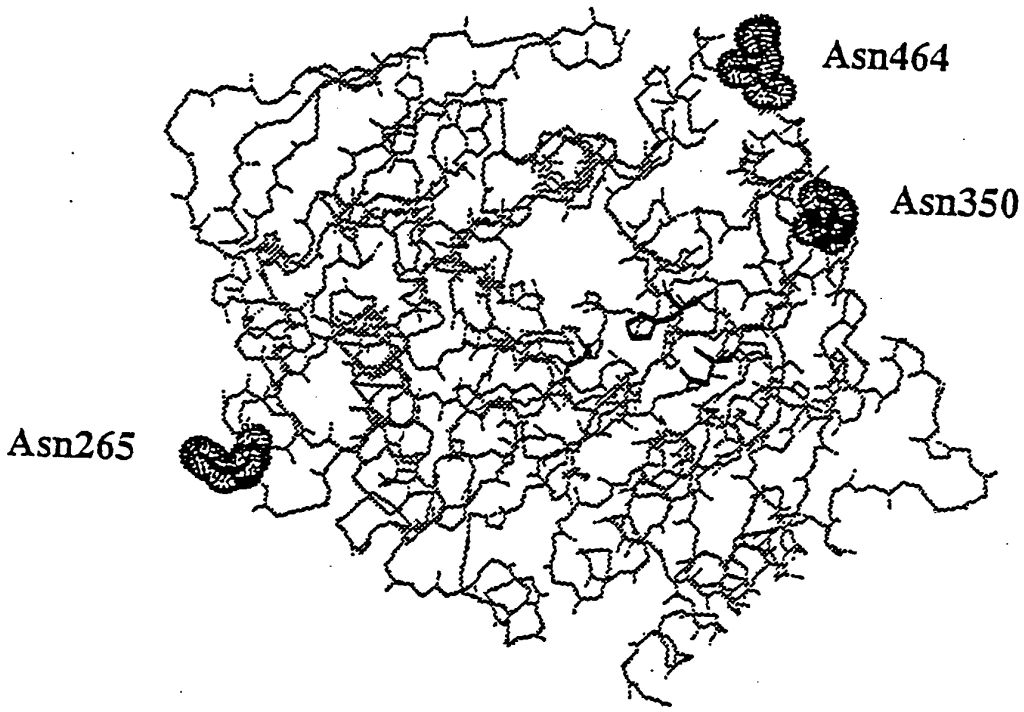

Fig. 32 - Mapping of the putative N-glycosylation targets on HuAChE.

Three-dimensional carbon-α backbone trace of HuAChE, highlighting residues Asn-265, Asn-350 and Asn-464 as well as the active site triad (in the center).

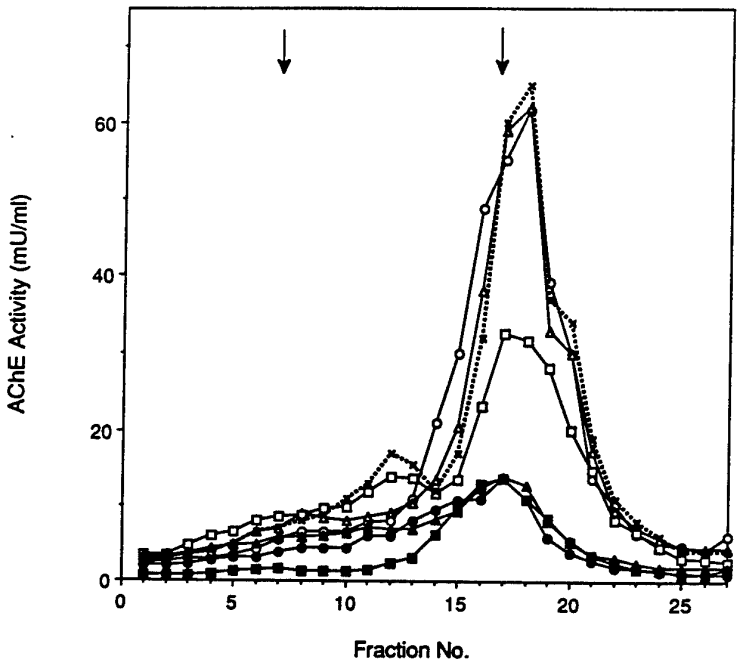

Fig. 33- Sucrose gradient profiles of HuAChE N-glycosylation mutants

Cell growth supernatants from 293 clone pools expressing WT AChE (0.2ml/gradient) or mutant AChE (1ml/gradient) were loaded on 5- 25% sucrose gradients. Left arrow marks sedimentation of β-galactosidase (16S) and right arrow marks sedimentation of bovine intestinal alkaline phosphatase (6S). HuAChE types analyzed include: wild-type enzyme (X) and the mutants N350Q (open circles), N265Q (open rectangles), N464Q (open squares), N265Q/N350Q (closed circles), N265Q/N464Q (closed rectangles) and N350Q/N464Q (closed squares).

HuAChE molecules were secreted from the cells into the medium, while most of the newly synthesized mutant-polypeptides were retained within the cells and could be recovered in lysates even 24 h after pulse (Fig. 34, right panel). Retention of non secreted AChE was also detected in cells expressing the single site mutant N265Q, although at a smaller proportion then that observed for the double-mutant.

Cell-associated AChE catalytic activity amounted to 6-8% of total activity produced within 24h by cell-cultures expressing the glycosylation-mutant AChEs, irrespective of location or number of N-glycosylation mutations. This value was identical to that observed in cells expressing WT rHuAChE. The accumulation of immunoreactive AChE suggested by the pulse chase experiments (Fig. 34) was not accompanied by a concomitant increase in cell associated enzyme activity. Thus, the AChE polypeptides retained in cells expressing the double mutant N350Q/N464Q appear to be non-active.

All these observations suggest that elimination of N-glycosylation sites leads to a less efficient folding of the nascent AChE polypeptides. In the double-site mutant N350Q/N464Q (Fig. 34) where the fate of newly synthesized molecules could be followed, the majority of the AChE molecules appear to undergo aberrant folding into non-active, secretion-incompetent forms, which are trapped in the cell. It is not clear whether the accumulated intracellular AChE is deleterious to the cells. Yet, one could speculate, that formation of intracellular non-active HuAChE pools may be responsible for difficulties to generate, in spite of repeated attempts, cell lines expressing other multiple-site glycosylation mutants.

N-Glycosylation Contributes to HuAChE Stability : The effect of N- glycosylation on thermostability of secreted HuAChE molecules was examined by comparing the time dependent loss of activity at 55^{0}C in WT vs. mutated enzyme (Fig. 35). The wild type enzyme, as well as all tested mutants exhibited a biphasic inactivation pattern (Edwards and Brimijoin, 1983; Velan *et al.*, 1991b), which is characteristic of multimeric ChEs (the major population in each of the pooled-clone preparations used consists of dimeric forms; Fig 33). Loss of side chain glycans affected AChE inactivation to different extent, yet in all cases the effect on the first phase appears to be more pronounced than on the second phase. Of the single-site mutants examined, the N350Q mutation had no effect on the heat inactivation pattern, the N265Q mutation had a minor effect, while the N464Q mutation led to a significant decrease in thermostability (The half life - $\tau_{1/2}$ - of the first phase is 2.2 min as compared to 4.5

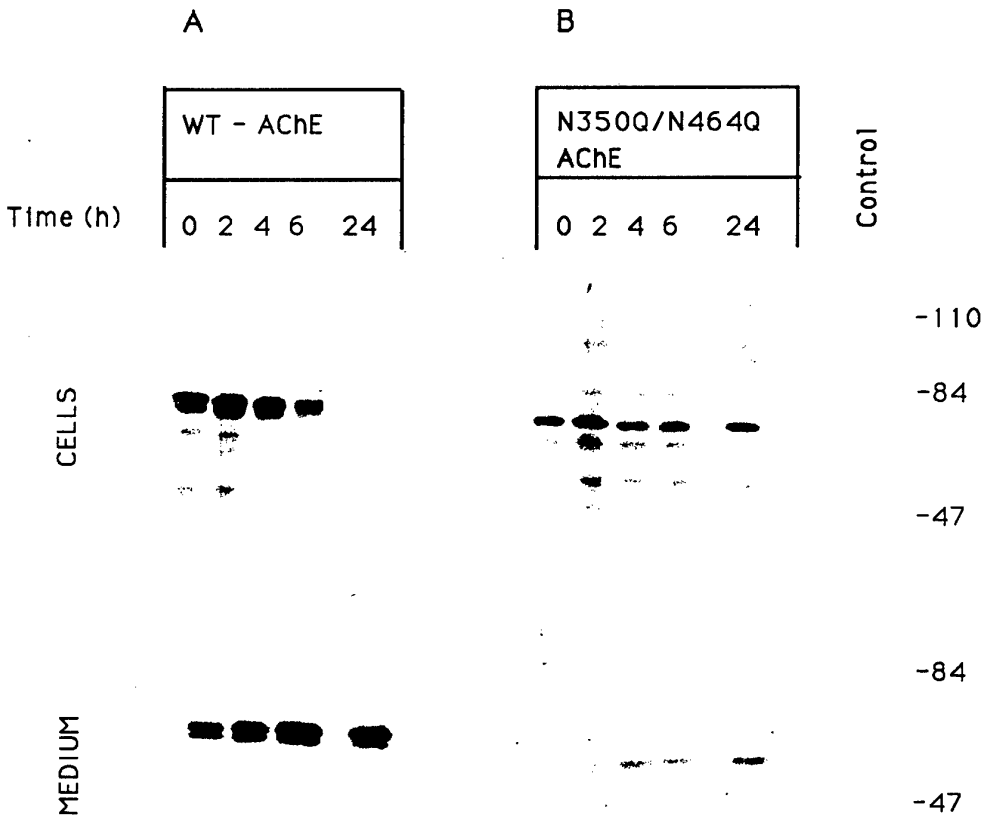

Fig 34 - Time course for secretion of WT rHuAChE and of the N350Q/N464Q mutant .

Cloned cells secreting ~30 U/ml WT-HuAChE (left panel) or ~1.5 U/ml N350Q/N464Q-HuAChE (right panel) were pulse labeled with [^{35}S] methionine for 30 min and chased for various times as indicated. rHuAChE was immunoprecipitated from solubilized cells and from medium. Non-transfected 293 cells served as control. Immunoprecipitated AChE was separated by SDS-PAGE under reducing conditions and visualized by fluorography. Exposure time of fluorographs was 2 days, the fluorograph of N350Q/N464Q AChE secreted into the medium (right, bottom) was exposed for 4 days. Positions of molecular size markers (prestained Bio-Rad standards) are shown on the right (in kilobases).

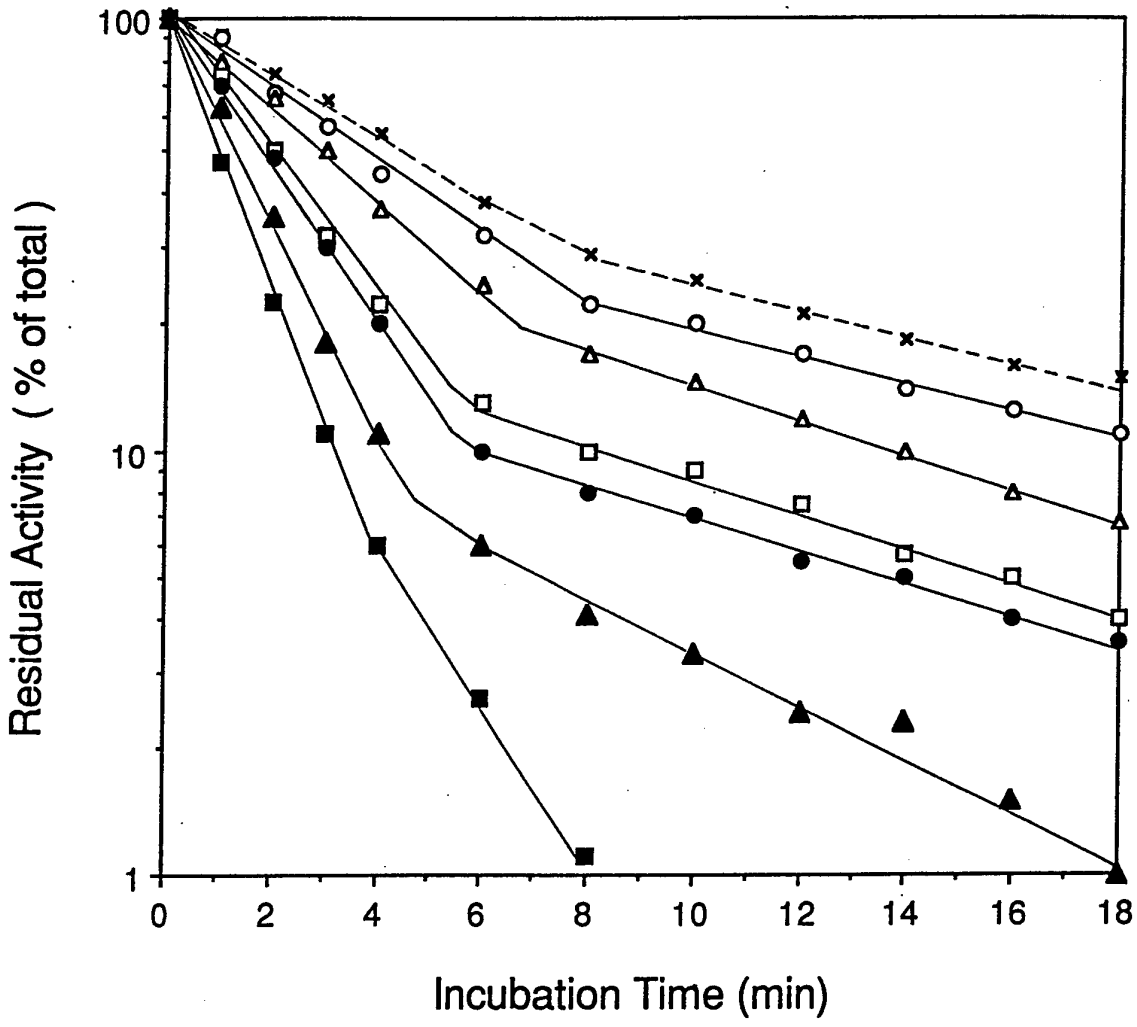

Fig 35 - Thermal inactivation kinetics of WT and glycosylation mutant rHuAChEs.
Aliquots of cell growth supernatant from stable clone pools, containing ca. 20 mU/ml of wild-type or mutant AChEs were incubated at 55°C in presence of 0.2 mg/ml BSA. At indicated intervals, aliquots were chilled on ice and tested for residual activity. HuAChE types analyzed include: wild-type enzyme (X) and the mutants N350Q (open circles), N265Q (open triangles), N464Q (open squares), N265Q/N350Q (closed circles), N265Q/N464Q (closed triangles) and N350Q/N464Q (closed squares).

in wild type). The double mutants are more thermosensitive then the single mutants, and molecules including the N464Q substitution are the most sensitive. The rank order of thermosensitivity among double mutants is [N350Q/N464Q] > [N265Q/N464Q] > [N265Q/N350Q] and the corresponding $\tau_{1/2}$s for the first component of the curve are 0.9 min, 1.2 min and 2.0 min respectively. Thermosensitivity of both double mutants carrying the N350Q substitution was greater than the sum of effects of the two corresponding single mutations. This synergism emphasizes the role of all the side chain glycans in maintaining a thermodynamically stable configuration of the mature enzyme. Accurate heat-inactivation analysis of the triple-site glycosylation mutant was prohibited by the low production level of these molecules, it appears, however that the triple-mutant is less thermostable than any of the double mutants.

One is tempted to draw correlations between the role of glycans in generating stable, secretion-compatible AChE configurations during the intracellular folding process and secretion, and their role in conferring resistance against thermal inactivation to the mature molecule. The overall N-glycosylation level, evidently, plays a key role in both processes, yet correlations at the level of individual glycosylation sites can not be found (for example the highly thermosensitive N464Q mutant is secreted at the same efficiency as other single-site mutants, compare Table 21 and Fig. 35). This stresses the fact that the thermodynamic considerations for formation of the folded polypeptide and those for maintaining the stability of the folded polypeptide are not necessarily similar.

N-Linked Oligosaccharide Side-Chains are not Required for Catalytic Activity of rHuAChE : In contrast to the significant effect on polypeptide biosynthesis, perturbation of N-glycosylation had no detectable effect on AChE catalytic activity of the secretion-compatible molecules. Specific activities calculated from the enzymatic activities of the various glycosylation mutants and the respective ELISA values (Shafferman *et al.*, 1992a) were found to be comparable to the wild type value of ca. 6±2 mU/ng (Table 22). The fact that none of the mutants exhibited a higher apparent specific-activity values indicates that lack of glycosylation does not affect the efficiency of the ELISA assay (the bulk of polyclonal antibodies used in the assay probably interacts with non-sugar epitopes).

Table 22: Catalytic functions of HuAChE and its N-glycosylation mutants.

AChE Type	Specific Activity mU/ng	K_m (mM)	k_{cat} (x10^{-5}) min^{-1}	k_{cat}/K_m (x10^{-8}) M^{-1}min^{-1}	IC_{50} (mutant)/IC_{50} (WT) a			
					Propidium	Edrophonium	Decame-thonium	BW284C51
Wild Type	6.6±2.2	0.14±0.01	4.0±1.0	29±7	1	1	1	1
N265Q	5.3±1.2	0.12±0.01	4.4±1.3	36±11	1	1	1	1
N350Q	3.7±0.9	0.14±0.02	4.2±0.8	30±6	1	2.2	7.5	3
N464Q	6.2±1.7	0.12±0.01	3.6±1.0	30±8	1	1	1	1
N265Q/N464Q	5.3±2.5	0.12±0.01	3.7±1.2	31±10	1	1	1	1
N265Q/N350Q	4.4±2.3	0.14±0.02	4.0±0.9	29±7	1	1.8	7.5	3
N350Q/N464Q	3.3±1.5	0.14±0.01	3.9±0.6	28±4	1	2	7.5	2.8
N265Q/N350Q/N464Q	3.8±2.5	0.15±0.02	3.5±1.0	23±7	ND	ND	ND	ND

[a] HuAChE Wild-type (WT) values for edrophonium, propidium, decamethonium and BW284C51 are 1.5, 1.5, 8.5 and 0.008 μM, respectively. Acetylthiocholine at 0.5 mM was used in inhibition studies.

Comparison of the catalytic constants for the hydrolysis of acetylthiocholine further establishes the similarity in the catalytic efficiency of the various glycosylation mutants. The Michaelis-Menten constant (Km), the apparent catalytic first order constant (kcat) and the apparent bimolecular rate constant (kcat/Km) were not affected by any of the mutations (Table 22). Even HuAChE molecules devoid of all three glycosylation sites exhibited normal catalytic properties. Nevertheless, some differences between mutants were revealed when interaction with the active site ligands was studied. AChE molecules carrying the N350Q substitution, alone or in combination with the other mutations, were less susceptible to inhibition by edrophonium, decamethonium and BW284C51 (Table 22). These results could indicate that the elimination of the oligosaccharide side-chain attached to Asn-350, triggers a subtle conformational change at the active center which affect interaction with the bulky inhibitor molecules. Interestingly, as noted before, a HuAChE glycoform lacking glycosylation at Asn-350 is probably generated during biosynthesis of the wild type enzyme in recombinant cells (Fig. 31).

Catalytic functions, in which the AChE peripheral anionic-site are believed to participate, were analyzed by examining interactions with the selective ligand propidium as well as inhibition by increased concentration of substrate. All single-site and double site mutants were inhibited by propidium at comparable efficiencies (Table 22) and exhibited the characteristic bell-shaped curve in response to high acetylthiocholine concentration (not shown). It appears therefore that the side chain oligosaccharides do not affect surface related AChE catalytic functions.

Taken together, all these results indicate that N-glycosylation contributes to the secretion-compatible folding of the AChE polypeptide in the cell and to the stabilization of conformation thereafter. Nevertheless, glycosylation-deficient molecules which escape the secretion related restrictions, are secreted in a folded form which permits all the interactions pertinent to catalysis. This conclusion is also substantiated by reports on *in-vitro* refolding of denatured, non-glycosylated, bacteria-derived recombinant cholinesterases into catalytically active polypeptides (Masson *et al.*, 1992; Fisher *et al.*, 1993).

Cholinesterases with different glycosylation patterns (probably generated through differential utilization of glycosylation sites or of biosynthetic pathways) have been isolated from various tissues of the same species. This was reported for *Electrophorus* AChE (Bon *et al.*, 1987), bovine and human AChE (Meflah *et al.*, 1984; Liao *et al.*, 1991; Liao *et al.*, 1992) as well as for chicken BuChE (Treskatis *et al.*, 1992). Only in bovine leukocytes (Meflah *et al.*, 1984)

was the different glycosylation pattern associated with differences in enzymatic properties. The various recombinant HuAChE glycosylation variants generated by us through elimination of N-glycosylation signals clearly exhibited very similar hydrolytic potentials. This was also true for recombinant HuAChE products in which additional N-glycosylation sites resembling those present in bovine AChE, were engineered into the human enzyme (unpublished results). These observations suggest that differential glycosylation of ChEs *in-vivo* is not involved in generation of variability in the catalytic profile, but is rather related to tissue specific processes which control glycoprotein biosynthesis in different cells. It is still possible, however, that N-glycosylation has a specific role in the, yet unsolved, non-cholinergic functions of cholinesterases in differentiation and development (Patinkin *et al.*,1990; Layer 1992).

XII - Manipulation of AChE Secretion from Mammalian Cells

INTRODUCTION

Protein secretion by eukaryotic cells involves an intricate organizational mechanism. Secretory proteins are first transported across the membrane into the lumen of the endoplasmic reticulum (ER) where folding of the polypeptide and assembly of most multisubunit proteins occur (for recent reviews see Gething and Sambrook 1992; Helenius *et al.*,1992). The folded molecules are then shuttled through the various compartments of the Golgi apparatus and are finally transported to secretion.

Soluble resident enzymes, confined to the lumen of the ER, are sorted from the proteins destined for secretion by a membrane-bound receptor through a signal mediated process (Munro and Pelham 1987). The receptor recognizes a specific signal, the tetrapeptide KDEL or a related sequence, at the COOH-terminus of the lumenal proteins and operates by continuous retrieval of these proteins from post ER 'salvage' compartments (Pelham, 1989; Pelham, 1990).

Besides the native resident ER enzymes, other groups of proteins are selectively retained in the ER, these include newly-synthesized misfolded polypeptides as well as multisubunit proteins which have failed to oligomerize properly. This is believed to be part of a quality control system which secures the functional integrity of exported proteins (Hurtly and Helenius, 1989).

The mechanisms which prohibit the export of unassembled subunits of multimeric proteins are not yet resolved and could vary in different proteins (Bonifacino *et al.*,1990; Hobman *et al.*,1992; Huth *et al.*, 1993, Rajagopalan *et al.*,1994). One could envision, therefore, a system in which secretion of properly assembled proteins is controlled by the same mechanism which controls sorting of lumenal ER proteins. This can be achieved if the signals for subunit assembly and for ER retention are coupled. Correct assembly will, thus, mask the retention

signal sequences and allow export from the ER, whereas unefficient assembly will lead to retrieval of unassembled polypeptides by the retention receptor.

Acetylcholinesterase which is a multimeric ectoenzyme (see recent reviews by Taylor, 1991; Massoulie *et al.*,1993), could be a good candidate for examining the interrelation between subunit-assembly and retention of secretory proteins in the ER. The soluble catalytic T subunit of AChE (Massoulie *et al.*,1992) serves as a precursor for several multi-subunit enzyme configurations (Lazar *et al.*,1984; Brockman *et al.*,1986; Velan et al 1991a; Duval *et al.*,1992). T- subunits polypeptides carry at their C-terminal part an exposed cysteine involved in subunit dimerization (Roberts et al 1991, Velan *et al.*,1991b) as well as C-terminal Leu residue which is preceded by a carboxylic-acid residue (see sequence compilation of AChEs in Gentry and Doctor 1991; Massoulie *et al.,* 1993). Interestingly, the Acid-Leu terminus appears to be the most critical structural element in the interaction between the ER lumenal proteins and their cognate receptor (Pelham, 1990; Andres *et al.*,1991, Haugejorden *et al.*,1991).

Recent kinetic analyses of HuAChE secretion by human embryonal cells have revealed preferential secretion of disulfide-bonded T- subunit dimers and restricted secretion of unassembled subunits (Kerem et al, 1993). This observation, together with the specific sequence motifs at the COOH-terminus of the AChE polypeptide could suggest the participation of a selective signal-mediated ER retrieval process in the controlled assembly of AChE catalytic subunits. In this report, we define the mutual effects of coresiding C-terminal signals on the process of selective secretion of assembled multisubunit proteins. This is done by engineering different amino acid configurations at the C-terminus of HuAChE and by analysing their effect on the biogenesis of HuAChE.

METHODS

Construction of Vectors and Expression of the Various AChE Mutants. : The wild-type human *ache* cDNA (Soreq *et al.*, 1990) and the HuAChE mutants altered at their C-terminus were expressed on multipartite vectors carrying also the *cat* reporter gene and the selective marker *neo* (Kronman *et al.*, 1992; Velan *et al.*, 1993).

Site directed mutagenesis was performed by DNA cassette replacement as described previously (Shafferman *et al.*,1992a; 1992b). Synthetic DNA duplexes carrying at their C-terminus the

sequences depicted in Fig. 36 were introduced into the *ache/cat/neo* tripartite plasmid vector (Velan *et al.*,1993) to replace the native HuAChE cDNA sequence between the unique restriction sites *BssHII* and *SalI* as described previously (Velan *et al.*,1991b).

Transient transfections of human embryonal 293 kidney cells were carried out as previously described (Shafferman *et al.*, 1992a). To release cell associated enzyme, transfected cells were resuspended in 0.02M phosphate buffer and disrupted by three freeze- thaw cycles. Buffer-soluble fraction was separated from cell debris by Eppendorf centrifugation, pellets were then extracted with phosphate buffer supplemented with 1% Triton X-100 and 1M NaCl to obtain the detergent-soluble fraction (Velan *et al.*,1991b). Total cell-associated AChE activity in transiently transfected cells was determined after combining the buffer-soluble fraction with the detergent-soluble fraction.

Selection of stably transfected clones and formation of stable clone pools were achieved as previously described (Kronman *et al.*,1992; Velan et al. 1991b). After reaching confluency, cell pools were submitted to subcellular fractionation as described below.

Subcellular Fractionation : Subcellular fractionation of the recombinant 293 cells was performed essentially as described by Leli *et al.*,(1993). Stably transfected cells were seeded onto eighteen 10mm culture plate at a density of $5x10^6$ cells/plate and propagated for 24 hrs in ChE-depleted medium (Shafferman *et al* ., 1992a). Cell growth media were collected and defined as the 'secreted-fraction'. Cells were washed twice with phosphate buffered-saline and resuspended in 7.5 ml homogenization buffer containing 0.25M sucrose, 20mM Tris-HCl pH 7.6, 1mM EDTA, 0,02U/ml Aprotinin (Sigma), 0.0005 mg/ml Leupeptin (Sigma) and 1mM benzamidine. Cells were homogenized with an ultrasonic probe and centrifuged at 100.000g for 60 min. Supernatant was collected and pellets were resuspended in 7.5 ml homogenization buffer, containing 1M NaCl, and centrifuged again as described above. The low salt extract and the high-salt extract were pooled and defined as the 'buffer- soluble cellular fraction. The pellets were then resuspended again in 7.5 ml homogenization buffer containing 0.15M KCl and 1% Triton X- 100. After ultrasonic homogenization, the suspension was centrifuged at 30.000g for 20 min The supernatants were collected and defined as 'detergent-soluble cellular fraction'.

Metabolic Labeling and Immunoprecipitation of Proteins : Cells were labeled for 1h

with [^{35}S]-methionine (200 μCi/ml;1000 Ci/mmol; Amersham) and chased in methionine-containing medium supplemented with 20 μg/ml Aprotinin (Sigma). At various chase periods, culture media were collected and cells were washed and then lysed (Kerem *et al.*,1993). AChE was immunoprecipitated from cleared cell lysates and media with rabbit anti-HuAChE antibodies (Shafferman *et al.*,1992a) followed by precipitation with protein-A bacterial adsorbent (Biomakor, Israel) and endo H treatment as described previously (Amitay *et al.*,1991).

Two alternative protocols were used for visualization of HuAChE bands. When protocol-A was used secreted, proteins were loaded directly on 10% SDS-polyacrylamide gels. Gel samples were electrotransfered to nitrocellulose paper and AChE bands were visualized using rabbit antibodies directed to bacteria-derived HuAChE polypeptides (Velan *et al.*,1991b).

When protocol-B was used, HuAChE was first immunoprecipitated from cell lysates with rabbit anti-HuAChE antibodies bound to Sepharose as previously described (Velan *et al.*,1993). Immunoprecipitates were eluted from the Sepharose beads by 30 min incubation in 1% SDS, 50mM Tris-HCl pH-8.0 at room temperature. Eluates were subjected to endo H treatment prior to SDS-PAGE as described previously (Kerem *et al.*,1993). Gels were electroblotted onto nitrocellulose filters and developed as described for protocol-A.

RESULTS

The C-terminal Tetrapeptide of HuAChE is not a Variant of the KDEL Retention Signal : The sequences of mammalian T-subunits (Gentry and Doctor, 1991) terminate with the tetrapeptide CSDL. This tetrapeptide carries the Acid-Leu terminus which is the most conserved functional element of the KDEL retention signal (Pelham, 1990).

Substitution of the Cys in CSDL by a Lys, to create KSDL, should increase similarity to the canonical retention signal, as well as prevent dimer formation. KSDL at the terminus of the AChE polypeptide is expected to act as an improved retention signal which cannot be masked by subunit dimerization. On the other hand, the putative interaction of the CSDL tetrapeptide with the retention-receptor should be abrogated by the concomitant substitution of the terminal Asp-Leu residues by Ala-Val, to generate a CSAV tetrapeptide. Similar substitutions (Glu to

Ala; Leu to Val) were shown previously, in other experimental systems, to prohibit cellular retention even when performed separately (Zagouras and Rose 1989; Haugejorden *et al.*, 1991; Andres *et al.*, 1991; Tang *et al* ., 1992; Vennema *et al.*, 1992).

To test these predictions, the two HuAChE mutants terminating with the tetrapeptides KSDL and CSAV were generated (Fig. 36). Transiently transfected cells expressing mutants C580K (KCDL-terminus) and D582A/L583V (CSAV-terminus) were compared to cells expressing WT- HuAChE (CSDL- terminus) and cells expressing the C580A HuAChE monomer (ASDL-terminus). Retention was monitored by determining the amounts of enzyme secreted into medium versus the amounts recovered from lysed cells. The ratio of intracellular vs. secreted activity in all four AChE variants appears to be about 1:10 (Table 23). Dimerization impairment *per-se* (ASDL terminus) did not effect secretion as shown previously (Velan *et al.*,1991b). The KSDL terminus did not induce the expected increase in cellular retention, and moreover, the CSAV terminus did not lead to decrease in the cell-associated AChE fraction, compared to WT HuAChE (Velan *et al.*,1991a).

To test whether HuAChE sequences are refractive, in some way, to efficient retention by 293 cells, a C580A HuAChE monomeric mutant tagged with the KDEL tetrapeptide was examined. Transfection results (Table 23, bottom) clearly indicate that this mutant (designated C580A-KDEL AChE; Fig. 36) is retained very efficiently in the recombinant cells.

Taken together, results presented in Table 23 suggest that the CSDL tetrapeptide at the C-terminus of AChEs does not act as a retention signal for unassembled HuAChE. Metabolic labeling experiments (not shown) appear to substantiate these observations: The C580K HuAChE mutant is secreted from cells in the monomeric form at rates comparable to those of the C580A mutant, whereas the D582A/L583V mutant is secreted in the dimeric form at rates comparable to those of WT enzyme, with no effect on the efficiency of dimerization.

KDEL Tagged HuAChE is Retained and Accumulates in the Cell as an Active Enzyme : The intracellular fate of the retained C580A-KDEL AChE was examined in stably transfected 293 cells. To overcome fluctuations related to AChE expression in individual transfected clones, cell pools, were prepared by combining ~100 different clones. These cells were submitted to partial subcellular fractionation and analyzed for cell-associated and secreted AChE. Stable clone pools expressing the C580A-KDEL AChE were compared to similar pools expressing the WT enzyme and the C580A mutant monomer.

AChE Type	C-Terminal Sequence
	580 ▼
Wild Type	—— Cys Ser Asp Leu —— TGC TCA GAC CTG
D582A/L583V	—— Cys Ser Ala Val —— TGC TCA GCC GTG
C580A	—— Ala Ser Asp Leu —— GCC TCA GAC CTG
C580K	—— Lys Ser Asp Leu —— AAG TCA GAC CTG
AChE-KDEL	—— Cys Ser Lys Asp Glu Leu —— TGC TCA AAG GAC GAG CTG
C580A-KDEL	—— Ala Ser Lys Asp Glu Leu —— GCC TCA AAG GAC GAG CTG

Fig 36. Mutagenesis of sequences at the carboxyl-terminus of HuAChE.

DNA sequences were altered downstream from the marked Cys-580 as described in the Methods

Table 23: Secreted and cell-associated enzymatic activities in transiently transfected cells expressing HuAChE carboxyl-terminus mutants

HuAChEs	C-terminal tetrapeptide	HuAChE (mU/plate) [a]		AChE Ratio Cells/medium
		Medium	Cells	
Wild Type	CSDL	760 ± 67	88 ± 20	0.11
D582A/L583V	CSAV	650 ± 45	68 ± 25	0.1
C580A	ASDL	680 ± 32	86 ± 17	0.13
C580K	KSDL	750 ± 90	60 ± 10	0.08
C580A-KDEL	KDEL	20 ± 4	855 ± 54	42.5

[a] HuAChE was recovered from a 100mm culture plate 48hrs post transfection. Activity was normalized to activity of coexpressed CAT as described previously (Shafferman *et al.*,1992a). Values represent the average of three experiments.

Table 24: Production of HuAChE by stable cell pools expressing WT AChE and the AChE mutants C580A and C580A-KDEL.

HuAChEs	Quantitation Method[a]	Amount of HuAChE [b]			
		Secreted	Cellular Buffer soluble	Cellular Detergent soluble	Total
WT	Activity	21.4	0.8	1.3	23.5
	Elisa	20	1	1	22
C580A	Activity	19.5	1.6	1.4	22.5
	Elisa	21	1	2	24
C580A -KDEL	Activity	2.3	10.5	12.2	25
	Elisa	2	9	12	23

[a] HuAChE quantitation is based either on enzymic activity measurments, using 6000 U/mg as specific activity (Kronman *et al.*,1992), or on ELISA quantitation (Shafferman *et al.*,1992a). Values represent micrograms AChE produced per plate within 48 hrs.
[b] Amounts of AChE are presented as micrograms enzyme produced per plate during 48hrs. Values represent the average of four experiments; the standard error range is ± 5-15%.

The non-KDEL appended AChE forms (oligomeric as well as monomeric) were secreted efficiently into the cell growth medium, as expected (Velan *et al*,. 1991b). On the other hand, most of the C580A-KDEL mutant enzyme was retained in a cell-associated fraction (Table 24). Nevertheless, the total level of AChE production (calculated by combining secreted and cellular AChE) by cells expressing the C580A-KDEL mutant was similar to that of cells expressing the WT enzyme or the mutant monomer (Table 24). This is true whether the HuAChE mass calculations are based on enzymatic activity or on total immunoreactive protein, as determined by ELISA. C580A-KDEL AChE recovered from cells displays a specific activity of about 6000 U/mg which is characteristic to secreted WT HuAChE . Moreover, the kinetic rate constants of the retained mutant enzyme (Km of 0.1±0.02 mM and kcat of 3.9± 0.4 x10^5/min) are identical to those of the secreted enzyme (Kronman *et al.*,1992).

The retained C580A-KDEL mutant enzyme is distributed in equal amounts between a buffer-soluble intracellular fraction and a detergent-soluble fraction. These two enzymatic fractions do not differ in their specific activity or kinetic parameters. A similar partitioning is observed also in the cell-associated AChE activity of 293 cells expressing WT enzyme, even though the amount of enzyme recovered from these cells is much smaller (Velan *et al.* ,1991a). Western blot analysis of secreted WT enzyme or cell-associated C580A-KDEL AChE with antibodies directed against non-conformational epitopes failed to detect a major proportion of inactive molecules in the retained enzyme. Integrated AChE band intensities in lanes containing equivalent amounts of enzyme units were similar, independent of AChE source or of the migration pattern (not shown). It appears, therefore, that the active cell-associated C580A-KDEL AChE molecules do not represent a sub-population within a larger pool of malfolded molecules. All these observations indicate that AChE-monomers retained in 293 cells by appendage of the KDEL signal acquire full enzymatic activity and are probably folded into the authentic functional configuration.

The fate of newly formed C580A-KDEL AChE molecules in the cell was studied by metabolic labeling with [^{35}S]-methionine followed by immunoprecipitation at various chase periods. Kinetics of biosynthesis were compared to those of C580A-AChE monomer (Fig. 37). Most of the newly synthesized non-KDEL appended monomers (C580A-AChE) were secreted from the cells into the medium within 6 hrs, as reported previously (Kerem *et al.*,1993). The intracellular C580A AChE molecules are endo H - sensitive , whereas the secreted enzyme is

endo H - resistant (Fig. 37A) and displays the two characteristic major glycoforms of terminally glycosylated HuAChE (Velan *et al.*,1993). On the other hand, newly formed C580A-KDEL mutant molecules were retained in the cells (Fig. 37B), and only a minute fraction of the labeled AChE was recovered in the medium (it should be noted that some of the C580A-KDEL monomers which appear in the medium, originate from cell lysis as indicated by their sensitivity to endo H; Fig. 37B). Judging by the intensity of the bands, the labeled KDEL-C580A AChE can be fully recovered from cells even after a 24 hrs of chase suggesting that the retained molecules are not susceptible to intracellular degradative processes. It should be noted also that the newly synthesized KDEL-retained enzyme does not acquire endo H - resistance for the first 6 hrs of chase, yet after 24 hrs a large fraction of the intracellular AChE population becomes endo H - resistant. This would suggests a dynamic recycling of KDEL tagged AChE monomers between the ER and the Golgi compartments.

Taken together, the intracellular AChE- measurements and the labeling experiments indicate that appendage of the KDEL tetrapeptide to a C580A-AChE catalytic subunit which is impaired in its ability to assemble, results in an effective intracellular retentation. The accumulated enzyme acquires full enzymatic activity and reaches average concentrations of 10 pg/cell.

Dimerization of AChE Subunits Overrides KDEL Mediated Intracellular Retention To examine the interrelationships between ER-retention and subunit assembly an HuAChE mutant which carries at its C-terminus the exposed native cysteine (Cys-580) juxtaposed to a KDEL tetrapeptide (designated AChE-KDEL) was created . Stably transfected cells, comprised of pooled clones expressing AChE-KDEL were established and analyzed for retained and secreted AChE. Results were compared to those of cells expressing WT-AChE and cells expressing the AChE mutants C580A and C580A-KDEL. Total AChE productivity in 293 cells is not affected by KDEL appendage and resembles that observed for WT and C580A-KDEL AChEs (Table 24). The relative proportion of retained enzyme in cells expressing the AChE-KDEL mutant is however clearly different from that in cells expressing the C580A-KDEL mutant (Fig. 38). While 93±2% of C580A-KDEL AChE produced by stable cells is retained in the cell only 23±4% of AChE-KDEL is found in the cell- associated form, while ~77% is secreted to the medium. In this respect AChE-KDEL AChE resembles the WT enzyme which at similar conditions exhibits a 87±3% secretion efficiency. This observation suggests that presence of a free cysteine in the vicinity of the KDEL signal

A. C580A AChE

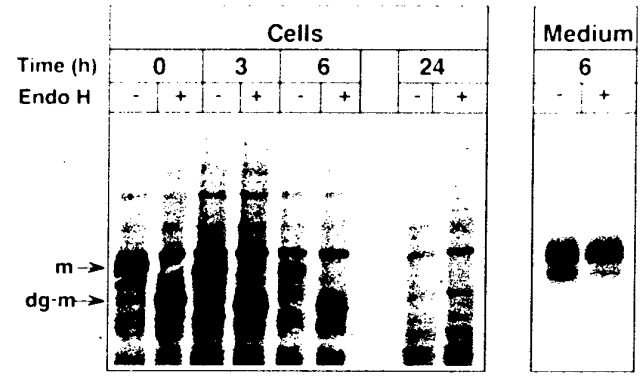

B. C580A-KDEL AChE

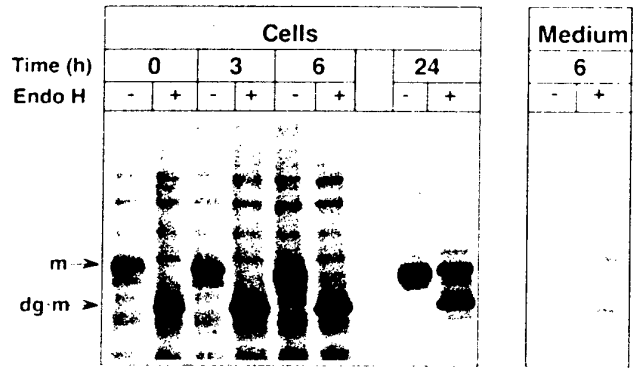

Fig. 37: Secretion of the C580A-AChE monomers and retention of C580A-KDEL AChE monomers.
Clone pools of 293 cells expressing either C580A-AChE (A) or C580A-KDEL (B) were grown to confluence, metabolically labeled for 1hr with [^{35}S]-methionine and chased with methionine - containing medium as described in "Methods". Cells were lysed at the indicated chase periods and HuAChE was immunoprecipitated from cleared lysates. AChE secreted into the growth medium was immunoprecipitated 6 hrs post chase. Immunoprecipitated AChE samples were divided into two equal aliquots, and incubated with (+) or without (-) endo H. Electrophoresis was performed at non-reducing conditions in 10% SDS gels, followed by fluorography. Migration of monomers (m), and deglycosylated monomers (dg- m) is marked by arrows.

abrogates the retention mediated by this tetrapeptide. Nevertheless the small, yet significant, decrease in the ratio of secreted to produced AChE in cells expressing AChE-KDEL as compared to WT AChE or to C580A monomers could indicate a delay in the transport of the enzyme through the secretory pathway.

To examine such a possibility, cells expressing WT enzyme and AChE- KDEL were metabolically labeled and AChE was immunoprecipitated from cell lysates at various chase periods (Fig. 39). In cells expressing WT enzyme (Fig 39A) nascent endo H - sensitive monomers are assembled into endo H - sensitive dimers which are then transported rapidly through the Golgi apparatus to be secreted as endo H - resistant dimers. This secretion profile resembles previous observations on secretion of HuAChE by single recombinant 293 cell clones (Kerem *et al.*,1993) yet is different from that of the AChE-KDEL mutant. While assembly of C580-KDEL monomers into dimers resemble the formation of WT dimers, the transport of mutant dimers through the Golgi appears to be significantly different from that of WT dimers. This is indicated by the detection of an endo H - resistant dimer population which accompanies the endo H - sensitive dimers at the various period of chase and, most surprisingly by the presence of these endo H-resistant molecules in cell lysates 24 hours after labeling. Differences are found also in the configuration of AChE secreted in the medium: in WT enzyme the majority of the secreted enzyme is composed of assembled mature forms whereas in the AChE-KDEL mutant a relatively large fraction of unassembled endo H resistant monomers is detected (Fig. 39A).

The effect of KDEL appendage on intracellular processing of AChE subunits can also be demonstrated by endo H treatment of the steady state pool of cell-associated AChE, followed by gel analysis in presence of β-mercaptoethanol. In cells expressing non KDEL appended AChE molecules such as WT enzyme or C580A monomers the intracellular pools of endo H - resistant AChE species can not be detected (Fig. 40). In the retained C580A-KDEL mutant a major population of endo H - resistant AChE subunits accompanies the endo H sensitive molecules. Moreover, within the endo H - resistant population one can identify a diffuse band of slow-migrating AChE species which is not present in the non KDEL-appended intracellular AChE. The migration profile of this band suggests that it represents AChE glycoforms (terminally glycosylated) which are trapped within the cell. The cell-associated species of AChE-KDEL resemble those of C580A-KDEL, and include endo H sensitive molecules, endo H - resistant molecules and endo H-resistant slow migrating molecules.

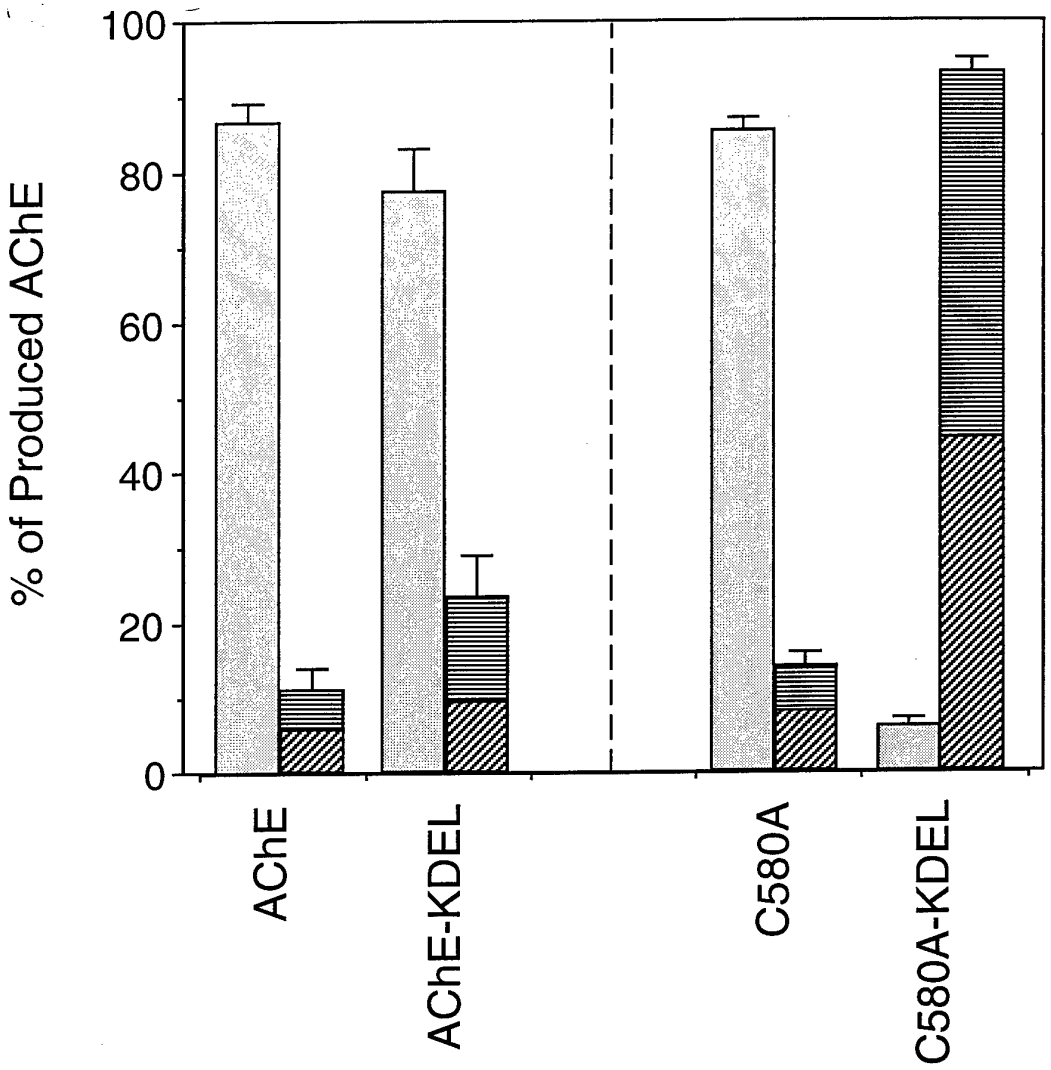

Fig. 38. Comparison of cell-associated and secreted enzyme levels in cells expressing KDEL-appended and non KDEL-appended HuAChE forms.

Stable cells expressing the dimerization competent wild-type AChE and its KDEL-appended derivative AChE-KDEL, (left panel), as well as the dimerization impaired C580A monomeric mutant and its KDEL appended derivative C580A-KDEL, (right panel) were submitted to partial subcellular fractionation. AChE activity was determined in growth medium (dotted bars) and in lysed cells (striped bars). The subcellular fraction (see "Methods") was divided into the buffer-soluble fraction (diagonal stripes) and the detergent-soluble cellular- fraction (horizontal stripes). Each bar represents the average of four independent experiments.

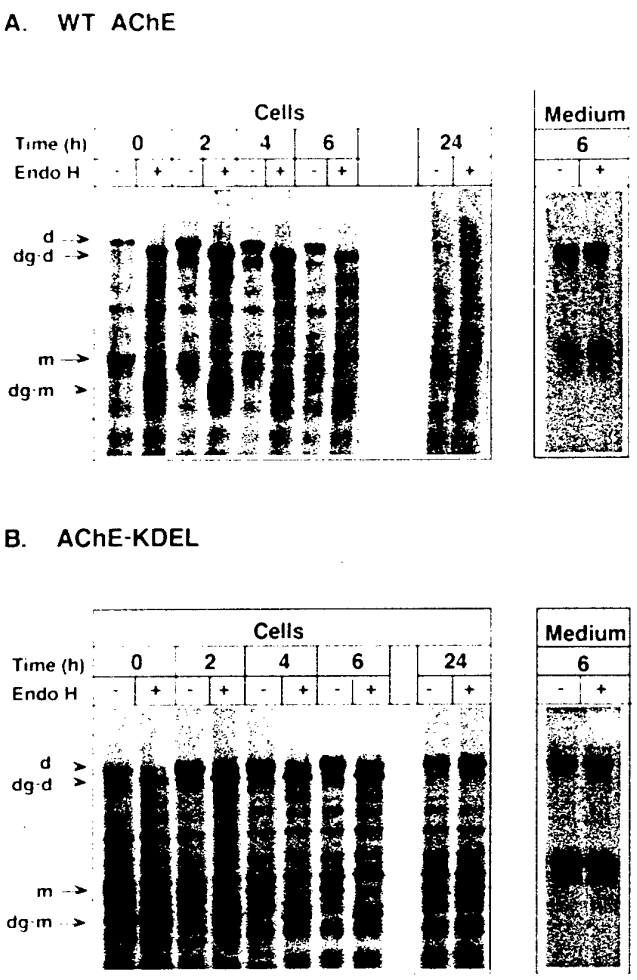

Fig. 39. Assembly, acquisition of endo H - resistance and secretion of wild-type and AChE-KDEL enzymes.

Clone pools of 293 cells expressing either WT AChE (A) or the AChE-KDEL mutant (B) were metabolically labeled and analysed as described above. Migration of monomers (m), deglycosylated monomers (dg-m), dimers (d) and deglycosylated dimers (dg-d) is marked by arrows.

Differences can be observed however in the relative proportion between the various forms, especially in the ratio of the various endo H resistant glycoforms.

These observations indicate that in 293 cells, like in other cell systems (Dean and Pelham, 1990; Peter *et al.*,1992) , the KDEL- receptor is recycled between the various compartments of the secretory pathway and can be sorted to the trans-Golgi cisternae. Nevertheless, the C580A-KDEL monomeric AChE is retrieved from these distal compartments into the ER and is thereby diverted from secretion. The dimerization-competent AChE-KDEL molecules can also interact with KDEL receptor, as reflected by the delay in transport, yet in these polypeptides the Cys-580 induced dimerization eventually overrides the retention process and directs the enzyme towards secretion.

In all the AChE variants tested in the present study, the cell associated AChE is partitioned at about equal proportions between the buffer-soluble and detergent- soluble cellular fractions. The origin of this partitioning is not clear and could be attributed to an unidentified post-translational process, to phase partition related to T-subunit amphiphilicity (Massoulie *et al.*,1993), or to differential lysis of different AChE- containing cellular vesicles. It should be noted that the AChE derived from the two cellular fractions were indistinguishable in catalytic activity, electrophoretic mobility, and resistance to endo H.

DISCUSSION

Interrelation Between Assembly and Retention Signals in Secretion of HuAChE.

The endoplasmatic reticulum functions as a specialized organelle for biogenesis and maturation of secretory proteins. This function is maintained by intricate processes which assist the correct folding and assembly of nascent polypeptides. Misfolded and unassembled polypeptides are selectively retained in the ER by a mechanism referred to as 'quality control' which is not completely understood. At the same time, the secretory system operates a well-characterized control mechanism which prevents the escape of the ER resident proteins and folding enzymes, through interaction of a membrane bound receptor with specific signals located on these proteins.

In this study, we have examined the possible involvement of the protein retention system in the control of subunit assembly of secreted complex proteins, utilizing HuAChE secretion as a specific target. To achieve this, we have created HuAChE derivatives which are mutated at putative native retention signals at the C-terminus of the polypeptide, as well as HuAChE derivatives, tagged with the ER- retention signal KDEL, which carry, or are defective in the native AChE-dimerization signal. Appendage of the ER-retention signal KDEL to a dimerization-impaired AChE-subunit (C580A-KDEL mutant) resulted in very efficient retention of AChE in the cell. On the other hand, attachment of KDEL to an AChE polypeptide which carries the native free cysteine at its C-terminus (AChE-KDEL mutant) did not lead to retention. This suggests that subunit dimerization mediated by Cys-580 (Velan *et al.*,1991b) overrides retention probably by masking recognition of KDEL by its cognate receptor. This observation is in line with our previous studies demonstrating that dimerization of HuAChE subunits occurs within the ER (Kerem *et al.*,1993) and with the concept that the KDEL- signal/receptor interaction occurs at a post-ER salvage compartment (Pelham, 1988). Thus, conjunction of an ER oligomerization process with a consecutive step of retrieval of non-oligomerized subunits can provide, in principle, a 'quality control' system for the proper sorting of assembled subunits from the ER.

Effect of Cellular Retention of AChE on Folding and Enzymatic Activity

Retention of the C580A-KDEL monomers is very efficient, leading to intracellular accumulation of almost all the enzyme mass (Table 24) produced by the high expression system (Kronman *et al.*,1992) used in this study. Concentrations of the retained enzyme is at least as high as 0.1mM in the whole cell and should be much higher in the secretory vesicles. Similar concentrations were calculated for native ER-resident folding proteins (Noiva and Lennarz, 1992). C580A-KDEL AChE extracted from the cells possesses the specific activity (Table 24) and kinetic parameters of the secretable enzyme, suggesting that most of the retained enzyme acquires conformational maturity. The correct folding of the intracellular enzyme is probably also reflected in the fact that the retained AChE polypeptides are not prone to pre-Golgi degradative processes. Such degradation processes can be triggered by malfolding of nascent polypeptides (Le *et al.*,1992; Wikstrom and Lodish, 1993) and appear to be involved in the abortive biosynthesis of AChE derivatives mutated at amino acids which are required for proper folding (Shafferman *et al.*,1992b). Indications that ER retention processes

can occur *in-vivo* during biosynthesis of AChE were provided in cells expressing AChE naturally. Chick brain cells (Chatel *et al.*,1993) as well as cultured muscle cells (Rotundo *et al.*,1989) contain distinct populations of endo H - sensitive AChE monomers which bind poorly to WGA. It should be noted however that these retained forms are devoid of enzymatic activity and in the case of muscle cells undergo proteolytic degradation. In this respect these intracellular form are different from the retained AChE monomers generated in recombinant 293 cells through the KDEL appendage. It should be noted that retained inactive HuAChE molecules can be formed in 293 cells, as demonstrated earlier (Velan *et al.*,1993) in cells expressing HuAChE molecules mutated at their N-glycosylation sites. These previous observations could suggest that oligosaccharide recognizing chaperones such as calnexin (Hammond *et al.*,1994) participate in the folding process of AChE polypeptides.

Effect of the KDEL Tetrapeptide on Cellular Transport of Dimerization-Competent and Dimerization-Impaired AChE Subunits. : Analysis of the retained AChE molecular forms reveals a large population of endo H - resistant molecules some of which appear to be terminally glycosylated, suggesting that KDEL-tagged AChE monomers can be retrieved from the distal Golgi compartments . This supports other observations on the relaxed rules which govern the recycling of the KDEL-receptor between the secretory vesicles (Pelham, 1988; Dean and Pelham, 1990; Peter et al, 1992).

Dimerization-competent AChE subunits tagged with the KDEL tetrapeptide are secreted efficiently from the recombinant cells, yet appear to be retarded in their transport to the cell surface. This is suggested by the identification of endo H - resistant cell associated AChE-KDEL molecules (dimeric as well as monomeric) in the later stages of chase. These species are not detected in cells expressing WT enzyme and in certain experiments, appear as a very small transient population (Kerem *et al.*,1993). One possible explanation for the observed retardation in AChE-KDEL secretion is the operation of a retrograde transport for receptor bound endo H resistant monomers from the Golgi back into the ER. This can be followed by dimerization in the ER of the endo H - resistant subunits and retransport of these dimers through the secretory pathway.

Alternatively, the increase in the intracellular endo H - resistant AChE fraction could originate from a receptor-mediated retardation in transport of assembled enzyme through the Golgi. This would implicate an equilibrium between AChE-KDEL dimers AChE-KDEL monomers

and a KDEL receptor docked in the Golgi membrane. The latter model would involve dissociation of disulfide bonded subunits in a post ER milieu and should be investigated carefully in the future. It should be noted, however, that equilibrium between monomers and oligomers in a post ER compartment was recently demonstrated in non-covalent assembly of VSV glycoprotein trimers (Zagouras and Rose 1993). Moreover, the mechanism proposed by Rotundo (1984) for assembly of asymmetric AChE, which implicates homo-dimerization in the ER followed by hetro-oligomerization in the Golgi, should also depend on post- ER dissociation of homodimers. Both models, the one invoking recycling of receptor-bound monomers and the one invoking dissociation of dimers in the late stages of transport are in accordance with the observed co-secretion of monomers and dimers in cells expressing the AChE-KDEL enzyme.

Involvement of the C-terminal Sequences of AChE in Cellular Retention. :

The possibility that the native C-terminal sequence of mammalian AChE provides a coupled oligomerization/retention signal through the C- terminal tetrapeptide CSDL was examined by site directed mutagenesis. Results obtained with various divergent forms of this C-terminal tetrapeptide suggest that CSDL does provide a subunit dimerization signal (Velan *et al.*,19921a) but fails to provide a retention signal (Table 23). Compilation of naturally occuring retention signal tetrapeptides (Pelham, 1990; Mazzarella *et al.*, 1990; Fliegel *et al.*,1990; Potter *et al.*,1992; Vennema *et al.*,1992; Robbi and Beaufray, 1991) as well as numerous mutagenesis studies (Haugejorden *et al.*,1991; Andres *et al.*,1991) suggest a strong functional stringency for conserving a Leu residue at position 4 and a carboxylic residue (preferentialy Glu) at position 3 of the tetrapeptide. In this respect the terminal tetrapeptides of AChE from mammalia (CSDL) and Torpedo (CSEL) conform with the basic structure of the retention signal for lumenal ER proteins. The comparative studies mentioned above also indicate that amino acids at position 1 and 2 of the KDEL tetrapeptide can be substituted by a large variety of amino acids, without effecting interaction with the cognate receptor. Nevertheless, results presented here indicate that the AChE terminal tetrapeptide CSDL can not function in retention. Incompatibility with retention can be attributed to the presence of a Ser at position 2, as indicated by lack of retention of an AChE mutant carrying the KSDL- terminus. (Table 23).

The failure to demonstrate the involvement of the AChE terminal tetrapeptide in retention

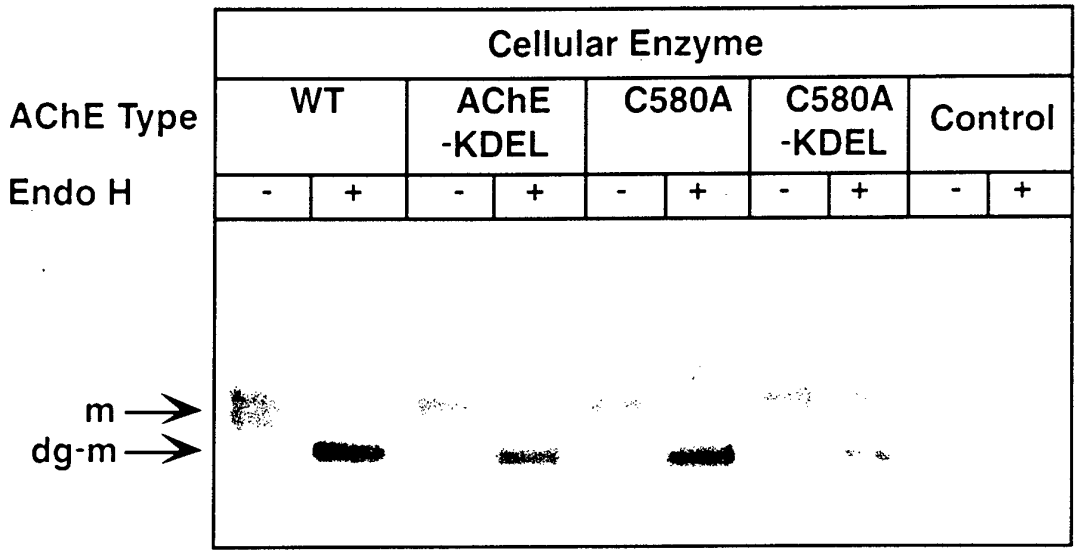

Fig. 40. Endo H - resistance of intracellular AChE in cells expressing WT enzyme and C-terminal mutants.

293 cells expressing WT AChE and the mutants AChE-KDEL, C580A and C580A-KDEL as well as non-transfected 293 cells (control) were submitted to partial subcellular fractionations. 1 ml aliquots of the buffer-soluble fraction, each containing 5 U/ml AChE were prepared by appropriate dilutions in the buffer-soluble fraction derived from non transfected cells, to maintain comparable levels of total protein. HuAChE was immunoprecipitated with Sepharose-bound antibodies prior to gel electrophoresis as described in protocol-B for Western blots (see Methods). Immunoprecipitates were divided into two equal aliquots, one of which was treated with endo H. Eluates were resolved by 10% SDS-PAGE at reducing conditions, electroblotted onto nitrocellulose and probed with antibodies directed against a HuAChE-peptide. Migration of subunit monomers (g-m) and deglycosylated subunit monomers (dg-m) is marked by arrows.

processes could indicate that secretion of dimerized AChE is controlled by a different mechanism. Selective pre- Golgi degradation of unassembled native AChE monomers, for example can assure preferential export of oligomeric forms. While KDEL- appended C580A monomers did not seem to undergo intracellular degradation it is still possible that the exposed thiol in the native subunit (Cys 580) triggers the degradative process, as recently suggested for degradation of non-assembled IgM molecules (Fra *et al.*,1993). On the other hand, the fact that the CSDL tetrapeptide of AChE does not act as a classical ER retention signal does not exclude the possible presence of non-KDEL related retention signals on the AChE polypeptide. Other retention signals, such as those identified recently at the C-termini of various soluble secreted proteins (Arber *et al.*,1992; Chen *et al.*, 1993; Fay *et al.*, 1993; Andersson *et al.*, 1994), could interact with Cys-580 to generate a retention/assembly quality control system for secretion of oligomeric AChE.

XIII - The Role of Oligosaccharide Side-Chains and Subunit-Assembly in the Clearance of Cholinestertases from the Circulation

INTRODUCTION

Acetylcholinesterase has been the subject of intense research due to its focal position in many fields of interest. Modification in the levels of human brain AChE have been reported in various disorders such as Down's syndrome (Yates *et al.*, 1980) and Alzheimer's disease (Coyle *et al.*, 1983). Several cholinesterase inhibitors have proven to be of value as medicinal agents and are used for the treatment of glaucoma or myasthenia gravis (Taylor, 1990). Previous reports have shown that plasma-derived AChE or butyrylcholinesterase can be used as a prophylactic antidote against organophosphate poisoning in animals (Wolfe *et al.*, 1987; Broomfield *et al.*, 1991; Ashani *et al.*, 1991; Raveh et al., 1993) or for treatment of humans exposed to organophosphate pesticides (Cascio *et al.*, 1988). Use of cholinesterase as a biological scavenger requires sources for large quantities of purified enzyme and depends on the retention of the enzyme in the circulation for sufficiently long periods of time. Recombinant DNA techniques may provide the method to establish efficient production systems along with the means for introduction of new traits into the enzyme. Production of AChE in a bacterial expression system was reported (Fisher *et al.*, 1993) yet the product accumulated in the cells as inclusion bodies and recovery of the nonglycosylated active enzyme was low. Animal cell lines which are capable of properly performing post-translational modifications may provide an attractive alternative for large scale production of recombinant protein possessing extended circulatory life-time (Furukawa and Kobata, 1992). We have previously reported the establishment of recombinant expression systems in which transfected human embryonal kidney (HEK) 293 cell clones produce and secrete high levels of active HuAChE (Kronman *et al.*, 1992). The recombinant enzyme is not O-glycosylated yet contains three sites for N-glycosylation, all of which were utilized (Velan *et al.*, 1993 and Section XI). Human AChE displays 90% homology to fetal bovine serum AChE (FBS-AChE) while both are equally divergent (50% homology) from human serum butyrylcholinesterase (HuS-BchE) (Gentry and Doctor, 1991). When administered to test animals, plasma-derived HuS-BChE

and FBS-AChE display clearance profiles characterized by $T_{1/2}$ values of several hours (Douchet *et al.*, 1982). However, recombinant human AChE produced in *E. coli* was rapidly cleared from the circulation (M. Fischer, personal communication). Since glycosylation plays a role in determination of circulatory life-time of proteins (reviewed by (Goochee, 1991), the accelerated elimination of the bacterial product may relate to the absence of posttranslation modification processes in bacteria . Indeed, when subjected to sialidase treatment, plasma-derived BuChE was rapidly cleared from the rat circulation. In this study, we use various engineered glycoforms of the enzyme which display an N-glycosylation pattern mimicking that of the slowly-cleared FBS-AChE, as well as dimerization-impaired AChE, to evaluate the potential contribution of N-glycan addition, oligosaccharide processing and subunit assembly to the residence of cholinesterases in the circulation.

METHODS

***Construction of Vectors for Expression of Hypo- and Hyper-Glycosylated rHuAChEs*:** Tripartite vectors expressing the human *ache* cDNA, the *cat* reporter gene and the selection marker *neo* gene were described previously (Velan *et al* .,1993). Mutagenesis was performed as describer previously (Shafferman *et al* 1992a). The hyperglycosylated D61N mutant was generated by substituting the *Apa* I -*Esp* I fragment of the human *ache* variant Ew7. The D61N mutation created a fourth N-glycosylation consensus sequence (Asn-Ala-Thr). The S541N mutant was generated by substituting the *BssH* I-*Sal* I fragment of the human *ache* cDNA. The S541N mutation also generated an additional N-glycosylation site (Asn-Ala-Thr). The HuAChE mutant D61N/S541N which contains five N-glycosylation sites was generated by replacing the *Bsu* II-*Spe* I DNA fragment of the D61N-containing construct, with that from the S541N-containing construct.

***Generation and Quantitation of Purified Cholinesterases*:** rHuAChE mutants were generated by transfecting 293 cells and establishment of stable cell clones. rHuAChE (wild-type and its glycoform-mutants) and fetal bovine serum AChE (FBS-AChE) were purified on procainamide columns (Kronman *et al.*, 1992). Human serum butyrylcholinesterase (HuS-BChE) was purified in a similar manner. rHuAChE was quantitated by three methods: a.

enzyme activity (assigning a specific activity value of 6300 U/mg protein, coupled to protein mass determination by the Lowry method (Lowry *et al* 1951), b. specific enzyme-linked immunosorbent assay (ELISA) based on polyclonal antibodies to native rHuAChE (Shafferman *et al* 1992a) and c. active-site titration with MEPQ [7-(methylethoxy-phosphonyloxy)-1-methylquinolinium iodide]

In-vivo Clearance Experiments : Following extensive dialysis against phosphate-buffered saline (PBS, pH 7.4) 20 microgram of enzyme (about 120 units of HuAChE or 6 units of HuS-BChE, 0.2 ml total volume) were injected into the tail vein of each of 3 to 6 ICR male mice (25-30 grams each). 5 microliter samples of blood were removed at various periods of time, diluted 1:20 in water and kept on ice until ChE activity was determined using acetylthiocholine (ATC) or butyrylcholinesterase (BTC) as substrate. ChE activity values in samples removed within 1 minute after injection were referred to as input activity and were used for calculation of residual activity throughout the experiment. All values were corrected for background activity determined in blood samples withdrawn 1 hour before performing the experiment. Exogenously administered cholinesterase was at least 10-fold higher than the background endogenous cholinesterase activity. Where specified, fetuin or asialofetuin (Sigma; 6 mg/mouse) were injected together with AChE. In some experiments asialofetuin was repeatedly administered at the same dosage, for a period of 8 hours at 1 hour intervals. When repeated injection coincided with blood sample collection, removal of blood preceded injection. When the experiment was completed, mice were euthanized with an overdose of anesthetics. The study was approved by the local ethical committee on animal experiments.

Analysis of Pharmacokinetic Profiles : The clearance patterns of the enzyme were biphasic and were fitted to a bi-exponential elimination pharmakokinetic model of the general form $Ct=Ae^{-k\alpha t}+Be^{-k\beta t}$, where Ct represented the concentration of enzyme in the circulation at time t and $k\alpha$ and $k\beta$ were the first-order constants of the first and second elimination phases, respectively. In all cases, the correlation coefficient was ≥ 0.997.

Desialylation of AChE and Determination of Sialic Acid : 0.5 mg of rHuAChE or FBS-AChE were incubated for 3 h at 30^0C with 0.25 units of agarose-bound neuraminidase (Sigma) in 30 mM phosphate buffer pH 6.8. Neuraminidase was removed by Eppendorf

centrifugation and enzyme was dialyzed against PBS to remove free sialic acid. Prior to administration, the dialyzed AChE was quantitated by determination of enzymatic activity.

Determination of sialic acid contents was performed on highly purified enzyme preparations. Sialic acid residues were released by incubation for 1 h at 80^0C in the presence of 0.1N H_2SO_4. Quantitation of sialic acid residues was achieved by the thiobarbituric acid method(Warren, 1959). Sialic acid extracted into cyclohexanone was quantitated at 549 nm alongside a standard curve of N-acetylneuraminic acid (Sigma) which was subjected to the same assay conditions.

Sucrose-Density Gradient Centrifugation and SDS-PAGE Electrophoresis: Analytical sucrose-density gradient centrifugation was performed on 4.5-25% sucrose gradients containing 1M NaCl/ 50 mM sodium phosphate buffer pH 8.0. Centrifugation was carried out in an SW41 Ti rotor (Beckman) for 22 h at 160,000g (36,000 rpm) at 4^0C. Fractions of 0.3 ml were collected and assayed for AChE activity. Alkaline phosphatase was used as a sedimentation marker.

Purified protein samples were denatured by boiling in the presence of 0.5% SDS/0.06% ß-mercaptoethanol.Where noted, samples were digested with 0.6 U of N-glycanase [peptide-N4-(N-acetyl-ß-glucosaminyl) asparagine amidase; Genzyme, USA] at 370C. Digestion buffer included 200 mM Na-phosphate buffer pH 8.0/0.17% SDS/ 1.25% NP-40/ 30 mM ß-mercaptoethanol. Purified enzyme was subjected to 0.1% SDS-7.5% polyacrylamide gel analysis (Laemmli, 1970) in the presence of ß-mercaptoethanol using the Phast System (Pharmacia LKB Biotechnology) with reagents and electrophoresis conditions supplied by the manufacturer. Bands were visualized by silver staining and apparent molecular weights were calculated based on a commercial mixture of polypeptide size markers (Biorad) which were run alongside.

RESULTS

Comparison of the Clearance Profiles of rHuAChE and Plasma Derived Cholinesterases: : To determine the residence of rHuAChE in the circulation, ICR mice were injected with 120 units of purified enzyme (6,300 U/mg protein). The clearance process of rHuAChE (Fig. 41) displays a pattern which fits a bi-exponential elimination pharmacokinetic

model; the initial decline is characterized by a first-order rate constant ($k\alpha$) of $9.5\times10^{-2}\times min^{-1}$ ($T_{1/2}\alpha = 7.5$ min), while the second phase decline exhibited a first-order rate constant ($k\beta$) of $9\times10^{-3}\times min^{-1}$ ($T_{1/2}\beta = 80$ min). These values were compared to clearance profiles of equivalent amounts of FBS-AChE and HuS-BChE, purified from the respective plasmas. Both of the plasma ChEs showed prolonged residence values in the circulation (FBS-AChE: $k\alpha = 1.7\times10^{-2}\times min^{-1}$, $k\beta = 7\times10^{-4}\times min^{-1}$; HuS-BChE:$k\alpha = 7\times10^{-3}\times min^{-1}$, $k\beta = 4.6\times10^{-4}\times min^{-1}$) as compared with the recombinant product (Table 25) . To determine whether the relatively rapid clearance rates of rHuAChE are due to an intrinsic instability of the product , 30 units of rHuAChE were incubated in 0.5 ml of blood samples drawn from ICR mice. After 24 h incubation at 37^{0}C no decrease in activity was detectable, suggesting that the rHuAChE is stable at these conditions and that the loss of AChE activity in the circulation is mediated by a clearance mechanism and does not reflect some instability/degradation of the recombinant product by blood factors.

Hyperglycosylated rHuAChE does not Display Extended Half-Life : Glycosylation is well known to influence residence values in many biological systems. One prominent feature in which rHuAChE differs from both FBS-AChE or HuS-BChE is the number of N-glycosylation consensus signals present on the enzyme. While FBS-AChE and HuS-BChE contain five and nine such sites respectively (Doctor and Gentry, 1991; Lockridge *et al.*, 1987) the rHuAChE sequence (Soreq *et al.*,1990) displays only three N-glycosylation sites. This difference could have been responsible for the relatively rapid clearance of rHuAChE from the circulation. Indeed,when mice were injected with a mutant rHuAChE which retains only one site for N-glycan attachment (Table 26, N350Q/N464Q) clearance was substantially enhanced in comparison to wild-type enzyme (N350Q/N464Q: $T_{1/2}\beta =$ 45min ; WT: $T_{1/2}\beta = 80$ min). In line with this observation, we generated rHuAChE molecules containing additional glycan-attachment sites to examine whether these species will be retained in the circulation for longer periods of time than the wild-type enzyme. FBS-AChE shows a high degree of homology to HuAChE and three of the five FBS-AChE glycosylation sites are identical to those found on recombinant AChE. We therefore used the FBS-AChE

Table 25: Comparison between the pharmacokinetic parameters of rHuAChE and plasma-derived cholinesterases.

ChE	No. of N-glycosyl. sites	Sialic acid /AChE [a]	A [b] (% Tot.)	kα ($x10^{-2}$ x min^{-1})	$T_{1/2}\alpha$ (min)	B (% Tot.)	kβ ($x10^{-3}$ x min^{-1})	$T_{1/2}\beta$ (min)
HuAChE	3	4	74 ± 5	9.5± 0.8	7.3 ± 0.7	25 ± 1.5	9 ± 0.4	80 ± 4
FBS-AChE	5	9	43 ± 2.2	1.7± 0.2	41 ± 5	57 ± 1.7	0.7 ± 0.05	990 ± 67
HuS-BChE	9	16	36 ± 2.2	0.7± 0.1	96 ± 13	64 ± 2.3	0.46 ± 0.02	1500 ± 73

[a] Molar ratio of sialic acid residues per cholinesterase catalytic subunit.

[b] A, B, kα and kβ are components of the bi-exponential elimination equation($Ct=Ae^{-k\alpha t}+Be^{-k\beta t}$). A and B are the amounts of enzyme at T=0 (expressed as percent of total enzyme) which are then cleared in the first and second elimination phases, respectively .

kα and kβ are the first-order constants and $T_{1/2}\alpha$ and $T_{1/2}$ß the half-life values of the first and second elimination phases, respectively.

Table 26: The pharmacokinetic parameters of rHuAChE and its various mutants.

rHuAChE	A (% Tot.) [a]	kα(x10^{-2} x min^{-1})	$T_{1/2}$ α (min)	B (% Tot.)	kβ(x10^{-3} x min^{-1})	$T_{1/2}$ β (min)
Wild-type	74 ±5	9.5±0.8	7.3 ± 0.7	25 ± 1.5	9 ± 0.4	80 ± 4
N350Q/N464Q	62 ±5	6 ± 0.6	11.0 ± 1.2	40 ± 2.2	15 ± 1	45 ± 3
S541N	68 ±8	10 ± 2	7.1 ± 1.2	32 ± 3	10 ± 0.7	71 ± 5
D61N	69 ±11	15 ± 4	4.6 ± 0.3	34 ± 4.6	17 ± 1	41 ± 3
S541N/D61N	78 ±5	18 ± 2	3.9 ± 1	34 ± 5	28 ± 6.4	25 ± 7
C580A	65 ±3	18 ± 3	3.8 ± 0.7	35 ± 2	13 ± 3	50 ± 8
asialoWT [b]	100	21 ± 1	3.3 ± 0.15	- [b]	- [b]	- [b]
WT+ASF [c]	63 ±3	1 ± 0.1	73.0 ± 8	36 ± 3	0.6 ± 0.04	1140 ± 77

[a] A, B, kα and kβ are components of the bi-exponential elimination equation($Ct=Ae^{-k\alpha t}+Be^{-k\beta t}$). A and B are the amounts of enzyme at T=0 (expressed as percent of total enzyme) which are then cleared in the first and second elimination phases, respectively. kα and kβ are the first-order constants and $T_{1/2}\alpha$ and $T_{1/2}\beta$ the half-life values of the first and second elimination phases, respectively.

[b] Wild-type rHuAChE pretreated with sialidase (see 'Methods'). This species displayed a single-phase clearance profile.

[c] Asialofetuin (ASF) was administered together with the initial bolus of wild-type (WT) rHuAChE and then reinjected at 1 hr intervals over a 8 hr period.

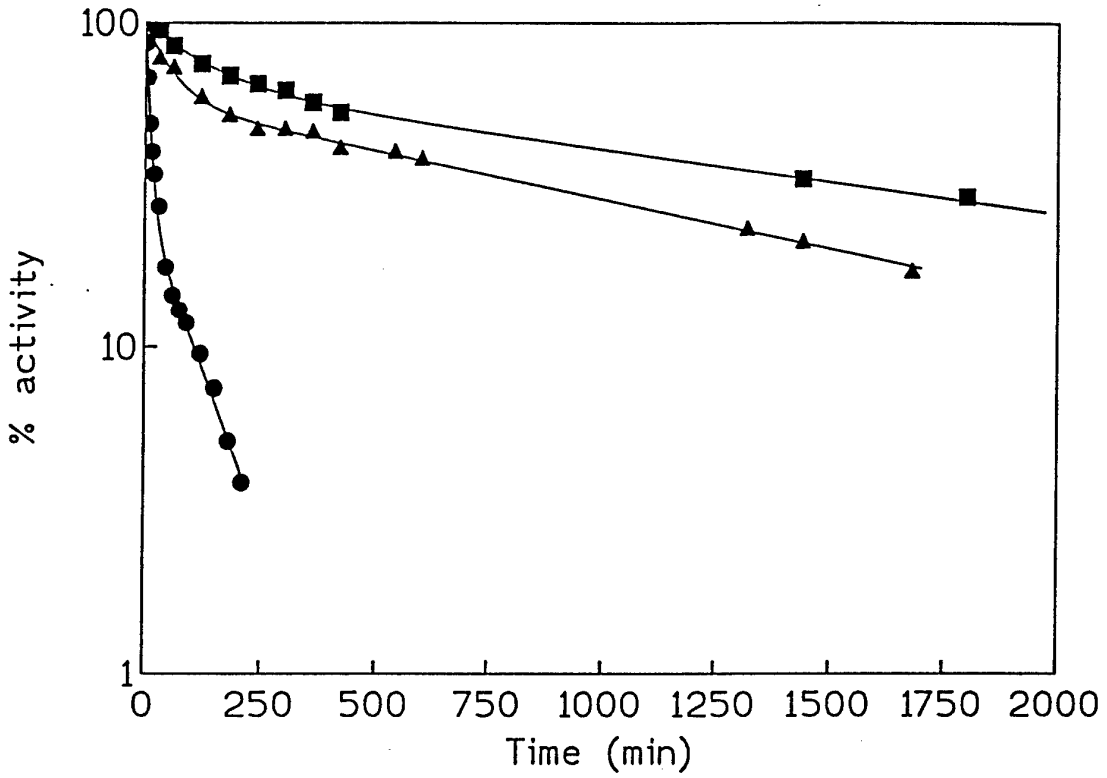

Fig. 41: Comparison of clearance rates of recombinant HuAChE and plasma-derived cholinesterases. Purified enzyme was administered to mice (20 µg/mouse in 0.2 ml). ChE activity values in samples removed immediately after injection were assigned a value of 100% and were used for calculation of residual activity. Values represent average of residual activity determined for 3-6 mice (standard deviation<10%). Circles: recombinant HuAChE; Triangles: FBS-AChE; Squares: HuS-BChE.

template as a guideline for construction of the HuAChE hyperglycosylated forms (Fig 42). Specifically, the Glu and Ser residues at positions 61 and 541 of HuAChE were substituted by aspargine to give rise to the Asn-X-Thr/Ser N-glycosylation consensus signals. These two engineered sites are analogous to two natural glycosylation sites present in the FBS-AChE. Analysis of the HuAChE hyperglycosylation mutants by SDS-PAGE (Fig. 43, inset) revealed that while the major band of the wild-type species exhibited an apparent molecular weight (MW) of 70 kDa, the HuAChE mutants D61N and S541N which contain four glycosylation sites each, had a higher apparent MW of 72 kDa. The double mutant D61N/S541N species which includes five N-glycan attachment sites, mimicking the potential N-glycosylation attachment site pattern of FBS-AChE, displayed an even higher MW of 74 kDa. Thus in all cases, the added N-glycosylation attachment sites appeared to be utilized. This conclusion is supported by the fact that both stepwise removal and addition of N-glycosylation sites gives rise to mutated enzymes whose apparent molecular weights show a linear dependence on the number of sites present on the molecule (Fig. 43). In addition, when subjected to N-glycanase digestion which catalyzes the hydrolysis of Asn-linked oligosaccharides, the wild-type and each of the mutants comigrated as a discrete band of approximately 63 kDa, proving that the differences in the MW of the various species is entirely due to differential N-glycosylation. All three hyperglycosylated species displayed catalytic values identical to those manifested by the wild-type enzyme suggesting that the number of attached N-glycosylation oligosaccharide side chains has no influence on the intrinsic biochemical traits or functional conformation of the enzyme. These results are consistent with previously published data which show that hypoglycosylated AChE retained full activity (Velan *et al.*, 1993; Mutero and Fournier, 1992). Though glycosylation has been shown to influence thermostability of proteins (Grinnel *et al.*, 1991), the engineered rHuAChE hyperglycoforms displayed very similar heat-inactivation profiles at 55^{0}C as well as comparable stabilities when incubated at 37^0 C in mouse serum.

Each of the three hyperglycosylated rHuAChE species was administered to mice and clearance profiles were determined. Unexpectedly, all of the hyperglycosylated forms displayed shorter half-lives in the circulation than the triglycosylated wild-type enzyme (Table 26). Furthermore, the two tetraglycosylated species were found to be markedly different from one another in respect to their clearance rates; while the tetraglycosylated S541N mutant exhibited a slightly

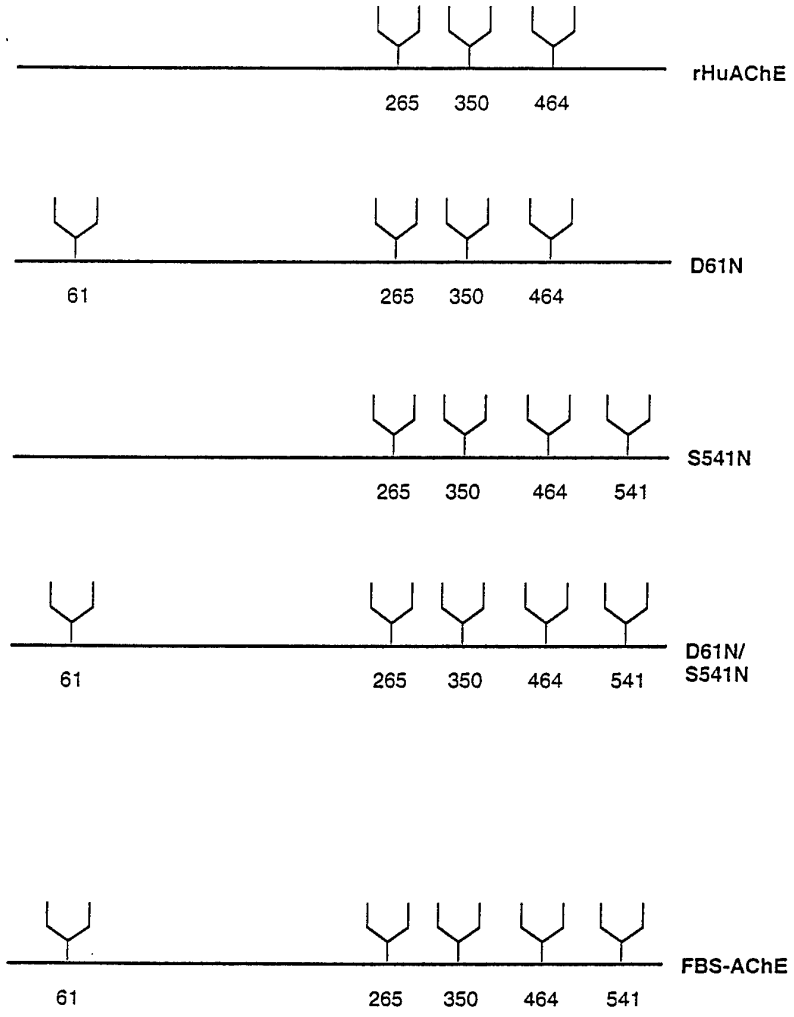

Fig. 42: Diagrammatic representation of hyperglycosylation mutant structures. The various hyperglycosylation mutants described in these studies are shown as amino-acid backbones (black line) with their corresponding N-glycans (oligosaccharide projections). Wild-type enzyme (top line) and FBS-AChE (bottom line) which served as a guideline for generation of the hyperglycosylated forms are shown as well. Numbers refer to the N-glycan attachment sites in the human enzyme amino-acid sequence (top 4 structures) or the FBS enzyme sequence (bottom structure). These are identical due to the colinearity of the two proteins

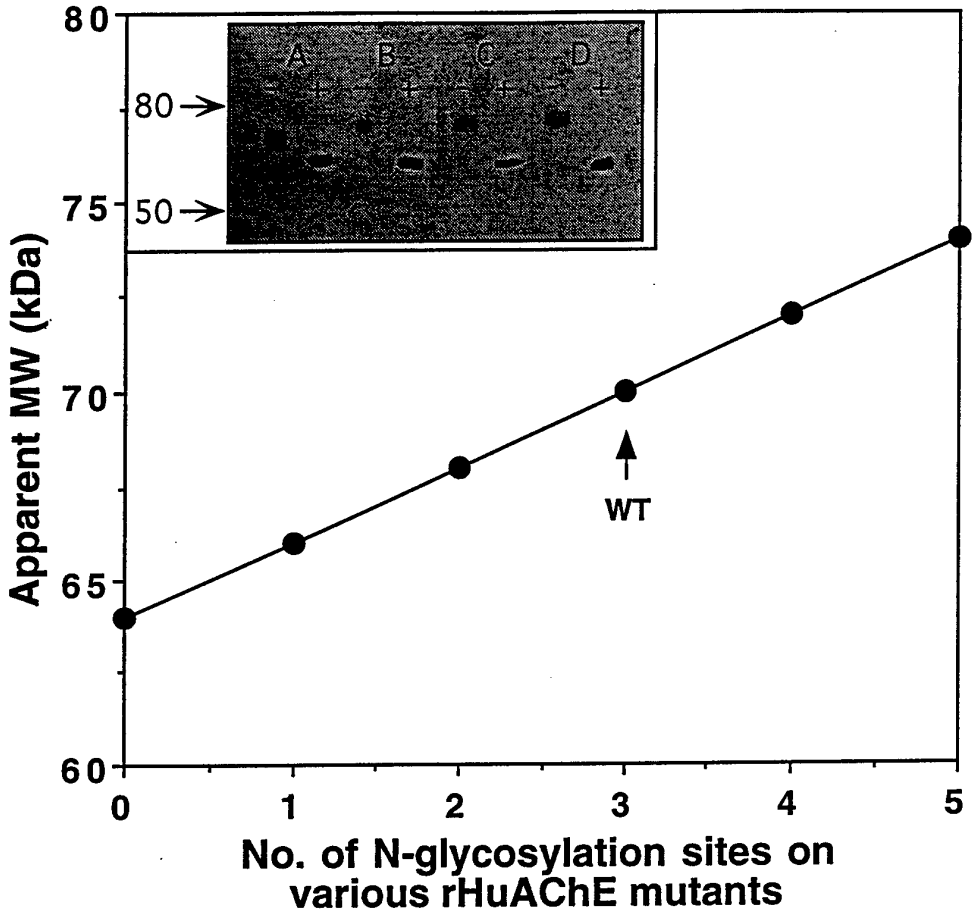

Fig 43: Correlation between apparent molecular-weights of rHuAChE derivatives and the number of N-glycosylation sites per enzyme subunit. Purified enzyme preparations (0.2 μg per lane) were subjected to 0.1% SDS-7.5% polyacrylamide gel analysis in the presence of ß-mercaptoethanol. Bands were visualized by silver staining. The apparent molecular weights of the major bands of D61N, S541N, D61N/S541N and wild-type are 72 kDa, 72 kDa, 74 kDa and 70 kDa, respectively, based on a commercial mixture of polypeptide size markers (Biorad). A curve displaying the apparent molecular-weight of the various rHuAChE glycoforms as a function of the number of N-glycosylation sites is shown. Data referring to hypoglycosylated forms of the enzyme (Section XI) were added. Inset: Silver stained SDS-polyacrylamide gel of wild type and hyperglycoforms of rHuAChE(-) and (+) denote untreated and N-glycanase treated samples, respectively. A: wild-type ; B: D61N; C: S541N; D: D61N/S541N. Arrows denote size marker molecular weights in kDa.

reduced half-life in comparison to the wild-type enzyme (S541N: $T_{1/2}\alpha$ =7.1 min, $T_{1/2}\beta$ = 70 min) the clearance rate of the D61N species was significantly faster than that of the wild-type species ($T_{1/2}\alpha$ =4.6 min, $T_{1/2}\beta$ =40 min). Moreover, the D61N/S541N pentaglycosylated species which has the highest number of N-attached oligosaccharides and mimics the N-glycosylation occupancy pattern of FBS-AChE, manifested the highest clearance rate ($T_{1/2}\alpha$ =3.9 min $T_{1/2}\beta$ = 25 min). Thus, extension of circulatory life-time was not achieved in the mutated species containing additional N-glycosylation sites, and therefore, there is no simple relationship between the number of N-glycan moieties and the circulatory residence of cholinesterases .

Clearance Rates of rHuAChE Glycoforms are Related to Sialic-Acid Contents

The fact that increased N-glycosylation had an adverse effect on circulatory life-time, raises the possibility that different rates of clearance exhibited by the various rHuAChE glycoforms may be due to differential processing and maturation of the N-glycan units on the various molecular species. N-glycan units of a given protein can have different structures and outer-chain moieties as a result of site-specific glycosylation at multiple sites.

Circulatory half-life values of glycoproteins are influenced by their sialic acid content (Ashwell and Morell, 1974). To test whether the presence of outer-chain sialic acid residues plays a determinal role in the circulatory life-time of rHuAChE, sialic acid residues were removed from the oligosaccharide chains by treatment with sialidase. Asialylated rHuAChE was administered to mice and clearance of the enzyme from the circulation was monitored. The asialo-rHuAChE indeed exhibited a rapid single- phase clearance pattern with a half-life value of 3.3± 0.15 minutes. Furthermore, when FBS-AChE which exhibits high $T_{1/2}$ values in the circulation was subjected to the same sialidase treatment, the resulting asialoFBS-AChE was cleared rapidly from the bloodstream at a rate similar to that of asialoHuAChE ($T_{1/2}$= 5.0 ± 0.4 min). These results suggest that sialylation is essential for retention of rHuAChE in the bloodstream and that the marked difference in the clearance rates of rHuAChE and FBS-AChE may relate to differences in N-glycan sialylation. To further test this possibility, we examined the ability to retain rHuAChE in the circulation in the presence of saturating amounts of asialofetuin. The latter should allow prolonged residence of undersialylated AChE in the

bloodstream (Hossner and Billiar, 1981; Clarenburg, 1983; Thomas and Zamcheck, 1983; Lefort et al, 1984) by saturating the hepatic asialoglycoprotein receptors which comprise the major system for clearance of hyposialylated glycoproteins.When mice were injected with rHuAChE or or any of its hyperglycosylated forms together with a single bolus of asialofetuin, the initial decline was markedly slower than that observed for the corresponding enzyme when administered without protein additives (Fig. 44) or together with fetuin. The accurate clearance rate was difficult to determine since the clearance process was visibly accelerated after a period of approximately two hours. Previous reports have shown that the effect of a single bolus of the asialylated protein is limited to a relatively short period of time (Vostal and McCauley, 1991) presumably due to regeneration of the asialoglycoprotein receptors. To overcome this problem AChE was administered to mice simultaneously with asialofetuin; thereafter saturating amounts of asialofetuin were injected into the tail vein at 1 hour intervals over a period of 8 hours. A dramatic increase in both clearance phases was seen in this case (Fig. 44). The calculated half-life values of both the α phase and the ß phase displayed approximately a 10-fold increase as compared to clearance rate of rHuAChE without asialofetuin (Table 26). Similar results were obtained for each of the hyperglycosylated forms of the enzyme when administered together with asialofetuin (not shown). It is worth noting that in the presence of steady-level asialofetuin, the $T_{1/2}$ values of rHuAChE clearance are similar to those displayed by the plasma-derived enzymes, FBS-AChE and HuS-BChE (Table 25). Taken together, these results indicate that the relative short half-life of rHuAChE stems from inefficient sialylation, and are in line with those reported by Douchet *et al.* (1982) which showed that sialylation plays an important role in retention of butyrylcholinesterase in the rat circulation. Most importantly, the results suggest that the primary structure of the rHuAChE can in principle allow prolonged residence of the recombinant protein within the bloodstream comparable to natural plasma cholinesterases.

To determine whether the variation in sialylation levels of the various rHuAChE mutants is related to their differential clearance rates, the average molar ratio of sialic acid per rHuAChE catalytic subunits was calculated. Sialic acid contents of the wild-type and hyperglycosylated rHuAChE species was determined. Purified enzyme was quantitated by three independent methods: 1- enzymatic activity and protein determination 2- immunoassay (quantitative ELISA) and by 3- active site titration. Results obtained by all the quantitation methods yielded similar

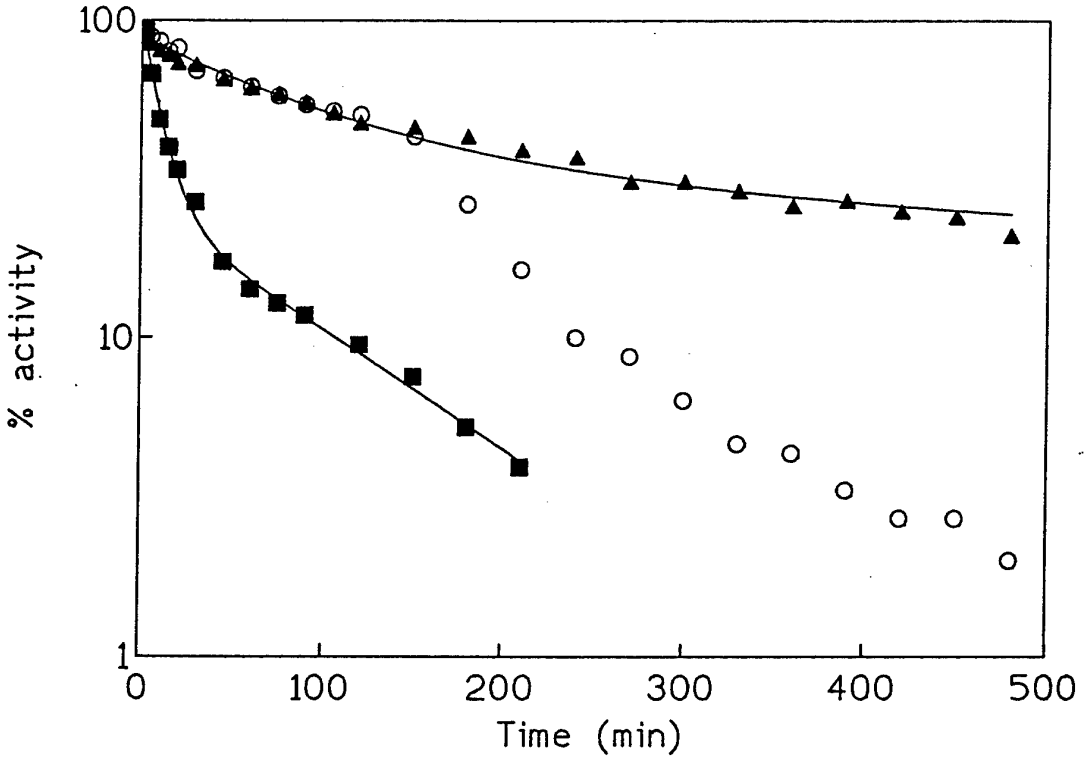

Fig 44: rHuAChE displays prolonged circulatory life-time when administered with asialofetuin. Wild-type rHuAChE was administered to mice without protein additives (squares); together with a single bolus of asialofetuin (circles); with asialofetuin and thereafter reinjection of asialofetuin at 1 hr intervals over a period of 8 hrs (triangles). The clearance profiles were determined as described above.

values for rHuAChE (±7%), indicating that the enzyme preparations were virtually free from impurities which can distort interpretation of the sialic acid quantitation.The wild-type rHuAChE species was found to contain four sialic acid residues per enzyme subunit (Table 27). This is lower than the value expected for an enzyme with three N-glycosylation sites each of which can be expected to contain a bi-antennary N-glycan unit with two sites for sialic acid attachment (see below). The two tetraglycosylated rHuAChE species were found to differ in their sialic acid contents; while the S541N species carries five sialic acid moieties per molecule, the D61N species displayed the same sialylation level as in the wild-type enzyme; namely, four sialic acid residues per molecule. Thus, the engineered N-glycan located on amino acid 61 is differently processed so that no sialic acid is terminally appended at this site. Indeed, the pentaglycosylated D61N/S541N species was found to contain only five sialic acid residues per enzyme subunit, confirming that the additional 541 but not the 61 N-glycan moiety is sialylated. The varying levels of sialylation displayed by the different rHuAChE glycoforms may possibly play a role in determining their different rates of clearance. In contrast to the various rHuAChE glycoforms which exhibit incomplete sialylation, the plasma-derived cholinesterases are efficiently sialylated. FBS-AChE and HuS-BChE which contain five and nine N-glycosylation sites respectively, exhibit a molar ratio of sialic acid to enzyme of (9±2) /1 and (16±3) /1 respectively.

Effect of rHuAChE Subunit Assembly on the Rate of Clearance :Plasma-derived cholinesterases are usually in the form of tetramers (Lockridge et al 1979; Ralston *et al.*, 1985). Wild-type rHuAChE as well as the hyperglycosylated species retain the ability to assemble into homo-oligomers consisting of dimers and tetramers, yet the relative proportions of the various assembled forms consisting the enzyme preparations may vary under different growth or storage conditions (Velan *et al* ., 1992; Lazar *et al.*, 1993). Tertiary structure as well as molecular weight have been shown to contribute to in-vivo circulatory life-time of proteins (Kanwar, 1984). To examine the possible influence of the assembled forms on clearance rates, two preparations of the wild-type enzyme with an equal ratio of sialic acid per subunit (4:1) but differing one from another in the ratio of assembled forms (as determined by sucrose gradients) were introduced into mice. Examination of enzyme removed from the bloodstream 2 hours after injection revealed that no significant alteration of subunit organization occurs in the

Table 27: Sialic acid occupancy of rHuAChE and its various mutants.

rHuAChE	No. of N-glycosylation sites	Sialic acid /AChE [a]	Calculated [b] Vacant sites/AChE
WT	3	4.2±0.3	2
asialoWT	3	< 0.1	6
C580A	3	2.1±0.2	4
D61N	4	4.1±0.1	4
S541N	4	5.4±0.3	3
D61N/S541N	5	5.3±0.2	5

[a] Molar ratio of sialic acid residues per catalytic subunit.
[b] No. of unoccupied sialic acid attachment sites per catalytic subunit was calculatedas [(number of N-glycosylation sites) x 2 - (number of sialic acid residues)].

circulation. In both cases, the time-course of enzyme elimination was found to be similar (data not shown). These findings suggest that the number of assembled subunits *per-se* does not play an important role in determining the clearance rate of the enzyme from the circulation.

To assess further the possible contribution of subunit assembly on circulatory retention, we tested the assembly-deficient mutant (C580A) described previously (Velan et al 1991b). The replacement of cysteine at position 580 by alanine, generated monomeric forms of rHuAChE that like the wild-type species, utilize all three N-glycosylation sites and are also catalytically indistinguishable from the wild-type. This monomeric variant of HuAChE was administered to mice and clearance profiles were determined. The $T_{1/2}\alpha$ and $T_{1/2}\beta$ values were 4.0± 0.7 min and 50 ±11 minutes respectively (Table 26), considerably shorter than the values exhibited by the wild-type enzyme. Incubation of the C580A HuAChE mutant in plasma at 37^{0}C for over 6 hours had no effect on its activity, demonstrating that the difference in clearance rates of the wild-type and C580A mutant can not be explained in terms of a greater lability of the monomeric form relative to wild-type. On the other hand, when subjected to sialic acid analysis, the dimerization-impaired species was found to contain only two sialic acid residues per molecule as compared to the 4:1 molar ratio found in the wild-type enzyme (Table 27). Thus, the relatively rapid clearance of the monomeric form can be explained in terms of sialic acid content. Previous studies (Kerem *et al.*, 1993; Velan *et al.*, 1994; see also Section XII) indicated that transit of monomers through the *trans* -Golgi apparatus and *trans* -Golgi network en-route to secretion is more rapid than that of the assembled wild-type AChE. This rapid transport may provide an explanation for the lower efficiency of monomer sialylation as compared to wild-type sialylation.

DISCUSSION

Comparison of the rates of clearance of rHuAChE and serum-derived cholinesterases reveals that the former is eliminated from the bloodstream faster than either FBS-AChE or HuS-BChE both of which are cleared from the circulation at comparable rates. rHuAChE is highly homologous to FBS-AChE (90% homology) while both are equally divergent from HuS-BChE (50% homology), suggesting that the relatively rapid rate of clearance of rHuAChE does

not stem from its primary sequence but rather from some post-translational process which differentiates it from the serum-derived cholinesterases. One salient feature which distinguishes rHuAChE from FBS-AChE and which may account for their differential clearance rates is their order of assembly. While FBS-AChE preparations consist entirely of tetramers, varying amounts of dimers, tetramers and monomers comprise different rHuAChE preparations. Since the filtration rate through kidney glomerular tubules is sensitive to the molecular weight of proteins allowing continuous removal of proteins with molecular weights of less than 70 kDa from the circulation (Kanwar,1984) one can speculate that subunit assembly may play a role in retention of exogenous ChEs from the circulation. Yet, the nearly identical clearance rates of rHuAChE preparations containing differently assembled forms of enzyme, contradicts the alleged importance of ChE assembly in circulatory longevity.

Comparison of the amino-acid sequences reveals that while FBS-AChE and HuS-BuChE contain five and nine sites for appendage of N-glycosylation side-chains respectively, HuAChE contains only three, all of which are utilized in established recombinant HEK 293 cell clones which efficiently produce and secrete active enzyme. N-linked side chains can control a wide variety of functions including resistance to thermal inactivation and proteolytic attack, signal transduction, receptor activation, intracellular folding and activity as well as playing a pivotal role in determining plasma clearance. Thus, it may be possible that the relatively rapid removal of rHuAChE from the circulation stems from low level of N-glycosylation. In the present study we found that an rHuAChE mutant which contains only one N-glycosylation site was indeed cleared more rapidly from the circulation of mice than the wild-type AChE expressed in the same HEK 293 cell type (Table 26) suggesting that N-glycan moieties are indeed essential for prolonged circulatory life-time of the enzyme. In accordance with these results, we examined whether the circulatory life-time of cholinesterases can be extended by increasing the number of N-glycosylation sites per enzyme. To this end, we generated a series of hyperglycosylated rHuAChE forms which contain either one or two additional sites for N-glycosylation at sites homologous to those present in FBS-AChE. This allows formation of catalytic subunits which bear the basic amino-acid backbone of human AChE yet which mimic the N-glycan occupancy pattern of the slowly-cleared fetal bovine serum AChE. Unexpectedly, all these hyperglycosylated mutants of rHuAChE were eliminated more rapidly than the wild-type enzyme even though all the additional sites are utilized, demonstrating that the circulatory life-time does not correlate exclusively to the number of N-glycosylation side-

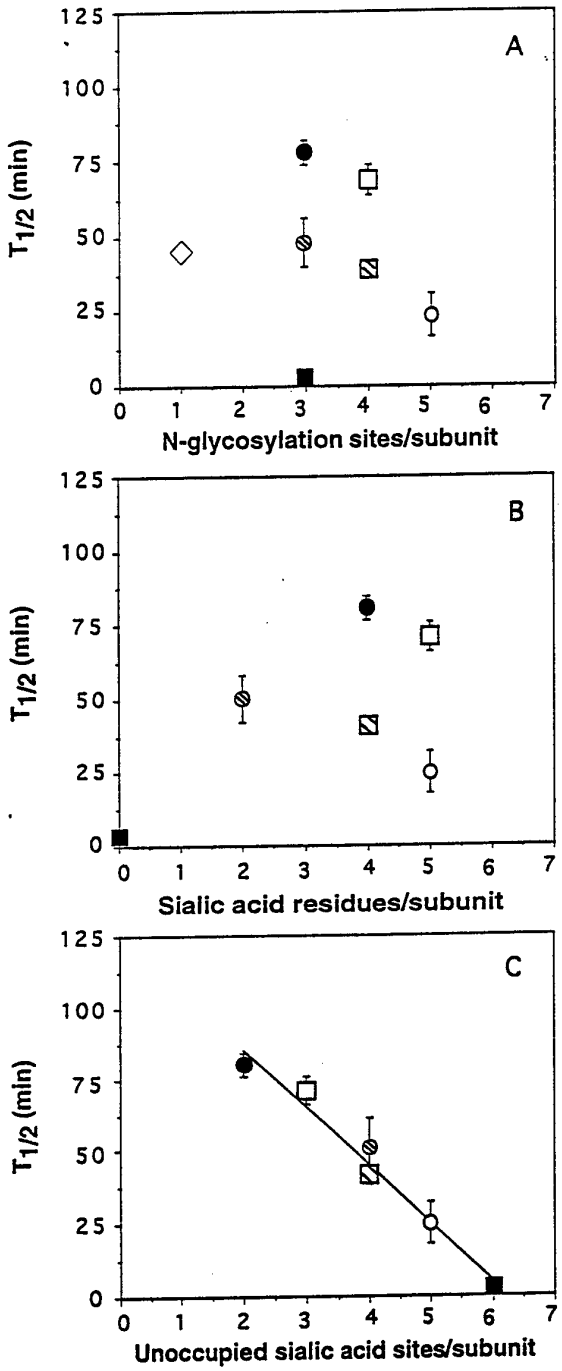

Fig 45: Dependence of clearance rates of rHuAChE and its various mutants on the number of: N-glycosylation side-chains, sialic acid residues, and unoccupied sialic acid attachment sites. The half-life values (second phase, T1/2β) of the various rHuAChEs were plotted against the number of N-glycosylation sites/subunit (A), the molar ratio of appended sialic acid residues/subunit (B) and the number of unoccupied sialic acid attachment sites/subunit (C) for each of the different rHuAChE species. The number of unoccupied sialic acid attachment sites was calculated as described in Table 27. Diamond: N350Q/N464Q monoglycosylated mutant; Filled-in circle: wild-type enzyme; Empty square: S541N tetraglycosylated mutant; Striped circle: dimerization-impaired C580A mutant; Striped square:D61N tetraglycosylated mutant; Empty circle: D61N/S541N pentaglycosylated mutant; Filled-in square: Sialidase-treated wild-type rHuAChE (asialoWT).

chains and that increasing the number of N-glycosylation side-chains in itself can not ensure sustained residence in the bloodstream but on the contrary, may have an adverse effect on enzyme residence in the bloodstream.

Enzymatically desialylated rHuAChE displayed an extremely short life-time in the circulation, suggesting an essential role for sialic acid in retention of AChE in the bloodstream. Comparison of the two tetraglycosylated species of rHuAChE (Table 26) which contain the same number of N-glycan moieties, demonstrates that the difference in rates of clearance is directly related to the sialic acid contents. Finally, when enzyme was administered together with excess asialofetuin to saturate the hepatic asialoglycoprotein clearance system, the circulatory residence of rHuAChE (Fig. 44) was dramatically increased. In this case, both the α and β elimination phases are similarly extended (approximately 10-fold increase) and exhibit $T_{1/2}$ values comparable to those of the plasma-derived FBS-AChE and HuS-BChE. Similar results were obtained for each of the hyperglycosylated forms of the enzyme when administered with asialofetuin (not shown). Extended circulatory residence was not observed when any form of the enzyme was administered together with fetuin. Taken together, these results argue against the possibility that the hyperglycosylated forms are more rapidly cleared due to the possible presence of immature high-mannose structures but rather suggest that the clearance rate of rHuAChE and its hyperglycosylated forms is determined by the sialylation efficiency of the N-glycan units. However, the sialic acid contents in itself can not provide an explanation for the residential half-life values of the various species since FBS-AChE and HuS-BChE contain significantly different amounts of sialic-acid residues per subunit, (Table 25) yet are similarly retained in the bloodstream. Moreover, the D61N tetraglycosylated species both contain the same proportion (4:1) of sialic acid residues per enzyme subunit yet display strikingly different half-life values in the circulation. Likewise, the tetraglycosylated S541N mutant and the pentaglycosylated D61N/S541N mutant both contain 5:1 sialic acid per enzyme, yet their elimination rates from the bloodstream are different and faster than that of wild-type.

The pioneering studies of Ashwell and coworkers have well established the fact that the hepatic asialoglycoprotein receptor provides a major system for the removal of undersialylated glycoproteins by binding and uptake of galactose-terminal glycoproteins (Ashwell and Harford, 1982). The latter is mediated by receptor recognition of sites on the N-linked

oligosaccharide which display non-sialylated galactose residues. In accordance with these findings our results indeed demonstrate that the decisive factor in determining the variance in clearance rates is related to the number of N-glycan termini *which are not occupied* by sialic acid residues, rather than to the absolute number of sialic acid residues present on the oligosaccharide chain. Estimation of the number of sites which are vacant of sialic acid depends upon the branching of the N-glycan unit. Experimental determination of branching by quantitation of terminal galactose residues present on desialylated enzyme is not possible due to the very large amounts of highly-purified enzyme required. Yet, we can expect rHuAChE produced in HEK 293 cells to be mostly bi-antennary since bisecting GlcNAc is detected in the sugar chains of enzymes expressed in kidney cells due to strong expression of GlcNAc transferase III (Kobata, 1992); this in turn should lead to commitment of the oligosaccharide to a processing pathway leading to a bisected bi-antennary complex-type structure (Goochee, 1992). In addition, studies with recombinant tissue factor pathway inhibitor (TFPI) have shown that in HEK 293 cells the recombinant TFPI is of the bi-antennary type, unlike that expressed in CHO cells where approximately 60 percent of the N-glycan units have tri- and tetra-antennary structures (Smith et al, 1992). Similarly, the most abundant species of oligosaccharides found on recombinant human protein C expressed in HEK 293 cells are of the biantennary type (Yan et al, 1993). Based on these facts, it is reasonable to assume that the N-glycan structures of rHuAChE expressed in HEK 293 cells contain primarily bi-antennary projections.Accordingly, we calculated the number of non-sialylated sites per enzyme subunit for each of the rHuAChE species as follows: Unoccupied sialic acid sites = the number of N-glycosylation sites times 2, minus the number of sialic acid residues (O-glycosylation of rHuAChE does not occur and therefore cannot contribute to the sialic acid content of the enzyme). When the clearance rates are plotted against the calculated unoccupied sites an inverse linear relationship is observed. Though these results are more pronounced for the β phase in which a more accurate measurement is possible (Fig 45), the general trend is clearly seen in the α phase as well (not shown). This linear correlation was retained also when the calculated number of antennary projections per glycosylation site was not precisely 2.0 but anywhere within the range of 1.5 to 2.5, suggesting that even if the rHuAChE N-oligosaccharides were to consist of equimolar amounts of bi-and triantennary moieties, the linear dependence of clearance on the number of unoccupied sialic-acid attachment sites is observed. This mode of presentation of the data provides a rationale for the unexplained

differences observed in the rates of clearance of the two tetraglycosylated species, or the rapid elimination of the pentaglycosylated form as well as the accelerated clearance of the assembly-impaired form (monomer) of the enzyme (C580A mutant). On the other hand, neither the number of N-glycosylation sites nor the number of appended sialic acid residues provided a linear dependence for the different rates of clearance observed for the various rHuAChE species. Moreover, enzyme molecules which display a higher content of sialic acid moieties concomitant with a greater number of vacant sialic acid attachment sites are removed from the circulation more rapidly than glycoforms containing less sialic acid residues but which display higher sialic acid occupancy (see Tables 26 and 27). It therefore appears that the number of unoccupied or vacant sialic acid attachment sites is the predominant factor in determining the rates of clearance, overriding the possible contribution of increased N-glycosylation or sialic acid contents to circulatory longevity. The fact that the clearance rate of monomeric AChE correlates with the sialic acid occupancy in a similar manner as that of the wild-type multimeric species and that when monomeric rHuAChE was administered together with asialofetuin , the enzyme was retained in the circulation to the same extent as the wild-type enzyme under the same conditions (not shown) supports our conclusion that oligomerization *per-se* is not an important factor in determining the circulatory half-life time.

While the linear relationship between nonoccupied sialylation sites and *in-vivo* circulatory half-life can be demonstrated for all the examined rHuAChE species in which two to six potential sites are indeed vacant, extrapolation to species with less or more vacant sites should be approached with caution. Ashwell and Morell (1974) have determined two as the minimal requirement of exposed galactose residues for clearance by the hepatocyte receptor. Thus, the linear relationship shown in the present study may probably be valid for those species which have at least two vacant sialic acid attachment sites. To our knowledge, our results are the first to show a strictly linear relationship between vacant sialic-acid attachment sites and circulatory life-time of exogenous glycoprotein and to provide the means to assess the potential contribution of varied factors such as state of assembly, number of N-oligosaccharides and sialic-acid contents to circulatory longevity, utilizing an array of engineered proteins of virtually identical primary sequences.

Fully sialylated cholinesterase species should display extended circulatory residence as suggested by the experiments in which rHuAcHE was administered together with asialofetuin.

In this case, circulatory half-lives are comparable to those of plasma cholinesterases. Glycoproteins purified from plasma in which they normally reside e.g. α_1- acid glycoprotein, human chorio-gonadotropin, carcinoembryonic antigen, rat transcortin and prothrombin (Hossner and Billiar, 1981; Clarenburg, 1983; Thomas and Zamcheck, 1983; Lafort et al, 1984) usually do not serve as ligands for the asialoglycoprotein receptor, presumably due to protective N-glycan processing. Indeed, plasma-derived FBS-AChE and HuS-BChE which exhibit extended circulatory life-times were found to be practically fully sialylated (Table 26). The undersialylation of the rHuAChE molecule may be due to some limitation of the biosynthetic pathway in HEK 293 cells. Indeed, when expressed in HEK 293 cells, recombinant human protein C contained a two-fold lower content of sialic acid than its plasma-derived counterpart (Yan *et al.*,1992) . On the other hand, undersialylation of rHuAChE in HEK 293 cells may depend on an intrinsic property of the polypeptide. Structure-related variations in processing of N-glycans of other proteins was reported previously (Yet *et al.*, 1988) as is indeed reflected by the difference in the sialic acid contents observed for the D61N and S541N tetraglycosylated mutants (Table 27).

To date, we have generated a panoply of mutagenized rHuAChE species which differ in their kinetic properties and affinity to various inhibitors. These may be usefully incorporated in a designed *in-vivo* bioscavenger of pernicious neurotoxins. The present study provides some clues regarding the design of such a bioscavenger with extended circulatory longevity.

XIV. Summary

We developed (under U.S contract DAMD17-89-C9117) efficient mammalian systems for expression of recombinant human acetylcholinesterase (rHuAChE) and methods for generation of rHuAChE mutants. These developments together with biochemical, biophysical, kinetic studies and molecular modeling of the three dimensional (3-D) structure, provide the tools for this research proposal. We proposed to elucidate the molecular basis of catalysis and inhibition events within the 'active site-gorge' and the periphery that may affect the catalytic machinery and specificity to substrates and various reversible and irreversible inhibitors including OP-agents. In addition we proposed to elucidate some of the factor(s) affecting enzyme stability in-vivo.

All the planned tasks were completed according to the SOW. The major achievements described in detail in the previous sections are highlighted below:

1. Specificity determinants of human acetylcholinesterase (HuAChE) towards ligands (substrate and some reversible and irreversible inhibitors) were identified by combination of molecular modelling and kinetic studies with enzymes mutated in active center residues Trp86, Gly121, Tyr133, Glu202, Phe295, Phe297, Tyr337, Phe338 and Glu450.

2. Replacement of Gly121 by alanine resulted in a protein devoid of any detectable catalytic activity, although its proper folding and secretion levels were not affected. The results are consistent with molecular model prediction of the role of Gly121 as a key element of the 'oxyanion hole'. Of all the substitutions tested to date (resulting in almost hundred enzyme variants) only the replacements of Gly121 and the catalytic triad (residues Ser203, His447 and Glu334) resulted in proteins without any detectable catalytic activity. We conclude that like the catalytic triad, the oxyanion hole is of paramount importance in facilitating catalysis in AChE.

3. The substitution of Trp86 by alanine and phenylalanine resulted in a 660 and 5 fold decrease, respectively, in affinity for acetylthiocholine but had no effect on affinity for the isosteric uncharged substrate (3,3 - dimethylbutyl thioacetate). The results demonstrate that

residue Trp86 is the anionic subsite which binds, through cation-π interactions, the quaternary ammonium moiety of choline. This conclusion was further supported by the <90,000 decrease in affinity of the Trp86Ala mutant towards the charged active center inhibitors edrophonium compared with only a 60 fold decrease in the case of the Trp86Phe mutant .

4. In the noncovalent complex, charged and noncharged substrates sharing a common acyl moiety (acetyl) bind to different molecular environments. The hydrophobic site for the alcoholic portion of the covalent adduct (tetrahedral intermediate) includes residues Trp86, Tyr337 and Phe338, which operate through nonpolar and/or stacking interactions, depending on the substrate. These three aromatic residues, constituting the alkoxy hydrophobic pocket have a limited effect on the affinity towards noncharged OP-agents unless the OP substituents are bulky or contain aromatic moieties.

5. Substrates containing choline but differing in the acyl moiety (acetyl, propyl, and butyryl) revealed that residues Phe295 and Phe297 determine substrate specificity of the acyl pocket for the covalent adducts (effects on k_{cat}).

6. Amino acid Phe295 also determines substrate specificity in the noncovalent enzyme substrate complex and thus, the HuAChE Phe295Ala mutant exhibits over 130 fold increase in the apparent bimolecular rate constant for butyrylthiocholine compared to wild type enzyme.

7. Residue Phe-295 is the dominant element in restricting the size of the organophosphate substituent accommodated in the acyl pocket and therefore in determining affinity toward OP-agents. The role of the second acyl pocket residue Phe-297 becomes evident with increasing size of the OP-substituents.

8. The glutamates 202 and 450 as well as Tyr133 modulate the catalytic activity of the enzyme for both charged and noncharged substrates and determine in a parallel manner the efficiency of the phosphylation process. It is suggested that these three amino acids participate in an H-bond network of HuAChE. The role of this network is to maintain the functional architecture of the active center and specifically to determine the configuration of the carboxylate of Glu202. Replacement of these residues leads to the largest reduction of the phosphorylation or phosphonylation processes.

9. The phosphorylation rates of the 15 HuAChE mutants studied with different organophosphates vary over a range of 4 orders of magnitude mainly due to changes in affinity (Kd). On the other hand the rates of the chemical transition from the noncovalent E.OP complexes of the various enzymes and organophosphates (k2), vary within a narrow range. We conclude that the differences in reactivity of HuAChE toward structurally distinct organophosphates results mainly from the spatial complementarity of the ligands with the enzyme active center during formation of the Michaelis complex.

10. Studying the kinetic behavior of three structurally distinct charged peripheral anionic site (PAS) ligands (propidium, decamethonium, BW284C51) and of two active center inhibitors (edrophonium and hexamethonium) with a large panel of mutants revealed the residues that constitute the PAS at the entrance to the active center gorge : Tyr72, Asp74, Tyr124, Glu285, Trp286 and Tyr341. Generation of different combination of multiple mutants based on these six amino acids revealed synergistic effects on interactions with PAS ligands and a functional degeneracy.

11. Fluorescence binding studies with propidium and different PAS mutants are consistent with the kinetic inhibition studies and demonstrate that the PAS is indeed the actual binding site of the peripheral charged ligands. In contrast the mutation of the active center residue Trp86 which results in several hundred fold increase in inhibition constant had no significant effect on binding affinity of propidium.

12. It is proposed that the allosteric effect in HuAChE , induced by binding of PAS ligands, involves a conformational transition between active and non-active states of the 'anionic' subsite -residue Trp86 - in the active center. In the non active state the indole side chain sterically occludes the active center, thereby lowering the enzyme affinity toward substrates and active center inhibitors.

13. A similar occlusion of the active center by residue Trp86 can be achieved through replacement of residue Tyr133 by alanine which apparently stabilizes the active confirmation of Trp86. In the Y133A HuAChE the allosteric effect, due to propidium binding, is abolished since the initial conformation of Trp86 is already extended. Removal of both Trp86 and Tyr133 restores access of ligands to the active center.

14. To determine the possible role of charge in catalysis or in physicochemical stability a series of 20 single or multiple site mutants were generated, where surface negative charged amino acids were replaced by neutral residues,. Up to seven negative surface charges were replaced on a single enzyme molecule with no significant effect on either apparent bimolecular rate constant or rate of catalysis (kcat). We concluded that surface electrostatic properties of AChE do not contribute to the catalytic rate or to binding constants of charged active center ligands.

15. The hypothesis of the "back door" for product clearance was tested using mutants of key residue along the putative back door channel. Turn over rates of all mutants tested, and in particular the one that should presumably seal the channel were similar to those of the wild type enzyme. We conclude that the proposed "back door" route for product clearance is of no functional relevance to catalytic activity.

16. Enzymes yielding OP-conjugates which are resistant to aging were engineered. The Glu202Gln, Glu450Ala and Tyr133Phe HuAChE's were completely resistant (days) to aging of their diisopropyl phosphoryl derivatives while the rates of aging for the pinacolyl methylphosphonyl derivative were 150-30 fold slower than in the wild type enzyme. More significantly the Phe338Ala mutant also demonstrated resistance to aging (150 fold reduction in rate of aging of its soman adducts relative to wild type enzyme with a half life time of approximately 30 hours) and yet this enzyme derivative was still as potent as wild type enzyme in scavenging the OP-agent. Thus residue F338 is a clear candidate for manipulation in the future HuAChE template-based bioscavenger.

17. To date we determined the catalytic properties of over 80 mutants and accordingly the functional assignment of various residues on HuAChE was proposed. A summary of these findings is compiled in Appendix A .

18. Large scale preparation of recombinant HuAChE was performed utilizing the microcarrier technology. Over 1000 milligrams of enzyme was prepared for x-ray crystallography pharmacological and kinetic studies. Material was supplied to various labs around the world mainly for structure function studies.

19. The role of N-glycosylation in the function of HuAChE was examined by site directed mutagenesis (Asn to Gln substitution) of the three potential N glycosylation sites Asn265, Asn350 and Asn464. In transiently or stably transfected embryonal human 293 kidney cells all three AChE N-glycosylation signals are utilized, yet not all the secreted molecules are fully glycosylated. Glycosylation at all sites is important for effective biosynthesis and secretion. Extracellular AChE levels decreases with a decrease in availability of wild type N-glycosylation signals.

20. Some N-glycosylation mutants display impaired stability as reflected by increased susceptibility to heat inactivation. Substitution of Asn464 has the most pronounced effect on thermostability.

21. Abrogation of N-glycosylation had no detectable effect on the enzymatic activity of HuAChE. In most mutants, inhibition profiles with edrophonium and with bisquaternary-ammonium ligands were identical to those of wild-type enzyme, the Asn350 mutants exhibit, nevertheless, a slight decrease in their affinity towards these ligands. Elimination of oligosaccharide side-chains had no detectable effect on the surface related 'peripheral-site' functions.

22. Newly formed AChE molecules can be folded into an active subunit through either a glycosylation independent or a glycosylation dependent mechanism, the latter being much more efficient than the former. Once folded monomers have been formed, they can accumulate in the ER at practically unlimited quantities. Non-folded molecules on the other hand are prone to rapid degradation.

23. Folding of AChE monomers is not coupled to subunit dimerization. Assembly is not a prerequisite for exit from the ER, yet there appears to be a mechanism which selects for preferential exit of dimerized forms. The native C-terminal tetrapeptide CSDL of HuAChE provides a dimerization signal but does not serve as a variant of the KDEL retention signal.

24. Subunit oligomerization does not play a significant role in determining clearance rate of recombinant HuAChE from blood stream of mice.

25. Oligosaccharide side chains contribute to the residence of HuAChE in the circulation. The asialoglycoprotein receptor plays a major role in the clearance of rHuAChE through the non sialylated glycans on the enzyme molecules.

26. HuAChE molecules with increased number of N-glycosylation site were generated to mimic the configuration of plasma fetal bovine AChE. We found that the potential contribution of increased number of N-glycosylation moieties to the circulatory longevity of rHuAChE is negated by a concomitant reduction in sialylation efficiency.

27. A linear relationship between non-occupied sialylation sites and in-vivo circulatory life time was demonstrated. These results suggests that engineering of improved sialylation efficiency should allow production of recombinant HuAChE with increased serum residence.

REFERENCES

Alber, T., Dao-pin, S., Nye, J.A., Muchmore, D.C., Matthews, B.W. (1987). Temperature-sensitive mutations of bacteriophage T4 lysozyme occur at sites of low mobility and low solvent accessibility in the folded protein. Biochemistry **26**:3754-3758.

Aldrich W.N., and Reiner E. (1972). Enzyme Inhibitors as Substrates, Elsevier, Amsterdam.

Allison, S.A., Bocquet, R.J. And McCammon, J.A. (1988). Simulation of diffusion-controlled reaction between superoxide and superoxide dismutase. II. Detailed methods. Biopolymers **27**:251-269.

Amitai, R., Bar-Nun, S., Haimovitch, J., Rabinovitch, E. and Shachar, I. (1991). Post translational regulation of IgM expression in B lymphocytes. Selective nonlysosomal degradation of assembled secretory IgM is temperature-dependent and occurs prior to the trans-Golgi. J. Biol. Chem. **266**:12568-12573.

Andersen, R.A., Aaraas, I., Gaare, G. and Fonnum, F. (1977). Inhibition of acetylcholinesterase from different species by organophosphorus compounds, carbamates and methylsulphonylfluoride. Gen. Pharamcol. **8**:331-334.

Andersson, M., Ostman, A., Wesrtermark, B., and Heldin, C.H. (1994). Characterization of the retention motif in the C-terminal part of the long splice form of the platelet-derived growth factor A-chain. J. Biol. Chem. **269**:926-930.

Andres, D.A., Rhodes, J.D., Meisel, R.L., and Dixon, J.E. (1991). Characterization of the C-terminus sequence responsible for protein retention in the endoplasmic reticulum. J. Biol. Chem. **266**:14277-14282.

Arber, S., Kraus, K.H. and Caroni, P. (1992). S-Cyclophilin is retained intracellularly via a unique COOH-terminal sequence and colocalizes with the calcium storage protein calreticulin. J. Cell. Biol. **116**:113-125.

Ashani, Y., Shapira, S., Levy, D., Wolfe, A.D., Doctor, B.P., and Raveh, L. (1991). Butyrylcholinesterase and acetylcholinesterase prophylaxis against soman poisoning in mice. Biochem. Pharmacol. **41**:37-41.

Ashwell, G., and Harford, J. (1982). Carbohydrate-specific receptors. Ann. Rev. Biochem. **51**:531-554.

Ashwell, G., and Morell, A.G. (1974). The role of surface carbohydrates in the hepatic recognition and transport of circulating glycoproteins. Adv. Enzymol. Relat. Areas Mol. Biol. **41**:99-128.

Augustinsson, K.-B. and Nahmansohn, D. (1949). Distinction between acetylcholine-esterase and other choline ester-splitting enzymes. Science **110**:98-99.

Axelsen, P.H., Harel, M., Silman, I., and Sussman, J.L. (1994). Structure and dynamics of the active site gorge of acetylcholinesterase : synergistic use of molecular dynamics simulations and x-ray crystallography. Prot. Sci. **3**:188-197.

Bajorath, J., Kitson, D.H., Kraut, J., and Hagler, A.T. (1991). Electron redistribution on binding of a substrate to an enzyme: folate and dihydrofolate reductase. Proteins **11**:1-12.

Barak, D., Ariel, N., Velan, B.,and Shafferman, A. (1992). Molecular models for human AChE and its phosphonylation products. In: *Multidisciplinary Approaches to Cholinesterase Functions*. (Shafferman A. and Velan B. Eds.),pp. 195-199, Plenum Pub. Co., New York .

Barak, D., Kronman, C., Ordentlich, A., Ariel, N., Bromberg, A., Marcus, D., Lazar, A., Velan, B., and Shafferman, A. (1994). Acetylcholinesterase peripheral anionic site degeneracy conferred by amino acid arrays sharing a common core. J. Biol. Chem. **264**:6296-6301.

Barnett, P. and Rosenberry, T.L. (1977). Catalysis by acetylcholinesterase. J. Biol. Chem. **252**:7200-7206.

Bazelyansky, M., Robey, E. and Kirsch,T. (1986). Fractional diffusion - limited component of reactions catalyzed by acetylcholinesterase. Biochemistry **25**:125-130.

Benschop, H.P. and De Jong, L.P.A. (1988). Nerve agent stereoisomers: analysis, isolation and toxicology. Acc. Chem. Res. **21**:368-374.

Benschop, H.P. and Keijer, J.H. (1966). On the mechanism of ageing of phosphonylated cholinesterases. Biochim. Biophys. Acta. **128**:586-588.

Benschop, H.P., Konings, C.A.G., Van Genderen, J. and De Jong, L.P.A. (1984). Isolation, anticholinesterase properties, and acute toxicity in mice of the four stereoisomers of the nerve agent soman. Toxicol. Appl. Pharmacol. **72**: 61-74.

Berman, H. A., Becktel, W., and Taylor, P. (1981). Spectroscopic studies on acetylcholinesterase : influence of peripheral-site occupation on active-center conformation Biochemistry **20**:4803-4810.

Berman H.A. and Decker M.M. (1986). Kinetic equilibrium and spectroscopic studies on dealkylation (aging) of alkylorganophosphonyl acetylcholinesterase. J.Biol.Chem. **261**:10646-10652.

Berman, H.A. and Decker, M.M. (1989). Chiral nature of covalent methylphosphonyl conjugates of acetylcholinesterase J.Biol.Chem. **264**:3951-3956.

Berman, H. A., Decker, M. M., Nowak, M.W., Leonard, K.J., McCauley, M., Baker, W.M., and Taylor, P. (1987). Site selectivity of fluorescent bisquaternay phenanthridinium ligands for acetylcholinestrase. Mol. Pharmacol. **31**: 610-616.

Berman, A.H., and Leonard, K. (1990). Ligand exclusion in acetylcholinesterase. Biochemistry **29**:10640-10649.

Berman H.A., and Leonard K. (1992). Interaction of tetrahydroaminocridine with acetylcholinestrease and butyrlcholinesterase.Mol. Pharmacol. **41**:412-418.

Berman, H.A. and Nowak, M.W. (1992). Influence of ionic composition of the medium on acetylcholinesterase conformation. In: *Multidisciplinary Approaches to Cholinesterase Functions*. (Shafferman A. and Velan B. Eds.), pp. 149-156, Plenum Pub. Co., New York.

Björkstén, J., Soares, C,M., Nilsson, O., and Tapia, O. (1994) . On the stability and plastic properties of the interior L3 loop in R.capsulatus porin. a molecular dynamics study.Protein Eng. **7**: 487-493.

Blacklow, S., Raines, R., Lim, W., Zamore, P., and Knowles, J. (1988). Triosphosphate Isomerase catalysis is diffusion controlled. Biochemistry **27**:1158-1167.

Bon, S., Meflah, K., Musset, F., Grassi, J. and Massoulie, J. (1987). An immunoglobulin M monoclonal antibody, recognizing a subset of acetylcholinesterase molecules from electric organs of *Electrophorus* and *Torpedo*, belongs to the HNK-1 anti-carbohydrate family. J. Neurochem. **49**:1720-1731.

Bone, R. and Agard, D.A. (1991). Mutational remodeling of enzyme specificity. Methods Enzymol. **202**:643-671.

Bonifacino, J.S., Cosson, P., and Klausner, R.D. (1990). Colocalized transmembrane determinants for ER degradation and subunit assembly explain the intracellular fate of TCR chains. Cell **63**:503-513.

Bourne, N. and Williams, A. (1984). Evidence for a single transition state in the transfer of the phosphonyl group ($-PO_3^{-2}$) to nitrogen nucleophile from Pyridino-N-phosphonates. J. Am. Chem. Soc. **106**:7591-7596.

Brockman, S.K., Usiak, M.F., and Younkin, S.G. (1986). Assembly of monomeric acetylcholinesterase into tetrameric and assymetric forms. J. Biol. Chem. **261**:1201-1207.

Broomfield, C.A., Maxwell, D.M., Solana, R.P., Castro, C.A., Finger, A.V. and Lenz, D.E. (1991). Protection by butyrylcholinesterase against organophosphorus poisoning in nonhuman primates. J. Pharmacol. Exp. Ther. **259**:633-638.

Burley, S.K. and Petsko, G.A. (1988). Weekly polar interactions in proteins. Advances in Protein Chemistry **39:**125-189.

Brünger, A.T., and Krukowski, A. (1990) . Slow cooling protocols for crystallographic refinement simulated annealing. Acta Crys. **A46:** 585-593.

Calef, D.F., and Deutch, J.M. (1983). Diffusion controlled reactions. Ann. Rev. Phys. Chem. **34**:493-524.

Cascio, C., Comite, C., Ghiara, M., Lanza, G., and Ponchione, A. (1988). Use of serum cholinesterases in severe organophosphorous poisoning. our experience. Minerva Anastesiol. **54**:337-338.

Cerutti, M., Fournier, D., Chaabihi, H, Fedon, Y. and Devauchelle, G. (1991). Expression of acetylcholinesterase gene from drosophila melanogaster by using baculovirus vectors. In: *Cholinesterases Structure, Function, Mechanism, Genetics and Cell Biology* (Massoulie, J., Bacou, F., Barnard, E.A., Chatonnet, A., Doctor, B.P. and Quinn, D.M. Eds.) pp.110, American Chemical Society, Washington D.C.

Changeux, J.P. (1966). Responses of acetylcholinesterase from torpedo marmorata to salts and curarizing drugs. Mol.Pharmacol. **2**:369-392.

Chatel, J.M., Grassi, J., Frobert, Y., Massoulie, J., and Vallette, F.M. (1993). Existence of an inactive pool of acetylcholinesterase in chicken brain. Proc.Natl. Acad. Sci. USA **90**:2476-2480.

Chatonnet, A., and Lockridge, O. (1989). Comparison of butyrylcholinesterase and acetylcholinesterase. Biochem. J. **260**:625-634.

Chen,H., Chan, W.Y., Chen, C.L., Mansfield, C.B., and Chou, J.Y. (1993). The carboxyl-terminal domain of the human pregnancy specific glycoprotein specifies intracellular retention and stability. J. Biol. Chem. **268**:22066-22075.

Clarenburg, R. (1983). Asialoglycoprotein receptor is involved in clearing intact glycoproteins from rat blood. Amer. J. Physiol. **244**:G247-G253.

Cohen, S.G., Chishti, S.B., Elkind, J.L., Reese, H. and Cohen, J.B. (1985). Effects of charge, volume, and surface on binding of inhibitor and substrate moieties to acetylcholinesterase. J. Med. Chem. **28:**1309-1313.

Cohen, S.G., Elkind, J.L., Chisti, S.B., Giner, J.L-P., Reese, H., and Cohen, J.B. (1984). Effects of volume and surface property in hydrolysis by Acetylcholinesterase. The trimethyl site. J. Med. Chem. **27**:1643-1647.

Conners, R.W., Sweet, R.W., Noveral, J.P., Pfarr, D.S., Trill, J.L., Shebuski, R.J., Berkowitz, B.A., Williams, D., Franklin, S. and Reff, M.E. (1988). DHFR coamplification of t-PA in DHFR bovine endothelial cells: In vitro characterization of the purified serine protease. DNA **7**:651-661.

Coyle, J.T., Price, D.L. and DeLong, M.R. (1983). Alzheimer's disease: A disorder of cortical cholinergic innervation, Science **219**:1184-1190.

Cygler, M., Schrag, J. D., Sussman, J. L., Harel, M., Silman, I., Gentry, M. K., and Doctor, B. P. (1993). Relationship between sequence conservation and three-dimensional structure in a large family of esterases, lipases, and related proteins. Prot. Sci. **2**: 366-382.

Davis, M.E., Madura, J.D., Sines, J., Luty, B.A., Allison, S.A. And McCammon, J.A. (1991). Diffusion controlled enzymatic reactions. Meth. Enzymol. **202**:473-497.

Dean, N., and Pelham, R.B. (1990). Recycling of proteins from the golgi compartment to the ER in the yeast. J. Cell. Biol. **111**:369-377.

De la Escalera, S.,Backamp, E,O.,Moya, F., Piovant, M, and Jimenez, F.(1990). Characterization and gene cloning of neurotactin a Drosophila transmembrane protein related to cholinesterase.EMBO J. **9**:3593-33601.

De Jong, L.P.A. and Kossen, S.P. (1985). Stereospecific reactivation of human brain and erythrocyte acetylcholinesterase inhibited by 1,2,2-trimethylpropyl methylphosphonofluoridate (soman). Biochim. Biophys. Acta. **830**:345-348.

Doctor, B.P., Chapman, T.C., Christner, C.E., Deal, C.C., De La Hoz, M.K., Gentry, R.K., Orget, R.A., Rush, R.S., Smyth, K.K. and Wolfe, A.D. (1990). Complete amino acid sequence of fetal bovine serum acetylcholinesterase and its comparison in various regions with other cholinesterases. FEBS Let. **266**:123-127.

Doctor B.P., Blick, D.W., Gentry, M.K., Maxwell, D.M., Miller, S.A., Murphy, M.R. and Wolfe, A.D. (1992). Acetylcholinesterase: a pretreatment drug for organophosphate poisoning. In: *Multidiciplinary Approaches to Cholinesterase Functions.* (Shafferman A. and Velan B. Eds.),pp. 277-286, Plenum Pub. Co., New York .

Dorner, A.J., Bole, D.G., and Kaufman, R.J. (1987). The relationship of N-linked glycosylation and heavy chain-binding protein association with the secretion of glycoproteins. J. Cell Biol. **105**:2665-2674.

Douchet, J.C., Masson, P., and Morelis, P. (1982). Elimination de la cholinesterase humaine purifee injectee an rat. Trav. Sci. **3**:342-347.

Dougherty, D.A. and Stauffer, D.A. (1990). Acetylcholine binding by a synthetic receptor: Implication for biological recognition. Science **250**:1558-1560.

Dreyfus, P.A., Seidman, S., Pincon-Raymond, M., Murawsky, M., Rieger, F., Schejter, E., Zakut, H., and Soreq, H. (1989) Tissue - specific processing and polarized compartmentalization of nascent cholinesterase in microinjected Xenopus oocytes. Molec. Cell. Neurobiol. **9**:323-341.

Dube, S., Fisher, J.W. and Powell, J.S. (1988). Glycosylation at specific sites of erythropoietin is essential for biosynthesis, secretion, and biological function. J. Biol. Chem. **263**:17516-17521.

Duran, R., Cervenansky, C., Dajas, F., & Tipton, K.F. (1994). Fasciculin inhibition of acetylcholinesterase is prevented by chemical modification of the enzyme at the peripheral site. Biochim. Biophys. Acta **1201**: 381-388.

Duval, N., Krejci, E., Grassi, J., Coussen, F., Massoulie, J., and Bon, S. (1992). Molecular architecture of acetylcholinesterase collagen-tailed forns, construction of a glycolipid-tailed tetramer. EMBO J. **11**:3255-3261.

Duval, N., Massoulie, J., and Bon, S.(1992) H and T subunits of acetylcholinesterase from Torpedo, expressed in COS cells, generate all types of globular forms. J. Cell Biol. **118**:641-653.

Edwards, J.A. and Brimijoin, S. (1983). Thermal inactivation of the molecular forms of acetylcholinesterase and butyrylcholinesterase. Biochim. Biophys. Acta. **742:**509-516.

Ellman, G.L., Courtney, K.D., Andres, V. and Featherstone, R.M. (1961). A new and rapid colorimetric determination of acetylcholinesterase activity: Biochem. Pharmacol. **7**:88-95.

Fambrough, D. M., Engel, A. G., and Rosenberry, T. L. (1982). Acetylcholinesterase of human erythrocytes and neuromuscular junctions: Homologies revealed by monoclonal antibodies. Proc. Natl. Acad. Sci. U.S.A. **79**: 1078-1083.

Fay, P.J., Haidrais, P.J. and Huggins, C.F. (1993). Role of the COOH terminal acidic region of A1 subunit retention in human factor VIIIa. J. Biol. Chem. **266**:8957-8962.

Fersht, A. (1985). *Enzyme Structure and Mechanism.*. 2nd Ed. Freeman, San Francisco, CA.

Filbin, M.T. and Tennekoon, G.I. (1990). High level expression of myelin protein Po in Chinese hamster ovary cells. J. Neurochem. **55**:500-505.

Fisher, M., Ittah, A., Liefer, I., and Gorecki, M. (1993). Expression and recognition of biologically active human acetylcholinesterase from E. coli. Molec. Cell. Neurobiol. **13**:25-38.

Fliegel, L., Newton, E., Burns, K., and Michalak, K. (1990). Molecular cloning of cDNA encoding a 55 kDA multifunctional thyroid hormone binding protein of skeletal muscle sarcoplasmic reticulum. J. Biol. Chem. **265**:15496-15502.

Forsberg, A., and Puu, G. (1984). Kinetics for the inhibition of acetylcholinesterase from the electric eel by some organophosphates and carbamates. Eur. J. Biochem. **140**: 153-156.

Fournier, D., Bride, J.-M., Hoffman, F. and Karch, F. (1992). Acetylcholinesterase: two types of modifications confer resistance to insecticide. J. Biol. Chem. **267**:12470-14274.

Fournier, D., Mutero, A., Pralavorio, M. and Bride, J.-M. (1993). Drosophila acetylcholinesterase: Mechanisms of resistance to organophosphates Chem.-Biol. Interactions **87**: 233-238.

Fra, M.A., Fagioli, C., Finazzi, R., Sitia, R., and Alberini, C.M. (1993). Quality control of ER synthesized proteins: an exposed thiol group as a three-way switch mediating assembly, retention and degradation. EMBO J. **12**:4755-4761.

Fraenkel, Y., Navon, G., Aronheim, A. and Gershoni, J. M. (1990) . Direct measurement of agonist binding to genetically engineered peptides of the acetylcholine receptor by selective T1 NMR relaxation. Biochemistry **29**: 2617-2622.

Friboulet, A., Rieger, F., Gougou, D., Amitai, G., and Taylor, P. (1990). Interaction of an organophosphate with a peripheral site on acetylcholinesterase. Biochemistry **29**: 914-920.

Friedman, J.S., Cofer, C.L., Anderson, C.L., Kushner, J.A., Gray, P.P., Chapman, G.E., Stuart, M.C., Lazarus, L., Shine J. and Kushner, P.J., (1989). High expression in mammalian cells without amplification. Bio/Technology, 7:359-362.

Froede, H.C. and Wilson, I.B. (1971). Acetylcholinesterase. In "*The Enzymes*" (Boyer P.D. Ed.), Academic Press New-York 5, pp. 87-114.

Furukawa, K., and Kobata, A. (1992). Protein glycosylation. Curr. Opin. Biotechnol. **3**:554-559.

Galzi, J-L., Bertrand, D., Devillers-Thery, A., Revah, F., Bertrand, S. and Changeux, J-P. (1991). Functional significance of aromatic amino acids from three peptide loops of the a7 neuronal nicotinic receptor site investigated by site-directed mutagenesis. FEBS Lett. **392:** 198-202.

Gao, J., Chou, L. W. and Auerbach, A. (1993). The nature of cation-π binding: Interactions between tetramethylammonium ion and benzene in aqueous solution. Biophys. J. **65**: 43-47.

Garel, L., Lozach, B., Dutasta, J.-P. and Collet, A. (1993). Remarkable effect of receptor size in the binding of acetylcholine and related ammonium ions to water soluble cryptophanes. J. Am. Chem. Soc. **115**: 11652-11653.

Gentry, M.K. and Doctor, B.P. (1991). Alignment of amino acid sequences of acetylcholinesterase and butyrylcholinesterases. In: *Cholinesterases: Structure, Function, Mechanism, Genetics, and Cell Biology*. (Massoulie, J., Bacou, F., Barnard, E.A. Doctor, B.P. and Quinn, D.M., Eds.), pp. 394-398. Am. Chem. Soc., Washington.

Gerstein, M., Lesk, M.L., and Chothia, C. (1994). Structural mechanisms for domain movements in proteins. Biochemistry **33**: 6739-6749.

Gething, M.J., and Sambrook, J. (1992). Protein folding in the cell. Nature **355**:33-45.

Giacobini, E., Becker, R., McIlhany, M. and Kumar, V. (1988) in: *Current Research in Alzheimer Therapy*. (Giacobini E., and Becker R., Eds) pp 113-122, Taylor & Francis, New York.

Gibney, G., Camp, S., Dionne, M., MacPhee-Quigley, K. and Taylor, P. (1990). Mutagenesis of essential functional residues in acetylcholinesterase. Proc. Natl. Acad. Sci. USA. **87**:7546-7550.

Gibson, R., Schlesinger, S. and Kornfeld (1979). The nonglycosylated glycoprotein of vesicular stomatitis virus is temperature-sensitive and undergoes intracellular aggregation at elevated temperatures. J. Biol. Chem. **254**:3600-3607.

Gilson, M.K., Straatsma, T.P., McCammon, J.A., Rippoll, D.R., Faerman, C.H., Axelsen, P.H.. Silman, I. And Sussman, J.L. (1994). Open "back door" in molecular dynamics simulations of acetylcholinesterase. Science **263**:1276-1278.

Glickman, A.H., Wing, K.D. and Casida, J.E. (1984). Profenofos insecticide bioactivation in relation to antidote action and the stereospecificity of acetylcholinesterase inhibition, reactivation and aging. Toxicol. Appl. Pharmacol. **73**:16-22.

Gnatt, A., Lowenstein, Y., Yaron, A., Schwarz, M. and Soreq, H. (1994) . Site directed mutagenesis of active-site residues reveals plasticity of human butyryochoinesterase in substrates and inhibitors interactions. J. Neurochem. **62**:749-755.

Goochee, C.F. (1992). Bioprocess factors affecting glycoprotein oligosaccharide structure. Develop. Biol. Stand. **76**:95-104.

Goochee, C.F., Gramer, M.J., Anderson, D.C., Bahr, J.B. and Rasmussen, J.R. (1991). The oligosaccharides of glycoproteins: bioprocess factors affecting oligosaccharide structure and their effect on glycoprotein properties. Bio/Technology **8**:1347-1355.

Gorman, C.M., Moffat, L.E. and Howard, B.H. (1982). Recombinant genomes which express chloramphenicol acetyltransferase in mammalian cells. Mol. Cell. Biol. **2**:1044-1051.

Goto, M., Akai, K., Murakami, A., Hashimoto, C., Tsuda, E., Ueda, M., Kawanishi, G., Takahashi, N., Ishomoto, A., Chiba, H. and Sasaki, R. (1988). Production of recombinant human erythropoietin in mammalian cells: Host-cell dependency of the biological activity of the cloned glycoprotein. Bio/Technology. **6**:67-71.

Gray, A.P. (1984). Design and structure-activity relationships of antidotes to organophosphorus anticholinesterase agents. Drug Metabolism Rev. **15**:557-589.

Gray, P.J., and Dawson, R.M. (1987). Kinetic constants for the inhibition of the eel and rabbit brain acetylcholinesterase by some organophosphates and carbamates of military significance. Toxicol. Appl. Pharmacol. **91**: 140-144.

Gray, P.J., and Duggleby, R.G. (1989). Analysis of kinetic data for irreversible enzyme inhibition. Biochem. J. **257**: 419-424.

Greenfield, S.A. (1984). AchE may have a novel function in the brain. TINS **7**::364-368.

Greenfield, S.A. (1992). AchE as a modulatory neuro-protein and its influence on motor control. In: *Multidisciplinary Approaches to Cholinesterase Functions*. (Shafferman A. and Velan B. Eds.),pp. 233-242, Plenum Pub. Co., New York .

Grinel, B.W., Walls, J.D., and Gerlitz, B. (1991). Glycosylation of human protein C affects its secretion, processing, functional activities and activation by thrombin. J. Biol. Chem. **226**:9778-9785.

Grunwald, J., Segal, Y., Shirin, E., Waysbrot, D., Steinberg, N., Silman, I. and Ashani, Y. (1989). Aged and non-aged pyrenebutyl-containing organophosphoryl conjugates of chymotrypsin. Biochem. Pharmacol. **38**:3157-3168.

Haas, R., Adams, E.W., Rosenberry, M.A., and Rosenberry, T.L. (1992) . Substrate-selective inhibition and peripheral site labeling of acetylcholinesterase by platinum(terpyridine)chloride. In *Multidisciplinary Approaches to Cholinesterase Functions* (Shafferman, A., and Velan, B., eds) pp 131-140, Plenum Publishing Corp., New York.

Hall, L.M,C,. and Spierer, P. (1986). The ace locus of Drosophila melanogaster: Structural gene for acetylcholinesterase with an unusual 5' leader. EMBO J. **5**:2949-2954.

Hammond, C., Braakman, I., and Helenius, A. (1994). Role of N-linked oligosaccharide recognition, glucose trimming and calnexin in glycoprotein folding and quality control. Proc. Natl. Acad. Sci. USA **91**:913-917.

Han, S. Y., Sweeney, J. E., Bachman, E. S., Schweiger, E. J., Forloni, G., Coyle, J. T., Davis, B. M., and Joullie M. M. (1992) Chemical and pharmacological characterization of galanthamine, an acetylcholinesterase inhibitor, and its derivatives. A potential application in Alzheimer's disease? Eur. J. Med. Chem. **27**: 673-687.

Harel, M., Schalk, I., Ehret-Sabatier, L., Bouet, F., Goelder, M., Hirth, C., Axelsen, P.H., Silman, I., and Sussman, J.L. (1993). Quaternary ligand binding to aromatic residues in the active-site gorge of Acetylcholinesterase. Proc. Natl. Acad. Sci. USA **90**:9031-9035.

Harel, M., Silman, I. and Sussman, J.L. (1992a). A model of butyrylcholinesterase based on the x-ray structure of acetylcholinesterase indicates differences in specificity. In: *Multidiciplinary Approaches to Cholinesterase Functions*. (Shafferman A. and Velan B. Eds.),pp. 195-199, Plenum Pub. Co., New York .

Harel, M., Su, C.T., Frolow, F., Ashani, Y., Silman, I. and Sussman, J.L. (1991). Refined crystal structure of "aged" and "non-aged" organophosphoryl conjugates of γ-chymotrypsin. J. Mol. Biol. **221**:909-918.

Harel, M., Sussman, J.L., Krejci, E., Bon, S., Chanal, P., Massoulie, J. and Silman, I. (1992b). Conversion of acetylcholinesterase to butyrylcholinesterase: modeling and mutagenesis. Proc. Natl. Acad. Sci. USA **89**:10827-10831.

Hart, G.J., and O'Brien, R.D. (1973). Recording spectrophotometric method for determination of dissociation and phosphorylation constants for the inhibition of acetylcholinesterase by oragnophosphates in the presence of substrate. Biochemistry **12**:2940-2945.

Hasinoff, B.B. (1982). Kinetics of Ach binding to electric eel AchE in glycerol/water solvents of increased viscosity. Biochim. Biophys. Acta **704**:52-58.

Hassan,F.B., Cohen, S.G. and Cohen, J.B. (1980). Hydrolysis by acetylcholinesterase. J. Biol. Chem. **255**:3898-3904.

Haugejorden, S.M., Srinivasan, M., and Green, M. (1991). Analysis of the retention signals of two resident luminal endoplasmic reticulum proteins by in vitro mutagenesis. J. Biol. Chem. **266**:6015-6018.

Hendricks, M.B., Luchette, C.A., Banker, M.J. (1989). Enhanced expression of an immunoglobulin-based vector in myeloma cells mediated by amplification with a mutant dihydrofolate reductase gene. Biotechnology **7**:1271-1274.

Hibert, M. F., Trumpp-Kallmeyer, S., Hoflack, J. and Bruinvels, A. (1993). This is not a G protein-coupled receptor. Trends Pharmacol. Sci.**14**: 7-12.

Hobbiger, F., (1955). Effect of nicotinhydroxamic acid methiodide on human plasma cholinesterase inhibited by organophosphates containing a dialkylphosphoro group. Brit. J. Pharmacol. **10**:356-359.

Hobbiger, F. and Peck, A.W. (1969). Hydrolysis of suxamethonium by different types of plasma. Br. J. Pharmacol. **37**:258-271.

Hobman, T.H., Woodwatd, L., and Farquahar, M.G. (1992). The rubella virus E1 glycoprotein is arrested in a novel post-ER pre-golgi compartment. J. Cell. Biol. **118**:795-811.

Hodge, A. S., Humphrey, D. R., and Rosenberry, T. L. (1992). Ambenonium is a rapidly reversible noncovalent inhibitor of acetylcholinesterase, with one of the highest known affinities Mol. Pharmacol. **41**:937-942

Hosea, N.A., Brman, H.A., and Taylor, P. (1995). Specificity and orientation of trigonal carboxyl esters and tetrahedral alkylphosphonyl esters in cholinesterases. Biochemistry **34**: 11528-11536.

Hossner, K.L. and Billiar, R.B. (1981). Plasma clearance and distribution of native and desyialyated rat and human transcortin , species specificity. Endocrinol. **108**:1780-1786.

Hucho, F., Jarv, J., and Weise, C. (1991). Substrate-binding sites in acetylcholinesterase. Trends Pharmacol. Sci. **12**:422-427.

Hurtly, S.M., and Helenius, A. (1989). Protein oligomerization in the endoplasmic reticulum. Ann. Rev. Cell. Biol. **5**:277-307.

Huth, J.R., Perini, F., Lockridge, O., Bedows, E., and Ruddon, R.W. (1993). Protein folding and assembly in vitro, parallel intracellular folding and assembly. Catalysis of folding and assembly of the human chorionic gonadotropin alpha, beta dimer by protein-disulfide isomerase. J. Biol. Chem. **268**:16472-16482.

Imai, N., Kawamura, A., Higuchi, M., Oh-eda, M., Orita, T., Kawaguchi, T. and Ochi, N. (1990). Physiochemical and biological comparison of recombinant human erythropoietin with human urinary erythropoietin. J. Biochem. **107**:352-359.

Jackson, F.B., and Ferscht, A.R. (1993). Contribution of long range electrostatic interactions to stabilization of the catalytic transition state of the serine protease Subtilisin BPN' . Biochemistry **32**:13909-13916.

Jacobs, K., Shoemaker, C., Rudersdorf, R., Neill, S.D., Kaufman, R.J. Mufson, A., Seehra, J., Jones, S.S., Hewick, R., Fritsch, E.F., Kawakita, M., Shimizu, T. and Miyake, T. (1985). Isolation and characterization of genomic and cDNA clones of human erythropoietin. Nature **313**:806-808.

Jarv, J. (1984). Stereochemical aspects of cholinesterase catalysis. Bioorganic Chem. **12**:259-278.

Jarv, J., Kesvatera, T. and Aaviksaar, A. (1976). Structure-activity relationships in acetylcholinesterase reactions. Eur. J. Biochem. **67**:315-322.

Kanwar, Y.S. (1984). Biophysiology of glomerular filtration and proteinuria. Lab. Invest. **51**:7-21.

Kearney, P.C., Mizoue, L.S., Kumpf, R.A., Forman, J.F., McCurdy, A. and Dougherty, D.A. (1993) . Molecular recognition in aqueous media. New binding studies provide further insights into the cation-π interaction and related phenomena. J. Am. Chem. Soc. **115:** 9907-9919.

Kemp, J.R. And Wallace, K.B. (1990) Molecular determinants of the species-selective inhibition of brain acetylcholinesterase. Toxicol. Appl. Pharmacol. **104**: 264-258.

Kempner, E.S. (1993). Movable lobes and flexible loops in proteins. FEBS Lett. **326**: 4-10.

Kerem,A., Kronman, C., Bar-Nun, S., Shafferman, A. and Velan, B. (1993). Interrelation between assembly and secretion of recombinant human acetylcholinesterase. J. Biol. Chem. **268**:180-184.

Kieffer, B., Goeldner, M., Hirth, C., Aebersold, R. and Chang J.Y. (1986). Sequence determination of a peptide fragment from electrical eel AChE, involved in the binding of quartenary ammonium. FEBS letters **202**:91-96.

Kobata, A. (1992). Structures and functions of the sugar chains of oligosaccharides. Eur. J. Biochem. **209**:483-501.

Kovach, I.M. (1991). Competitive irreversible inhibition of enzymes in the presence of a substrate: scope and limitations. J.Enzyme Inhibition **4**: 201-212.

Kreienkamp H.J., Weise C., Raba R., Aaviksaar A. and Hucho, F. (1991). Anionic subsites of the catalytic center of acetylcholinesterase from *Torpedo* and from cobra venom. *Proc. Natl. Acad. Sci. USA*. **88**:6117-6121.

Kronman C., Velan B., Gozes Y., Leitner M., Flashner Y., Lazar A., Marcus D., Serry T., Papier Y., Grosfeld H., Cohen S., and Shafferman A. (1992). Production and secretion of high levels of recombinant human acetylcholinesterase in cultured cell lines. Gene **121**:295-304.

Kronman, C.,Ordentlich, A., Barak, D., Velan, B. and Shafferman, A. (1994). The Back Door Hypothesis for Product Clearance in Acetylcholinesterase Challenged by Site Directed Mutagenesis. J. Biol. Chem. **269**: 27819-27822.

Krupka, R. M. (1966). Chemical structure and function of the active center of acetylcholinesterase. Biochemistry **5**:1988-1998.

Laemmli, U.K. (1970). Cleavage of structural proteins during the assembly of the head of the bacteriophage T_4. Nature **227**:680-685.

Laughton, C.A. (1994). A study of simulated annealing protocols for use with molecular dynamics in protein structure predictions. Protein Eng. **7**: 235-241.

Layer P.(1992). Towards a functional analysis of cholinesterases in neurogenesis: histological, molecular and regulatory features of BChE from chicken brain In: *Multidisciplinary Approaches to Cholinesterase Research* (Velan, B. and Shafferman A. Eds.), pp 223-231, Plenum Pub. Co., New York

Lazar, A., Reuveny, C., Kronman C., Velan, B., and Shafferman, A. (1994). Evaluation of anchorage-dependent cell propagation system for production of human acetylcholinesterase by recombinant 293 cells. Cytotechnology **13**:115-123.

Lazar, M., Salmeron, E., Vigny, M., and Massoulie, J. (1994). Heavy isotope-labeling study of the metabolism of monomeric and tetrameric acetylcholinesterase forms in the murine neuron-like T28 hybrid cell line. J. Biol. Chem. **259**:3703-3713.

Le, A., Ferrel, G.A., Dishon, D.S., Le, Q.A., and Sifers, R.N. (1992). Soluble aggregates of the human Pi Z alpha 1-antitrypsin variant are degraded within the endoplasmic reticulum by mechanism sensitive to inhibitors of protein synthesis. J. Biol. Chem. **267**:1072-1080.

Lefort. G.P., Stolk, J.M., and Nisula, B.C. (1984). Evidence that desialyatiion and uptake by hepatic receptors for galactose-terminated glycoproteins are immaterial to the metabolism of human choriogonadotropin in the rat. Endocrinol. **115**:1551-1557.

Legay , C., Bon, S., Vernier, P., Coussen, F., and Massoulie J. (1993). Cloning and expression of acetylcholinesterase subunit; generation of multiple molecular forms, complementarity with a Torpedo collagenic subunit. J. Neurochemistry, **60**:337-346.

Leli, U., Shea, T.B., Cataldo, A., Hauser, G., Grynspan, E., Beermann, M.L., Leipkalns, V.A., Nixon, R.A., and Parker, P.J. (1993). Differential expression and subcellular localiztion of Protein kinase C alpha, beta, gamma, delta, epsilon isoforms in SH-SYSS neuroblastoma cells. Modification during differentiation. J, Neurochem. **60**:289-298.

Levy D., and Ashani Y. (1986). Synthesis and in vitro properties of a powerful quaternary methylphosphonate inhibitor of acetylcholinesterase. Biochem. Pharmacol. **35**:1079-1085.

Liao, J., Heider, H., Sun, M.-C., Stieger, S. and Brodbeck, U. (1991). The monoclonal antibody 2G8 is carbohydrate-specific and distinguishes between different forms of vertebrate cholinesterases. Eur. J. Biochem. **198**:59-65.

Liao, J., Heider, H., Sun, M.-C. and Brodbeck, U. (1992). Different glycosylation in acetylcholinesterases from mammalian brain ad erythrocytes. J. Neurochem. **58**:1230-1238.

Lim, A.W., Farruggio, D.C. and Sauer, R.T. (1992). Structural and energetic consequences of disruptive mutations in protein core. Biochemistry **31**:4324-4333.

Lin, R.K., Suggs, S., Lin C.-H., Browne, J.K., Smalling, R., Egrie, J.C., Chen, K.K., Fox, G.M., Martin, F., Stabinski, Z., Badrawi, S.M., Lai, P.-H. and Goldwasser, E. (1985). Cloning and expression of the human erythropoietin gene. Proc. Natl. Acad. Sci. **82**:7580-7584.

Lind, W., Jager, V., Lucki-Lange, M., and Wagner, R. (1991). Characterization of protease activity in serum-free culture supernatants of hybridomas and recombinant mammalian cells. In: *Production of Biologicals from Animal Cells in Culture*. Spier, R.E., Griffiths, J.B., and Meignier, B. (Eds.), (pp. 196-202), Butterworths Scientific Publishers UK.

Liu, W. and Tsou, C. (1986) Determination of rate constants for the irreversible inhibition of acetylcholine esterase by continuously monitoring the substrate reaction in the presence of the inhibitor. Biochim. Biophys. Acta **870**: 185-190.

Lockridge, O., Bartels, C.F., Vaughan, T.A., Wong, C.K., Norton, S.E., and Johnson L.L. (1987). Complete amino acid sequence of human serum cholinesterase. J. Biol. Chem. **262**:549-557.

Lockridge, O., Eckersen, H.W., and LaDu, B.N. (1979).Interchain disulfide bonds and subunit organizaion in human serum cholinesterase. J. Biol. Chem. **254**:8324-8330.

Lowenatein, Y., Gnatt, A., Neville, L.F., and Soreq, H. (1993). Chimeric human Cholinesterase. Identification of interaction sites responsible for recognition of Acetyl or BuChE - specific ligands. J, Molec. Biol. **234**:289-296.

Lowry, O.H., Rosenbrough, N.J., and Farr, A.L. (1951). Protein measurement with the folin phenol reagent. J. Biol. Chem. **193**:265-267.

Lullmann, H., Ohnesorge, F. K., Tonner, H. D., Wassermann, O., and Ziegler, A. (1971). Influence of alkane-bis-onium compounds upon the activity of the AChE and upon its inhibition by DFP. Biochem. Pharamcol. **20**: 2579-258.

Luty, B.A., Wade, R.C., Madura, J.D., Davis, M.E., Briggs, J.M., and McCammon, J.A. (1993). Brownian dynamics simulations of diffusional encounters between Triose Phosphate Isomerase and Glyceraldehyde Phosphate. J. Phys. Chem. **97**:233-237.

Machamer, C.E. and Rose, J.K. (1988). Vesicular stomatitis virus G proteins with altered glycosylation sites display temperature-sensitive intracellular transport and are subject to aberrant intermolecular disulfide bonding. J. Biol. Chem. **263**:5955-5960.

Macphee-Quigley, K., Taylor, P. and Taylor, S.S. (1985). Primary structures of the catalytic subunits from two molecular forms of acetylcholinesterase: A comparison of NH_2-terminal and active center sequences. J. Biol. Chem. **260**:12185-12189.

Macphee-Quigley, K., Taylor, P., and Taylor, S.S. (1988) Expression of active, glycosylated acetylcholinesterase using the insect vector Baculovirus system. FASEB J. **2**:A361.

Main, A.R. and Iverson, F. (1966) Measurement of the affinity of phosphorylation constants governing irreversible inhibition of cholinesterase by diisopropylphosphorofluoridate. Biochem. J. **100**: 265-275.

Main, A.R. (1976). In: *Biology of Cholinergic Function* (Goldberg, A.M. and Hanin, A. Eds.) pp. 269-353, Random Press, New York.

Marchot, P., Khelif, A., Ji, Y-H., Mansuelle, P., and Bougis, P.E. (1993). Binding of ^{125}I-fasciculin to rat brain acetylcholinesterase. J. Biol. Chem. **268**: 12458-12467.

Masson, P., Adkins, S., Pham-Trong, P., and Lockridge, O. (1992). Expression and refolding of functional human butyrylcholinesterase from E. coli. In: *Multidisciplinary Approaches to Cholinesterase Functions.* (Shafferman, A. and Velan, B. Eds.), pp. 49-52, Plenum Press, New York.

Massoulie, J., Pezzementi, L., Bon, S., Krejci, E., and Vallette, F.-M. (1993). Molecular and cellular biology of Cholinesterases. Prog. Neurobiol. **41**:31-91.

Massoulie, J., Sussman, J.L., Doctor, B.P., Soreq, H., Velan, B., Cygler, M., Rotundo, R., Shafferman, A., Silman, I. and Taylor, P. (1992). Recommendations for nomenclature in cholinesterases. In: *Multidisciplinary Approaches to Cholinesterase Functions.* (Shafferman A. and Velan B. Eds.), pp.285-288, Plenum Pub. Co., New York.

Matthews, B.W. (1993). Structural and genetic analysis of protein stability. Annu. Rev. Biochem. **62**:139-160.

Matzuk, M. M. and Boime, I. (1988). The role of the asparagine-linked oligosaccharides of the α subunit in the secretion and assembly of the human chorionic gonadotropin. J. Cell Biol. **106**:1049-1059.

Matzuk, M.M., Keene, J.L. and Boim, I. (1989). Site specificity of chorionic gonadotropin *N*-linked oligosacchrides in signal transduction. J. Biol. Chem. **264**:2409-2414.

Mazzarella, R.A., Srinivasan, M., Haugejorden, S.M., and Green, M. (1990). ERp72 an abundant luminal endoplasmic reticulum protein, contains three copies of the active-site sequence of protein disulfide isomeras. J. Biol. Chem. **265**:1094-1101.

McCurdy, A., Jimenez, L., Stauffer, D. A., and Dougherty, D. A. (1992). Biomimetic catalysis of S_N2 reactions through cation-π interactions. The role of polarizability in catalysis. J. Am. Chem. Soc. **114**: 10314-10321.

Meflah, K, Barnard, S., and Massoulie, J. (1984) Interactions with lectins indicate differences in the carbohydrate composition of the membrane-bound enzymes acetylcholinesterase and 5'-nucleotidase in different cell types. Biochemie **66**:59-69.

Michel, H.O., Hackley Jr, B.E., Berkowitz, L., List, G., Hackley, E.B., Gilliam, W.and Paukan, M., (1967). Ageing and dealkylation of soman-inactivated eel cholinesterase. Arch. Biochem. Biophys. **121**:29-34.

Millard, C.B., and Broomfield, C.A. (1992). A computer model of glycosylated human butyrylcholinesterase. Biochem. Biophys. Res. Commun. **189**:1280-1286.

Mooser, G., Schulman, H., and Sigman, D. (1972) . Fluorescent probes of acetylcholinesterase. Biochemistry **11**: 1595-1602.

Munro, S., and Pelham, H.R.B. (1987). A C-terminal signal prevents secretion of luminal proteins. Cell **48**:899-907.

Mutero, A. and Fournier D. (1992). Post-translational modifications of Drosophila acetylcholinesterase. J. Biol. Chem. **267**:1695-1700.

Nair, H. K., Seravalli, J., Arbuckle, T. and Quinn, D. M. (1994). Molecular recognition in acetylcholinesterase catalysis: free-energy correlations for substrate turnover and inhibition by trifluoroketone transition state analogs. Biochemistry: **33**, 8566-8576.

Neville, L.F., Gnatt, A., Lowenstein, Y., Seidman, S., Erlich, G., and Soreq, H. (1992). Intramolecular relationships in Cholinesterases revealed by oocyte expression of site-directed and natural variants of human BuChE. EMBO J. **11**:1641-1649.

Noiva, R., and Lennarz, W.J. (1992). Protein disulfide isomerase. A multi-functional protein resident in the lumen of the endoplasmic reticulum. J. Biol . Chem. **267**: 3553-3556.

Nolte H.J, Rosenberry T.L. Neuman E.,(1980).Effective charge on acetylcholinesterase active sites determined from the ionic strength dependence of association rate constants with cationic ligands. Biochemistry **19**: 3705-3711.

O'Brien, R.D. (1971). The design of organophosphate and carbamate inhibitors of cholinesterases. in Drug Design (Ed. Ariens) Vol. **2**, pp. 161-212

Ollis, D.L., Cheah, E., Cygler, M., Dijkstra, B., Frolow, F., Franken, S.M., Harel,M., Remington, S.J., Silman, I., Schrag, J., Sussman, J.L., Verscchueren, K.H.G., and Goldman, A. (1992). The α/ß hydrolase fold. Protein Eng.: **5**, 197-211.

Olson,P.F., Fessler,L.I., Nelson R.E., Cambell,A.G., and Fessler J.H. (1990). Glutactin, a novel Drosophila basement membrane-related glycoprotein with sequence similarity to serine esterase.EMBO J. **9**: 3593-3601.

Ordentlich A., Barak D., Kronman C., Flashner Y., Leitner M.,Segall Y., Ariel N., Cohen S., Velan B.,and Shafferman A. (1993a) Dissection of the human acetylcholinesterase active center - determinants of substrate specificity: Identification of residues constituting the anionic site, the hydrophobic site, and the acyl pocket. J. Biol. Chem. **268**:17083-17095.

Ordentlich, A., Kronman, C., Barak, D., Stein, D., Ariel, N., Marcus, D., Velan, B., and Shafferman, A. (1993b). Engineering resistance to 'aging' in phosphylated human acetylcholinesterase - role of hydrogen bond network in the active center. FEBS Lett. **334**:215-220.

Ordentlich, A., Barak, D., Kronman, C., Ariel, N., Segall, Y., Velan, B., and Shafferman, A. (1995). Contribution of aromatic moieties of tyrosine 133 and of the anionic subsite tryptophan 86 to catalytic efficiency and allosteric modulation of acetylcholinesterase. J. Biol.Chem. **270**: 2082-2091.

Paterson, Jr. M.K. (1979). Measurement of cell growth and viability of cells in culture. Methods Enzymol. **58**:141-143.

Patinkin, D., Seidman, S., Eckstein, F., Benseler, F., Zakut, H. and Soreq, H. (1990). Manipulation of cholinesterase gene expression modulate murine megakaryocytopoiesis *in vitro*. Molec. Cell Biol., **10**:6046-6050.

Pattison, S., and Bernhard, S.A. (1978). Functional consequences of ligand-dependent conformational changes in trypsin-solubilized and in membrane particle constrained-acetylcholinesterase. Proc. Natl. Acad. Sci USA **75**: 3613-3617.

Pearlman, D.A., Case, D.A., Caldwell, J.C., Seibel, G.I., Singh, U.S., Weiner, P. & Kolmann, P.A. (1991) AMBER 4.0, University of California, San Fransisco.

Pelham, H.R.B. (1988). Evidence that luminal ER proteins are sorted from secreted proteins in a post-ER compartment. EMBO J. **7**:913-918.

Pelham, H.R.B. (1989). Control of protein exit from the endoplasmic reticulum. Ann. Rev. Cell. Biol. **5**:1-23.

Pelham, H.R.B. (1990). The retention signal for soluble proteins of the endoplasmic mice reticulum. Trends Biochem. Sci. **15**:483-486.

Peter, F., Nguyen van P., and Soling, H.D. (1992). Different sorting of Lys-Asp-Glu-Leu proteins in rat liver. J. Biol. Chem. **267**:10631-10637.

Potter, S.M., Johnson, B.A., Henschen, A., and Aswad, D.W. (1992). The type II isoform of bovine brain protein L-isoaspartyl methyltransferase has an endoplasmic reticulum retention signal at its C-terminal. Biochemistry **31**:6339-6347.

Prody, C.A., Zevin-Sonkin, D., Gnatt, A., Goldberg, O., and Soreq, H. (1987). Isolation and characterization of full length cDNA clones coding for cholinesterase from fetal human tissues. Proc. Natl. Acad. Sci. USA. **84**:3555-3559.

Qian, N. and Kowach, I.M. (1993). Key active site residues in the inhibition of acetylcholinesterase by soman. Medical Defense Bioscience Review, **3**:1005-1014.

Quinn, D.M. (1987). AChE: Enzyme structure, reaction dynamics and virtual transition states. Chem. Rev. **87**:955-979.

Rachinsky,T.L., CampS.,Li, Y.,Ekstrom, T,J.,Newton, M.,and Taylor P.(1990). Molecular cloning of mouse acetylcholinesterase: Tissue distribution of alternatively spliced mRNA species. Neuron **5**:317-327.

Radic, Z., Reiner, E., and Taylor, P. (1991) Role of the peripheral anionic site on acetylcholinesterase: inhibition by substrates and coumarin derivatives. Mol. Pharmacol., **39**: 98-104.

Radic, Z., Gibney, G., Kawamoto, S., MacPhee-Quigley, K., Bongiorno, C., and Taylor, P. (1992) Expression of recombinant acetylcholinesterase in Baculovirus system: kinetic properties of glutamate 199 mutant. Biochemistry **31**:9760-9767.

Radic, Z., Pickering, N.A., Vellom, D.C., Camp, C., and Taylor, P. (1993). Three distinct domains in the cholinesterase molecule confer selectivity for acetyl and butyrylcholinesterase inhibitors. Biochemistry **32**:12074-12084.

Radic, Z., Duran, R., Vellom, D. C., Li, Y., Cervenansky, C., and Taylor, P. (1994) Site of fasciculin interaction with acetylcholinesterase. J. Biol. Chem. **269**: 11233-11239.

Radic, Z., Quinn, D.M., Vellom, D.C., Camp, S. and Taylor, P. (1995) Allosteric control of acetylcholinesterase catalysis by fasciculin. J. Biol. Chem. **270**: 20391-20399.

Rajagopalan, S., Ku, Y., and Brenner, M.B. (1994). Retention of unassembled components of integral membrane proteins by calnexin. Science **263**:387-390.

Ralston, J.C., Rush, R.S., Doctor, B.P. and Wolfe, A.D. (1985). Acetylcholinesterase from fetal bovine serum, purification and characterization of soluble G4 enzyme. J. Biol. Chem. **260**:4312-4318.

Randall, W.R. (1991). Cellular expression of murine AChE from cloned brain transcript. In: *Cholinesterases Structure, Function, Mechanism, Genetics and Cell Biology* (Massoulie, J., Bacou, F., Barnard, E.A., Chatonnet, A., Doctor, B.P. and Quinn, D.M. Eds.) pp. 152-156, American Chemical Society, Washington D.C.

Raveh, L., Ashani, Y., Levi, D., De La Hoz, D., Wolfe, A.D. and Doctor, B.P. (1989). Acetylcholinesterase prophylaxis against organophosphate poisoning: Quantitative correlation between protection and blood-enzyme level in mice. Biochem. Pharmacol. **38**:529-534.

Raveh, L., Grunwald, J., Marcus, D., Papier, Y., Cohen, E., and Ashani, Y. (1993). Human butyrylcholinesterase as a general prophylactic antidote for nerve agent toxicity. Biochem. Pharmacol. **45**:2465-2472.

Remers, W.A. (1971) in The Chemistry of Heterocyclic Compounds (Weissberger, a. and Taylor, E.C. Eds.), Vol. **25**, Part 1, pp.57-58,Wiley-Interscience, New York.

Reuveny, S., Zheng, Z.B., and Epstein, L. (1986). Evaluation of a cell culture fermentor. American Biotechnol. Lab. 28-39.

Ripoll, D.L., Faerman, C.H., Axelsen, P.H., Silman, I., and Sussman, J.L. (1993). An electrostatic mechanism for substrate guidance down the aromatic gorge of AchE. Proc. Natl. Acad. Sci. USA **90**:5128-5132.

Robbi, M., and Beufray, H. (1991). the COOH terminal of several liver carboxylesterases targets these enzymes to the lumen of the endoplasmic reticulum. J. Biol. Chem. **266**:20489-20503.

Robert, J., Cote, J. and Archambault, J. (1991). Surface immobilization of anchorage-dependent mammalian cells. Biotechnol. Bioeng. **39**:697-706.

Roberts, W.L., Doctor, B.P., Foster, J.D., and Rosenberry, T.L. (1991). Bovine brain acetylcholinesterase primary sequence involved in inter-subunit disulfide linkages. J. Biol. Chem. **266**:7481-7487.

Rogers, D. F. and Adams, J. A. (1990) in Mathematical Elements of Computer Graphics , McGraw Pub., New York, pp. 247.

Rosenberry, T.L. (1975). Acetylcholinesterase. Adv. Enzymol. Relat. Areas. Mol. Biol. **43**:103-219.

Rosenberry, T.L. and Berhnard, S.A. (1972). Studies of catalysis by acetylcholinesterase: synergistic effects of inhibitors during the hydrolysis of acetic acid esters. Biochemistry **11**:4308-4321.

Rotundo, L.R. (1984). Assymetric acetylcholinesterase is assembled in the golgi apparatus. Proc. Natl. Acad. Sci. USA **81**:497-483.

Rotundo, L.R. (1988). Biogenesis of acetylcholinesterase molecular forms in muscle: evidence for a rapidly turning over, catalytically inactive precursor pool. J. Biol. Chem. **263**: 19398-19406.

Rotundo, L.R., Thoma, K., Portr-Jordan, K., Benson, R.J., Fernandez-Valle, C., and Fine, R.E. (1989). Intracellular transport, sorting and turnover of acetylcholinesterase. J. Biol. Chem. **264**:3146-3152.

Roufogalis, B. D., and Quist, E. E. (1972) Relative binding sites of pharmacologically active ligands on bovine erythrocyte acetylcholinesterase. Mol. Pharmacol. **8**: 41-49

Roussaux, C.G. and Dua, A.K. (1989). Pharmacology of HI-6 an H-series oxime. Can. J. Physiol. Pharmacol. **67**:1183-1189.

Ryu, S. , Lin, J. And Thompson, C.M. (1991) Comparative anticholinesterase potency of chiral isoparathion methyl. Chem. Res. Toxicol. **4**: 517-520.

Salih, E. (1992). Catalysis by acetylcholinesterase in two-hydronic-reactive states.Biochem. J. **285:**451-460.

Sanford, K.K., Earle, W.R., Evans, V.S., Walltz, J.K. and Shanon, J.E. (1951). The measurement of proliferation in tissue cultures by enumeration of cell nuclei. J. Natl. Cancer Inst. **11**: 773-795.

Satow Y ,Cohen G.H., Padlan E.A and Davies D.R.(1986). Phosphocholine binding immunoglobulin Fab McPC603. An X-ray diffraction study at 2.7A . J.Mol.Biol. **190**:593-604.

Saunders, B.C. And Stacy, G.J. (1948). Esters containing phosphorus. J. Chem. Soc. 695-699.

Saxena, A., Doctor, B.P., Maxwell, D.M., Lenz, D.E., Radic, Z. and Taylor, P. (1993). The role of glutamate-199 in the aging of cholinesterase. Biochem. Biophys. Res.Comm. **197**: 343-349.

Schalk, I., Ehret-Sabatier, L., Bouet, F., Goeldner, M. and Hirth, C. (1992) Structural analysis of acetylcholinesterase ammonium binding sites. In: *Multidisciplinary Approaches to Cholinesterase Functions.* (Shafferman A. and Velan B. Eds.), pp.117-120, Plenum Pub. Co., New York.

Schneider, H.J. (1991). Mechanisms of molecular recognition: investigations of organic host-guest complexes. Angew. Chem. Int. Ed. Engl. **30:**1417-1436.

Schumacher, M., Camp, S., Maulet, Y., Newton, M., MacPhee-Quigley, L., Taylor, S.S., Friedman, T., and Taylor, P. (1986). Primary structure of Torpedo californica acetylcholinesterase deduced from its cDNA sequence. Nature **319**:407-409.

Semenkovich, C.F., Luo, C.-C., Nakanishi, M.K. Chen, S.-H., Smith, L.C. and Chan, L. (1990). *In vitro* expression and site-specific mutagenesis of the cloned human lipoprotein lipase gene. J. Biol. Chem. **265**: 5429-5433.

Shafferman, A. and Velan, B. Eds. (1992). "*Multidisciplinary Approaches to Cholinesterase Functions*". Plenum Pub. Co., New York .

Shafferman, A., Kronman, C., Flashner, Y., Leitner, S., Grosfeld, H., Ordentlich, A., Gozes, Y., Cohen, S., Ariel, N., Barak, D., Harel, M., Silman, I., Sussman, J.L. and Velan. B., (1992a). Mutagenesis of human acetylcholinesterase. J. Biol. Chem. **267**:17640-17648.

Shafferman, A., Ordentlich, A., Barak, D., Kronman, C., Ber, R., Bino, T., Ariel, N., Osman, R., and Velan, B. (1994). Electrostatic attraction by surface charge does not contribute to the catalytic efficiency of acetylcholinesterase. EMBO J. **13**:3448-3455.

Shafferman, A., Velan, B., Ordentlich, A., Kronman, C., Grosfeld, H., Leitner, M., Flashner, Y., Cohen, S., Barak, D., and Ariel, N. (1992b). Substrate inhibition of acetylcholinesterase: residues signal transduction from the surface to the catalytic center. EMBO J. **11**:3561-3568.

Shafferman, A., Velan, B., Ordentlich, A., Kronman, C., Grosfeld, H., Leitner, M., Flashner, Y., Cohen, S., Barak, D., and Ariel, N. (1992c). Acetylcholinesterase catalysis-protein engineering studies. In: *Multidisciplinary Approaches to Cholinesterase Functions*. (Shafferman A. and Velan B. Eds.),pp. 165-175, Plenum Pub. Co., New York .

Shafferman, A., Velan, B., Barak, D., Kronman, C., Ordentlich, A.,Flashner, Y., Leitner, M., Segal, Y., Grosfeld, H., Stein, D and Ariel, N. (1993). Recombinant human acetylcholinesterase - Enzyme engineering. Medical Defense Bioscience Review, **3**:1111-1123.

Sharp, K.A., and Honig, B. (1990). Electrostatic interactions in macromolecules - theory and applications. Ann. Rev. Biophys. Biophys. Chem. **19**:301-332

Sikorov, J.L., Krejci E. and Massoulie J. (1987). cDNA sequence of Torpedo marmorata acetylcholinesterase: Primary structure of the precursor of a catalytic subunit: existence of multiple 5' untranslated regions. EMBO J. **6**:1865-1873.

Sines, J.J., Allison, S.A., and McCammon, J.A. (1990). Point charge distributions and electrostatic steering in enzyme/substrate encounter: brownian dynamics of modified copper/zinc superoxide dismutase. Biochemistry 29:9403-9412.

Smith, P.L., Skelton, T.P., Fiete, D., Dharmesh, S.M., Beraneck, M.C., MacPhail, L., Broze, G.J. and Baenzinger, J.U. (1992). The Asparagine-linked oligosaccharides of tissue factor pathway inhibitor terminate with SO_4-GalNac-beta1,4GlcNAc-beta1,2Man.J. Biol. Chem. **267**:19140-19146.

Soman, K., Yang, A.S., Honig, B., and Fletterick, M. (1989). Electrostatic potential in Trypsin isoenzymes. Biochemistry **28**:9918-9926.

Soreq, H., Parvari, R., and Silman, I. (1982) Biosynthesis and secretion of catalytically active acetylcholinesterase in Xenopus oocytes microinjected with mRNA from rat brain and from Torpedo electric organ. Proc. Nat. Acad. Sci. USA **79**:830-834.

Soreq, H., Ben-Aziz, R., Prody, C., Gnatt, A., Neville, A., Lieman-Hurwitz, J., Lev-Lehman, E., Ginzberg, D., Seidman, S., Lapidot Lifson, Y. and Zakut, H. (1990). Molecular cloning and construction of the coding region for human acetylcholinesterase reveals a G+C reach attenuating structure. Proc. Natl. Acad. Sci. USA. **87**:9688-9692.

Soreq, H.. and Seidman, S. (1992) Xenopus oocyte microinjection: from gene to protein. Meth. Enzymol. **207**:225-265.

Southern, P.J. and Berg, P. (1982).Transformation of mammalian cells to antibiotic resistance with a bacterial gene under control of the SV40 early region promoter. Mol. Appl. Genet. 1, 327-341. Taylor, P. (1991) J. Biol. Chem. **266**:4025-4028.

Steiner, H., Pohl, G., Gunne, H., Hellers, M., Elhammer, A. and Hansson, L. (1988). Human tissue-type plasminogen activator synthesized by using a baculovirus vector in insect cells compared with human plasminogen activator produced in mouse cells. Gene **73**:449-457.

Sussman J.L, Harel M., Frolow F.,Oefner C. Goldman A. and Silman I.(1991). Atomic resolution of acetylcholinesterase from Torpedo californica: A prototypic acetylcholine binding protein.Science. **253**:872-879.

Sussman, J.L., Harel, M. and Silman, I. (1992). Three dimensional structure of acetylcholinesterase. In: *Multidisciplinary Approaches to Cholinesterase Functions.* (Shafferman A. and Velan B., Eds.), pp.95-107, Plenum Pub. Co., New York.

Tainer, J.A., Getzoff, E.D., Richardson, J.S. And Richardson, D.C. (1983). Structure and mechanism of copper and zinc superoxide dismutase. Nature **306**:284-287.

Tan, R.C., Truong, T.N., McCammon, J.A. , And Sussman, J.L. (1993). Acetylcholinesterase: electrostatic steering increases the rate of ligand binding. Biochemistry **32**:401-403.

Tang, B.L., Wong, S.H., Low, S.H., and Hong, W. (1992). Retention of a type II surface membrane protein in the endoplasmic reticulum by the Lys-Asp-Glu-Leu sequence. J. Biol. Chem. **267**:7072-7076.

Taylor, P., Lwebuga-Mukasa, J., Lappi, S. and Rademacher, J. (1974) Propidium - a fluorescence probe for a peripheral anionic site on acetylcholinesterase. Mol. Pharmacol. **10**: 703-708.

Taylor P. and Lappi S. (1975). Interaction of fluorescent probes with acetylcholinesterase : the site and specificity of propidium binding.Biochemistry **14**:1989-1997.

Taylor P. (1990). In: "*Pharmacological Basis of Therapeutics*" (Gilman A.G., Goodman L.S., Rall T., and Murad F. Eds.); MacMillan New York, pp 131-149.

Taylor P. (1991). The Cholinesterases. J.Biol.Chem. **266**:4025-4028.

Taylor, P., and Radic, Z. (1994). The cholinesterases: from genes to proteins. Ann. Rev. Pharmacol. Toxicol. **34**:281-320.

Thomas, P., and Zamcheck, N. (1983). Role of the liver in clearance and excretion of circulating carcino-embryonic antigen. Digest. Dis. and Scie. **28**:216-224.

Tomlinson, G., Mutus, B., and McLennan, I. (1980) Modulation of aceytlcholinestrase activity by peripheral site ligands Mol. Pharmacol. **18**: 33-39.

Trestakis, S., Ebert, C., and Layer, P.G. (1992) Butyrylcholinesterase from chicken brain is smaller than that from serum: its purification, glycosylation and membrane association. J. Neurochem. **58**:2236-2247.

Trifft, C.J., Proia, R. L. and Camerini-Otero, D.R. (1992). The folding and cell surface expression of CD4 requires glycosylation. J. Biol. Chem. **267**:3268-3273.

Van der Drift, A.C.M., Beck, H.C., Decker, A.G., Hulst, A.G. and Wils, E.R.G. (1985). ^{31}P NMR and mass spectrometry of atropinesterase and some serine proteases phosphorylated with a transition-state analogue. Biochemistry **24**:6894-6903.

Velan, B., Grosfeld, H., Kronman, C., Flashner, Y., Leitner, M., Cohen, S., and Shafferman, A. (1993). N-glycosylation of human acetylcholinesterase : efects on activity, stability and biosynthesis. Biochem. J. **296**:649-656.

Velan, B., Kronman, C., Grosfeld, H., Leitner, M., Gozes, Y., Flashner, Y. Serry, T., Cohen, S., Benaziz, R., Seidman, S., Shafferman, A. and Soreq, H. (1991a). Recombinant human acetylcholinesterase is secreted from transiently transfected 293 cells as a soluble globular enzyme. Cell. Mol. Neurob. **11**:143-156.

Velan B.,Grosfeld H.,Kronman C.,Leitner M.,Gozes Y.,Lazar A.,Flashner Y.,Marcus D., Cohen S., and Shafferman A. (1991b). The effect of elimination of intersubunit disulfide bonds on the activity, assembly and secretion of recombinant human acetylcholinesterase. J.Biol.Chem. **266**:23977-23984.

Velan, B., Kronman, C., Leitner, M., Grosfeld, H., Flashner, Y., Marcus, D., Lazar, A., Kerem, A., Bar-Nun, S., Cohen, S., and Shafferman, A. (1992). Molecular organization of recombinant human acetylcholinesterase. In: In: *Multidisciplinary Approaches to Cholinesterase Functions.* (Shafferman A. and Velan B., Eds.), pp.39-48, Plenum Pub. Co., New York.

Velan, B., Kronman, C., Ordentlich, A., Flashner, Y., Leitner, M., Cohen, S., and Shafferman, A. (1993). N-glycosylation of human acetylcholinesterase affects enzyme stability and secretion efficiency but not enzyme activity. Biochem. J. **296**:649-656.

Velan, B., Kronman, C., Flashner, Y., and Shafferman, A. (1994). Reversal of signal mediated cellular retention by subunit assembly of human acetylcholinesterase. J. Biol. Chem. **269**:22719-22725.

Vellom , D.C., Radic, Z., Li, Y., Pickering, N.A., Camp, S. and Taylor, P. (1993). Amino acid residues controlling acetylcholinesterase and butyrylcholinesterase specificity. Biochemistry **32**:12-17.

Vennema, H., Heijnen, L., Rottier, P.J.M., Horzinek, M.C., and Spann, W.J.M. (1992). A novel glycoprotein of feline infectious peritonitis coronavirus contains a KDEL-like endoplasmic reticulum retention signal. J. Virol. **66**:4951-4956.

Vostal, J.G., and McCauly, R.B. (1991). Pro-thrombin plasma clearance is mediated by hepatic asialoglycoprotein receptors. Thromb. Res. **63**:299-309.

Walls, J. D., Berg, D.T., Yan, S.B. and Grinnell, B.W. (1989). Amplification of multicistronic plasmids in human 293 cell line and secretion of correctly processed recombinant human protein C. Gene **81**:139-149.

Wang, C. And Murphy, S.D. (1982) Kinetic analysis of species difference in acetylcholinesterase sensitivity to organophosphate insecticides. Toxicol. Apll. Pharmacol. **66**: 409-419.

Warren, L. (1959). The thiobarbituric acid assay of sialic acids. J. Biol. Chem. **234**:1971-1975.

Weiner, S.J., Kolman, P.A., Nguyen, D.T. And Case, D.A. (1986). An all-atom force field for simulations of proteins and nucleic acids. J. Comput. Chem. **7**:230-252.

Weise C. Kreienkamp h-J.,Raba R.,Pedak A., Aaviksaar A., and Hocho F. (1990). Anionic subsites of the acetylcholinesterase from Torpedo californica : affinity labelling with the cationic reagent N,N-dimethyl-2-phenyl-aziridinium. EMBO **9**:3885-3888.

Weitz, G., and Proia, R.L. (1992). Analysis of the glycosylation and phosphorylation of the α-subunit of the lysosomal enzyme, β-hexosaminidase A, by site directed mutagenesis. J. Biol. Chem. 267, 10039-10044 Wigler, M., Silverstein, S., Lee, L.S., Pellicer, A., Cheng, Y. C. and Axel, R. (1977) Cell **11**:223-232.

Wess, J. (1993). Mutational analysis of muscarinic acetylcholine receptors: Structural basis for ligand/receptor/G-protein interactions. Life Sci. **53**: 1447-1463.

Wickstrom, L., and Lodish, H.F. (1993). Unfolded H2b asialoglycoprotein receptor subunit polypeptides are selectively degraded within the endoplasmic reticulum. J. Biol. Chem. **268**:14412-14416.

Wilchek, M., and Miron, T. (1982). Immobilizations of enzyme and affinity ligands on to agarose via stable and uncharged carbamate linkages. Biochem. Int. **4**: 629-635.

Wilson, I. B. (1952) . Acetylcholinsterase XII. Further studies of binding forces.*J.* Biol. Chem. **197**: 215-225.

Wilson, I. B., and Quan, C. (1958). Acetylcholinesterase studies on molecular complementariness. Arch. Biochem. **73**: 131-143

Wolfe, A.D., Rush, R.S., Doctor, B.P., Koplovitz I., and Jones, D., (1987). Acetylcholinesterase prophylaxis against organophosphate toxicity. Fundam Appl Toxicol. **9**: 266-270.

Yan, S.B., Chao, Y.B., and van Halbeek, H. (1993). Novel Asn-linked oligosaccharides terminating in GalNac beta (1,4) the (alpha1,3)GlcNac are present in recombinant human PKC expressed in HEK293 cells. Glycobiol. **3**:597-608.

Yan, S.B., Grinell, B.W. and Wold, F. (1989). Post-transnational modifications of proteins: Some problems left to solve. TIBS **14**:264-268.

Yates, C.M., Simpson,J., Moloney, A.F.J., Gordon,A. and Reid, A.H. (1980). Alzheimer like cholinergic deficiency in Down Syndrome, Lancet, **2**:979-980.

Yet. M.G., Chin, C.C.Q., and Wolfe, F. (1980). The covalent structure of individual N-linked glycopeptides from ovmucoid and asialofetuin. J. Biol. Chem. **263**:111-117.

Zagouras, P., and Rose, J.K. (1989). Carboxy-terminal SEKDEL sequences retard but do not retain two secretory proteins in the endoplasmic reticulum. J. Cell. Biol. **109**:2633-2640.

Zagouras, P., and Rose, J.K. (1993). Dynamic equilibrium between vesicular stomatitis virus glycoprotein monomers and dimers in the golgi and at the cell surface. J. Virol. **67**:7533-7538.

APPENDIX A

Compilation of Catalytic Properties[a] of HuAChE and Mutants Generated During the Research and Functional Assignment of Residues

AChE Type	K_m (mM)		k_{cat} ($x10^{-5}$x min^{-1})		k_{cat}/K_m ($x10^{-8}$ M^{-1}xmin^{-1})		Comment
	ATC	TB	ATC	TB	ATC	TB	
WT	0.14	0.28	4.0	0.50	29.0	1.8	
D61N	0.14	ND	5.0	ND	38.0	ND	Extra N-glycosylation
Y72A	0.14	ND	4.7	ND	32.0	ND	PAS
Y72N	0.14	ND	4.2	ND	30.0	ND	PAS
D74E	0.50	ND	4.4	ND	8.8	ND	PAS/signal transduction/allosteric
D74N	0.58	0.23	2.7	0.50	4.6	2.2	PAS/signal transduction/allosteric
D74G	0.63	ND	3.6	ND	5.7	ND	PAS/signal transduction/allosteric
D74K	4.50	0.30	3.5	0.58	0.8	1.9	PAS/signal transduction/allosteric
E84Q	0.27	0.28	4.0	0.44	15.0	1.6	carboxyl/attraction studies
W86A	93.30	0.44	0.8	0.18	0.009	0.4	anionic subsite/signal transduction
W86E	90	0.36	0.4	0.07	0.004	0.2	anionic subsite/signal transduction
W86F	0.8	0.30	2.1	0.47	2.6	1.6	anionic subsite/signal transduction
D95N	0.13	ND	4.4	ND	34.0	ND	reduced biosynthesis
G121A			No activity detected				oxyanion hole
G122A			Marginal activity				oxyanion hole

AChE Type	K_m (mM)		k_{cat} ($x10^{-5}x\ min^{-1}$)		k_{cat}/K_m ($x10^{-8}\ M^{-1}x min^{-1}$)		Comment
	ATC	TB	ATC	TB	ATC	TB	
Y124Q	0.22	ND	4.0	ND	18.2	ND	PAS
Y124A	0.25	ND	2.5	ND	10.0	ND	PAS
D131N	0.10	0.3	3.8	0.55	38.0	1.8	external charge
V132K	0.9	0.35	2.2	0.3	2.4	0.9	"backdoor" hypothesis
V132A	0.12	0.21	3.4	0.58	29.0	2.8	"backdoor" hypothesis
Y133A	12.8	NAD	0.5	NAD	0.04	NAD	active center/H-bond network
Y133F	0.48	0.24	2.0	0.05	4.2	0.2	active center/H-bond network
R152C	No activity detected/non-producer						folding/salt bridge
D175N	No activity detected/non-producer						folding/salt bridge
D175C	No activity detected/non-producer						folding/salt bridge
E202Q	0.35	0.23	0.75	0.1	2.1	0.4	H-bond network/acylation,
E202D	0.30	0.50	0.55	0.09	1.8	0.17	phosphylation,aging,substrat
E202A	0.44	0.42	0.1	0.004	0.23	0.01	inhibition
S203A	No activity detected						catalytic triad
S203C	0.29	ND	0.05	ND	0.15	ND	catalytic triad
S203T	No activity detected/low production						catalytic triad
S203Y	No activity detected/low production						catalytic triad
N265Q	0.12	ND	4.4	ND	36.0	ND	N-glycosylation
E285A	0.30	0.26	4.0	0.5	13.3	1.92	PAS
W286A	0.30	0.40	3.6	0.52	12.0	1.2	PAS
E292A	0.16	0.28	4.1	0.36	26.0	1.3	"electrostatic attraction" hypothesis

AChE Type	K_m (mM)		k_{cat} ($x10^{-5}x\ min^{-1}$)		k_{cat}/K_m ($x10^{-8}\ M^{-1}x min^{-1}$)		Comment
	ATC	TB	ATC	TB	ATC	TB	
F295A	0.13	ND	3.8	ND	29.2	ND	acyl pocket
F295L	0.27	ND	1.5	ND	5.5	ND	acyl pocket
F295H							acyl pocket
F297A	0.43	ND	2.0	ND	4.7	ND	acyl pocket
F297H	2.60	ND	0.7	ND	0.3	ND	acyl pocket
F297V	1.20	ND	2.2	ND	1.8	ND	acyl pocket
D333A	0.12	ND	0.5	ND	4.2	ND	triad definition
D333E	0.11	ND	1.2	ND	11.0	ND	triad definition
D333N	0.13	ND	3.1	ND	24.0	ND	triad definition
E334A			No activity detected				catalytic triad
E334Q			No activity detected/low production				catalytic triad
Y337A	0.13	0.20	1.0	0.20	7.7	1.0	signal relay/substrate inhibition
Y337F	0.18	0.33	4.0	1.3	22.6	3.9	signal relay/substrate inhibition
F338A	0.24	0.30	2.4	0.13	10.0	0.43	hydrophobic subsite
Y341A	0.40	0.31	3.2	0.56	8.0	1.8	PAS
D349N	0.17	0.25	4.4	0.44	26.0	1.8	"electrostatic attraction" hypothesis
N350Q	0.14	ND	4.2	ND	30.0	ND	N-glycosylation
E358Q	0.16	0.25	4.0	0.5	25.0	2.0	"electrostatic attraction" hypothesis
E389Q	0.14	0.24	4.0	0.5	29.0	2.0	"electrostatic attraction" hypothesis

AChE Type	K_m (mM)		k_{cat} ($x10^{-5}x\ min^{-1}$)		k_{cat}/K_m ($x10^{-8}\ M^{-1}x min^{-1}$)		Comment
	ATC	TB	ATC	TB	ATC	TB	
D390N	0.14	0.24	4.0	0.5	29.0	2.0	"electrostatic attraction" hypothesis
D404N			No secretable protein/intracellular activity				salt bridge
H447A			No activity detected				catalytic triad
E450A	0.35	0.20	0.10	0.006	0.3	0.03	H-bond network/active center modulation
N464Q	0.12	ND	3.6	ND	30.0	ND	N-glycosylation
S541N	0.13	ND	4.0	ND	30.0	ND	extra N-glycosylation
C580A	0.14	ND	4.3	ND	30.0	ND	subunit dimerization
C580K	0.14	ND	4.2	ND	30.0	ND	Potential retention signal
D61N/S541N	0.10	ND	4.0	ND	40.0	ND	extra N-glycosylation
Y72A/Y124A	0.07	ND	2.5	ND	35.7	ND	PAS
Y72A/E285A	0.24	ND	4.0	ND	16.7	ND	PAS
Y72A/W286A	0.30	ND	4.2	ND	14.0	ND	PAS
E84Q/E292D	0.33	0.32	3.9	0.53	12.0	1.7	"electrostatic attraction" hypothesis
N265/350Q	0.14	ND	4.0	ND	29.0	ND	N-glycosylation
N265/464Q	0.12	ND	3.7	ND	31.0	ND	N-glycosylation
E285A/W286A	0.43	ND	4.2	ND	9.8	ND	PAS

AChE Type	K_m (mM)		k_{cat} ($x10^{-5}$x min^{-1})		k_{cat}/K_m ($x10^{-8}$ M^{-1}xmin^{-1})		Comment
	ATC	TB	ATC	TB	ATC	TB	
F295L/F297V	0.40	ND	0.9	ND	2.2	ND	acyl pocket
D349N/E358Q	0.16	0.20	5.2	0.43	32.0	2.15	"electrostatic attraction" hypothesis
N350/464Q	0.14	ND	3.9	ND	28.0	ND	N-glycosylation
E389Q/D390Q	0.14	0.24	3.9	0.50	28.0	2.0	"electrostatic attraction" hypothesis
Y72A/E285A/ W286A	0.30	ND	2.0	ND	6.7	ND	PAS
E84Q/D349N/ E358Q	0.34	0.26	4.1	0.43	12.0	1.7	"electrostatic attraction" hypothesis
Y124A/E285A/ W286A	0.28	ND	1.4	ND	5.0	ND	PAS
N265/350/ 464Q	0.15	ND	3.5	ND	23.0	ND	N-glycosylation
E292A/D349N/ E358Q	0.16	0.25	4.0	0.4	25.0	1.6	"electrostatic attraction" hypothesis
E292A/E389Q/ D390N	0.12	0.24	4.2	0.44	35.0	1.8	"electrostatic attraction" hypothesis
E84Q/E292A/ D349N/E358Q	0.45	0.22	4.4	0.41	10.0	1.86	"electrostatic attraction" hypothesis

AChE Type	K_m (mM)		k_{cat} (x10^{-5}x min^{-1})		k_{cat}/K_m (x10^{-8} M^{-1}xmin^{-1})		Comment
	ATC	TB	ATC	TB	ATC	TB	
D349N/E358Q E389Q/D390N	0.13	0.24	4.3	0.42	33.0	1.8	"electrostatic attraction" hypothesis
E84Q/E285A/E292A/ D349N/E358Q	0.39	0.29	4.1	0.5	10.5	1.7	"electrostatic attraction" hypothesis
E292A/D349N/E358Q/ E389Q/D390N	0.16	0.27	4.3	0.5	27.0	1.9	"electrostatic attraction" hypothesis
E84Q/D349N/E358Q/ E389Q/D390N	0.29	0.29	3.9	0.47	13.4	1.6	"electrostatic attraction" hypothesis
E84Q/E292A/D349N/ E358Q/E389Q/ D390N	0.35	0.26	4.3	0.41	12.3	1.6	"electrostatic attraction" hypothesis
E84Q/E285A/E292A/ D349N/E358Q/ E389Q/D390N	0.35	0.26	4.3	0.5	12.3	1.9	"electrostatic attraction" hypothesis

a The averaged values displayed in this table were derived from studies (described in this report) under standard conditions (pH 8.0, 27 °C, and 50 mM sodium phosphate or 50 mM Tris buffer).
The abbreviations used are:ND- not done; NAD- No activity detected; PAS- peripheral anionic site.

APPENDIX B

List of publications originating from the research contract

1. Ordentlich, A., Barak, D., Kronman, C., Flashner, Y., Leitner, M.,Segall , Y., Ariel N., Cohen S., Velan B.,and Shafferman A. (1993) Dissection of the human residues constituting the anionic site, the hydrophobic site, and the acyl pocket. ***J.Biol.Chem.*** 268, 17083-17095.

2. Velan, B., Kronman, C., Ordentlich, A., Flashner, Y., Leitner, M., Cohen, S., and Shafferman, A. (1993). N-Glycosylation of human acetylcholinesterase affects enzyme stability and secretion efficiency but not enzymatic activity. ***Biochem J.*** 296, 649-656.

3. A. Shafferman, B. Velan, D. Barak, C. Kronman, A. Ordentlich, Y. Flashner, M. Leitner, Y. Segall, H. Grosfeld, D. Stein and N. Ariel (1993). Recombinant human acetylcholinesterase - Enzyme engineering. ***Proceedings of Medical Defense Bioscience Review,*** Vol. 3, 1111-1124.

4. Velan, B., Kronman, C., Lazar, A., Ordentlich, A., Flashner, Y., Leitner, M., Marcus,D., Reuveny,S., Grosfeld, H., Cohen, S. and Shafferman, A. (1993) Recombinant human acetylcholinesterase - Production and post-translation processing. ***Proceedings of Medical Defense Bioscience Review, 1993,*** Vol 3, 1097-1108.

5. Lazar, A., Reuveny, S., Kronman, C., Velan, B. and Shafferman. A. (1993). Comparative studies of cell propagation systems for production of human acetylcholinesterase by recombinant cells. in: ***"Animal Cell Technology, Products of Today Prospects for Tomorrow".*** (Eds. R.E. Spier, J.B. Griffiths and W. Bethold) Butterworth-Heinermann Lts.

6. Lazar, A., Reuveny, S., Kronman, C., Velan, B. and Shafferman, A. (1993). Evaluation of anchorage-dependent cell propagation systems for production of human acetylcholinesterase by recombinant 293 cells. ***Cytotechnology,*** 13, 115-123.

7. Ordentlich, A., Kronman, C., Barak, D. , Stein, D., Ariel, N., Marcus, D., Velan, B., and Shafferman, A. (1993). Engineering Resistance to 'Aging' in Phosphylated Human Acetylcholinesterase - Role of Hydrogen Bond Network in the Active Center. ***FEBS Lett*** 334, 215-220.

8. Barak, D., Kronman, C., Ordentlich, A., Ariel, N., Bromberg, A., Marcus, D., Lazar, A., Velan, B. and Shafferman, A. (1994). Acetylcholinesterase peripheral anionic site degeneracy conferred by amino acid arrays sharing a common core. ***J.Biol.Chem.*** 264, 6296-6305.

9. Shafferman, A., Ordentlich, A., Barak, D., Kronman, C., Ber, R., Ariel, N., Osman, R. and Velan, B. (1994) Electrostatic Attraction by Surface Charge Does Not Contribute to the Catalytic Efficiency of Acetylcholinesterase. ***EMBO J.*** 13, 3348- 3455.

10. Velan, B., Kronman, C., Flashner, Y. and Shafferman, A. Reversal of signal-mediated cellular retention by subunit assembly of human acetylcholinesterase (1994). ***J. Biol. Chem.*** 269, 22719-22725.

11. Kronman, C., Ordentlich, A., Barak, D., Velan, B., and Shafferman, A. (1994). The Back Door Hypothesis for Product Clearance in Acetylcholinesterase Challenged by Site Directed Mutagenesis. ***J.Biol.Chem*** . 269, 27819-27822.

12. Ordentlich, A., Barak, D., Kronman, C., Ariel, N., Segall, Y., Velan, B., and Shafferman, A. (1995). Contribution of Aromatic Moieties of Tyr-133 and of the "Anionic Subsite" Trp-86 to Catalytic Efficiuency and Allosteric Modulation of Acetylcholinesterase. ***J. Biol. Chem.*** 270, 2082-2091.

13. Shafferman, A., Ordentlich, A., Barak, D., Kronman, C., Ariel, N., Leitner,M., Segall,Y., Bromberg, A., Reuveny, S., Marcus, D., Bino,T., Lazar, A., Cohen, S. and Velan, B. (1995). Molecular aspects of catalysis and of allosteric regulation of acetylcholinesterases. In ***Enzymes of the Cholinesterase Family*** (Balasubarmanian, A.S., Doctor, B.P., Taylor, P., Quinn, D.M., Eds.) Plenum Publishing Corp. 189-196.

14. Velan, B., Kronman, C., Ordentlich, A., Flashner, Y., Ber, R., Cohen, S. and Shafferman, A. (1995). Post translation processing of acetylcholinesterase - cellular control of biogenesis and secretion. In ***Enzymes of the Cholinesterase Family*** (Balasubarmanian, A.S., Doctor, B.P., Taylor, P., Quinn, D.M., Eds.) Plenum Publishing Corp.269-276.

15. Lebleu, M., Clery, C., Masson, P., Reuveny, S., Marcus, D., Velan, B. and Shafferman, A. (1995) Denaturation of Recombinant Human Acetylcholinesterase. In: ***Enzymes of the Cholinesterase Family*** (Balasubarmanian, A.S., Doctor, B.P., Taylor, P., Quinn, D.M., Eds.) Plenum Publishing Corp. 131-132.

16. Kronman, C., Velan, B., Marcus, D., Ordentlich, A., Reuveny, S. and Shafferman, A. (1995) Involvement of oligomerization, N-Glycosylation and sialylation in the clearance of cholinesterases from the circulation. ***Biochem. J.*** **311:** 959-967.

17. Barak, D., Ordentlich, A., Bromberg, A., Kronman, C., Marcus, D., Lazar, A., Ariel, N., Velan, B. and Shafferman, A. (1995) Allosteric Modulation of Acetylcholinesterase Activity by Peripheral Ligands Involves Conformational Transition of the Anionic Subsite. ***Biochemistry***. **34:** 15444-15452.

18. Ordentlich, A., Barak, D., Kronman, C., Ariel, N., Segall, Y., Velan, B.and Shafferman, A. (1996) The Architecture of Human Acetylcholinesterase Active Center Probed by Interactions with Organophophate Inhibitors. ***J. Biol. Chem.*** In press.

Abstracts and Short Communication in Meetings

1. Shafferman, A. Determinants of the Catalytic Machinery and of Allosteric Regulation of Cholinesterases.(1994) ESN Meeting, Amsterdam Holland.

2. Shafferman, A., Kronman, C. and Ordentlich, A. Compilation of evaluated mutants of cholinesterases. In Enzymes of the Cholinesterase Family (Balasubarmanian, A. S., Doctor, B.P., Taylor, P., Quinn, D.M., Eds.) Plenum Publishing Corp.481-488 (1995). Meeting Madras India Sept 1994.

3. Kronman, C., Flashner, Y., Shafferman, A. and Velan, B. Signal-mediated cellular retention and subunit assembly of human acetylcholinesterase. In Enzymes of the Cholinesterase Family (Balasubarmanian, A.S., Doctor, B.P.,Taylor, P.Quinn, D. M. Eds.) Plenum Publishing Corp. 293-294 (1995) Meeting Madras India Sept 1994.

4. Barak, D., Ordentlich, A., Kronman, C., Ber, R., Bino, T., Arie, N., Osman, R., Velan, B., and Shafferman, A. Electrostatic attraction by surface charge does not contribute to the catalytic efficiency of acetylcholinesterase. In Enzymes of the Cholinesterase Family (Balasubarmanian, A.S., Doctor, B.P.,Taylor, P.Quinn, D.M. Eds.) Plenum Publishing Corp. 223-224 (1995). Meeting Madras India Sept 1994.

5. Ordentlich, A., Kronman, C., Stein, D., Ariel, N., Reuveny, S., Marcus, D. Segall, Y. Barak, D., Velan, B. and Shafferman, A. Amino acids determining specificity to OP-agents and facilitating the "ageing" process in human acetylcholinesterase. In Enzymes of the Cholinesterase Family (Balasubarmanian, A.S., Doctor, B.P.,Taylor, P.Quinn, D.M. Eds.) Plenum Publishing Corp. 221-222 (1995) Meeting Madras India Sept 1994.6

6. Shafferman, A., Ordentlich, A., Barak, D., Kronman, C., Grosfeld, H., Stein, D., Ariel, N., Segall, Y. and Velan, B. (1996) Enzyme Engineering Towards Novel OP-Hydrolases based on the Human Acetylcholinesterase Template. Phosphorus, Sulfur and Silicon.109-110 pp393-396. Meeting Jerusalem, Israel 1995.

7. Velan, B., C. Kronman, D. Marcus, A. Ordentlich, L. Motola, N. Zeliger, S. Reuveny and A. Shafferman. The Role of Oligosaccharide Side-Chains in the Clearance of Cholinesterases from the Circulation. Proceedings of Medical Defense Bioscience Review,in press. Baltimore U.S.A 1996

8. Ariel, N., D. Barak, B. Velan and A. Shafferman. Molecular Dynamics Simulation of the Cys69-Cys96 Surface Loop in Human Acetylcholinesterase. Relevance to the Conformational Mobility of the 'Anionic' Subsite Trp86. Proceedings of Medical Defense Bioscience Review,in press. Baltimore U.S.A 1996.

9. Barak D.,, A. Ordentlich, A. Bromberg, C. Kronman, D. Marcus, A. Lazar, N. Ariel, B. Velan and A. Shafferman.The Role of Active Center Aromatic Residues in the Allosteric Modulation of Acetylcholinesterase Activity by Peripheral Ligands. Proceedings of Medical Defense Bioscience Review, in press. Baltimore U.S.A 1996.

10. Ordentlich, A., D. Barak, C. Kronman, N. Ariel, Y. Segall, B. Velan and A. Shafferman. Determination of Amino Acids in the Active Center of Human AChE Affecting Reactivity Toward Phosphorylating Agents. Proceedings of Medical Defense Bioscience Review,in press. Baltimore U.S.A 1996.

11. Shafferman, A., D. Barak, A. Ordentlich, C. Kronman, N. Ariel, H. Grosfeld, D. Marcus, A. Lazar, Y. Segall and B. Velan. Molecular Manipulation of Bio-Scavengers for Organophosphorus Agents. Proceedings of Medical Defense Bioscience Review,in press. Baltimore U.S.A 1996.

Personnel Receiveng Pay*

BARUCH VELAN	DOV BARAK
ARIE ORDENTLICH	CHANOCH KRONMAN
NAOMI ARIEL	DINO MARCUS
SHAUL REUVENI	TAMAR SERRY
HAIM GROSFELD	NEHAMA ZELIGER
DANA STEIN	LEA SILBERSTEIN
ARIE LAZAR	TAMAR BINO
SARA COHEN	LEVANA MOTULA
ABRHAM BROMBERG	THEODOR CHITLARU
YOEL PAPIER	YEHUDA FLASHNER
RAFI BER	MOSHE LEITNER
GILA FRIEDMAN	AVIGDOR SHAFFERMAN

* Partial or full salary.